UNIVERSIDADE DE LISBOA
FACULDADE DE CIÊNCIAS
DEPARTAMENTO DE QUÍMICA E BIOQUÍMICA

Synthesis of Building Blocks for Assembly of Protozoan Galactofuranose-containing Surface Glycans

Eduardo Cláudio de Sousa

Mestrado em Química
Especialização em Química

Dissertação orientada por:
Professora Doutora Amélia Pilar Rauter
Professor Doutor Daniel Varón Silva

2022

Acknowledgments

I want to express my deep gratitude to my supervisors, Prof. Dr. Amélia Pilar Rauter and Prof. Dr. Daniel Varón Silva, for all the support and advice. I also thank my colleagues from the GPI group at MPIKG and the Carbohydrate Chemistry group at CQE: Antonella Rella, Hyun-Il Oh, Paula Guerrero, Rafael Nunes, Sandra Pinzón, and Tânia Moreira, for the great work environments and their assistance.

I want to thank my friends Andreia Fortuna, Bernardo Henriques, João Pais, Patrícia Calado, and Vitor Martins, for the emotional support and for tolerating my nearly constant ramblings. Last, I want to thank my family: my parents Madalena and Carlos Sousa, and my brothers Filipe and Luís Sousa, for their unconditional love and support.

Abstract

Glycosylphosphatidylinositols (GPIs) are eukaryote glycolipids which attach proteins and glycans to the cell membrane. Trypanosomatide parasites of the *Trypanosoma cruzi* (*T. cruzi*) species and the *Leishmania* genus, the etiologic agents of American trypanosomiasis (also known as Chagas' Disease, ChD) and Leishmaniasis, contain many GPIs and the structurally related glycoinositolphospholipids (GIPLs). These protein-free glycolipids are key membrane glycoconjugates found throughout the parasites' life cycle. Some of these glycan structures contain D-Galactofuranose (Gal*f*) residues, which are not present in mammalian glycans. Gal*f*-containing GPIs and GIPLs are potential virulence factors for *T. cruzi* and *Leishmania*. However, there is little information about their bioactivity. Further research with these glycoconjugates requires pure and structurally defined samples. These cannot be obtained from natural sources and must be accessed by chemical synthesis.

This dissertation covers the syntheses of four orthogonally protected thioglycoside building blocks required to assemble oligosaccharides from *T. cruzi* and *Leishmania major* (*L. major*) GIPLs. These structures include a galactofuranose having a 3-*O*-(2-naphtylmethyl) group (Nap), two mannopyranose units having either a Nap or Benzyl (Bn) ether as protecting group in the 3-O-position, and a galactopyranose with two orthogonal groups, a 6-*O*-Levulinoyl ester (Lev) and a O-4 benzoyl ester for remote participation. These structures were designed for use in conventional oligosaccharide synthesis and Automated Glycan Assembly (AGA) on a solid support.

The synthesis of the Gal*f* building block using two reported methods, starting from 1,2:5,6-Di-*O*-isopropylidene-α-D-galactofuranose and benzyl α-D-galactofuranoside, was inefficient to deliver the target molecule. Thus, an approach for synthesizing Gal*f* thioglycosides was developed using an open-form D-galactose diethyldithioacetal as a precursor. A critical step in this strategy was the cyclization of 5,6-*O*-isopropylidene-D-galactose diethyldithioacetal into a galactofuranoside, which required extensive optimization to achieve a scalable and reproducible reaction. In addition, access to the Gal*f* building block was hindered by poor regioselectivity and product degradation in subsequent reaction steps. Thus, a change in the protecting group strategy from benzyl to acetyl was required to access a building block suitable for synthesizing the target oligosaccharides. A mannose building block bearing a Nap group was synthesized from ethyl 4,6-*O*-benzylidene-1-thio-β-D-mannopyranoside in four steps. The process involved a regioselective etherification using a stannyl ether-assisted nucleophilic substitution on NapBr and the benzoylation of the O-2 position. Removal of the benzylidene acetal and benzylation under basic conditions induced side reactions involving the O-2 benzoyl group. Alternatively, a sequence of reductive cleavage of benzylidene and one-pot silylation and reductive benzylation delivered the benzylated product. This strategy was applied to obtain a second mannopyranose building block containing three benzyl groups. The galactopyranose building block was assembled from ethyl 4,6-*O*-benzylidene-1-thio-β-D-galactopyranoside in four steps, with a regioselective Steglich esterification of the O-6 position as the key reaction step.

The results of this work include the syntheses of the four monosaccharide building blocks and the required optimization of critical cyclization and protection steps. In addition, these compounds are valuable materials for the assembly of GIPL glycans, which are required for evaluating the activity of these glycolipids and their potential application for the diagnosis of ChD and leishmaniasis.

Keywords: *Trypanosoma cruzi*, *Leishmania major*, Glycoinositolphospholipid, Synthesis, Galactofuranose.

Resumo

Glicosilfosfatidilinositois (GPIs, do inglês *Glycosylphosphatidylinositols*) são uma classe de glicoconjugados presentes em todos os eucariotas, que têm a função de ancorar proteínas à membrana celular através de um grupo fosfatidiletanolamina. Parasitas protozoários da ordem Tripanosomatida produzem também glicolípidos idênticos aos GPIs denominados fosfolípidos de glicoinositol (GIPLs, do inglês *Glycoinositolphospholipids*), que não ancoram proteínas. Os GPIs e GIPLs partilham a mesma estrutura geral: um fosfolípido ligado a mioinositol, conectado a um núcleo de manose por glucosamina. A grande variedade de GPIs e GIPLs naturais resulta da presença de diferentes funções lipídicas (ceramida, alquilglicerol, alquiacilglicerol e diacilglicerol) e modificação do núcleo de manose com resíduos de carbo-hidratos (manopiranose, galactopiranose, galactofuranose, glucosamina e ácido siálico) ou grupos fosfatados. Alguns GPIs e GIPLs dos agentes etiológicos da tripanossomíase americana (ou doença de Chagas, causada por *Trypanosoma cruzi*, *T. cruzi*) e leishmaniose (causada por várias espécies do género *Leishmania*), contêm resíduos de galactofuranose (Gal*f*), uma hexofuranose que não está presente em oligossacáridos de vertebrados. Ambas as doenças são incluídas na lista de doenças tropicais negligenciadas da Organização Mundial de Saúde, que compila 20 patologias pouco investigadas, com pouco investimento económico para tratamento ou prevenção, e que afetam maioritariamente regiões pobres. Embora sejam os principais glicoconjugados membranares em *T. cruzi* e *Leishmania major* (*L. major*), sabe-se pouco sobre a bioatividade dos GPI e GIPLs com Gal*f*. Elucidação da atividade destes gliconjugados necessita de quantidades significativas de amostras puras e caracterizadas estruturalmente. Tais amostras não são facilmente obtidas de fontes naturais, dado a natureza anfifílica destes glicolípidos e a grande diversidade de estruturas produzidas por cada espécie/estirpe. Alternativamente, GPIs e GIPLs podem ser obtidos por síntese. A síntese de GPI e GIPLs é complexa, uma vez que exige a síntese regioselectiva e estereoseletiva de mioinositois e oligossacáridos (que podem conter ramificações), bem como a instalação de funcionalidades fosfato e de diversos lípidos. As estratégias de síntese de GPIs/GIPLs são normalmente divididas entre estratégias lineares, onde o mioinositol oligossacárido é montado por glicosilação sequencial com monossacáridos, começando com mioinositol, e estratégias convergentes, que constroem o mioinositol oligossacárido a partir de vários percursores (mono e oligossacáridos). As estratégias convergentes são mais comuns, uma vez que minimizam a manipulação de grupos protetores no oligossacárido em construção.

Foram previamente reportadas duas sínteses de fosfatos de glicoinositol (GIPLs sem lípido) com Gal*f*. Um dos principais desafios na síntese de GIPLs de *L. major* e *T. cruzi*, bem como de outras estruturas com resíduos internos de Gal*f*, é a obtenção de *building blocks* de Gal*f* com grupos protetores ortogonais, uma vez que as estratégias para obtenção e proteção seletiva de galactofuranósidos são limitadas e menos estandardizadas que a síntese de hexopiranoses protegidas ortogonalmente. Ainda assim, várias sínteses de diferentes percursores derivados de Gal*f* já foram reportadas. Estas baseiam-se em estratégias de um só passo, que obtêm galactofuranosidos através da proteção regioselectiva ou glicosilação de galactose livre, e estratégias de vários passos, que sintetizam galactofuranosidos a partir da conversão de outros carbo-hidratos (glucofuranosidos, galactopiranosidos ou D-galactose ditioacetais) ou galactolactonas após a instalação de alguns grupos protetores.

Esta dissertação teve como objetivo sintetizar quatro precursores tioglicósido, necessários à preparação de oligossacáridos com Gal*f*, a serem utilizados para desenvolvimento de novos métodos de diagnostico para doença de Chagas e leishmaniose. Estes precursores incluem um derivado de Gal*f* com um grupo protetor participante na posição O-2 e um grupo protetor temporário em O-3, um galactopiranósido com um grupo participante remoto na posição O-4 e um grupo temporário em O-6, e dois manopiranósidos, com um grupo participante em O-2 e proteção variável em O-3 (benzilo ou 2-

naftilmetilo). A seleção de grupos protetores e rejeitados permite a utilização destes precursores em síntese convencional de oligossacáridos (em fase líquida), ou para *Automated Glycan Assembly* (AGA), uma técnica de síntese automatizada de oligossacáridos onde as reações de desproteção e glicosilação são feitas sobre um aceitador de glicósido montado numa resina sólida.

Foram testadas três estratégias distintas para obter o precursor de Gal*f*. Inicialmente, tentou-se preparar 1,2:5,6-di-*O*-isoprolideno-α-D-galactofuranose a partir de D-galactose por condensação com acetona ou 2,2-dimetoxipropano (DMP). Foram testadas condições reacionais propostas na literatura e variações nestas, mas não se obteve o precursor desejado. Foi também testada mono-benzilação regioselectiva de galactose para produzir o percursor α-D-galactofuranosido de benzilo; esta reação utiliza o solvente não volátil *N,N'*-dimetilpropilenoureia (DMPU), dificultando o tratamento de misturas reacionais e impedindo escalamento da reação. Após instalação de 5,6-isopropilideno, foram testadas duas estratégias de proteção regioselectiva de O-2, acilação direta com cloreto de pivaloílo (PivCl), e acilação mediada por éter de estanho com PivCl ou cloreto de benzoílo (BzCl). Esta segunda estratégia não foi anteriormente reportada para a proteção regioselectiva de posição O-2 de uma Gal*f* em competição com O-3, e proporcionou melhores resultados que acilação direta. No entanto, a impossibilidade de escalamento dos primeiros paços reacionais inviabilizou esta estratégia. Foi, portanto, testada uma terceira estratégia, a condensação de galactose com tioetanol catalisada por $FeCl_3$. Este catalisador produz galactofuranoses quando usado na condensação de Gal com álcoois; no entanto, em vez de produzir o desejado 1-tio-D-galactofuranósido de etilo, esta reação produziu D-galactose dietilditioacetal num rendimento moderado. Este derivado aberto de galactose é convencionalmente sintetizado utilizando HCl fumegante, e pode ser empregue como precursor para tiogalactofuranosidos. O ditioacetal foi utilizado numa nova estratégia reacional, não foi previamente reportada na literatura. Instalação seletiva de 5,6-*O*-isopropilideno foi conseguida com rendimento moderado, após modificação de condições reportadas na literatura. A ciclização do resultante 5,6-*O*-isopropilideno-D-galactose dietilditioacetal com *N*-iodosuccinimida (NIS) exigiu controlo cuidadoso da temperatura, concentração e tempo de reação para evitar sobre-reação do galactofuranosido com subprodutos da ativação do grupo tioetoxi. Após otimização extensiva destes parâmetros obteve-se um protocolo escalável, que oferece uma mistura de anómeros (com produto α maioritário) em rendimentos elevados. Ao contrário do galactofuranosido de benzilo da estratégia anterior, acilação regioselectiva mediada por éter de estanho não funcionou com o tiogalactofuranosido, pelo que se utilizou acilação convencional com PivCl. O grupo protetor temporário levulinilo (Lev) foi de seguida instalado em O-3 por esterificação de Steglich. Após hidrolise de isopropilideno, testou-se a benzilação de O-5 e O-6 em meio básico (com brometo de benzilo e hidreto de sódio) que resultou na migração indesejada de Lev para O-6, e em meio ácido (com tricloroacetimidato de benzilo), que não produziu reação. Alternativamente, utilizou-se o grupo protetor 2-naftilmetilo (Nap), que é estável em meio básico, para proteção temporária de O-3. No entanto, a benzilação de O-5 e O-6 foi novamente impossível em meio básico (devido a hidrolize de Piv) e num conjunto de reações alternativas em meio neutro e ácido, pelo que se instalou acetilo como grupo protetor permanente em O-5 e O-6. Embora se tenha obtido o percursor desejado, o método atual produziu um rendimento global baixo. Perda de rendimento ocorreu principalmente durante a instalação de isopropilideno, ciclização (devido á formação de uma mistura anomérica), e durante a acilação (pela baixa seletividade da reação).

O precursor de galactopiranose foi preparado a partir de 4,6-*O*-benzilideno-1-tio-β-D-galactopiranosido de etilo em quatro passos. Após benzilação dos grupos O-2 e O-3, testou-se a clivagem oxidativa do benzilideno, que é reportada produzir um grupo benzoilo em O-4 e uma posição O-6 livre. No entanto, a reação oxidou o grupo tioetoxi na posição anomérica. Alternativamente, removeu-se benzilideno por metanolise, protegeu-se regioselectivamente O-6 com Lev por esterificação de

Steglich, e benzilou-se O-4, obtendo-se o precursor desejado. Um dos manopiranosidos, com o grupo protetor temporário Nap em O-3, foi preparado partir de 4,6-*O*-benzilideno-1-tio-β-D-manopiranosido de etilo. A posição 3 foi regioselectivamente protegida com Nap por substituição nucleofílica mediada por éter de estanho. Após benzoilação de O-2 e remoção de benzilideno, testou-se a benzilação das posições livres em meio básico e ácido, mas ambos os casos resultaram em degradação do substrato. Alternativamente, realizou-se clivagem redutiva de benzilideno com BH_3.THF, fornecendo um grupo benzilo em O-4, seguido de benzilação de O-6 por sililação e benzilação redutiva *one-pot*. O segundo precursor de manose foi preparado a partir de 4,6-*O*-benzilideno-3-*O*-benzo-1-tio-β-D-manopiranosido de etilo utilizando a mesma estratégia.

Palavras-Chave: *Trypanosoma cruzi*, *Leishmania major*, Fosfolípidos de glicoinositol, Síntese, Galactofuranose.

Contents

List of Figures

List of Schemes

List of Tables

List of Abbreviations

2-AEP – 2-Aminoethylphosphonate
Ac – Acetyl
Ac_2O – Acetic anhydride
AcOEt – Ethyl acetate
AcOH – Acetic acid
AGA – Automated Glycan Assembly
AgOTf – Silver trifluoromethanesulfonate
$BF_3.Et_2O$ – Boron trifluoride diethyl ether complex
BH_3.THF – Borane tetrahydrofuran complex
Bn – Benzyl
BnBr – Benzyl bromide
BnTCAI – Benzyl trichloroacetimidate
Bu_2SnO – Dibutyltin oxide
$(Bu_3Sn)_2O$ – Bis(tributyltin) oxide
Bz – Benzoyl
BzCl – Benzoyl Chloride
cat. – catalytic
CCC – Chronic Chagas Cardiomyopathy
ChD – Chagas' Disease
CL – Cutaneous Leishmaniasis
COSY – Correlation Spectroscopy
CSA – Camphorsulphonic acid
d – Doublet
DAG – 1,2:5,6-Di-*O*-isoprolylidine-α-D-glucofuranose
DBU – 1,8-Diazabicyclo[5.4.0]undec-7-ene
DCC – Di-cyclohexylcarbodiimide
DCM – Dichloromethane
dd – Doublet of doublets
ddd – Doublet of doublet of doublets
DDQ – 2,3-Dichloro-5,6-dicyano-1,4-benzoquinone
DIC – Di-isopropylcarbodiimide
DIPEA – *N,N*-Diisopropyletylamine
DMAP – 4-(Dimethylamino)pyridine
DMF – Dimethylformamide
DMP – 2,2-Dimethoxypropane
DMPU – *N,N*′-Dimethylpropyleneurea
DTU – Discrete Typing Unit
equiv. – Equivalent
Et – Ethyl
Et_3N – Triethylamine
EtNP – Ethanolamine phosphate
EtSH – Ethanethiol
Fmoc – Fluorenylmethoxycarbonyl
Gal – Galactopyranose
Gal*f* – Galactofuranose
GIPL – Glycoinositolphospholipids
Glc – Glucopyranose
GlcN – Glucosamine
GlcNAc – N-acetylglucosamine
GPI – Glycosylphosphatidylinositol
Hex – Hexane
HMBC – Heteronuclear Multiple Bond Correlation
HMDS – Hexamethyldisilazane
HMDSO – Hexamethyldisiloxane
HPLC – High Performance Liquid Chromatography
HSQC – Heteronuclear Single Quantum Correlation
Lev – Levulinoyl
LevOH – Levulinic acid
LG – Leaving Group
LPG – Lipophosphoglycan
m – Multiplet
Man – Mannopyranose
Me – Methyl
MeOH – Methanol
MeCN – Acetonitrile
MP – Melting point
MS/IR – Mass spectrometry/ infrared spectroscopy
myo-Ins – *myo*-Inositol
NaOMe – Sodium methoxide
Nap – 2-Naphtylmethyl
NapBr – 2-(bromomethyl)naphthalene
NIS – *N*-iodosuccinimide
NMR – Nuclear Magnetic Resonance
NOESY – Nuclear Overhauser Effect Spectroscopy
NP-HPLC – Normal phase HPLC
NTD – Negleted tropical disease
Nu – Nucleophile
PG – Protecting Group
Ph – Phenyl
PhCHO – Benzaldehyde
$PhCH(OMe)_2$ – Benzaldehyde dimethyl acetal
PIF – Pyranose-into-furanose

Piv – Pivaloyl
PivCl – Trimethylacetyl chloride
PMB – *p*-Methoxybenzyl
PTSA – *p*-Toluenesulfonic acid
$Py.SO_3$ – Sulfur trioxide pyridine complex
qC – Quaternary carbon
R_f – Retention factor
rt – Room temperature
s – Singlet
t – Triplet
td – Triplet of doublets
TBABzO – Tetrabutylammonium benzoate
TBAF – Tetrabutylammonium Fluoride
TBAI – Tetrabutylammonium Iodide
TBDPS – *tert*-Butyldiphenylsilyl
TBDPSCl – *tert*-Butyldiphenylsilyl chloride
TBS – Tributylsilyl
TBSCl – Tributylsilyl chloride
TCA – Trichloroacetyl
TCAI – Trichloroacetimidate
TES – Triethylsilane
TfOH – Triflic acid
THF – Tetrahydrofuran
TLC – Thin-layer chromatography
TLR – Toll-like receptor
TMSCl – Trimethylsilyl Chloride
TMSI – Trimethylsilyl Iodide
TMSOTf – Trimethylsilyl triflate
Tol – *p*-Toluyl
TolSH - 4-Methylbenzenethiol
tPG – Temporary protecting group
TriBOT – 2,4,6-tris(benzyloxy)-1,3,5-triazine
TrCl – Trytil chloride
Ts – Tosyl
TsCl – *p*-Toluenesulfonyl Chloride
tt – Triplet of triplets
UDP – Uridine diphosphate
VL – Visceral leishmaniasis

1. Introduction

1.1. Protozoa Parasites

Protozoa is an informal group of heterotrophic single-celled eukaryotes. Protozoa ecology is varied, but parasitism is common in many species. In particular, the taxonomic order Trypanosomatida encompasses parasitic species, including the pathogens causing Human African trypanosomiasis (or sleeping sickness), American trypanosomiasis (Chagas Disease, ChD) and leishmaniasis.[1] These diseases are included in the World Health Organization (WHO) list of neglected tropical diseases (NTDs), a compilation of 20 under-researched and under-invested diseases and disease groups, affecting mostly poor tropical and subtropical regions, causing significant health and economic impacts in developing nations.[2]

1.1.1. Chagas' Disease and *Trypanosoma cruzi*

Chagas' disease is a zoonotic disease caused by infection with the protozoa parasite *Trypanosoma cruzi* (*T. cruzi*). ChD is endemic to Latin America, although it can be found worldwide, resulting from the migration of infected individuals.[3] Three main stages characterize ChD; an acute phase, occurring shortly after infection with *T. cruzi*, followed by an indeterminate (asymptomatic) phase, which may develop into chronic ChD decades after infection.[4] In 2018, the WHO estimated that 6 to 7 million cases of ChD existed worldwide.[5]

T. cruzi has a two-host life cycle with four distinct stages, the insect stage epimastigotes and (metacyclic) trypomastigotes, and the mammalian stage amastigotes and trypomastigotes (**Figure 1.1**). Only epimastigotes and amastigotes can reproduce, inside the triatomine gut and mammalian host cells, respectively, while trypomastigotes transfer the infection between hosts and disseminate the infection in mammals.[6,7] Modulation of host immune response is essential for *T. cruzi* proliferation and maintenance of a large parasite population to infect the triatomine vector.[8] This modulation ensures the survival of the mammalian host, which is rapidly killed when immune response is absent.[9]

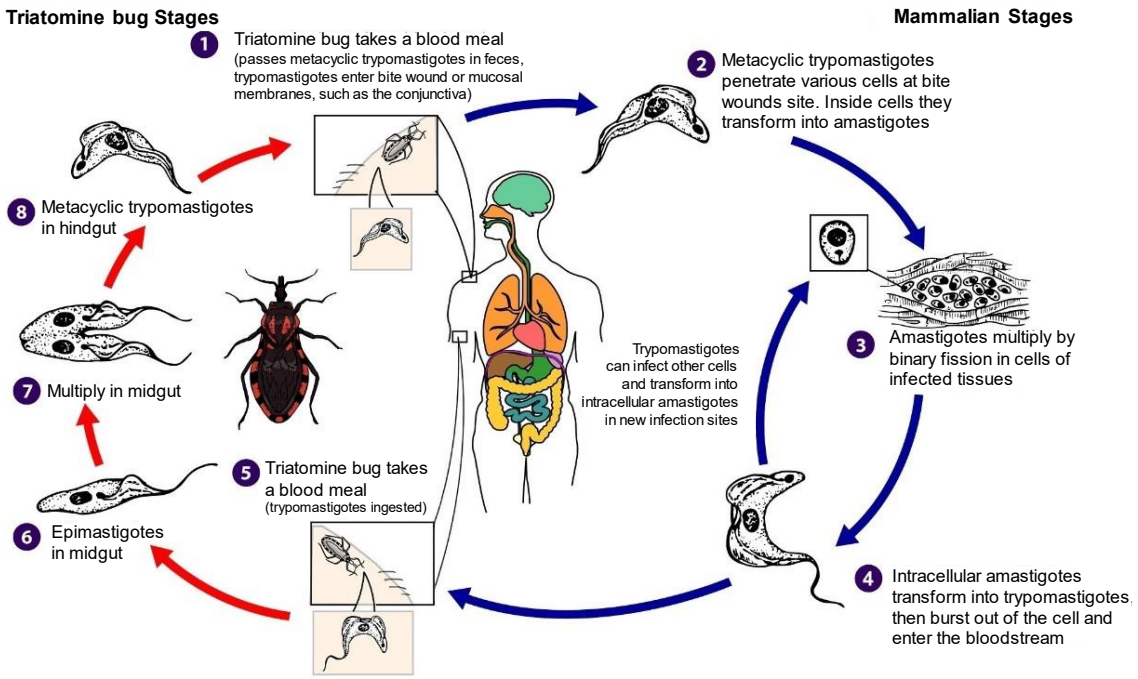

Figure 1.1: *T. cruzi* life cycle, adapted from Center for Disease Control and Prevention (CDC).[7]

Most ChD cases are vector-borne (insects of the *Triatominae* subfamily, commonly known as kissing bugs) or result from vertical transmission during gestation.[4,10] Infection can also occur by oral transmission (through consumption of contaminated food and beverages), blood transfusions, and organ transplants from infected donors.[4,10] Acute ChD can be asymptomatic, cause mild, unspecific symptoms [11] which may be mistaken for other illnesses,[12] and in rare instances lead to skin nodules (chagomas) or prolonged eyelid edema (Romaña's sign) in the inoculation site.[11] Acute ChD is very rarely life-threatening,[10] although the risk of severe complications increases after disease reactivation in immune-compromised individuals, in particular, those co-infected with HIV.[4]

Acute ChD can be treated with benznidazole and nifurtimox; the effectiveness of these drugs varies with *T. cruzi* strains and host genetic backgrounds.[13] They are estimated to cure 60 % to 85 % of patients.[14,15] However, adverse reactions to both drugs are common and potentially severe (especially with nifurtimox), leading to treatment discontinuation.[14,15] While some prophylactic and therapeutic ChD vaccine prototypes improve survivability in murine models, none have yet reached the clinical trial stage.[16,17]

Without treatment, ChD develops into an intermediate (or indeterminate) phase, where the host immune response maintains a low parasite population without being able to eliminate it. Decades after infection, an estimated 30 % to 40 % of patients develop a form of chronic ChD,[3] characterized by multiple gastrointestinal and cardiac complications. Unlike acute ChD, benznidazole or nifurtimox chemotherapies for chronic ChD are ineffective and controversial.[18]

The most common gastrointestinal manifestations of chronic ChD are megaesophagus (enlarged esophagus) and megacolon (enlarged colon), resulting from damage to the enteric nervous system.[19] While not life-threatening, gastrointestinal ChD is severely debilitating and related to several other gastrointestinal diseases.[19] Chronic Chagas Cardiomyopathy (or chronic chagasic cardiomyopathy, CCC) is the leading cause of ChD mortality. It is a consequence of accumulated damage to heart tissue from several years of inflammation and significant morphological changes in the heart.[12] These morphological changes lead to arrhythmia and increased risk of heart failure and thromboembolic events (such as strokes), which rise with the progression of the disease.[20] CCC pathogenesis is still debated, although the presence of parasites in the cardiac tissue is likely required.[21]

1.1.2. Leishmaniasis and the *Leishmania* genus

Leishmania genus encompasses multiple species of parasites, which can cause different forms of leishmaniasis, a mammalian vector-born disease. Various clinical manifestations may occur depending on *Leishmania* species and host/environmental factors, and are classified as cutaneous and visceral leishmaniasis.[22] Geographic distribution of different species of *Leishmania* will determine both the host and type of leishmaniasis that is endemic to a region.

Leishmania parasites share similar, two-host life cycles, with two main morphological stages. Promastigotes reproduce in the female sandflies' gut, infect mammals during the sandflies' bloodmeal, and are phagocytized by host macrophages. Promastigotes then differentiate into amastigotes, which reproduce intracellularly, proliferate around the inoculation site (and possibly disseminate around the body), and infect the insect vector during feeding (**Figure 1.2**).[23,24]

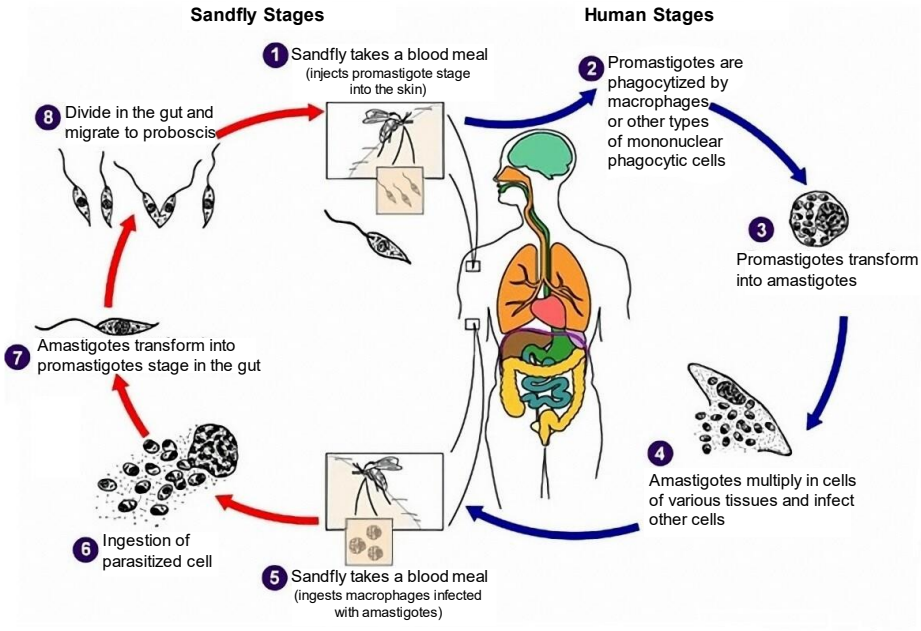

Figure 1.2: *Leishmania* life cycle, adapted from CDC.[24]

Cutaneous leishmaniasis (CL) is the most common and least dangerous form of the disease. According to the WHO, as of 2019, there are 600 thousand to one million new cases annually, 95 % of which occurred in the Americas, Mediterranean Basin, Middle East and Central Asia.[25] CL may manifest differently depending on parasite species/strain, and host and environmental factors.[26] Most CL cases are classified as localized CL, characterized by the formation of painless, self-healing ulcers in the inoculation site.[27]

The formation of multiple lesions can occur, either from various inoculations or by disseminating parasites through the circulatory and lymphatic systems. These disease forms are classified as disseminated CL and mucosal CL, and are most common and severe in species from the American *Viania* subgenus.[26] Disseminated CL is characterized by multiple skin lesions around the inoculation site and/or in non-adjacent body parts.[27] Mucosal CL produces lesions in the upper respiratory and gastric tract mucosa, which occur months after initial infection or simultaneously with localized CL.[27] Without treatment, mucosal CL causes severe, highly disfiguring and potentially life-threatening damage to the mucosa.[27]

Visceral leishmaniasis (VL), also known as kala-azar, is a life-threatening result of infection by *Leishmania donovani* (*L. donovani*) or *Leishmania infantum* (*L. infantum*).[28] In 2019, the WHO estimated 50 thousand to 90 thousand new yearly cases of VL, mainly occurring in Brazil, East Africa and the Indian subcontinent.[25] VL may be preceded by CL, and is caused by parasite dissemination to visceral organs, including the spleen and bone marrow.[29] VL causes fevers, weight loss, anemia, internal bleeding, and infection by opportunistic bacteria.[28,30] Without treatment, this form of leishmaniasis is usually fatal.[28]

Current therapeutic approaches are effective in immunocompetent patients, but there is a growing concern with drug resistance.[31,32] Moreover, anti-leishmanial drugs are expensive and produce significant adverse reactions.[32] During VL or after successful treatment of VL caused by *L. donovani* (and possibly *L. infantum*),[33] patients can develop a third type of CL, known as post-kala-azar dermal leishmaniasis. Most cases occur in Indian subcontinent and East Africa, with different characteristics.[26,33,34]

Hosts may become immune to some forms of leishmaniasis after disease resolution, which supports the development of prophylactic vaccines.[35] Several vaccine candidates have been developed, but either lack sufficient evidence to be used, or fail to produce helpful protection in humans or animals.[36] Thus, while some vaccine clinical trials are still ongoing,[37] there are currently no vaccines against leishmaniasis approved for human use.

1.2. Glycosylphosphatidylinositols (GPIs) and related structures

Glycosylphosphatidylinositols (GPIs) are glycoconjugates common to all eukaryotes, functioning as cell membrane anchors for proteins.[38] Some trypanosomatids produce similar protein-free, low molecular weight Glycoinositolphospholipids (GIPLs), and use GPIs as anchors for complex phosphoglycans (Lipophosphoglycans, LPGs).[39] GIPLs, LPGs, and GPI-anchored proteins are virulence factors for *T. cruzi*, *Trypanosoma brucei*, and the *Leishmania* genus.[39]

All GPIs and GIPLs share the motif Man1α-4GlcNα1-6*myo*-Ins-PO_4^--Lipid (**Scheme 1.1**), and most known GPI anchors have the glycan core NH_2EtOPO_3H-6Man1α-2Man1α-6Man1α-4GlcN, which connects to the proteins' C-terminus through ethanolamine phosphate (EtNP).[38,40] GIPLs are more diverse and are classified into three types. Type 1 GIPLs contain Man II in the O-6 position of Man I (like GPI protein anchors); type 2 GIPLs have Man II' in the O-3 position of Man I instead of O-6; hybrid type GIPLs contain mannose in both O-3 and O-6 (**Figure 1.3**).[40]

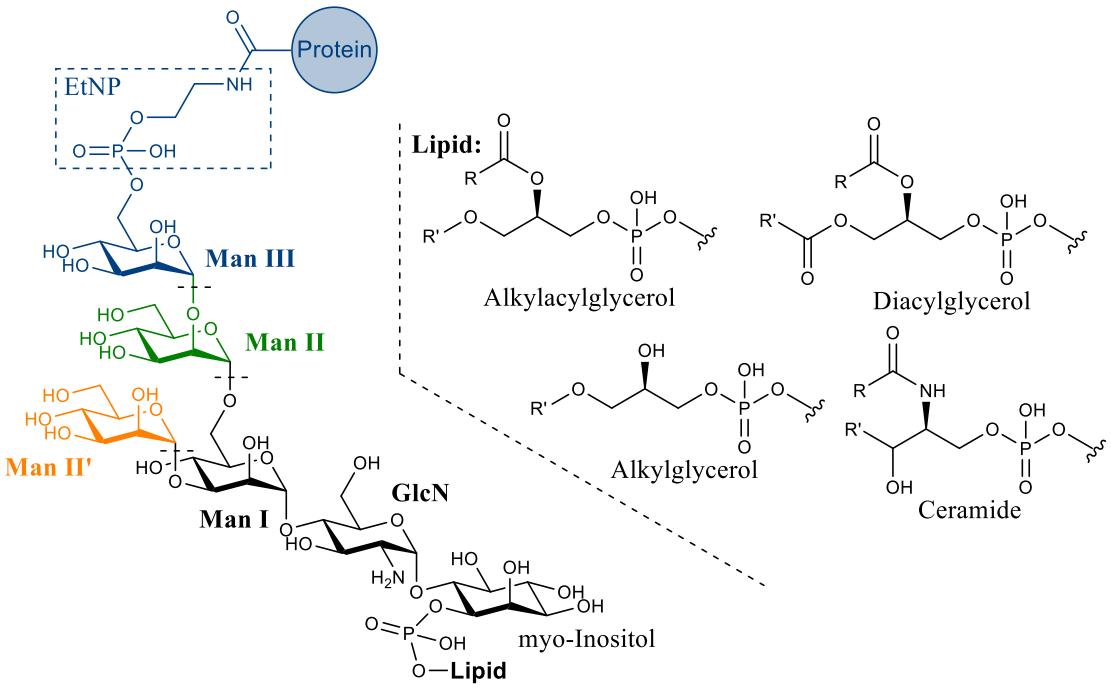

Figure 1.3: Structure of GPIs and GIPLs. Type 1 GIPLs have Manα1,6 (ManII), Type 2 have Manα1,3 (ManII'), and Hybrid type GIPLs have both units; GPIs share the Type 1 structure, with the addition of NH_2EtOPO_3H-Manα1,2 (blue); R and R' represent saturated or unsaturated alkyl chains.

Beyond these shared motifs, GPIs and GIPLs have various modifications with glycosyl units, such as mannopyranose (Man), galactopyranose (Gal), galactofuranose (Gal*f*), glucosamine (GlcN) and sialic acid. They can have phosphorylations with 2-aminoethylphosphonate (2-AEP), EtNP and or Glcα1-PO_4^- units.[41] The phospholipid moiety is also heterogeneous, with variable chemical structure (alkylacylglycerol, alkylglycerol, diacylglycerol and ceramide), and containing distinct alkyl chain length and saturation.[38]

Gal*f* containing glycan moieties are a peculiarity of some *T. cruzi* and *Leishmania* GPIs, GIPLs and GPI anchored proteins. Galactofuranose is not produced by any vertebrate, unlike galactopyranose, which is found in mammalian glycans and glycoconjugates. Galactofuranosides exist in several species, including human pathogenic *Mycobacteria* and opportunistic *Aspergillus* fungi.[42,43]

The biosynthesis of Gal*f* containing glycans is similar in all species: UDP-Gal is isomerized into UDP-Gal*f* by the enzyme UDP-Gal mutase,[44] and is used as a glycosyl donor substrate by a Gal*f*-glycosyltransferase.[45] These processes do not exist in mammals, and are therefore potential therapeutic targets.[46] This motivates research into Gal*f* derivatives and analogues as transferase substrates, required to study enzyme activity,[47–49] and as mutase and transferase inhibitors.[50]

1.2.1. Galactofuranose in *T. cruzi* mucins and GIPLs

The cell surface of all life stages of *T. cruzi* contains mucins, a family of highly glycosylated GPI-anchored proteins. The glycan moieties of these glycoconjugates are composed mainly of galactose,[51] and contain terminal β-Gal*p*, acting as an acceptor for sialic acid transferred from host glycans by *T. cruzi trans*-sialidases.[52] Sialylation of surface glycans is a strategy used by many pathogens, including *T. cruzi* and *Leishmania*, to evade the immune response and modulate interactions with host cells.[53]

Strains from Discrete Typing Unit I (DTU I) and DTU IV (DTU system is used to group *T. cruzi* strains that share defined molecular markers)[54] present mucins with β-Gal*f* units, with or without galactose in O-2. These structures are present during the epimastigote and metacyclic trypomastigote life stages but not in amastigotes or blood trypomastigotes.[51] Mucins with terminal Gal*f* (from Dm28c strain, DTU 1), in particular with the trisaccharide motif Gal*f*1β-4-[Gal1α-6]-GlcNAcα, participate in parasite adhesion to triatomine (*Triatominae infestans*) hindgut, which is inhibited by synthetic glycans bearing this trisaccharide.[55] The effect of Gal*f*-containing mucins from metacyclic trypomastigotes on the initial stages of mammalian infection is yet to be clarified.

Unlike mucins, Gal*f* containing type 1 GIPLs (incorrectly named lipopeptidophosphoglycans, LPPGs, when first identified) [56] are present in all life-stages of most described *T. cruzi* strains.[57–60] *T. cruzi* GIPLs share a common glycan core, Man1α-2Man1α-6Man1α-4GlcNα1-6*myo*-Ins-PO_4^--Lipid, as well as the 2-AEP substitution in O-6 of GlcN.[60] Man III is modified in a strain-specific fashion, dividing *T. cruzi* GIPLs into two series. Series 1 GIPLs contain EtNP or 2-AEP in O-6, while series 2 GIPLs have Gal*f* in O-3 (**Figure 1.4**, **Table 1.1**).[60] Most characterized GIPLs from stationary phase epimastigotes have ceramide lipid units,[60,61] except for GIPLs from *T. cruzi* CL strain, which may bear either ceramide or alkylacylglycerol moieties.[60]

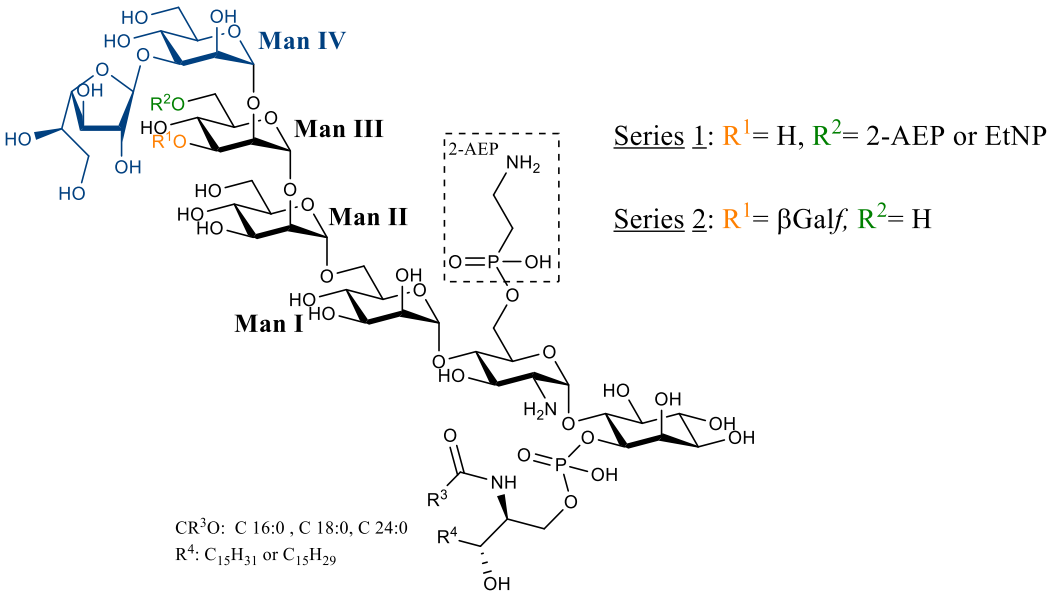

Figure 1.4: General structure of GIPLs from *T. cruzi* stationary phase epimastigotes.

Table 1.1: Glycan cores from *T. cruzi* epimastigote GIPLs, adapted from Mendonça-Previato *et al.*.[60]

GIPL Series	Glycan Core	*T. cruzi* strain
Series 1	EtNP (6), 2-AEP (6) — Galf1β-3Man1α-2Man1α-2Man1α-6Man1α-4GlcN1α-6Ins-PO_4	G, G-645, CL, Y
	2-AEP (6), 2-AEP (6) — Galf1β-3Man1α-2Man1α-2Man1α-6Man1α-4GlcN1α-6Ins-PO_4	G-645, CL, Y
	EtNP (6), 2-AEP (6) — Man1α-2Man1α-2Man1α-6Man1α-4GlcN1α-6Ins-PO_4	G, G-645, Tulahuen, Y
	2-AEP (6), 2-AEP (6) — Man1α-2Man1α-2Man1α-6Man1α-4GlcN1α-6Ins-PO_4	G, Y
Series 2	Galf1β (3), 2-AEP (6) — Galf1β-3Man1α-2Man1α-2Man1α-6Man1α-4GlcN1α-6Ins-PO_4	CL, Y, G, G-645
	Galf1β (3), 2-AEP (6) — Man1α-2Man1α-2Man1α-6Man1α-4GlcN1α-6Ins-PO_4	CL, Y
	Galf1β (3), 2-AEP (6) — Man1α-2Man1α-6Man1α-4GlcN1α-6Ins-PO_4	Y

Only GIPLs from stationary phase epimastigotes have been fully characterized. However, partial characterization of GIPL from other growth phases and life stages shows variation in the glycan core and the lipid content. In Y strain epimastigote cultures, 20% of the GIPL pool during the exponential growth phase contains galactopyranose, which is not found in stationary phase GIPLs.[62] Both ceramide and alkylacylglycerols are found in high amounts in Y strain growth phase GIPLs,[62] instead of only ceramide.[61] Changes in lipid structure were also identified during the transition from trypomastigote to amastigote stages, with Y strain GPIs and GIPL lipid moieties (mainly glycerolipids

in the early stages of differentiation) being remodeled to ceramide; inhibition of this process stops the differentiation of trypomastigote to amastigote.[63] Thus, changes on GIPL structure are developmentally regulated and influence parasite differentiation and proliferation. Most research into *T. cruzi* GIPL activity has used GIPL mixtures isolated from stationary phase epimastigotes, which disregards possible variations in activity of different glycan and lipid structures, and the effect of developmental and life-stage related changes in GIPL structure.

GIPLs participate in epimastigote adhesion to triatomine gut. Using GIPLs isolates from Y and Dm28c strains significantly hinders the adhesion of epimastigotes from these strains to *Rhodnius prolixus* larvae gut (up to 90 %).[64] The adhesion is mediated by Gal*f*, as selective hydrolysis of Gal*f* reduced this inhibition by 50 %, and is independent of epimastigote adhesion mediated by Gal*f* containing mucins.[64] In mammalian hosts, both Y strain GIPLs and Gal*f*1β-3Man1α-Me (the reducing end of the major GIPLs of this strain) inhibit trypomastigote internalization.[65] The ceramide moiety of epimastigote GIPLs can also induce macrophage apoptosis,[66] and suppress the release of some proinflammatory cytokines.[67–69]

T. cruzi GIPLs are known agonists to some macrophage Toll-like receptors (TLR), which participate in the innate and acquired immune responses to infection by regulating proinflammatory cytokine production.[8] TLR4 is activated *in vitro* and *in vivo* by G strain GIPLs, leading to cytokine production and subsequent recruitment of neutrophils [70,71] and lymphocyte activation in mice.[71] This innate immune response is vital for the survival of mice infected with *T. cruzi* Y strain, as TLR4 deficiency leads to fatal infections.[70] TLR2 also binds Y strain GIPLs, although less than GPI protein anchors.[72] GIPLs activate B lymphocytes through their glycan moiety, inducing the production of IgG and IgM antibodies;[67] this activity is potentiated by interleukin 4, one of the cytokines released after GIPL exposure *in vivo*.[71] These anti-GIPL antibodies are present in the sera of acute and chronic ChD patients, and react to GIPLs isolated from Y strain epimastigotes.[57,73] This recognition is attributed to their Gal*f* epitopes, as their removal significantly reduced reactivity.[57]

1.2.2. Galactofuranose in *Leishmania* LPGs and GIPLs

All *Leishmania* species produce LPGs almost exclusively during the promastigote life stage.[74] LPGs have several unique features, including a saturated alkylglycerol ($C_{24}H_{49}$ or $C_{26}H_{53}$) phospholipid moiety, and a glycan core containing an internal Gal*f* unit, shared by all *Leishmania* species (**Figure 1.5**). This GPI binds a large phosphoglycan composed of repeating units of phosphodisaccharide HPO_4-6Gal1β4Man1α, which is terminated by a cap oligosaccharide.[74,75] Several changes to this conserved structure, including phosphate-bound Glc in position O-6 of Man II',[75] variable lengths and branching of the phosphoglycan with Man or Glc, and distinct cap structure and size,[74–76] lead to a large diversity of species and life-stage specific LPG structures.[74] *Leishmania* LPG activity is commonly assessed *in vitro* and *in vivo* using mixtures of extracted LPGs, and by characterization of *Leishmania* mutants lacking LPGs and other membrane glycoconjugates. These approaches disregard the structural diversity of LPG structures.[75]

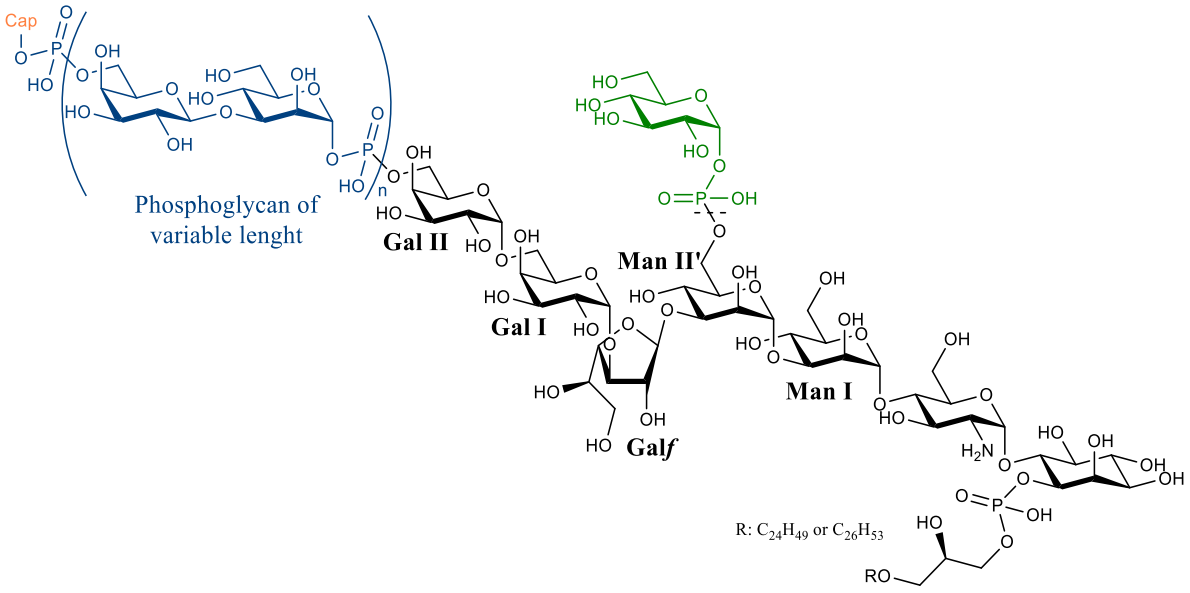

Figure 1.5: *Leishmania* LPG.

LPGs participate in promastigote binding to the sandflies' gut, and structural changes to the phosphoglycan chain release the parasite from the epithelium.[77] LPGs may modulate the early immune response and macrophages' activity, ensuring promastigote survival in mammalian hosts before differentiation into amastigotes.[75,76,78] They do not have the same functions in all *Leishmania* species,[79,80] as evidenced by the distinct virulence of LPG deficient mutants. In particular, *Leishmania major* (*L. major*, an "Old World" species that causes localized CL)[27] mutant promastigotes have significantly decreased survival inside macrophages,[81] while a similar mutation has little effect on *Leishmania mexicana* (*L. mexicana*) virulence.[82] Moreover, LPGs from different species and strains also elicit distinct immune responses from host macrophages.[80,83] This diversity of activity and immunogenicity may result from the diverse composition of LPGs, and relate to the clinical manifestation of leishmaniasis.[83]

Unlike LPGs, *Leishmania* GIPLs are produced throughout the entire life cycle.[76] Both type 1, type 2, and hybrid type GIPLs have been identified in different species.[76,84] Only some type 2 GIPLs contain Gal*f*, which were initially discovered in *L. major* as the main membrane glycoconjugates in both promastigotes and amastigotes.[84,85] They are also found in *L. mexicana* promastigotes (as 10 % of the GIPL pool),[86] but not in amastigotes.[87] Type 2 GIPLs were also identified as the main glycolipid of *Leishmania braziliensis*.[88] However, it is unknown if these contain Gal*f* (like *L. major*) or only galactopyranose (like the type 2 GIPLs of *Leishmania panamensis*).[89]

L. major GIPLs share the glycan core Gal*f*1β-3Man1α-3Man1α-4GlcN of LPGs (initial characterization [85] incorrectly assigned the anomeric configuration of Gal*f* as α instead of β).[90] Three main GIPLs have been classified according to their glycan moiety. GIPL-1 only has the shared glycan core with terminal Gal*f*, GIPL-2 bears an α-Gal (Gal I) in the O-3 position of Gal*f*, and GIPL-3 contains an additional α-Gal (Gal II) on the O-6 position of Gal I (**Figure 1.6**).[84,85] A fourth structure, GIPL-A, was identified in some *L. major* strains and contains a galactose dimmer (with a 1-3 glycosyl bond) on the O-3 position of Gal*f*. However, there is disagreement on whether these are in furanose or pyranose form, and on the configuration of the two glycosyl bonds.[76,85,88,91] The ratio of type 2 GIPLs and the presence of phosphate-bound Glc in the O-6 position of Man II' is strain specific.[84] All *Leishmania* GIPLs have alkylacylglicerol lipid moieties,[84] but type 2 GIPLs have a higher diversity of

alkyl ($C_{18}H_{33}$, $C_{22}H_{25}$, $C_{24}H_{49}$ and $C_{26}H_{53}$) and acyl (C12:0, C14:0, C16:0 and 15-hydroxypentadecanoic ester) moieties than type 1 and hybrid type GIPLs, even in GIPLs from the same strain and with the same glycan core.[85] Amastigotes present higher amounts of *lyso*-GIPL variants with alkylglycerol lipid moieties.[91]

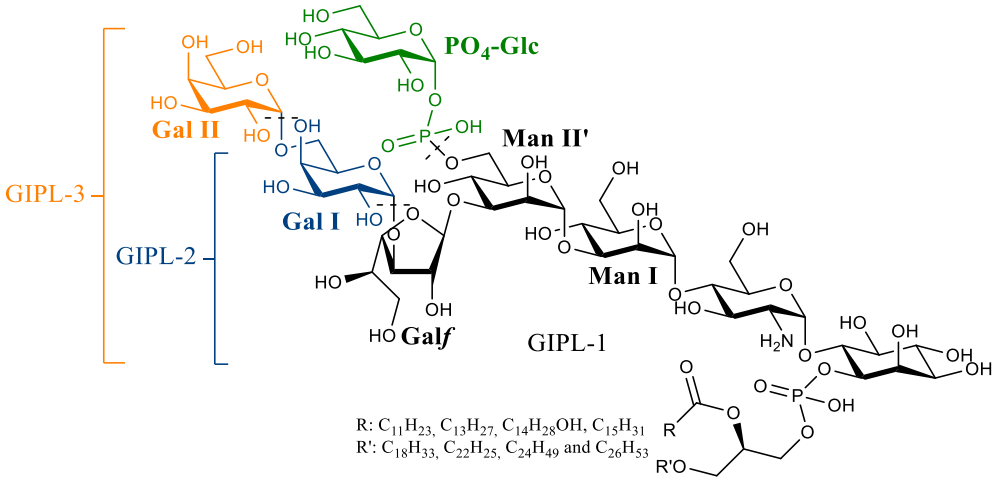

Figure 1.6: *Leishmania* type 2 GIPLs: GIPL-1 is represented in black; GIPL-2 in blue and black, and GIPL 3 in orange, blue and black; strain-specific phosphate-bound Glc in green.

L. major GIPLs are known immunogens,[85,92,93] but their function during infection is poorly understood. GIPL-1 may participate in *L. major* cell binding and macrophage invasion. Promastigotes and amastigotes incubated with monoclonal antibody MEST-1, which binds glycolipids with Gal*f*1β-3Man*p* and Gal*f*1β-6Man*p* epitopes, had a significant reduction of macrophage infectivity (80 % for promastigote, 30 % for amastigotes).[94] *L. major* GIPLs, but not LPGs, can inhibit nitrous oxide production by macrophages through their lipid moiety, improving parasite survival.[95]

The relevance of these results is undermined by research on *L. major* mutant strains. Promastigotes producing only type 2 GIPLs and no LPGs,[81] and UGM-suppressed mutants, which produce truncated GIPLs and no LPGs,[96] suffer similar reductions in infectivity and delayed disease onset in murine models. Amastigote activity and disease progression were largely unaffected in either case. Since no significant change in amastigote infectivity or survival was observed between strains with complete, truncated or no type 2 GIPLs,[97] these structures may be unnecessary for amastigote survival inside macrophages.[96,97]

1.2.3. Syntheses of GPIs and GIPLs

Further research into GPIs and GIPLs must consider structure-activity relationships. This requires significant amounts of pure and structurally defined samples. However, the heterogeneity of glycan and lipid moieties in a single species/strain, and the amphiphilic nature of GPIs/GIPLs, renders the preparation of such samples from biological sources virtually impossible. Thus, chemical synthesis is required. There is no standard method for the synthesis of GPIs and GIPLs. Most structures have been synthesized through target-oriented approaches, limiting access to the compound libraries needed to assess the effect of structure variation on bioactivity. Generally, these approaches involve a linear or convergent synthesis of a *myo*-inositol oligosaccharide (**A**, **Scheme 1.1**), with a late-stage phosphorylation with the required phosphates and phosphonates.[98–100]

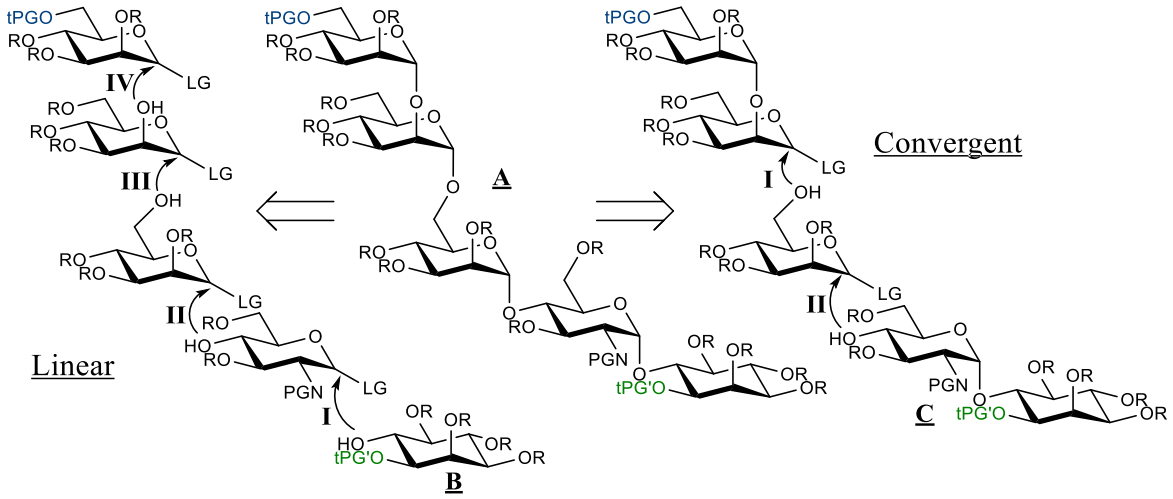

Scheme 1.1: Linear and convergent approaches to GPI and GIPL synthesis.

Linear synthesis is achieved through successive additions of monosaccharide residues, usually starting with the glycosylation of a *myo*-inositol glycosyl acceptor (**B**, **Scheme 1.1**).[99] Convergent approaches build the *myo*-inositol oligosaccharide **A** from multiple monomers or oligomer building blocks, reducing protecting group manipulation steps on the oligosaccharide.[99] Convergent strategies can also be designed to access various glycan cores.[101] A common method in convergent synthesis uses an oligosaccharide (comprising the mannose core and glycosyl modifications) and pseudodisaccharide **C** as the final building blocks.[102] This approach was used in the synthesis of glycoinositolphosphate fragments (GIPLs without the lipid moiety) from a *T. cruzi* series 2 GIPL [103] and *L. major* GIPL-3,[104] as well as a *L. major lyso*-GIPL-1.[105]

Several challenges are associated with GPI and GIPL synthesis. The *myo*-inositol precursor must be both selectively protected and enantiomerically pure.[98] The stereo and regioselective assembly of the oligosaccharide, with added complexity in branched structures, requires careful design of appropriately protected glycosyl building blocks. The removal of permanent protecting groups must be compatible with modifications and functionalities of the lipid. Particularly, acyl protecting groups are removed by basic methanolysis (NaMeO in methanol solutions), which can also remove ester lipids (present in alkylacylglycerol and alkylglycerol lipids); unsaturated lipids may be reduced through catalytic hydrogenation, used to remove benzyl (Bn) and benzylidene protecting groups.[106]

1.3. Oligosaccharide Synthesis

Oligosaccharide structures can contain multiple different monosaccharide residues, branching positions and anomeric configurations. Thus, glycan synthesis requires selectivity regarding the position and configuration of every new glycosidic bond (α- and β-). This selectivity is achieved through selectively protected building blocks, appropriate glycosylation reaction conditions and manipulation of protecting groups.

1.3.1. Glycosylation reaction

Glycosylations are coupling reactions between a carbohydrate bearing a leaving group (LG) in the anomeric positions (glycosyl donor) and a nucleophile (glycosyl acceptor), commonly a glycan with a free hydroxy group. Regioselectivity is generally achieved using fully protected glycosyl donors and a glycosyl acceptor with a single free hydroxy group. Chemoselective removal of

orthogonal (or "temporary") protection groups (tPG) from the glycosyl acceptor is usually required for linear chain elongation and branching.[107] Synthesis of protected building blocks requires regioselective protection strategies, contributing to the complexity of glycan synthesis.

Most glycosylation reactions have been described with an S_N1-like mechanism.[108] The reaction proceeds by activation and displacement of the leaving group in the anomeric position of the glycosyl donor, yielding carbocation **A**, which is stabilized by resonance with oxocarbenium **B**. Nucleophile attack can occur through either face of these structures, delivering a mixture of stereoisomers (*i.e.* anomeric mixture) (**Scheme 1.2**). It is currently understood that the counterion to oxocarbenium can also participate in the reaction mechanism, to a variable extent. Thus, glycosylation reactions are more accurately described in a continuum between S_N1 and S_N2 mechanisms, better explaining glycosylation kinetics and known reaction intermediates.[109]

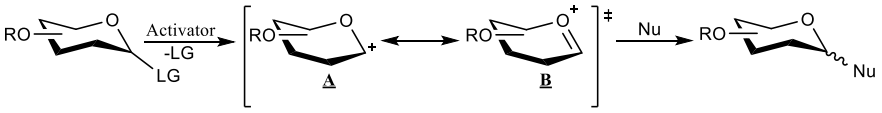

Scheme 1.2: Glycosylation through S_N1-like mechanism.

Glycosylation stereoselectivity is affected by the structure and protecting groups of the glycosyl donor and acceptor, the leaving group, the reaction promotor (and other additives), reagent concentration/stoichiometry, solvent, and reaction temperature.[107,110,111] 1,2-*trans* selectivity (such as β-Glc, β-Gal, or α-Man linkages) is usually enhanced through neighboring group participation, enabled by an acyl protecting group in position 2 of the glycosyl donor. This effect is commonly explained by the stabilization of the glycosyl donors' intermediate oxocarbenium **A** through equilibrium with a bicyclic dioxolenium **B**, formed between the carbonyl of the participating acyl group and the anomeric center.[112] This hinders the attack of the nucleophile from forming a 1,2-*cis* product (**Scheme 1.3**).

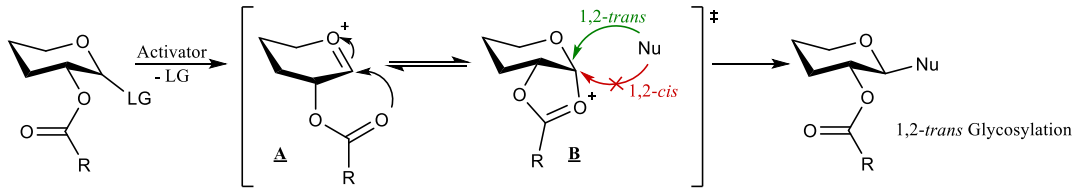

Scheme 1.3: Neighboring group participation.

Selective formation of 1,2-*cis* glycosidic bonds (such as α-Glc, α-Gal or β-Man linkages) is more demanding. Extensive optimization of solvents, reaction promotors and temperature is usually required to attain good 1,2-*cis* selectivity.[111] The protection pattern of the glycosyl donor can also direct stereoselectivity. In particular, acyl protecting groups in positions other than C-2 of the glycosyl donor can induce *trans* selectivity (relative to the remote group). This effect is known as remote group participation, and can be helpful when designing donors for 1,2-*cis* glycosylation.[113]

The mechanism of remote participation of esters is controversial.[114] A bicyclic dioxolenium intermediates may block nucleophile access to one face (**Scheme 1.4**),[113] as in neighboring group participation. These species are present in the gas phase and detected by MS/IR technics,[115–117] but have not been identified in solution.[118] Alternatively, protecting groups may indirectly affect selectivity through a combination of stereoelectronic effects.[114]

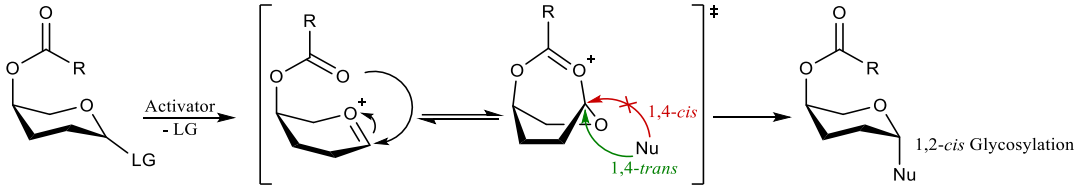

Scheme 1.4: Proposed mechanism for remote group participation of an axial O-4 acyl protecting group via a diaoxolenium intermediate.

Remote participation is less reliable than neighboring group participation,[113] and only directs stereoselectivity when a non-participating group protects O-2/N-2; otherwise, glycosylation is controlled by this group. The effect on 1,2-*cis* selectivity is also highly dependent on the participating group position.[113,117] This is evident in Gal building blocks, having O-3, O-4, and O-6 *trans* to an anomeric substituent with α configuration. Participation of O-3 [119] and O-6 [116] is relatively small, while acylated O-4 can produce significant increases in stereoselectivity.[116] In galactopyranose donors, stereoselectivity is also influenced by the nature of the acyl group, and O-4 benzoyl (Bz) gives better selectivity than acetyl (Ac).[119,120]

1.3.2. Automated Glycan Assembly

Conventional glycan synthesis is time-consuming and requires workup and purification procedures after each reaction step (glycosylation and protecting group manipulation). Many strategies have been developed to overcome these issues, either by using unprotected building blocks in regioselective chemical [121] and enzymatic [122] reactions, or by avoiding/streamlining workup between each reaction step in one-pot [123] and solid/tag supported approaches.[124]

Automation of glycan synthesis is a significant focus of current research in carbohydrate chemistry. It will eliminate time-consuming syntheses, give access to synthetic glycans to non-specialists, and improve reaction reproducibility by using easily replicable (standardized) reaction conditions, while also reducing human error. Presently, no single technology fulfils these goals, and current approaches still require highly specialized operators, personalized equipment, and individual optimization of reaction parameters.[124]

Automated Glycan Assembly (AGA), a solid-supported glycan synthesis approach developed by Seeberger's group over the last two decades (**Scheme 1.5**),[125] is one of the better-implemented approaches to automated glycan synthesis. The process starts with the glycosylation of a linker-modified Merrifield resin with the reducing end monosaccharide (**A**) of target glycan (**E**). Next, chain elongation is done linearly, through successive selective deprotection (**II**) of the resin-bound glycan (**D**), followed by glycosylation (**I**) of the resulting glycosyl acceptor (**B**) with an excess of glycosyl donor building block (**C**).[125] The reaction vessel is purged after each reaction step, removing excess reagents and side products. The growing glycan remains bound to the resin and is subsequently washed, thus eliminating time-consuming manual work up and purification steps.

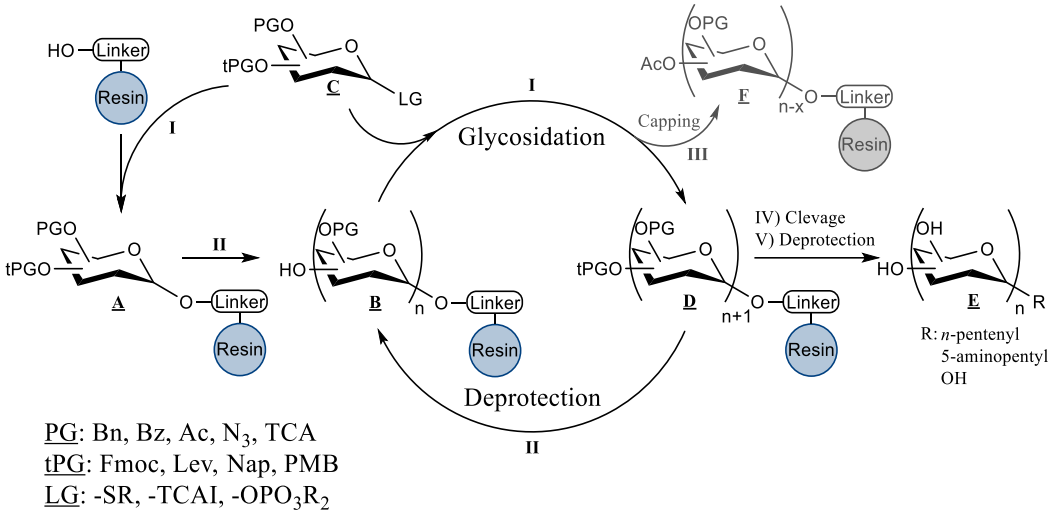

Scheme 1.5: Automated glycan assembly on solid phase.[125]

After each glycosylation step, the unreacted acceptor is capped by a fast and quantitative acid-catalyzed (Methanesulphonic acid, MsOH) acetylation with acetic anhydride (Ac_2O) (**III**). Ac group is often compatible with protecting groups used in AGA, and blocks deletion sequences from subsequent glycosylation (**F**).[126] Capping decreases building block use (less building block is wasted in glycosylation of deletion sequences), simplifies product purification (absence of large deletion sequences), and improves total yields.[126] Once glycan assembly is complete, the product is cleaved from the resin (**IV**), purified by preparative normal-phase high-performance liquid chromatography (NP-HPLC), fully deprotected (**V**), then purified by reverse-phase HPLC. Different linkers will require distinct reactions to cleave (metathesis, methanolysis or photocleavage), and yield other anomeric groups (*n*-pentenyl, 5-aminopentyl, OH).[127]

Regioselectivity is assured by using orthogonally protected building blocks. 1,2-*Trans* stereoselectivity is achieved using building blocks with a participating group in O-2. 1,2-*Cis* glycosylation can also be achieved with high selectivity through remote participation and reaction conditions optimization.[128,129] Due to inherent the limitations of AGA, and the need for standardized reaction conditions, AGA building blocks have a limited number of available leaving and protecting groups.

Thioglycosides, glycosyl phosphates, and imidates are used as AGA building blocks.[125] Phosphate and imidate leaving groups are activated through acid catalysis (trimethylsilyl triflate, TMSOTf). Triflic acid (TfOH) catalyzed iodination with N-Iodosuccinimide (NIS) is used for thioglycoside activation.[125] Thioglycosides are preferentially used as donors, as they are more stable under normal storage conditions and are less susceptible to hydrolysis at glycosylation temperatures (0 ^{o}C).[125]

Standard AGA building blocks include benzyl (Bn), Bz and Ac as permeant O-protecting groups.[125] Azides (N_3) and trichloroacetyl (TCA) are used to protect amines,[125] such as those found in GlcN. Acyl protecting groups are employed as participating groups, and Bn and N_3 are used as non-participating permanent protecting group. Permeant protecting groups are removed after the glycan is assembled and cleaved from the resin through Pd-catalyzed hydrogenolysis (Bn and N_3) and basic methanolysis (Ac, Bz and trichloroacetyl).

Fluorenylmethyloxycarbonyl (Fmoc), levulinoyl (Lev), 2-napthylmethyl (Nap) and *p*-methoxybenzyl (PMB) are used as temporary protecting groups.[125] Fmoc is preferred over other groups, as it is removed quantitatively with piperidine or triethylamine (Et_3N) in very short deprotection cycles (5 min),[129,130] minimizing synthesis time. Branched structure synthesis requires building blocks with two or more orthogonal protecting groups. Lev is usually used as a second protecting group and is removed with hydrazine.[125] Nap and PMB are alternative non-participating temporary groups, removed through selective oxidation with 2,3-dichloro-5,6-dicyano-1,4-benzoquinone (DDQ).[131,132]

1.4. Galactofuranose Chemistry

Research into Gal*f* derivative synthesis is motivated by the need for galactofuranose building blocks for Gal*f*-containing glycan and glycoconjugate synthesis, together with the potential use of galactofuranoses as biosynthesis substrates and inhibitors.[133] Syntheses of these compounds require Gal*f* precursors assembled through one-step or multistep synthetic strategies.

1.4.1. Synthesis of Gal*f* derivatives

As an aldohexose, galactose exists in solution in an equilibrium of its open, pyranose, and furanose forms. Galactopyranose is thermodynamically favored at room temperature and is therefore the most prevalent form.[134,135] Abundancy of galactofuranose increases at high temperatures, representing more than 50 % of the galactose content in refluxing dimethylformamide (DMF).[136] One-step syntheses of Gal*f* derivatives use selective protection or modification of the furanoses' anomeric position to block rearrangement into galactopyranosides. This is achieved by increasing the furanose to pyranose ratio in solution (usually through heating) and using reagents that react preferentially with Gal*f* (**Scheme 1.6**).

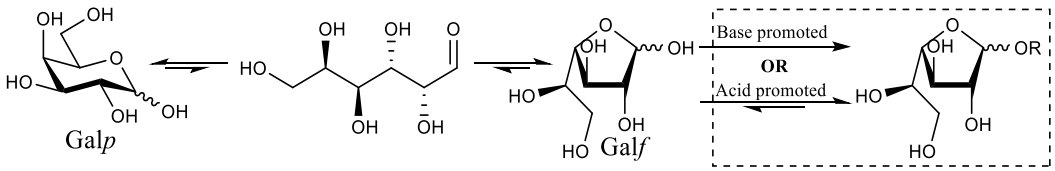

Scheme 1.6: Galactose tautomerization and regioselective protection of Gal*f*.

Gal*f* derivatives can be directly obtained from D-Gal through several approaches, including per-acylation, per-silylation, Fischer glycosylation, and mono-alkylation (**Scheme 1.7**). These approaches deliver either fully protected (**I-1**, **I-2,** and **I-3**) or deprotected (**I-4** and **I-5**) furanose precursors. Selective protection of these structures and their derivates, particularly of positions O-2 and O-3, is complex and limits access to orthogonally protected Gal*f* building blocks.[133]

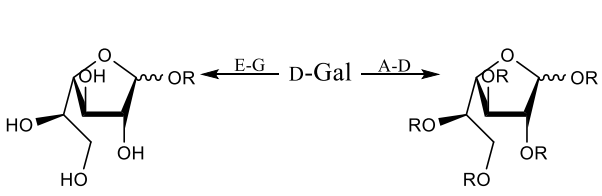

Reagents	R	Product
A) Pyridine (reflux), then Ac_2O	Ac	**I-1**
B) Pyridine (reflux), then BzCl	Bz	**I-2**
C) TBSCl, Imidazol, DMF	TBS	**I-3**
F) $FeCl_3$, MeOH (60 °C)	Me	**I-4**
E) BnBr (1 equiv.), NaH, DMPU	Bn	**I-5**

Scheme 1.7: Galactofuranose synthesis through direct acylation, alkylation and silylation of D-Gal.

Acylation of D-Gal is achieved in two steps. Galactose is first refluxed in pyridine, increasing the ratio of Gal*f* in solution, then acylated with Ac_2O or benzoyl chloride (BzCl).[137,138] Benzoylation is generally regioselective to furanose, while acetylation also delivers per-acetylated galactopyranose.[138] Per-acylated galactofuranoses **I-1** and **I-2** are versatile and widely used as precursors in Gal*f* building block synthesis. They can function as a glycosyl donor for β-glycosylation through activation with a Lewis acid ($SnCl_4$),[139] or be converted into various O-1 protected glycosides and thioglycosides, which are valuable precursors for orthogonally protected Gal*f* building blocks. All these conversions produce exclusively β anomers because of neighboring group participation.

Persilylation selectivity is dependent on the nature of the electrophile. Trimethylsilyl chloride (TMSCl) gives the pyranose form exclusively at room temperature, while the larger silane tributylsilyl chloride (TBSCl) forms only **I-3**.[140,141] **I-3** can be produced through a fast, high-temperature reaction, or at room temperature. The latter method is more selective to furanose and stereoselective to β anomers.[140,141] Product **I-3** can be converted into **I-1** through acid-catalyzed acylation (*p*-toluenesulfonic acid, PTSA).[141] Using an intermediate iodination step with trimethylsilyl iodide (TMSI), **I-3** can also be used as a β glycosyl donor or as a precursor for alkyl glycosides and thioglycosides.[140,142]

1-*O*-Alkylated Gal*f* derivatives can be obtained from D-Gal in one step, by acid-catalyzed Fischer glycosylation or through basic alkylation. The selectivity of Fischer glycosylation depends on reaction conditions and acid catalyst (**Scheme 1.8**). Conventional (batch), high-temperature glycosylation of 4-penten-l-ol with galactose, catalyzed by a Brønsted acid (camphorsulfonic acid, CSA),[143] delivers both penten-4-yl D-galactofuranose (**I-6*f***) and its pyranose isomer (**I-6*p***).[143,144] $FeCl_3$ catalyzed glycosylation yields almost exclusively 1-*O*-alkyl furanoses at room temperature, for reactions in tetrahydrofuran (THF) with 4-penten-l-ol, n-octanol, and n-decanol.[144–146] Glycosylation of methanol requires heating to reach complete conversion into **I-4**.[147] Reactions with $FeCl_3$ produce anomeric mixtures, with β anomers as the main product.[145–147] Addition of $CaCl_2$ improves regioselectivity to furanoses,[144] and increases β stereoselectivity for n-octanol and n-decanol.[145,146] Recently, **I-4** was obtained in a high yield using a flow reaction with a sulfonic acid functionalized silica column (HO-SAS) to enforce kinetic control.[148]

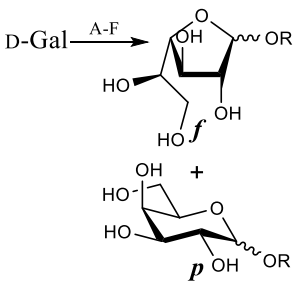

Reagents	R	Product	η (%, *f*/*p*)
A) 4-Penten-1-ol, CSA, DMSO (100 ºC).[143]	$C_3H_6CH{=}CH_2$	**I-6*f***, **I-6*p***	45 / 16 (10 % mix)
B) 4-Penten-1-ol, $FeCl_3$, $CaCl_2$, THF.[144]	$C_3H_6CH{=}CH_2$	**I-6*f***	54 / 0 (after acetylation)
C) n-Octanol, $FeCl_3$, $CaCl_2$, THF.[146]	C_8H_{17}	**I-7**	56 / 0
D) n-Decanol, $FeCl_3$, $CaCl_2$, THF.[146]	$C_{10}H_{21}$	**I-8**	55 / 0
E) MeOH, $FeCl_3$ (60 ºC).[147]	Me	**I-4**	75 / minor
F) MeOH, HO-SAS (60 ºC, flow).[148]	Me	**I-4**	86 / 0

Scheme 1.8: Synthesis of alkyl galactofuranosides by acid-catalyzed glycosylation.

Basic mono-alkylation of D-Gal with alkyl bromides (benzyl bromide, BnBr, or Acyl bromide) delivers Gal*f* derivatives and favors α anomers.[149–151] The reaction does not require heating, and is performed at 0 ºC to room temperature. *N,N*′-Dimethylpropyleneurea (DMPU) is used instead of conventional polar aprotic solvents. This reaction is not selective to furanoses for D-Glc and D-Man, delivering only pyranose products.[149] Per-benzylation of D-Gal in DMF with excess BnBr and NaH, and catalytic KI, at 0 ºC, also yields exclusively Benzyl 2,3,5,6-tetra-*O*-benzyl-α-D-galactofuranose.[152]

1,2:5,6-Di-*O*-isoprolylidene-α-D-galactofuranose (**I-9**) can also be obtained directly from D-Gal, through acid catalyzed condensation with excess of acetone or 2,2-dimethoxypropane (DMP). **I-9** is a valuable precursor, as it contains a single free hydroxy group, facilitating orthogonal protection. Condensation of free carbohydrates with an excess of acetone or DMP delivers products with the highest number of isopropylidene groups, thus favoring isomers with the highest number of vicinal *cis* hydroxy groups. The reaction yields furanose or pyranose derivatives exclusively when applied to some carbohydrates (glucose delivers 1,2:5,6-Di-*O*-isoprolylidene-α-D-glucofuranose, DAG, a very common precursor in carbohydrate chemistry). However, in galactose, both α-Gal*f* and α-Gal*p* can form two isopropylidene acetals, in positions 1-2 and 5-6 for α-Gal*f*, and positions 1-2 and 3-4 for α-Gal*p*. Thus, the reaction can deliver both **I-9** and pyranose isomer **I-10**. Proper kinetic and thermodynamic control can favor one of the structures (**Scheme 1.9**).

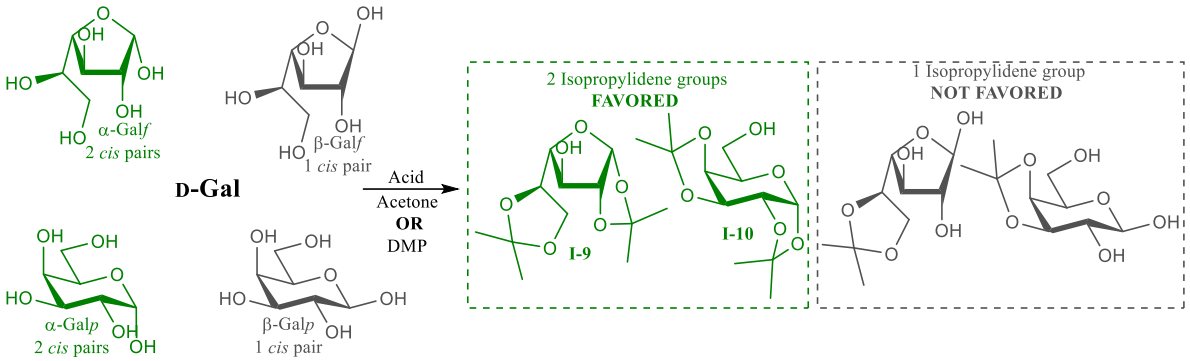

Scheme 1.9: Condensation of Galactose with acetone or DMP into **I-9** and **I-10**.

There are one-step and multistep strategies for **I-9** synthesis. One-step approaches optimize the regioselectivity of galactose condensation with acetone or DMP, by using different Lewis [136] or Brønsted acids,[153–155] under tuned reaction conditions. However, all reported conditions also deliver **I-10**, reducing the reaction yield of **I-9**. Alternatively, multistep strategies start with DAG and invert the configuration of C-4 through the formation of a double bond between C-3 and C-4, either via oxidation [156] or elimination,[157] and following selective reduction and substitution reactions (**Scheme 1.10-A**) or through an addition reaction (**Scheme 1.10-B**). Although more time-consuming than one-step synthesis, multistep strategies produce **I-9** exclusively and can give high yields.

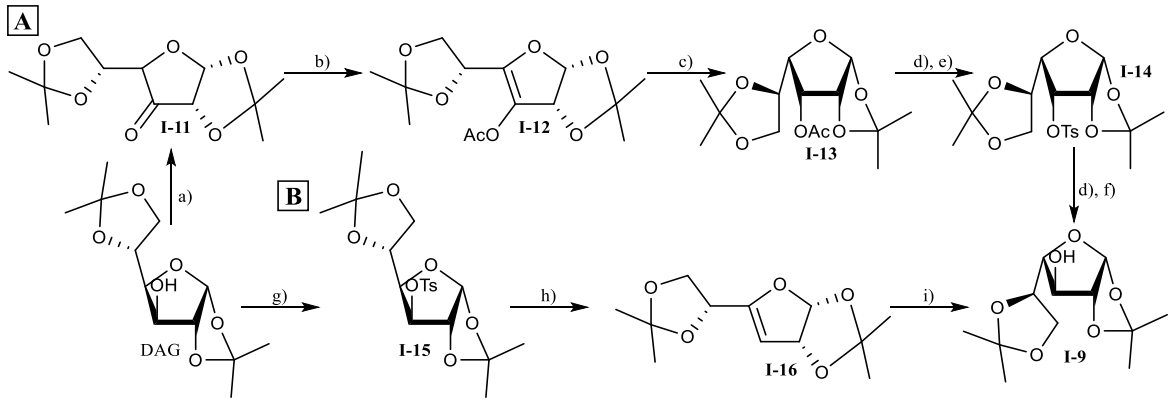

Scheme 1.10: Multistep synthesis of **I-9**, as described by Stick *et al.* (**A**) [156] and Sato *et al.* (**B**).[157] Reagents: a) RuO_2, $NaIO_4$; b) Ac_2O, pyridine; c) H_2, Pd/C; d) MeOH, basic resin; e) TsCl, pyridine; f) TBABzO, g) TsCl, h) DBU, DMSO; i)BH_3.THF; followed by NaOH, H_2O_2, THF.

D-Galactose diethyldithioacetal (**I-21**) is an alternative precursor for multistep synthesis of **I-1** and **I-4**. **I-21** is commonly obtained in acid media from D-Gal and ethanethiol (EtSH).[158] As described

for D-Glc, the reaction proceeds with the formation of open form hemi-thioacetal **I-18**, and subsequently dithioacetal **I-19**, kinetically favored over intramolecular condensation (**Scheme 1.11**). Cyclization of D-Glc and D-Man into thermodynamically favored pyranosides (**I-20**) will occur after several hours at room temperature,[158] but this is not reported for D-Gal.

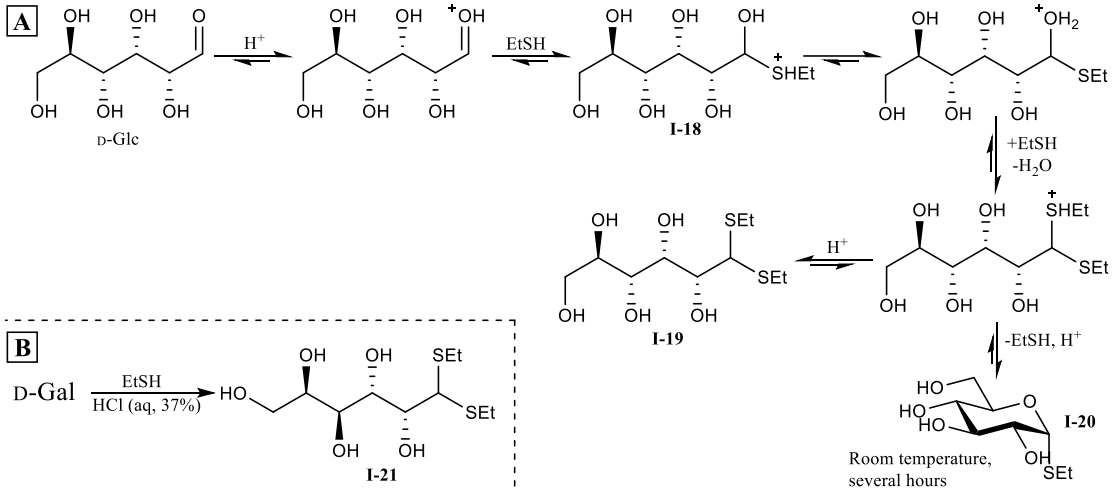

Scheme 1.11: Acid-catalyzed condensation of glycosides with EtSH. **A**- Reactions of D-Glucose with EtSH in acid media;[158] **B**- Synthesis of **I-21**.

I-21 is converted into **I-1** by acetylation with Ac_2O and a strong acid (H_2SO_4 or a combination of H_2SO_4 and acetic acid, AcOH), a process known as acetolysis (**Scheme 1.12**).[159] Conversion of **I-21** into **I-4** uses I_2 activation in alcohol solutions,[48] delivering intermediate thioglycoside **I-22**, which is further activated by I_2 and reacts with the solvent. Reaction yields vary significantly for different alcohols.[48] **I-21** can also cyclize into **I-22** with $HgCl_2$ in water, using either HgO [160] or HCl [161] as catalysts. However, the overreaction of **I-22** with $HgCl_2$ also gives free galactose as a side product.[160,161]

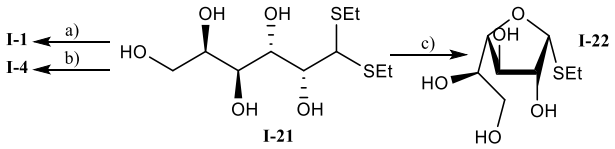

Scheme 1.12: Cyclization of dithioacetal **I-21**. Regents: a) Ac_2O, H_2SO_4, AcOH;[159] b) I_2, MeOH;[48] c) $HgCl_2$, HCl or HgO H_2O.[160,161]

D-Galactono-1,4-lactone (**I-23**) is used as an alternative to galactofuranosides precursors. It is prepared through the oxidation of galactose with Br_2 (in an aqueous solution of $NaHCO_3$).[162] The relative nucleophilicity of O-2 over O-3 increases in the lactone, facilitating the synthesis of orthogonally O-2 and O-3 protected glycosyl acceptors.[133] After protection or glycosylation of the lactone (**A**), it is reduced into an O-glycoside (**B**) and can then be converted into a glycosyl donor (**Scheme 1.13**).[133]

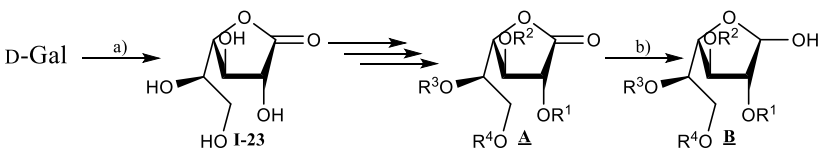

Scheme 1.13: General strategy for Gal*f* synthesis from **I-23**. Reagents: a) $NaHCO_3$, Br_2, H_2O;[162] b) dialkyl borane,THF.[133]

Another strategy for protected galactofuranoses is the isomerization of partially protected or glycosylated galactopyranoses, an approach known as Pyranoside-Into-Furanoside (PIF) rearrangement. Acid methanolysis of derivatives of galactopyranose **I-10** at reflux temperatures (70 ºC) provides α:β mixtures (β anomers are favored) of 1-methoxy furanosides, and has been used on 6-*O*-benzylated (**I-24**, **A**)[163] and glycosylated derivatives (**B**)[164] (**Scheme 1.14**). This approach uses widely available reagents but only delivers Gal*f* derivatives solely functionalized in O-6. PIF rearrangement of alkyl β-galactopyranoses with free O-2 and O-4 positions (**C**) using sulfur trioxide pyridine complex ($Py.SO_3$) can produce galactofuranoses selectively protected or glycosylated in O-3 and O-6.[165–168] The reaction is incompatible with thioglycosides since $Py.SO_3$ can oxidize the anomeric thioalkyl group.[167]

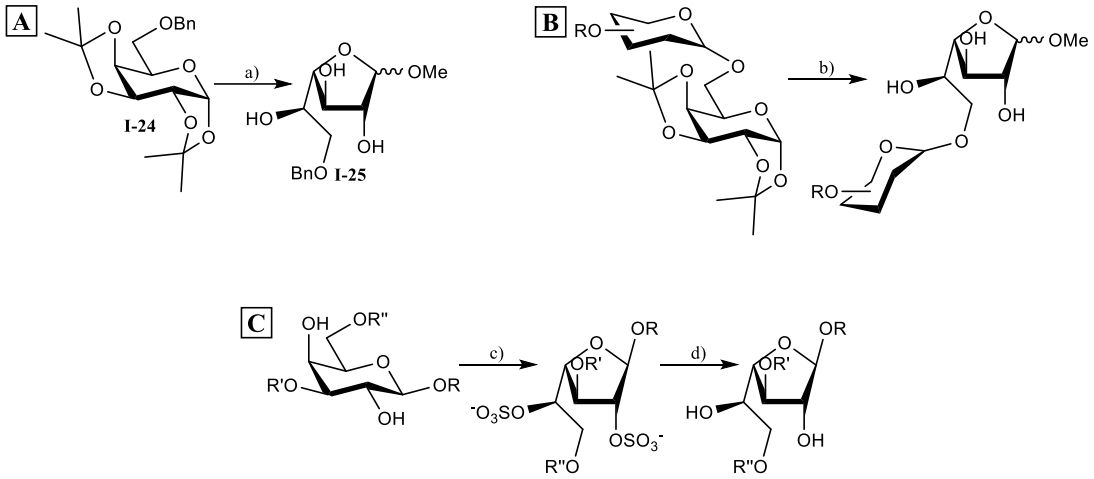

Scheme 1.14: PIF rearrangement. Reagents: a) PTSA, MeOH, reflux;[163] b) $HClO_4$, SiO_2, MeCN, 70 ºC;[164] c) $Py.SO_3$, HSO_3Cl, d) $NaHCO_3$, then H^+.[165]

1.4.2. Synthesis of Galactofuranose-containing glycans

Most natural glycans and glycoconjugates contain β-Gal*f* as either terminal (non-reducing) or internal, mono-glycosylated residues.[42] Assembly of these structures will require distinct building blocks, accessed from the previously discussed precursors.

Syntheses of glycans with terminal (non-reducing) β-Gal*f* require fully protected Gal*f* glycosyl donors with a participating group in O-2 and are easily accessed from per-acylated galactofuranoses. This stratagy is demonstrated in two syntheses of a terminal tetrasaccharide from a *T. cruzi* GIPL (**Scheme 1.15**). In the first example, selenoglycoside **I-26** (prepared in quantitative yield from **I-1** by $BF_3.Et_2O$ catalyzed glycosylation with benzeneselenol)[169] was used as a Gal*f* donor, selectively activated by NIS and TfOH (cat.).[169,170] The same oligosaccharide was later assembled from disaccharide **I-30** (and derivative **I-31**), prepared by glycosylation of **I-29** with **I-1,** though $SnCl_4$ activation.[103] **I-1** was also used in the synthesis of an *L. major lyso*-GIPL-1.[105]

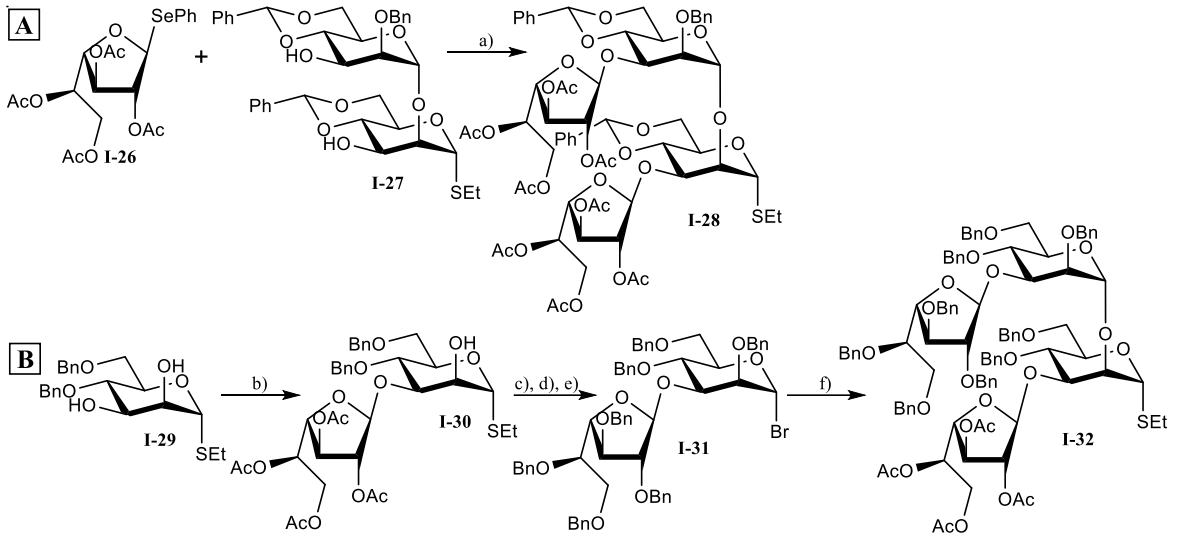

Scheme 1.15: Syntheses of tetrasaccharides from a *T. cruzi* GIPL, by Pinto *et al.* (**A**)[170] and Konradsson *et al.* (**B**).[103] Reagents: a) NIS, TfOH, DCM; b) $SnCl_4$, **I-1**, DCM; c) NaOMe, MeOH:$CHCl_3$ (1:2); d) BnBr, KI, Ag_2O, DMF; e) Br_2, DCM; f) AgOTf, DCM.

Synthesis of glycans containing an internal, O-2 glycosylated Gal*f*, such as epitopes of *T. cruzi* mucins, usually requires a building block with a free or orthogonally protected O-2 group. These are obtained from deprotected Gal*f* derivatives by blocking hydroxy groups O-5 and O-6 with an isopropylidene acetal, followed by regioselective installation of a temporary protecting group in position O-2 (**Scheme 1.16**), and further manipulation of protecting groups.[133,151] The synthesis of *T. cruzi* mucin epitopes is an example of this approach.[151] The O-2 group of precursor **I-33** was first masked with *tert*-butyldiphenylsilyl chloride (TBDPSCl), which offers better regioselectivity than acylation; this was followed by removal of isopropylidene, benzoylation, and the replacement of TBDPS for participating group Lev (to enhance stereoselectivity).[151] After assembly of disaccharide **I-39**, the O-2 Lev group was removed, and the resulting acceptor was glycosylated with Gal*f* donor **I-40**.[171]

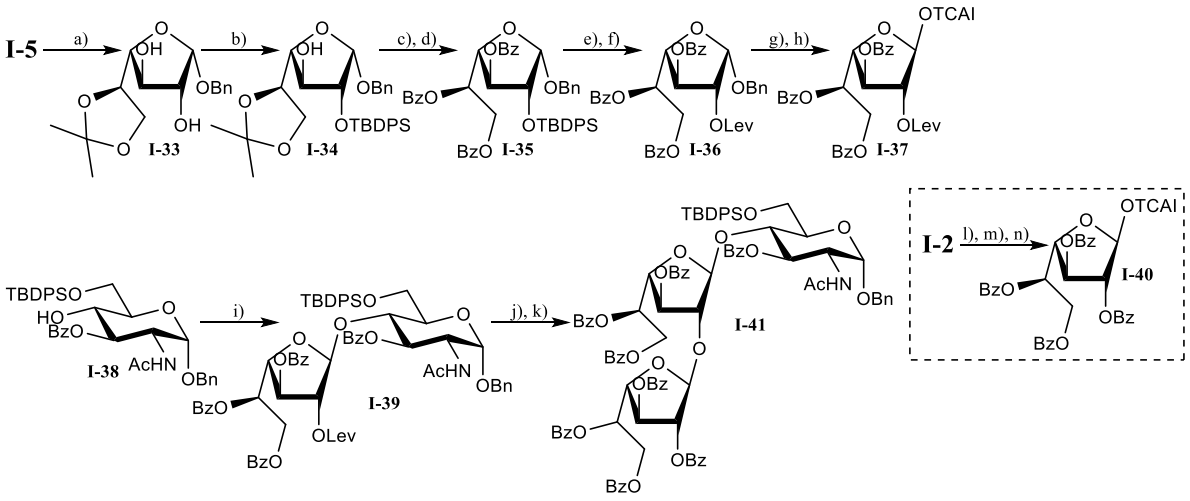

Scheme 1.16: Synthesis of a *T. cruzi* mucin epitope.[151,171] Reagents: a) DMP, PTSA, acetone; b)TBDPSCl, imidazole, DMF; c) AcOH, H_2O; d) BzCl, pyridine; e) TBAF, AcOH, DMF, THF; f) LevOH, DCC, DMAP, DCM; g) H_2, Pd/C, AcOEt; h) TCAICl, DBU, DCM; i) TMSOTf, DCM; j) hydrazine, pyridine, AcOH; k) **I-40**, TMSOTf, DCM; l) HBr, AcOH; m) Ag_2CO_3, acetone, H_2O; n) Cl_3CCN, DBU, DCM.

Gal*f* building blocks for 1-3Gal*f* glycosylation are accessed by the same strategy as O-2 Gal*f* acceptor,[133] or by using **I-9** as a precursor, avoiding regioselective protection of O-2.[104] Both approaches have been used in the synthesis of *L. major* GIPL glycan cores. Synthesis of the glycan core of *L. major* GIPL-3 used O-3 glycosyl acceptor **I-45** (**Scheme 1.17**), prepared from **I-9** in six steps.[104] **I-9** was obtained by Cu (II) catalyzed condensation of D-Gal with acetone, which gives poor yields.[136] Approaches with **I-9** require the selective hydrolysis of 5,6-isopropylidene with AcOH,[172] since simultaneous removal of both acetals would result in rearrangement into pyranose. Lactone **I-23** was used in the synthesis of the terminal trisaccharide of GIPL-2.[173] After installing isopropylidene,[174] **I-35** was regioselectivity protected with either trimethylacetyl chloride (PivCl, **I-49a**) or BzCl (**I-49b**), then glycosylated with **I-50**. While acylation with PivCl was significantly more effective, Piv containing disaccharide **I-52a** was unstable, unlike **I-52b**.[173]

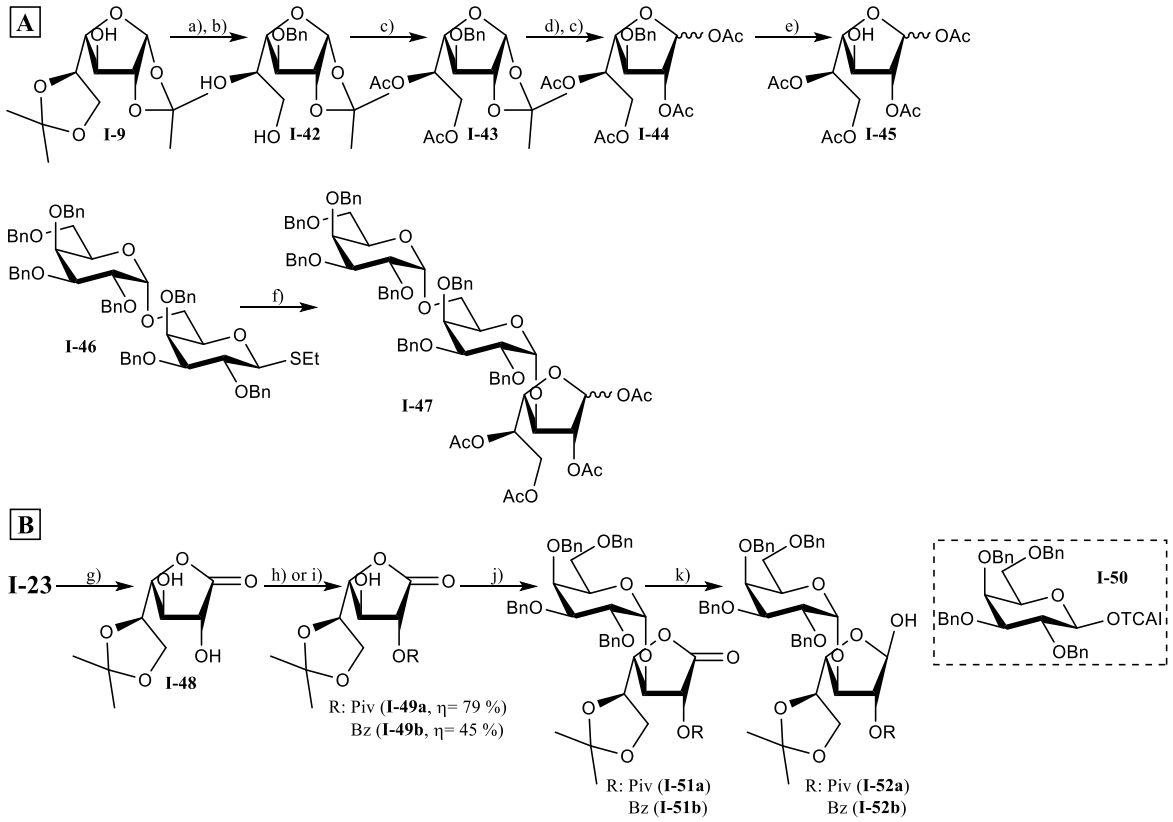

Scheme 1.17: Synthesis of *L. major* GPI glycan cores by Konradsson *et al.* (**A**)[104,172] and de Lederkremer *et al.* (**B**).[173] Reagents: a) BnBr, NaH, THF; b) AcOH, H_2O; c) Ac_2O, pyridine; d) Trifluoroacetic acid, $CHCl_3$; e) H_2, Pd/C; f) TMSOTf, DCM; g) PTSA, DMP, acetone;[174] h) PivCl, pyridine; i) BzCl, pyridine; j) **I-50**, TMSOTf, Et_2O; k) bis(2-butyl-3-methyl)borane, THF.

Gal*f* glycosyl acceptors for O-6 glycosylation are conventionally obtained by regioselective protection of the O-6 position, followed by protection of the remaining hydroxy groups, and a final deprotection of O-6.[133] Acyl protecting groups can migrate from O-5 to O-6, which is used to synthesize O-5 glycosyl acceptors.[133,175] This allowed the synthesis of oligosaccharide substrates for *Mycobacterium tuberculosis* galactofuranosyltransferases (**Scheme 1.18**).[48] Thioglycoside precursor **I-53** was regioselectively tritylated, then benzoylated; removal of trityl yielded O-6 glycosyl acceptor **I-55**, as well as O-5 acceptor **I-56**, by migration of Bz from O-5 to O-6.[48]

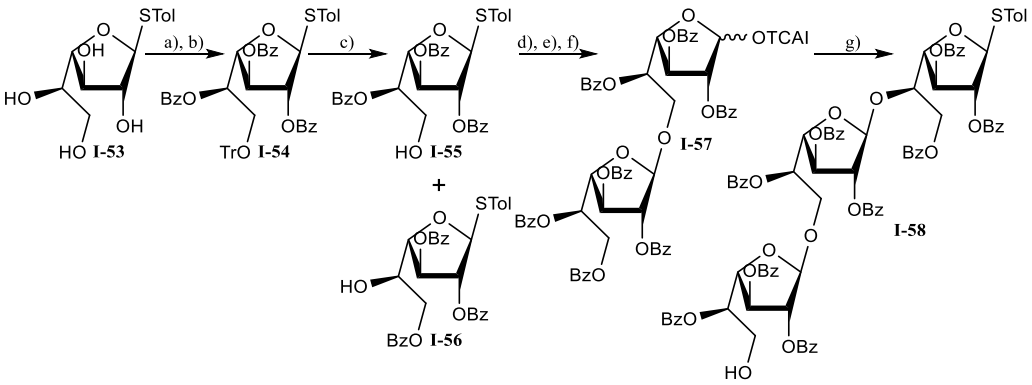

Scheme 1.18: Partial synthesis of a *Mycobacterium tuberculosis* galactofuranosyltransferases substrate.[48] Reagents: a) TrCl, pyridine; b) BzCl, pyridine; c) TFA, H_2O, DCM; d) **I-40**, TMSOTf, DCM; e) H_2O, N-Bromosuccinimide, AgOTf, AcOEt; f) Cl_3CCN, DBU, DCM; g) **I-56**, TMSOTf, DCM.

Alternatively, O-5 glycosyl acceptors can be assembled from deprotected Gal*f* derivatives by sequential blocking of O-5 and O-6 with isopropylidene, protection of O-3 and O-2, removal of isopropylidene and regioselective protection of O-6.[133] This approach was used in the synthesis of a tetrasaccharide epitope from an *Aspergillus fumigatus* galactomannan (**Scheme 1.19**).[137]

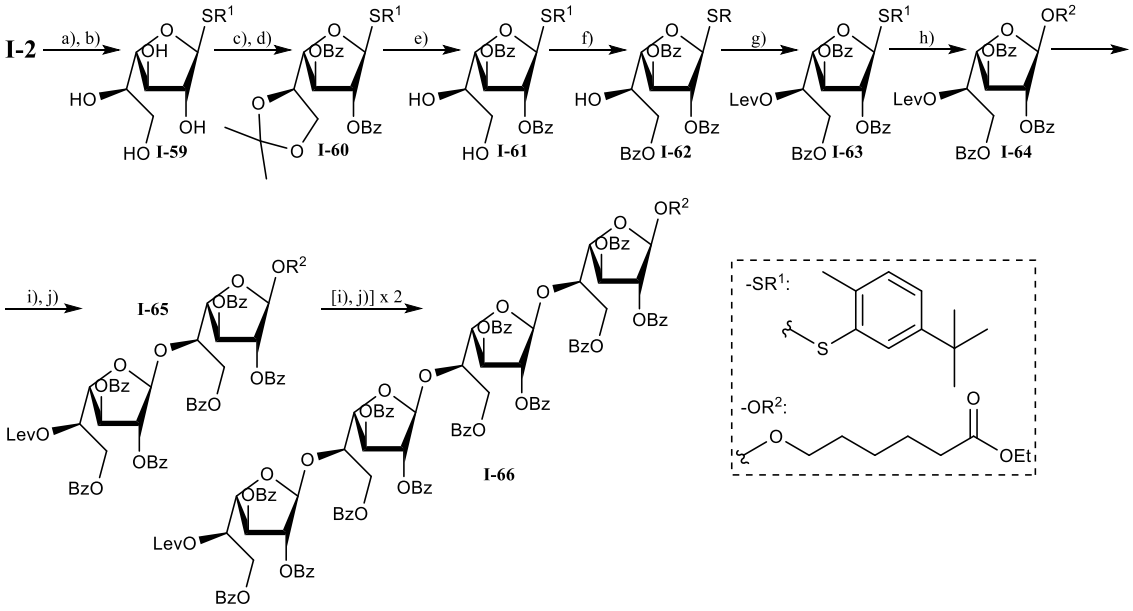

Scheme 1.19: Synthesis of a *Aspergillus fumigatus* tetrasaccharide.[137] Reagents: a) 2-methyl-5-*tert*-butyl-thiophenol, $BF_3.Et_2O$, DCM; b) NaOMe, MeOH; c) DMP, CSA, acetone; d) BzCl, DMAP, Et_3N, DCM; e) AcOH, H_2O; f) BzCl, DMAP, Et_3N, DCM (-20 ºC); g) LevOH, DCC, DMAP, DCM; h) ethyl 6-hydroxy hexanoate, NIS, DCM; i) hydrazine, pyridine, AcOH; j) **I-63**, N-Bromosuccinimide, TfOH, DCM.

2. Objectives

The function and immunogenicity of Gal*f* containing GIPLs of *T. cruzi* and *L. major* remains largely undetermined. Nevertheless, recent examples demonstrate synthetic GIPL derived structures may be useful in disease prevention and diagnosis.[176,177] Synthesis of GIPLs and their glycan moieties is a necessity not only to further establish the function of these structures, but also to develop novel therapeutic and diagnostic technics.

This dissertation covers the synthesis of building blocks needed for assembly of GIPL glycan moieties containing Gal*f*. With this aim, two model structures, the glycan moieties of GIPL-3 (from *L. major*) and a series 2 *T. cruzi* GIPL, were analyzed by retrosynthesis (**Scheme 2.1**). To access synthons **A** to **J**, four thioglycoside building blocks were designed, which can be used to assemble several Gal*f* containing GIPL glycan moieties, through either AGA or conventional synthesis.

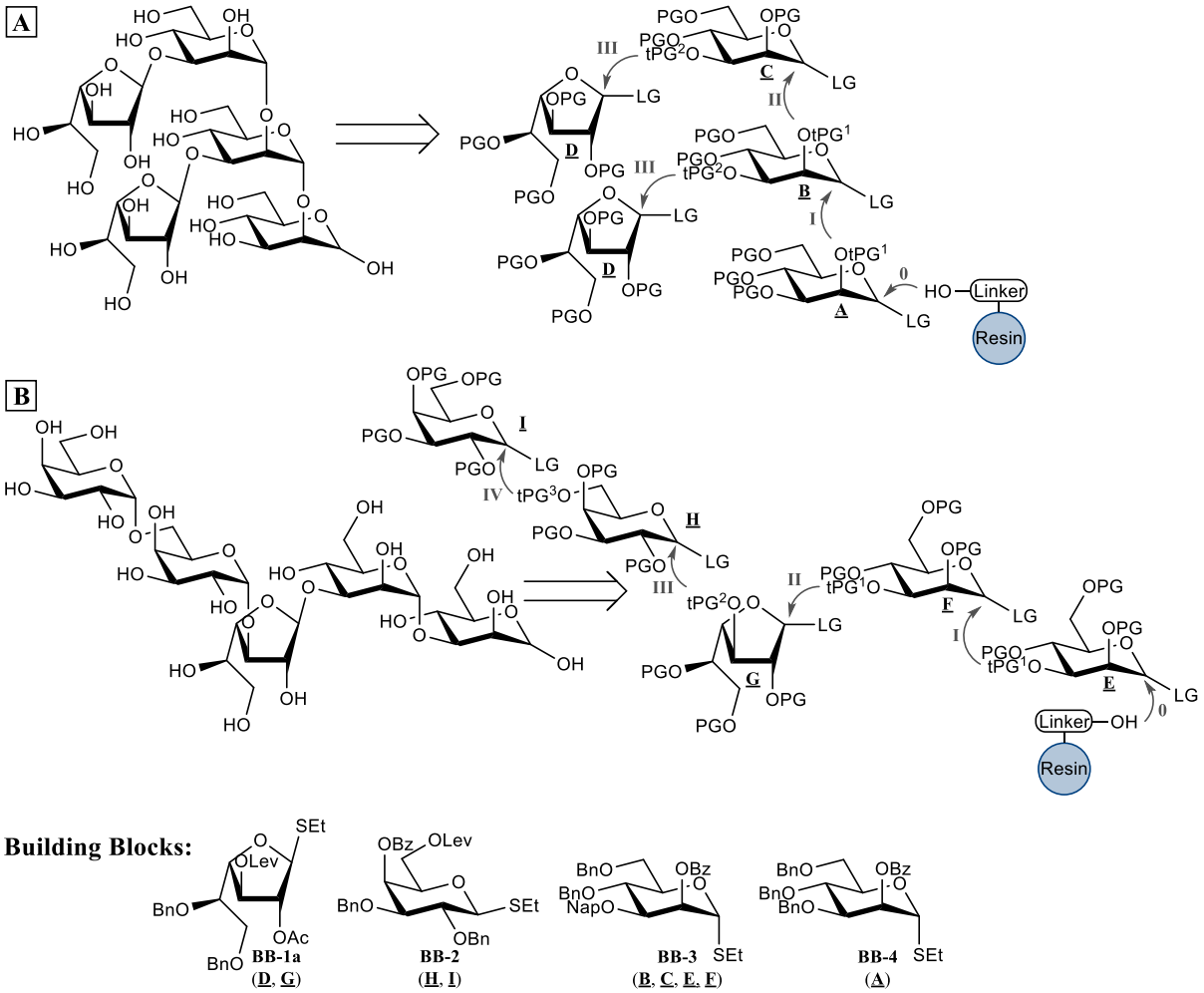

Scheme 2.1: Retrosynthesis of glycan fragments of *T. cruzi* (A) and *L. major* (B) GIPLs. All reaction steps (**0**-**IV**) represent a sequence of removal of the temporary protecting group and glycosylation.

BB-1a includes a participating group in O-2 and a temporary protecting group in O-3, and can function as synthons **D** and **G**. **D** could more effectively be accessed from **I-2** in a single step ($BF_3.Et_2O$ catalyzed glycosylation), thus avoiding the unnecessary reaction steps, but this building block was not prepared. While the synthesis of selectively protected pyranose building blocks is well implemented, preparation of orthogonally protected galactofuranoses is still challenging. Thus,

developing a reproducible, scalable, and short protocol for these building blocks was also an aim of this work.

BB-2 can be used in the synthesis of *L. major* glycans (synthons **H** and **I**); it contains a temporary protecting group in O-6 (Lev), a remote participating group in O-4 (to facilitate α stereoselectivity) and a non-participating group in O-2. **BB-3** contains a temporary protecting group in O-3 (Nap) and an acyl participating group (Bz) in O-2. This building block can be used for synthesis of the glycan moiety of *L. major* GIPL (synthons **E** and **F**) through AGA, conventional synthesis of *T. cruzi* GIPLs (with Bz functioning as an orthogonal protecting group), or as a precursor for AGA building blocks for *T. cruzi* GIPL glycan moieties (after replacing Bz for Fmoc). These later applications are also possible with **BB-4**.

3. Results and Discussion

3.1. Galactofuranose building block

A main objective of this work was to establish a strategy for synthesizing a Gal*f* building block containing a O-3 orthogonal protecting group and a O-2 participating group, to favor β-glycosylation. As will be discussed in this chapter, this was a challenging process. Previously reported methodologies proved unsatisfactory to get the desired compound. Major difficulties during the protection steps led to low overall yield and significant changes to the synthesis strategy and protection pattern of the Gal*f* building block.

3.1.1. First Strategy: Isopropylidene Acetal Protection

Synthesis of **BB-1a** was conceived using a similar strategy to the one reported by Konradsson *et al.* (**Scheme 3.1**).[104] Starting from di-isopropylidene protected galactofuranose **I-9**, the free hydroxy group in position 3 is protected with Lev through Steglish esterification [178] to get **A**. The more labile 5,6-isopropylidene group is selectively hydrolyzed with a weak acid (e.g. AcOH) to get **B**,[172] and the two free hydroxy groups benzylated, giving **C**. Hydrolysis of 1,2-isopropylidene with a stronger acid delivers **D**, and following acetylation would yield galactose **E**, with a participating group in position 2. Finally, the anomeric position is converted into the desired thioglycoside by treatment of **E** with EtSH, and $BF_3.Et_2O$ catalysis (**F**). To reduce the number of reaction steps, **I-9** synthesis from D-Gal was envisaged using a one-step strategy.

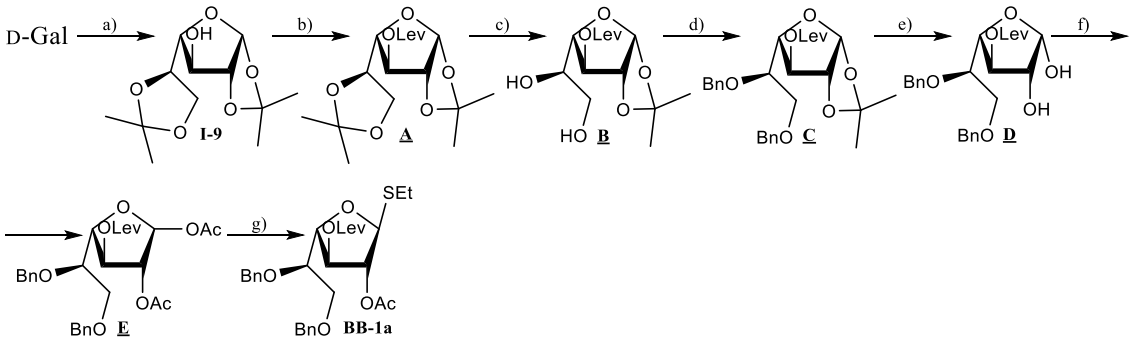

Scheme 3.1: Initial strategy for Gal*f* building block. Reagents: a) acetone or DMP, H^+; b) LevOH, DIC, DMAP; c) AcOH, H_2O; d) BnBr, NaH; e) H^+, H_2O; f) Ac_2O, pyridine; g) EtSH, $BF_3.Et_2O$.

The first attempt to synthesize **I-9** from D-Gal involved the treatment of D-Gal with sulfuric acid in a 2:1 mixture of DMF and acetone, 4 Å molecular sieves and reflux. A low conversion of the starting material was observed after 39 hours; the major product was isolated in only 10 % yield, and corresponded to the galactopyranose isomer **I-10**, according to ^{1}H-NMR (Appendix A.1, confirmed by comparison of with the literature).[153] A residual product with a lower R_f on TLC was assumed to be the galactofuranose **I-9**, although this could not be confirmed by NMR. The low formation of **I-9** was attributed to the acidity of H_2SO_4, which is a stronger acid than the acid resins that are reported in the literature to deliver **I-9** in 50 % yield.[154,155] As such, the regioselectivity of the acetal formation results from the interplay between reaction conditions, the relative abundance of different galactose forms, and the acid catalyst. This interplay is clear in other examples in the literature, such as HY zeolite catalysis, which produce **I-9** in 40 % yield,[153] under reaction conditions which yield almost exclusively **I-10** with $CuSO_4/H_2SO_4$ catalysis.[179]

The second attempt to obtain **I-9** was based on a reported method using acid resins.[154,155] H_2SO_4 was replaced by Amberlite IR 120 H^+ form resin, which was used directly from the package and after washing it with acetone and drying to remove water from the resin. However, no reaction was observed with either resin preparation. Considering that both Dowex 50 H^+ resin (used in the original report) and Amberlite IR 120 H^+ contain sulfonic acid, catalytic amounts (0.2 equiv.) of CSA were evaluated in the same 2:1 DMF/acetone reaction mixture. This method also failed to produce **I-9**.

DMP also tested as a source of isopropylidene. Using a 2:1 mixture of DMF/DMP and CSA as a catalyst, the reaction delivered a mixture of products containing both **I-9**, **I-10** and other unidentified side products. The main component of the product mixture was identified by ^{1}H-NMR (Appendix A.2) as **I-9**, through signals at 5.81 ppm (d, 1H, H-1), 4.48 ppm (dd, 1H, H-2), and singlets from isopropylidene groups at 1.48 ppm, 1.38 ppm, 1.31 ppm, and 1.28 ppm, which are consistent with the literature.[153] However, the product could not be purified, and was obtained in a yield lower than 20%. Further optimization of the reaction by increasing reagent concentration or using exclusively DMP as solvent (at room temperature) did not improve reaction outcome. Complete conversion of starting material was never observed, and **I-9** could not be purified from product mixtures. Based on these results, **I-9** was abandoned for preparation of **BB-1a**.

3.1.2. Second Strategy: Regioselective Benzylation of Galactose

An alternative strategy was envisioned using **I-5** as the Gal*f* percursor, prepared from D-Gal in one step.[151] The approach required the installation of a 5,6-isopropylidene acetal and a regioselective acylation step of product **I-33**. Previous reports showed that O-2 is more reactive than O-3 position in Gal*f* derivatives, and it can be selectively acylated with PivCl in high yields.[173,180] To complete the synthesis, the process envisioned the installation of Lev in O-3 (**A**), followed by hydrolysis of 5,6-isopropylidene (**B**), benzylation of the free hydroxy groups (**C**) and the conversion into thioglycoside **BB-1b** by treatment of **C** with EtSH, and $BF_3.Et_2O$ catalysis (**Scheme 3.2**).

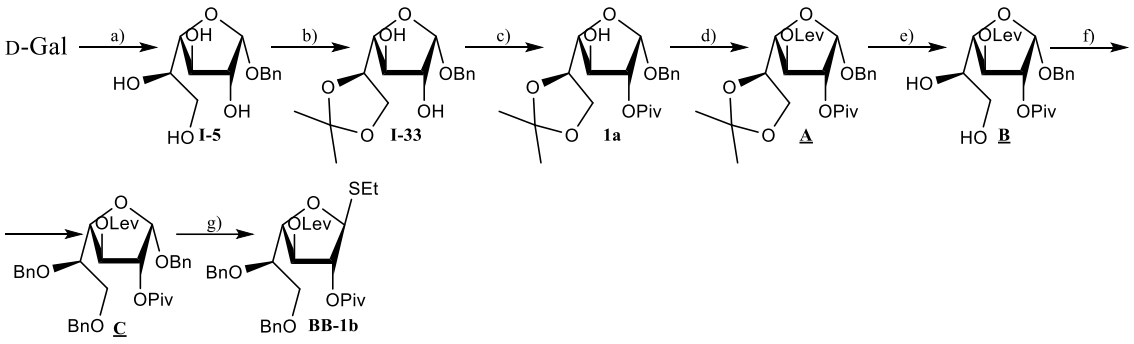

Scheme 3.2: Alternative strategy for synthesis of Gal*f* building block. Reagents: a) NaH (1.5 equiv.), BnBr (1.2 equiv.), DMPU, 49 %; b) DMP (3.6 equiv.), PTSA (0.02 equiv.), Acetone, 67 %; c) PivCl, Et_3N, DMAP, THF, 35 %; d) AcOH (60 %, aqueous); e) LevOH, DIC, DMAP; f) BnBr, NaH; g) EtSH, $BF_3.Et_2O$.

The synthesis of benzyl α-D-galactofuranoside (**I-5**) was studied using small excesses of BnBr and NaH in the polar aprotic solvent DMPU. DMPU has a high boiling point (246 ºC at 1 atm) and is difficult to remove by evaporation. Thus, the solvent was mostly removed by multiple extractions of the reaction mixture with hexane, following the reported protocol.[151] The process delivered a thick oil containing the reaction products and residual DMPU, which was still present after overnight stirring in high vacuum. This oil was dissolved in water and the product extracted with AcOEt, until **I-5** could not be detected in the aqueous phase by TLC. This process was unpractical and tedious, requiring over 20 extractions with AcOEt.

When the reaction was scaled up to 2 g of D-Gal, DMPU was extracted with hexane and the product directly purified by chromatography using a DCM/MeOH (15:1) eluent mixture, thus skipping the water extraction step. This afford **I-5** as a white solid in 49 % yield, which was lower than the reported yield of 67 %.[151] ^{1}H-NMR signals (Appendix A.3) and the meting point of the product were in agreement with the literature.[151] Efforts to replace DMPU with THF, MeCN or DMF resulted in either no reaction (THF and MeCN) or formation of multiple side products, with low conversion of starting material (DMF) after 15 hours and 26 hours, respectively. This outcome was attributed to the low solubility of D-galactose in the evaluated solvents.

To avoid the chromatography purification step, the crude **I-5** obtained by extraction with AcOEt was reacted to deliver the 5,6-*O*-isopropylidene protected product **I-33**, following a protocol by the same authors. The tetrol **I-5** was subjected to condensation with excess DMP in acetone under PTSA catalysis. Contrary to the report by Gallo-Rodriguez *et al.*, the reaction delivered multiple products. Purification of product **I-33** was not possible, as it coeluted with DMPU from the first reaction, which was present in the crude **I-5** mixture. This contamination was identified in the ^{1}H-NMR spectrum of the mixture (Appendix A.4), by signals at 3.14 ppm (t, 4H), 2.81 (s, 6H) and 1.86 (p, 2H), in a ratio of 1:1 with **I-33**. The yield for this approach was 32 %, over two steps. To avoid DMPU contamination, the synthesis of **I-33** was scaled up with pure **I-5**; TLC analysis of the reaction mixture also showed multiple side products, which hindered product purification; this process delivered **I-33** in 67 % yield, which is significantly lower than the reported yield of 94 %.[151]

The following regioselective protection of **I-33** was tested using a direct acylation with excess PivCl and Et_3N (**Scheme 3.3**). TLC analysis (Hex/AcOEt, 2:1) of this reaction showed the formation of three major products, which were assigned to the regioisomers **1a** and **1b**, having identical R_f values (0.35 and 0.38) and the di-acylated product **1c**, with a higher R_f of 0.9. Separation of the polar products by chromatography gave two fractions. The first fraction contained the desired product **1a**, identified by a correlation in HMBC of the Piv carbonyl group (179.33 ppm) and H-2 (4.82-4.76 ppm, overlapped with C*H*$_2$Ph) (Appendix A.5), corresponding to the Piv group at O-2. The second fraction contained a mixture of product **1a** and presumably **1b**, although this was not confirmed by HMBC. As a result of the poor regioselectivity, product **1a** was isolated in only 35% yield.

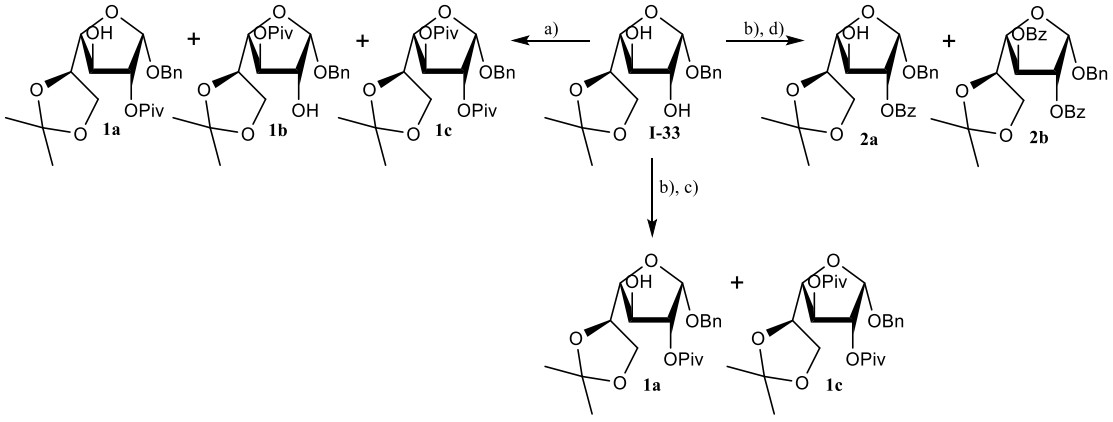

Scheme 3.3: Regioselective acylation of **I-33**. Reagents: a) PivCl (1.5 equiv.), Et_3N (3 equiv.), DMAP (cat.), THF, 35 %; b) $(Bu_3Sn)_2O$ (1.3 equiv.), Toluene, 4 Å molecular sieves, reflux; c) PivCl (1.5 equiv.), Et_3N (3 equiv.), DMAP (cat.), THF, 0 ºC, 53 %; d) BzCl (2 equiv.), Et_3N (3 equiv.), DMAP (cat.), THF, 0 ºC, 57%.

To increase the regioselectivity of acylation of **I-33**, the reaction was tested using stannyl ethers. In this method, bis(tributyltin) oxide ($(Bu_3Sn)_2O$) was condensed with the diol, to increase the nucleophilicity of the hydroxy groups. In pyranoses, stannyl ethers favor the reaction of electrophiles

with primary and equatorial hydroxy groups with vicinal *cis* oxygen atoms.[181] This is clearly shown in the benzoylation of 1-methyl-α-D-glycosides, that gives O-2 and O-6 benzoylated products for α-glucopyranose and O-3 and O-6 benzoylation for α-mannopyranoside and β-galactopyranoside.[181] The mechanism behind this selectivity is not clearly understood. However, it does not appear to be result of a selective stannyl ether formation with a specific hydroxy group of the carbohydrate, because stannyl ethers can migrate freely between hydroxy groups.[182] Thus, it is assumed that an intermediate penta-coordinated Sn (I) complex, having the vicinal *cis* oxygen atoms as a bident ligand, may explain the selectivity,[181,182] although this remains unconfirmed.

The O-2 position of α-galactofuranoses (like in **I-33**) fulfils the requirements observed for selectivity acylation with stannyl ethers in pyranoses; it is *cis* to O-1 and more reactive than O-3 under standard conditions (**Scheme 3.4**). Therefore, stannyl ethers were tested for preparation of Gal*f* derivatives. The reaction was performed in a one-pot approach. First, the stannyl ether was formed by refluxing $(Bu_3Sn)_2O$ and **I-33** in toluene, with a combination of 4 Å molecular sieves and Dean-Stark trap to remove the water formed during the condensation. The solvent was removed, the product was dissolved in THF, and subjected to a basic acylation with PivCl. TLC analysis of the reaction after 1 h showed formation of **1a** as the main reaction product and small amounts of **1c** and **I-33**. The side product **1b** was not detected. The yield of **1a** increased to 53 % under these conditions, showing a better regioselectivity of the process with the stannyl ether mediated acylation.

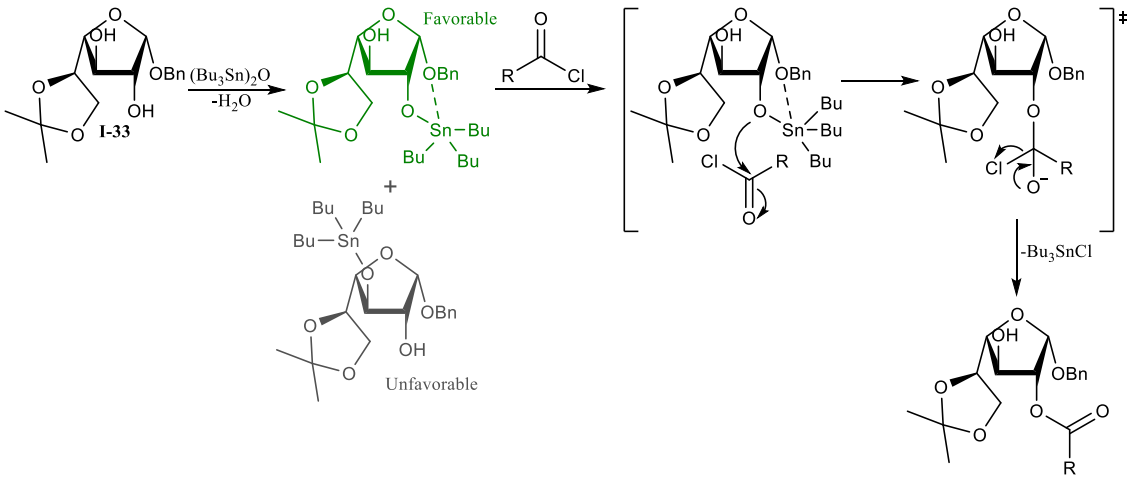

Scheme 3.4: Proposed mechanism for O-2 regioselective acylation through stannyl ether activation.

The stannyl ether mediated acylation of **I-33** with BzCl was evaluated, since a benzoyl is easier to remove after glycan assembly then a Piv group. The reaction was first tested using the same conditions used with PivCl, with an excess of electrophile (1.5 equiv). TLC analysis (Hex/AcOEt, 2:1) of the reaction showed two major products having R_f values of 0.36 and 0.7 on TLC, which were attributed to products **2a** and **2b**, respectively (**Scheme 3.3**). Product **2a** was obtained in 32 % yield after purification and confirmed by NMR analysis, showing a correlation in HMBC of the Bz carbonyl group (167.28 ppm) with H-2 (5.11 ppm) (Appendix A.6). The reaction was repeated with 1 equiv. of BzCl to avoid perbenzoylation, which resulted in significantly slower conversion of **I-33**. Successive additions of BzCl to a total of 2 equiv. over 19 h delivered **2a** in 57 % yield, with reduced formation of **2b** but without complete conversion of **I-33**. It was not assessed if Et_3N is necessary for second step and 0.5 equiv. of $(Bu_3Sn)_2O$ would avoid multiple acylations, as previously reported.[183]

Despite the relatively successful regioselective protection of **I-33**, this strategy was still inadequate for preparing significant amounts of the target building block. All reaction steps delivered

low to moderate yields and were difficult to scale up, particularly the initial benzylation. Thus, another strategy was explored for preparing the desired Gal*f* unit.

3.1.3. Third Strategy: Galactose Dithioacetal Route

A strategy using a thiogalactofuranoside **I-22** as an initial precursor was considered to circumvent the difficult regioselective benzylation of D-Gal (**Scheme 3.5**). There are no reported reactions that deliver this product from D-Gal in a single step. However, Fe (III) catalyzed condensation of D-Gal with alcohols, such as MeOH,[147] n-octanol, and n-decanol,[145] are reported to deliver 1-*O*-alkyl-galactofuranosydes. Thus, it was hypothesized that a reaction of galactose and ethanethiol under Fe (III) catalysis would deliver the desired thiogalactofuranoside **I-22**.

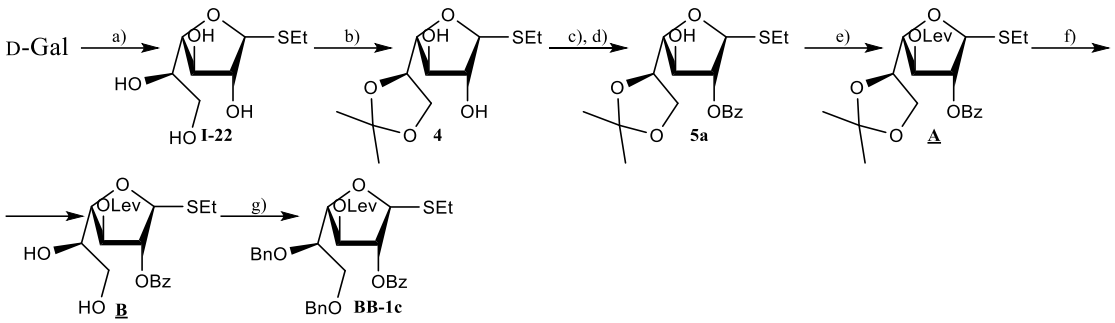

Scheme 3.5: Third stratagy for synthesis of Gal*f* buidling block. Reagents: a) $FeCl_3$, EtSH; b) DMP, PSA, acetone; c) $(Bu_3Sn)_2O$, Toluene, 4 Å molecular sieves, reflux; d) PivCl, Et_3N, DMAP (cat.), THF, 0 ºC; e) LevOH, DIC, DMAP; f) AcOH, H_2O; g) BnBr, NaH.

To test this hypothesis, D-Gal and $FeCl_3$ were dissolved in ethanethiol and stirred for 4 days to deliver a single product, which was characterized by H^1-NMR (Appendix A.8). The spectra of the product were inconsistent with the intended product, as it contained a multiplet at 2.76-2.59 ppm (4H) and two overlapped triplets at 1.21 ppm (6H), coupling in H-H COSY, corresponding to two CH_2 and CH_3 signals from two thioethoxy moieties. The integration of all other signals showed the presence of a single product and not a mixture of anomers. These signals indicated the formation of dithioacetal **I-21**, wish was isolated in a 48.9 % yield. The excess of acid catalyst and EtSH are conditions commonly employed for dithioacetal synthesis. The process generally involves reacting a carbohydrate with EtSH in an aqueous solution of a strong Brønstead acid (usually 37 % HCl), at 0 ºC.[158]

Dithioacetal **I-21** is a common precursor in Gal*f* synthesis (Chapter 1.4.1), and a useful intermediate in the synthesis of building block **BB-1b**. However, the reaction in EtSH was both slow and inefficient, and showed to be impractical due to difficulties in removing Fe (III) during work up. Therefore, 37 % HCl and EtSH were used for upscaling the reaction. The reaction was much faster under these conditions (less than 20 minutes), with **I-21** precipitating five minutes after addition of EtSH, turning the reaction mixture into a wet, compact mass, which was neutralized, concentrated, and crystalized from EtOH. This procedure gave pure **I-21** in high yield (82 %, from 12 g of D-Gal), as a white solid, with characterization consistent with the literature.[158] Efforts to optimize the work up protocol, using filtration and washing,[158] reduced the yield of **I-21** to 47 %.

A direct cyclization of **I-21** with N-iodosuccinimide (NIS) to obtain **I-22** produced multiple products that could not be identified. To limit **I-21** cyclisation to Gal*f* thioglycosides, hydroxy groups in positions 5 and 6 were protected with an isopropylidene group. Intermediate **I-21** has multiple vicinal hydroxy groups that can form isopropylidene acetals, since it lacks the conformational

limitations enforced by a ring geometry. By using near-stoichiometric quantities of DMP, the 4,5, 5,6 and 4,6 acetals are all formed (**Scheme 3.6**), with the envisioned 5,6-isopropylidene **3** being the favored product through a kinetic control.[184,185]

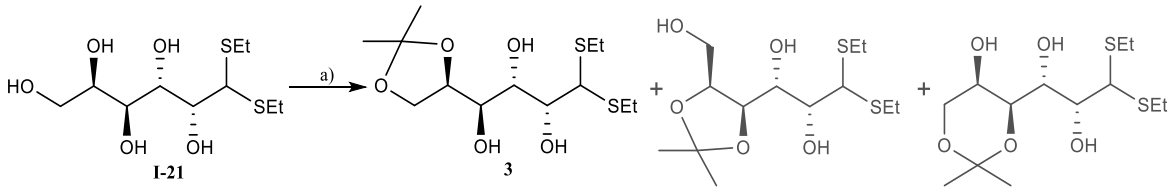

Scheme 3.6: Condensation of **I-21** with DMP. Reagents: a) DMP (1.2 equiv.), TfOH (0.1 equiv.), DMF, 0 ºC, 59%.

Multiple attempts were needed to achieve a reliable acetal formation protocol (**Table 3.1**). The reaction in THF failed due to poor solubility of **I-21** in this solvent (**Table 3.1**, Entry 1). **I-21** was soluble in DMF, which was used in subsequent reactions. Synthesis of acetal **3** was further hindered by the incomplete conversion of **I-21** and by the formation of side products that were difficult to separate from **3**. This product was distinguished from other acetals by the HMBC correlation of the quaternary carbon of isopropylidene (109.33 ppm) and both H-6 signals (4.08 ppm and 3.95-3.85 ppm) and H-5 (4.37 ppm) (Appendix A.9).

Using excess of DMP did not improve the reaction outcome, as it led to formation of side products with multiple isopropylidene groups. Better results were obtained using only 1.2 equiv. of DMP. Performing the reaction at temperatures higher than 0º C, or increasing the temperature during the reaction, favored the formation of 4,5 and 4,6 acetals over acetal **3** (**Table 3.1**, Entry 2). Thus, reactions had to be kept constantly at 0 ºC. The amount of PTSA also affected the rate of the reaction. An increase from 0.02 equiv. to 0.05 equiv. leads to complete conversion of **I-21** and increased the yield from 39 % to 63 % (**Table 3.1**, Entry 4). However, reactions with 0.05 equiv. PTSA were very inconsistent. A substitution of PTSA for 0.1 equiv. TfOH resulted in reproductible reactions, with complete conversion of **I-21** and moderate product yields (**Table 3.1**, Entry 5).

Table 3.1: Optimization of product **3** synthesis.

Entry	Solvent	Temperature	Catalyst	DMP (equiv.)	Time	Yield (%)
1	THF	rt	PTSA (cat.)	2	24 h	0
2	DMF	- 10 ºC to rt	PTSA (0.04 equiv.)	1.1	1 h (-10 º C) + 4 h (rt)	36
3	DMF	0 ºC	PTSA (0.02 equiv.)	1.2	22 h	39
4	DMF	0 ºC	PTSA (0.05 equiv.)	1.2	17 h	63
5	DMF	0 ºC	TfOH (0.1 equiv)	1.2	18 h	59

Cyclization of **3** with NIS was evaluated at room temperature, using a 0.03 M concentration of **3** (**Table 3.2**, Entry 1). After 15 minutes, TLC analysis (AcOEt/Hex, 2:1) showed the formation of three new products. The two major products presented R_f values of 0.88 and 0, inconsistent with expected behavior of **4** in TLC. These compounds were assigned to be products of intermolecular coupling and degradation, respectively. A minor product was detected having an R_f lower than **3**,

which was assigned to **4**. However, this product was not recovered in a sufficient amount for NMR characterization. Reducing the concentration of **3** to 0.015 M eliminated the less polar side product, which supports the assumption of glycan coupling. There was still significant product degradation under these conditions, and product **4** could not be recovered without contamination with succinimide (**Table 3.2**, Entry 2), a byproduct of NIS activation (**Scheme 3.7**). Thus, the reaction was neither clean nor high yielding, unlike previous syntheses of other thioglycosides with the same protocol.[186–188] To solve the issues of low yield, product degradation, and contamination by succinimide, reaction conditions were extensively optimized. Alternative methods using *N*-(pheniylthio)-ε-caprolactam [189] or N-Bromosuccinimide for thiol activation were also tested but resulted in product degradation.

Table 3.2: Optimization of product **4** synthesis.

Entry	Temperature	Concetration of **3** (mol dm^{-3})	NIS (equiv.)	Time (min)	NaOH quench	Yield (%)	α:β
1	rt	0.03	1.2	35	No	0	-
2	rt	0.015	1.1	15	No	18 (**4**/succinimide 1:1.5 mix)	1:0
3	rt	0.015	1	6	No	41	1:0.3
4	rt	0.015	1	7	Yes	47	1:0.5
5	-10 ºC	0.03	1.2	5	Yes	83	1:0.25

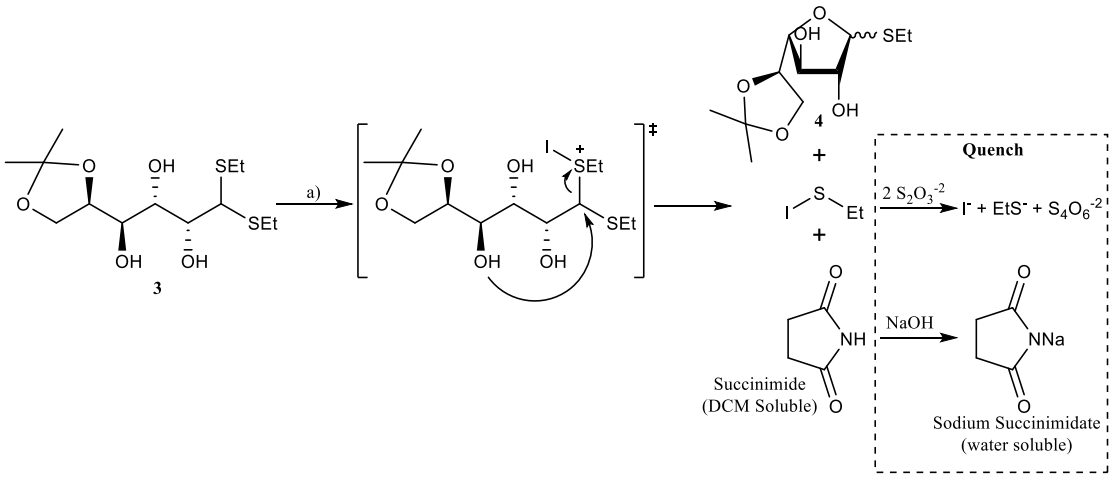

Scheme 3.7: Final, optimized NIS cyclization reaction conditions and quenching. Reagents: a) NIS (1.2 equiv.), DCM, -10 ºC, 5 min, 83 % (1α:0.25β).

During NIS-mediated cyclization of **3**, the color of the reaction mixture varied significantly. In the first 5 min, the reaction changed from bright to dark red and progressively turned orange. After 10 to 15 min, the reaction was visibly clouded by insoluble degradation products. To evaluate how the reaction progressed over time, a test reaction was analyzed by TLC at 1 min intervals after NIS addition. Complete conversion of **3** and minor product degradation were both observed after 6 min, but the degradation significantly progressed after this time. This analysis demonstrated that the reaction was time sensitive, and that the outcome was affected by the fast degradation of **4** and not by a side reaction of **3**. Considering that NIS is consumed by the end of the reaction, it is assumed that **4**

reacts with an iodine-containing byproduct, likely EtSI, forming an oxocarbenium, which may react with any nucleophile in solution and produce many different side products (**Scheme 3.8**). Thus, it was assumed quenching the reaction mixture with saturated aqueous $Na_2S_2O_3$ solution could stop the degradation of **4**.

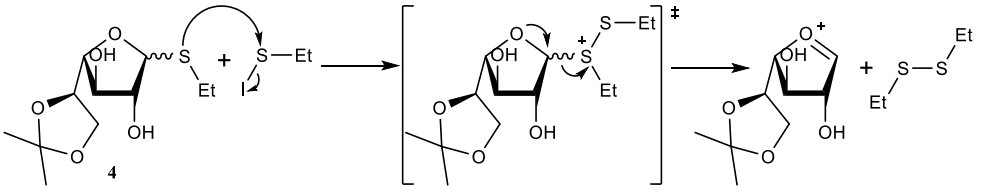

Scheme 3.8: Proposed mechanism for degradation of **4**.

Contamination of product **4** with succinimide was also a major issue in this process, identified in ^{1}H-NMR by the presence of two singlets, at 9.25 ppm (1H, N*H*) and 2.72 ppm (4H, CH_2) (Appendix A.9, **Figure A.25**). Chromatographic separation of **4** from succinimide was not possible and mainly resulted in coelution of both compounds. Only using comparatively high ratios of Hex/AcOEt (1.75:1) minimized this issue, but led to slow and unreliable chromatography steps, and subsequent loss of **4** (**Table 3.2,** Entry 3). An alternative separation method was thus developed, exploiting the acidity of succinimide and its reaction with strong bases, which deliver water-soluble salts. Accordingly, NaOH was added to the $Na_2S_2O_3$ quenching solution. This treatment removed all succinimide from the reaction mixture, which was evident even in ^{1}H-NMR spectra of crude products (Appendix A.9, **Figure A.26**); this quenching method was used in subsequent reactions.

Cyclization of **3** using NIS delivered anomeric mixtures of **4** that were difficult to separate by chromatography. Using ^{1}H-NMR spectra, anomer ratios were determined by integration of the H-1 signals of both products, which appeared as a doublet overlapping a less intense singlet at 5.34-5.30 ppm (Appendix A.9, **Figure A.27**). This suggested **4*α*** was the main reaction product, since the ^{1}H NMR spectrum of a previous synthesis of **4*α*** showed H-1α as a doublet with $J_{1\text{-}2}$= 4.2 Hz.[190] Moreover, it is expected H-1β signals appear as a singlets or a doublets with $J_{1\text{-}2}$ < 1Hz due to the dihedral angle between H-1 and H-2, which is close to 90 º.[191] Anomer content was further confirmed by NOESY, showing a correlation between H-4 of the major product and the H-1 multiplet, which is only possible in the α anomer, that has these hydrogens in the same orientation (**Figure 3.1**).

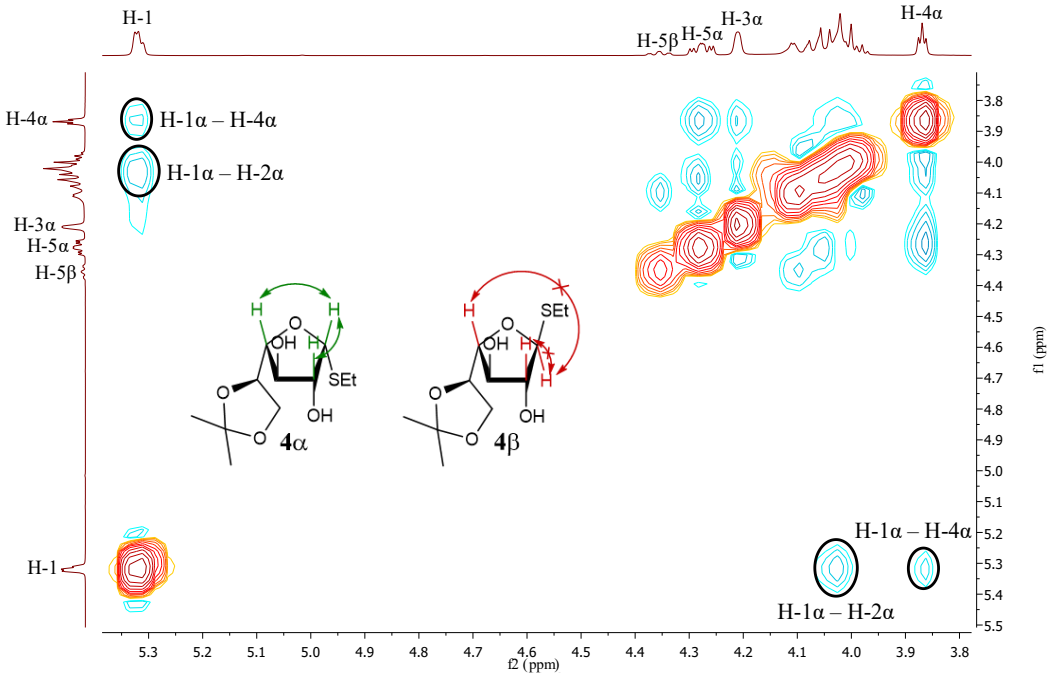

Figure 3.1: NOESY correlation of H-1α with H-4α.

Despite the optimization of reaction time and work up, yields were still modest (**Table 3.2**, Entry 4) and unreproducible. Thus, the effect of temperature on the reaction was also assessed using the TLC method. At 0 ºC the conversion of starting material was slower than at room temperature, and **3** still present after 20 min. Product degradation was unaffected and already observed after 6 min. A reaction temperature of -10 ºC, in combination with an increase of concentration of **3** to 0.03 M, resulted in complete conversion after 5 min, with very minimal degradation of product **4**. Using these conditions for cyclization of 0.5 g of **3** improved significantly both the yield (83 %) and α anomer selectivity (α/β, 1:0.25) (**Table 3.2**, Entry 5). A scaling of the process to 4 g of **3** delivered a decreased yield and selectivity (71 %, α/β 1:0.35), likely caused by both slower NIS homogenization and slower quenching.

A regioselective protection at the O-2 position of product **4** (α/β 1:0) using the established stannyl ether mediated protection with BzCl delivered two main products, assigned by TLC analysis to mono (**5a**) and diacylated (**5b**) galactofuranosides (**Scheme 3.9**). The signals of the ^{13}C-NMR and ^{1}H-NMR spectra of monoacylated product **5a** were consistent with a single Bz group, which showed a HMBC correlation of the Bz carbonyl group at 166.95 ppm with the H-2 at 5.30 ppm (Appendix A.10). The yield of the reaction was only 21 %. The reaction was repeated without addition Et_3N, to assess if stannyl ether mediation was occurring. Under these conditions no **5a** was formed. This result showed that the SEt group has a detrimental effect on stannyl ether formation. Conventional benzoylation of **4** (α/β 1:0.12) using stoichiometric amount of BzCl delivered both **5a** and **5b**, with a yield of 46 % (α only; corrected to α content of **4**), demonstrating that **4** and **5a** compete as reactants for acylation. This yield is comparable to the selective benzoylation of *p*-toluil 5,6-*O*-isopropylidene-1-thio-β-D-galactofuranoside.[192]

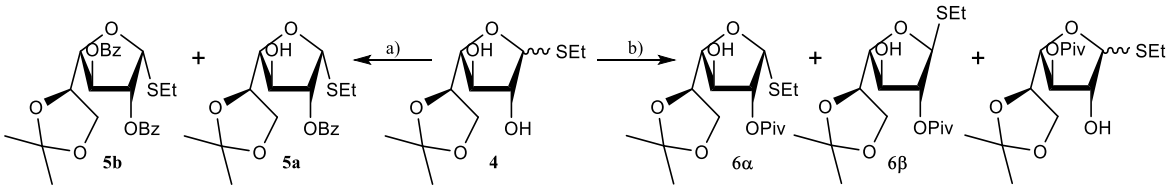

Scheme 3.9: Acylation of **4**. Reagents: a) **4** (α/β 1:0.12), BzCl (1 equiv.), Et_3N (3 equiv.), DMAP (cat.), THF, 46 %; b) **4** (α/β 1:0.35), PivCl (1.2 equiv.), Et_3N (1.5 equiv.), DMAP (0.3 equiv.), THF, 47 %.

Acylation of **4** (α/β 1:0.12) using PivCl was more selective than with BzCl and delivered exclusively **6α** in 65 % yield (corrected to α content of **4**). The structure of **6α** was confirmed by correlation in HMBC of the Piv carbonyl group (179.08 ppm) and H-2 (5.01 ppm), and the high coupling constant of H-1 signal (5.38 ppm, d ,1H, $J_{1\text{-}2}$ = 4.82 Hz), through coupling with H-2 (5,31 ppm, dd, 1H, $J_{1\text{-}2}$= 4.82 Hz, $J_{2\text{-}3}$= 3.10 Hz), in ^{1}H NMR (Appendix A.11). Scale up of the reaction with a different anomer ratio of **4** (2.31 g, α/β 1:0.35) was significantly less effective. The reaction did not proceed with complete conversion of **4** and was less selective, delivering **6α** in a yield of only 47 % (corrected for α portion of **4**). Multiple side products were also observed through TLC analysis, including compounds with similar polarity to **6α**, presumably **6β** and O-3 acylated regioisomers.

Product **6α** was protected with Lev through Steglich esterification,[178] using di-isopropylcarbodiimide (DIC), DMAP and levulinic acid (LevOH) (**Scheme 3.10**). This reaction gave the fully protected galactofuranose **7** in high yield (89 %), which was then treated with AcOH (60%, aqueous) to obtain diol **8** in quantitative yield. Final benzylation of **8** with excess BnBr and NaH did not deliver the desired building block **BB-1b**. Instead, a migration of the Lev group from O-3 to O-6 and following benzylation of the resulting free hydroxy group in position 3 gave product **9**. The structure of **9** was confirmed by ^{1}H-NMR, showing integrals equivalent to a monobenzylated product, and the HMBC correlations of *C*H_2Ph (72.71 ppm) with H-3 (4.26 ppm) and of C-1' Lev (172.73 ppm) with H-6 (4.19/4.12 ppm), corresponding a Bn group in O-3 and Lev in O-6, respectively (Appendix A.14). Acid-catalyzed benzylation with trichloroacetimidate (BnTCAI),[193] a common alternative for benzylation of base labile substrates, was also tested using three different acid catalysts (PTSA, TfOH or BF_3.Et_2O), but no reaction was observed with any of these reagents, at room temperature or under reflux in THF.

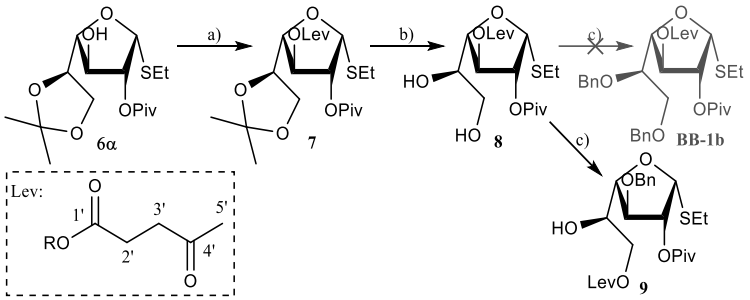

Scheme 3.10: Steglish esterification of product **7α**, followed by hydrolysis of isopropylidene. Reagents: a) LevOH (1.3 equiv.), DIC (1.3 equiv.), DMAP (0.3 equiv.), DCM, 89 %; b) AcOH (aqueous, 60 %), quantitative; c) BnBr (3 equiv.), NaH (3 equiv.), DMF.

A precursor replacing Lev with Nap as the orthogonal protecting group was considered as an alternative substrate for basic benzylation (**Scheme 3.11**). Nap was installed on **6α** using Williamson etherification, with NaH and 2-(bromomethyl)naphthalene (NapBr) in dry DMF, delivering product **10** in 92 % yield. Correlation in HMBC of *C*H_2 Nap (72.42 ppm) with H-3 (3.90 ppm) and of the Piv carbonyl group (177.68 ppm) with H-2 (5.36 ppm) demonstrated that no migration or hydrolysis of

Piv occurred during the reaction (Appendix A.15). The 5,6-isopropylidene of **10** was then hydrolyzed in near quantitative yield (99 %). In contrast to **7**, compound **10** was unreactive at room temperature and required heating to 60 ºC to achieve full acetal hydrolysis.

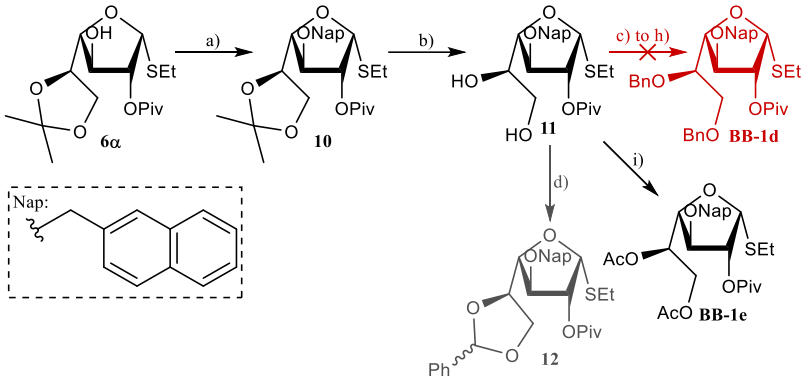

Scheme 3.11: Basic protection of product **6α** with NapBr, and final protection step for Gal*f* building block. Reagents: NapBr (1.5 equiv.), NaH (1.5 equiv), DMF, 92 %; b) AcOH (aqueous, 60 %), 60 ºC, 99 %; c) NaH, BnBr, DMF; d) i) HMDS, TMSOTf, DCM; ii) PhCHO, TMSOTf ; iii) TES, TMSOTf, 60%; e) DIPEA, BnBr, TBAI, reflux; f) Ag_2O, BnBr; g) TriBOT, TfOH; h) Ac_2O (4 equiv.), DMAP (0.5 equiv.), Pyridine, 97 %.

Final benzylation of **11** using NaH as a base delivered multiple products that were not separable by column chromatography. Two products were identified by NMR in the major chromatography fraction, in a 1:0.8 ratio (Appendix A.17). Only one of these products contained the Piv group, with ^{13}C-NMR showing a single Piv carbonyl signal (178.36 ppm), and the characteristic methyl singlet of Piv (1.19 ppm) in ^{1}H-NMR with integration corresponding to nine protons. It was not possible to identify the H-2 signal in ^{1}H-NMR, or the position of Piv using HMBC. Thus, there was no confirmation if this was product **BB-1d** or if the Piv group migrated to another position.

Alternative benzylation methods were explored to complete the synthesis. First, one pot silylation and reductive benzylation was tested on **11**, using a large excess of benzaldehyde (PhCHO). This method had previously proved useful to benzylate base labile mannose substrates (products **23** and **26**, Chapter 3.3). NMR data from the reaction product suggests the formation of a 1:1 mixture of the two 5,6-benzylidene diastereomers **12** instead of **BB-1d** (**Scheme 3.11**). ^{1}H-NMR signals in the aromatic range integrated to a total of 24 H, instead of the expected 17 H. These integration values are only possible a mixture of two products (1:1, 12 H each) is present. The two singlets at 5.92 ppm (1 H) and 5.82 (1 H), corelating in HMBC with both aromatic and aliphatic carbons, corresponding to the two C-6 signals (at 66.58 ppm and 66.42 ppm), further suggested the presence of two benzylidene groups (Appendix A.18).

A solventless benzylation approach using excess di-isopropyl ethyl amine and BnBr, with TBAI as a catalyst and at high temperatures (110 ºC to 150 ºC) was also tested. This reaction relies on a milder base and was reported to work on ester protected substrates.[194] However, this reaction only led to degradation of **11**. Ag_2O-mediated benzylation with BnBr was tested next. This reaction works in neutral media, involves the activation of the electrophile instead of the hydroxy group, and is compatible with esters. Initial experiments with this strategy involved a co-solvent approach using a Hex/DCM (4:1) mixture as solvent.[195] The reactions suffered from poor conversion of **11** and gave multiple residual products that could not be purified or characterized by NMR. Replacing the solvent mixture for toluene and performing the reaction under reflux led to complete consumption of **11**, but multiple products were formed. A characterization by ^{1}H-NMR of the major fraction obtained from

chromatography, which appeared pure in TLC, showed a complex mixture of products without the desired product **BB-1d**.

Finally, an acid-catalyzed benzylation using 2,4,6-tris(benzyloxy)-1,3,5-triazine (TriBOT) was tested. TriBOT is an air-stable solid that donates three benzyl groups (**Scheme 3.12**) and can be used as an alternative to BnTCAI.[196] TriBOT was synthesized from cyanuric chloride, NaOH and excess of benzoic acid following reported protocols.[196] Benzylation of **11** using 0.4 equiv. of TfOH and 1 equiv. of TriBOT at room temperature did not show any product formation. Increasing the amount of TfOH to 1 equiv. and refluxing for 23 h led to complete degradation of diol **11** into two side products lacking the thiolethyl group, as observed by ^{1}H-NMR.

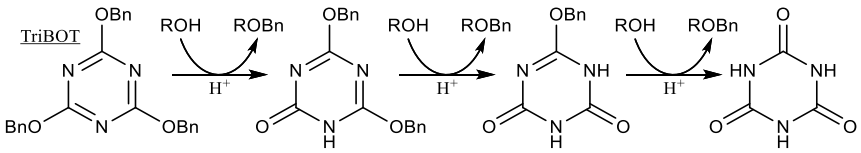

Scheme 3.12: Acid catalyzed benzoylation of three hydroxy groups with TriBOT and its derivatives.

Considering the lack of an efficient method for benzylation of the diol, acetyl was selected as an alternative permanent protecting group. This protecting group was initially disregarded since the electron-withdrawing effect of multiple ester protecting groups "disarms" a glycosyl donor by destabilizing the oxicarbenium ion formed during glycosylation.[197] Thus, acetyl protection can reduce the reactivity of the donor and hinder the use of the building block.

Acetylation of **11** in pyridine, with acetic anhydride (Ac_2O) and DMAP, gave the final building block **BB-1e** very high yield (97 %). NMR spectra of the product were consistent with di-acetylation (Appendix A.19), with two methyl signals as singlets (integrating to 3H) at 1.99 ppm and 1.97 ppm in ^{1}H-NMR, and two carbonyl signals at 170.67 ppm and 170.32 ppm in ^{13}C-NMR, which correlated in HMBC with the aforementioned methyl groups. However, it was not possible to determine if migration of Piv occurred during the reaction. HMBC showed correlation between carbonyl carbon of an Ac and H-6 (ABX system, 4.34, 4.31 ppm and 4.12, 4.09 ppm), but correlations of the other Ac carbonyl group and the Piv carbonyl group were significantly weaker, and both occur with the multiplet in 5.39-5.31 (2H), corresponding to the overlap of H-2 and H-5 signals.

3.1.4. Final considerations on Gal*f* synthesis

The initial objective of obtaining a Gal*f* building block for O-3 glycosylation was accomplished. However, the final protocol was not ideal to produce the desired benzylated building block, requiring further optimization to improve the very low overall yield of 11 % (based on the optimized, upscaled reactions and on the α content after the cyclization).

There are some possible approaches to optimize the synthesis of the key precursor **4** that remain untested. Improving regioselectivity in the synthesis of product **3** by lowering reaction temperature may enhance the overall yield of the strategy, but this could not be achieved with current reaction setup. Nevertheless, the present protocol can be easily used in multigram scale and is an improvement on a previous reports, which described yields lower than 40 %.[184] The optimized cyclization protocol produces high total yields, but it is still hindered by the formation of the β anomers, having a negative impact on the regioselective of O-2 acylation, reducing the global yield of the strategy. There is an apparent relation between temperature and stereoselectivity. Further studies should explore the reaction at temperatures lower than -10 ºC.

There are some reported approaches which may have offered precursor **4** in substantial yields. Synthesis of **4α** has been performed by cyclization of **I-21** with $HgCl_2$, followed by installation of isopropylidene**,** with both steps delivering high yields (**Scheme 3.13-A**).[190] However, this approach is difficult to reproduce due to the lack of a report describing the protocol for the $HgCl_2$-mediated cyclization. Product **I-2** can be synthesized from D-Gal in high yields [137,198] and converted into various thioglycosydes through $BF_3.Et_2O$ catalyzed glycosylation.[199,200] This approach has been used to prepare analogues of product **4**, through high yielding debenzoylation and protection with isopropylidene acetal (**Scheme 3.13-B**).[137,201] Product **I-4** has been used in similar strategies (**Scheme 3.14-C**), usually including a redundant per-benzoylation step that simplifies purification and improves the stereoselectivity to β-thioglycosides through neighboring group effect (**Scheme 3.13-C**).[48,202,203]

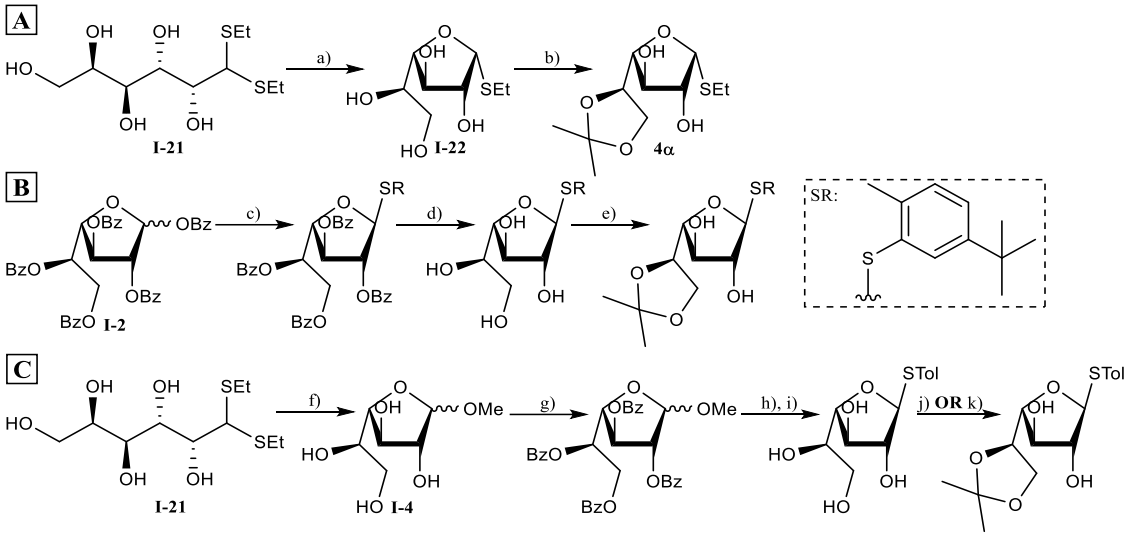

Scheme 3.13: Synthesis of product **5** analogues using precursor **I-21** (**A**),[190] **I-2** (**B**) [137] and **I-4** (**C**).[48,202,203] Reagents: a) $HgCl_2$, H_2O (η= 74 %); b) DMP, PTSA, acetone (η= 88 %), c) 2-methyl-5-tert-butyl-thiophenol, $BF_3.Et_2O$, DCM (η= 97 %); d) NaOMe, MeOH (η= 94 %); e) DMP, CSA, acetone (η= 90 %); e)f) MeOH, I_2; g) BzCl, pyridine (η= 71 %, two steps); h) TolSH, $BF_3.Et_2O$, DCM (η= 89 %); i) NaOMe, MeOH (η= 88 %); j) acetone, $CuSO_4$,H_2SO_4 (η= 88 %); k) DMP, CSA, DCM (η= 80 %).

Two different approaches to selective protection O-2 were explored for the synthesis of the Gal*f* building block. Direct acylation of either **I-33** or **4** delivered the product in poor yields. A stannyl ether mediated acylation was efficient to obtain products **1a** and **2a**, but the method did not work on thioglycosides. This approach should also not be compatible with β-galactofuranoses lacking the required 1,2-*cis* configuration and is therefore of limited interest as a general protection strategy.

An alternative to the stannyl ether protocol is stannyl acetal mediated acylation, achieved though condensation of a diol with Bu_2SnO, which is used in pyranoses to modulate the reactivity of hydroxy groups.[181] Unlike stannyl ether mediated acylation, it does not require participation of the anomeric position (**Scheme 3.14**); although it is reported that anomeric configuration affects regioselectivity in pyranoses,[181] this may not occur in furanoses. Thus, this strategy could potentially be used in both α and β-galactofuranoses, as well as in thioglycosides, and may significantly simplify the selective protection of Gal*f* derivatives.

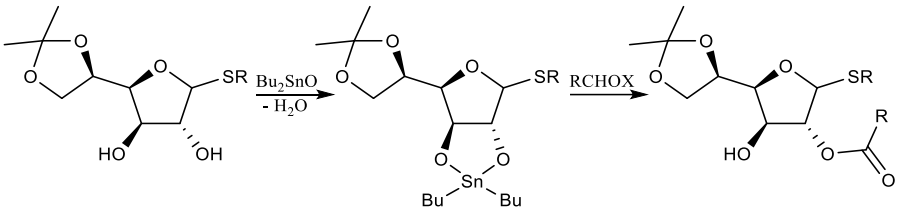

Scheme 3.14: Proposed stannyl acetal mediated acetylation.

3.2. Galactopyranose building block

The building block **BB-2** required orthogonal protection at the O-6 position, a remote participating group to favor α-glycosylation and a non-participating group in the O-2 position. A synthetic strategy for building block **BB-2** was envisioned starting from ethyl 4,6-*O*-benzylidene-1-tio-β-D-galactopyranoside (**13**). The hydroxy groups in positions 2 and 3 are first protected with non-participating benzyl group. Then, a benzoyl ester is selectively installed in O-4 through oxidative cleavage of benzylidene and finally O-6 is protected with tPG Lev through Steglish esterification (**Scheme 3.15**).

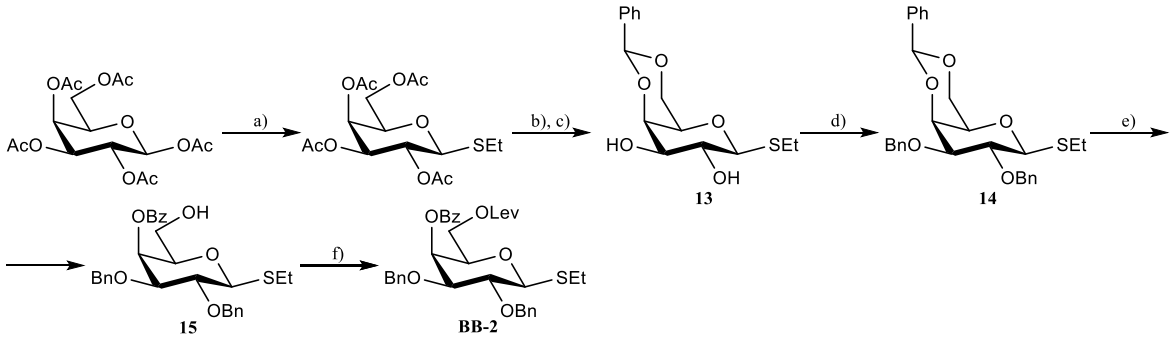

Scheme 3.15: Initial synthetic strategy for Gal building block **BB-2**. Reagents: a) TfOH, EtSH; b) NaMeO; c) $PhCH(OMe)_2$, CSA, 88 % (three steps); d) BnBr, NaH, DMF, 68 %; e) H_5IO_6, TBABr; f) LevOH, DIC, DMAP.

The thioglycoside **13** was previously prepared in three steps starting with 25 g of per-acetylated D-galactose. The process involved the preparation an ethylthioglycoside, basic methanolysis of Ac groups and acetalation of hydroxy groups in positions 4 and 6 with benzylidene, in an overall yield of 88 %. **13** was benzylated under standard Williamson conditions in 68 % yield, which was lower than expected, as TLC analysis of the reaction after 19 h at room temperature showed only residual amounts of starting material.

Oxidative cleavage of benzylidene with periodic acid and tetrabuthylamonium bromide in wet alumina was evaluated on **14** (**Scheme 3.16**).[204] Instead of obtaining product **15** having an O-4 benzoylation, as reported in the literature for glactopyranoses,[204] NMR characterization of the resulting product did not show the characteristic signals for either SEt group (in ^{1}H-NMR) or Bz carbonyl (in ^{13}C-NMR, Appendix A.21). Thus, the thioethyl group of compound **14** was oxidized, either by the periodic acid or by the bromine formed *in situ*, giving a sulfoxide that hydrolyzed under the reaction conditions to deliver product **16** (**Scheme 3.16-B**). Therefore, this reaction is unsuitable for installation of O-4 benzoyl groups in thioglycosides.

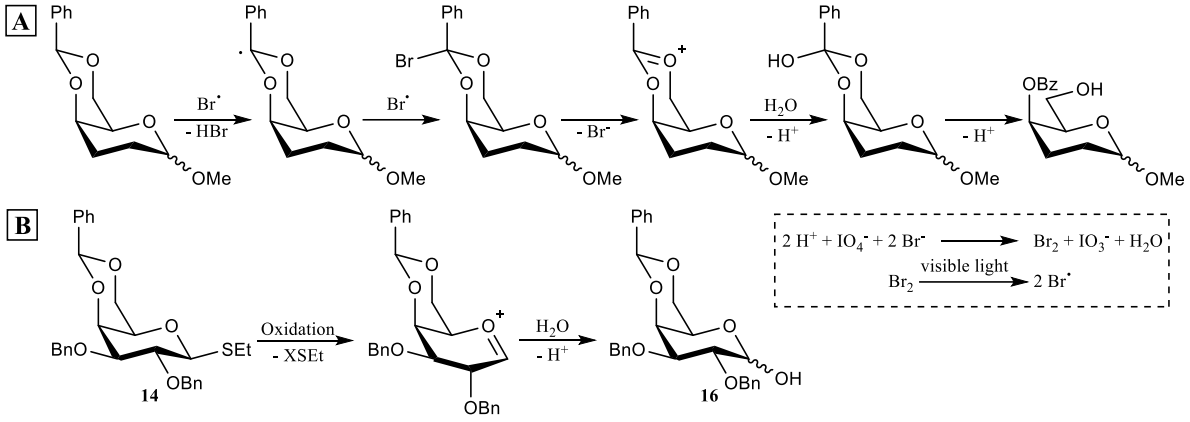

Scheme 3.16: Oxidative cleavage of benzylidene. **A**- Reaction mechanism;[204] **B**- Proposed mechanism for degradation of **14**.

Removal of benzylidene acetal and following regioselective Steglich esterification of O-6 with LevOH and benzoylation of O-4 was tested as an alternative to oxidative cleavage of benzylidene (**Scheme 3.17**). The benzylidene acetal was successfully removed by hydrolysis with aqueous AcOH 70%, and methanolysis, with PTSA in a MeOH/DCM (4:1) solvent mixture. Both reactions delivered **17** in high yields (97 % and 84 %, respectively), although the methanolysis reaction proceeded faster. Product **17** was selectively protected using Steglich esterification with equimolar amounts of **17**, LevOH and DIC. As expected, the reaction was selective to O-6 over the axial hydroxy group and delivered **18a** in a moderate yield of 66 %. The structure of the main reaction product was confirmed with the correlation of C-1' Lev (172.77 ppm) with both H-6 signals (4.38-4.27 ppm, as an overlap of 2 dd signals) in HMBC, indicated that Lev was present in O-6 (Appendix A.23). A small portion of O-4 Lev regioisomer **18b** was formed and coeluted with **18a** during chromatography, hindering product purification.

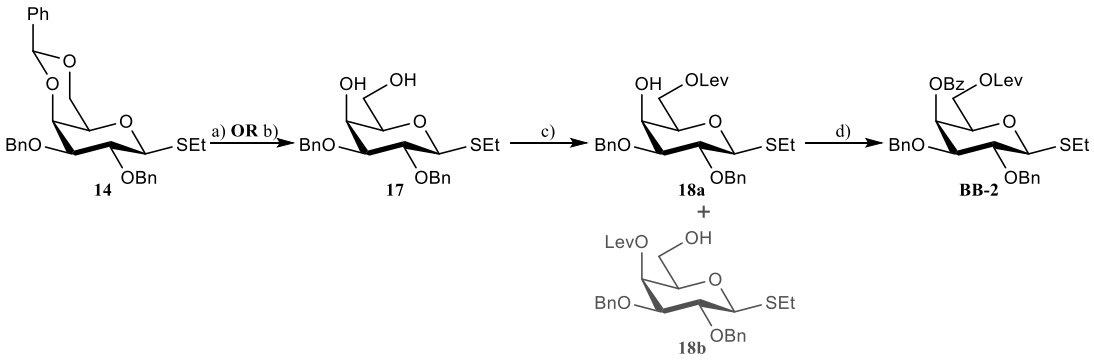

Scheme 3.17: Alternative synthesis of building block **BB-2**. Reagents: a) AcOH (70 %, aqueous), 97 %; b) PTSA (0.5 equiv.), MeOH: DCM (4:1), 84 %; c) LevOH (1 equiv.), DIC (1 equiv.), DMAP (0.3 equiv.), DCM, 66 %; d) BzCl (1.5 equiv.), Et_3N (3 equiv.), DMAP (0.3 equiv.), THF, 87 %.

A benzoylation of alcohol **18a** delivered the final building block **BB-2** in 87 % yield. HMBC correlation of C-1'' Lev (172.47 ppm) with H-6 (ABX system, 4.30 ppm, 4.27 ppm, 4.15 ppm, 4.12 ppm, 2H) and of the Bz carbonyl (165.83 ppm) with H-4 (5.81 ppm, d, 1H) indicated that no migration of Lev occurred under these mild basic conditions, confirming the structure of **BB-2** (Appendix A.24). Starting from **13**, the total yield for the synthesis of this building block was 37 %.

3.3. Mannopyranose building blocks

Two Man*p* building blocks differing only in the inclusion of a Nap (**BB-3**) or Bn (**BB-4**) group in O-3 were required. These mannoses contain both a participating group in O-2 and permanent protection with Bn in O-4 and O-6 and can thus be assembled though similar synthetic strategies. Starting from commercially available ethyl 4,6-*O*-1-thio-benzylidene-α-D-mannopyranoside (**19**), the synthesis of building block **BB-3** was envisioned in 4-steps (**Scheme 3.18**).

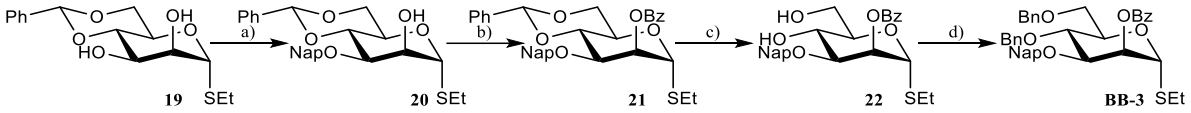

Scheme 3.18: Strategy for Man building block BB-3 synthesis. Reagents: a) $(Bu_3Sn)_2O$ (1.3 equiv.), toluene, 4 Å molecular sieves, reflux, then NapBr (1.3 equiv.), TBAI (1.3 equiv.), toluene, reflux; b) BzCl (1.5 equiv.), Et_3N (3 equiv.), DMAP (0.3 equiv.), THF, reflux; c) PTSA (0.5 equiv.), MeOH:DCM (4:1), 74 % (three steps); d) NaH, BnBr, DMF.

A small scale regioselective protection of the hydroxy group in position 3 with NapBr through stannyl ether activation of **19** delivered exclusively product **20** after 4 h. The structure was confirmed by the HMBC correlation of CH_2-Nap (73.10 ppm) with H-3 (3.96 ppm, dd, 1H) (Appendix A.25). Product purification by chromatography was hindered by two contaminants, identified by NMR: NapOH, with ^{1}H-NMR signals for CH_2 (in the 4.90-4.83 ppm multiplet,1.14 H) and an hydroxy group proton (1.93 ppm, 0.57 H, t), which correlate in COSY, as well as a higher than expected integration of aromatic signals (16 H instead of 12 H), and a product with a butyl moiety (likely a derivative of Bu_3Sn (I)), identified in ^{1}H-NMR by signals at 1.70-1.60 (m, 0.7 H), 1.42-1.32 (m, 0.7 H) and 0.94 (t, 0.7H). Contaminated product **20** was then benzoylated at room temperature, delivering product **21** in 63 % yield (over two steps), which was easily separated from the contaminants of the previous reaction. Subsequent removal of benzylidene via acid methanolysis gave diol **22** in 94 % yield.

Upscaling of the process to 2.3 g of **19** resulted in a slower regioselective protection, requiring a 24 h reaction at reflux to reach completion. Similarly, product **20** could not be isolated from the contaminants and was benzoylated without further purification. The benzoylation was also slower than expected and required over 3h under reflux to achieve complete conversion. Purification of the reaction though chromatography yielded pure product **21**, and a fraction contaminated with benzoic acid (from degraded BzCl stock). This contaminant was removed after benzylidene methanolysis of combined fractions of **21**, which delivered product **22** in 74 % yield, over three steps.

Benzylation of diol **22** with NaH in dry DMF delivered multiple products. Purification by chromatography produced 2 fractions that were characterized by NMR. In ^{13}C-NMR of the first fraction, a Bz carbonyl signal was present (at 165.84 ppm), and correlated with H-2 (5.79 ppm, dd, 1H) in HMBC, showing Bz was still present and did not migrate. The signals and respective integration in ^{1}H-NMR were consistent with 2 benzyl groups, confirming this fraction as product **BB-3** (Appendix A.29), which was obtained in a yield of 16 %. The second fraction contained multiple products lacking a Bz group. Alternatively, acid catalyzed benzylation, using TfOH and BnTCAI delivered a complex product mixture, without formation of the desired **BB-3**.

A one-pot, three-step procedure involving silylation and reductive benzylation was evaluated on **22** (**Scheme 3.19**). The process started with a TMSTOTf catalyzed silylation of **22** with hexamethyldisilazane (HMDS) or hexamethyldisiloxane (HMDSO), delivering intermediate **A**. Benzaldehyde is then added to form a silylated hemiacetals (intermediates **B** and **C**), which may be reduced with triethyl silane (TES) into the Bn protecting groups.[205] However, treatment of diol **22**

under these conditions resulted in the formation of product **21** in 95 % yield. This outcome was attributed to the intramolecular reaction being faster than the formation of two silylated hemiacetals. This result overlaps with previous applications of this approach for regioselective, one-pot protection of hexapyranosides, as it allows a sequential introduction of 4,6-benzylidene acetals and selective benzylation of O-3, producing a single free O-2 position.[206,207]

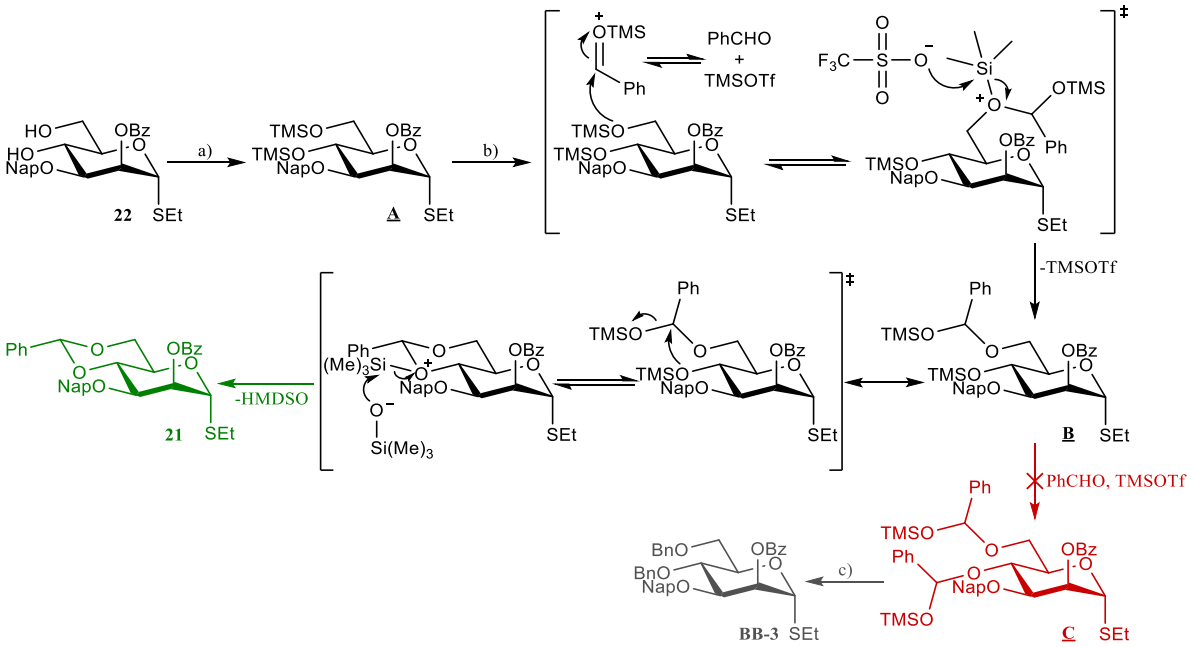

Scheme 3.19: Failed one pot silylation-reductive benzylation of **22**, and proposed reaction mechanism. Reagents: a) HMDSO (6 equiv.), TMSOTf (0.5 equiv.), THF; b) PhCHO (6 equiv.), 95 %; c) TES (4 equiv.).

Reductive cleavage of the benzylidene in product **21** would furnishes either a O-6 or O-4 position with a benzyl group, resulting in a single free hydroxy group that could be benzylated (**Scheme 3.20**). Many methods are available for reductive opening of benzylidene. These can favor either O-4 or O-6 benzylation, depending on reduction agent, acid catalyst, solvent and substrate.[208] Because a free hydroxy group in position 6 would be more reactive for subsequent benzylation, a protocol for selective opening to O-4 Bn was selected.

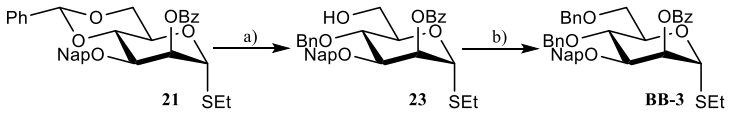

Scheme 3.20: Regioselective reductive cleavage of benzylidene and one pot silylation-reductive benzylation. Reagents: a) BH_3.THF (5 equiv.), TMSOTf (0.15 equiv.), DCM, 78 %; b) i) HMDS (1.5 equiv.), TMSOTf (0.15 equiv.), DCM; ii) PhCHO (2 equiv.) TMSOTf (0.15 equiv.); iii) TES (2 equiv.), TMSOTf (0.15 equiv.), 71%.

Benzylidene protected substrate **21** was treated with BH_3.THF and TMSOTf (**Scheme 3.21**),[209] delivering two products. The major product was obtained in 78 % yield, and was identified by NMR as alcohol **23**. NMR characterization showed a correlation between C-4 (74.23 ppm) and C*H*$_2$ Bn (AB system, 4.98 ppm, 4.95 ppm, 4.72 ppm, 4.69 ppm, 2H) by HMBC, and coupling between H-6 (3.88 ppm, broad s, 2H) and a hydroxy group (1.90 ppm, broad s, 1H) by COSY (Appendix A.28). The side product resulted from benzoyl reduction of **23** since NMR characterization did not show a Bz carbonyl signal in ^{13}C-NMR or C*H* singlet from benzylidene in ^{1}H-NMR.

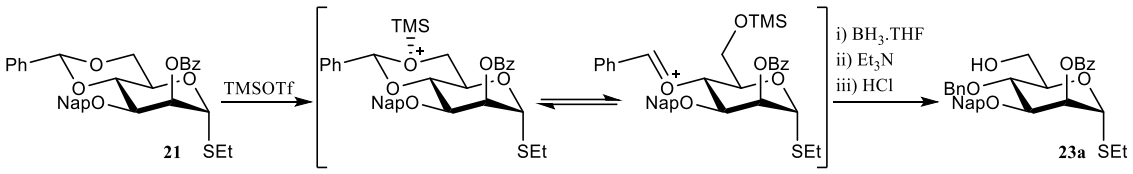

Scheme 3.21: Mechanism for selective reductive cleavage of benzylidene to O-4 Bn.

Product **23** was benzylated through one pot silylation (with HMDSO) and reductive benzylation. Even with large reagent excesses, the reaction did not proceed with full conversion, and delivered **BB-3** in only 55 % yield (76 % yield, based on recovered starting material). 28 % of the starting material was recovered after chromatography, but not the TMS-protected intermediate. Incomplete reaction could be a result of hemiacetal hydrolysis by residual water competing with a slow reduction step. HMDS was also tested as an alternative to HMDSO. Silylation with HMDS generates ammonia, which is soluble in THF, and can quench TMSOTf (**Scheme 3.22**). To avoid this neutralization of TMSOTf, DCM was used as a solvent and the reaction mixture was concentrated and redissolved after the first step. This method increased the yield to 71 %, with little starting material being detected by TLC 1 h after TES addition. The overall yield for **BB-3**, starting from **20**, was 39 %.

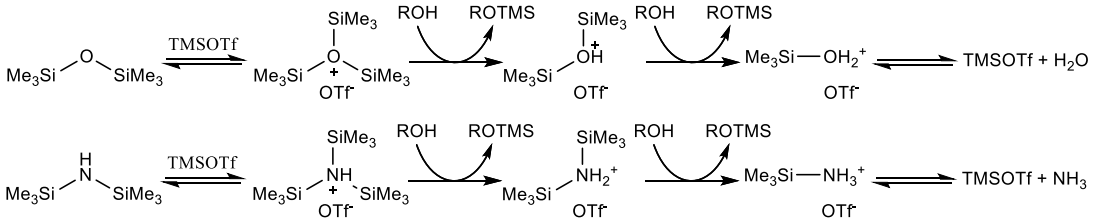

Scheme 3.22: HMDSO and HMDS silylation.

Starting from previously prepared product **24**, the building block **BB-4** was prepared with a similar approach as **BB-3** (**Scheme 3.23**). Benzoylation of alcohol **24** gave **25** in 78 % yield, without contamination of the product with BzOH. A reductive opening of the benzylidene in **25** using BH_3.THF delivered product **26** in 95 % yield, without reduction of benzoyl. The structure of **26** was confirmed by HMBC correlation of C-4 (74.24 ppm) with the C*H*$_2$-Bn (AB system, 4.95 ppm, 4.92 ppm, 4.69 ppm, 4.66 ppm, 2H), and by COSY coupling between H-6 (3.89-3.82 ppm, m, 2H) and O*H* (1.88 ppm, t, 1H) (Appendix A.31). Benzylation of **26** though silylation and reductive benzylation, using HMDSO as the TMS source, was also more effective with this O-3 benzylated precursor, and delivered **BB-4** in 77 % yield. The total yield for this approach was 57 %.

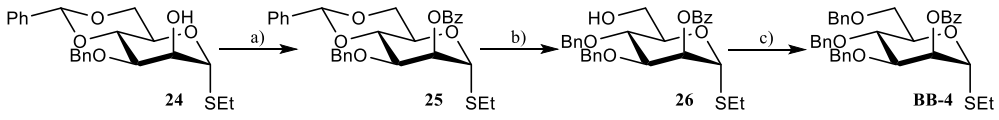

Scheme 3.23: Synthesis of building block **BB-4**. Reagents: a) BzCl (1.5 equiv.), Et_3N (3 equiv.), DMAP (0.3 equiv.), THF, reflux, 78 %; b) BH_3.THF (5 equiv.), TMSOTf (0.15 equiv.), DCM, 95 %; c): i) HMDSO (6 equiv.), TMSOTf (0.5 equiv.), THF; ii) PhCHO (3 equiv.): iii) TES (3 equiv.), 77 %.

4. Conclusions

This dissertation encompassed the syntheses of four thioglycoside building blocks, requiring the design, evaluation, and optimization of synthetic strategies for all structures. Preparing a Gal*f* building block with an orthogonal protecting group in the O-3 position was particularly challenging. Testing three approaches for Gal*f* precursor synthesis, and a significant change in the final building block structure, were necessary to obtain this key building block.

Synthesis of di-isopropylidene protected galactofuranoside **I-9** by acid catalyzed condensation of D-Gal with acetone or DMP was first tested. However, attempts to replicate or optimize a previously published protocol were unsuccessful. Low conversion of starting material and formation of pyranose isomer **I-10** led to meager yields. Other published one-step syntheses of **I-9** reportedly deliver low yields and were not tested. An alternative strategy involving the regioselective benzylation of D-Gal to deliver O-alkyl galactofuranoside **I-5** was also tested but was unsatisfactory, delivering poor yields. Product purification and reaction upscaling were hindered by the used of non-volatile polar aprotic solvent DMPU, which could not be replaced for a conventional solvent (THF, DMF, acetonitrile). Other published strategies for *O*-alkyl galactofuranoside synthesis are likely superior to monobenzylation but were not tested.

A novel three-step approach for Gal*f* precursor synthesis was developed. The strategy presented some limitations, but there are further possibilities for its improvement that were not evaluated in this work. Starting with the synthesis of dithioacetal **I-21** from D-Gal, the process involved the regioselective protection of positions O-5 and O-6 with isopropylidene and cyclization into thiogalactofuranoside **4**. The protocol developed for installation of 5,6-isopropylidene on dithioacetal **I-21** improves on previously published approaches; it is scalable and reliably delivers product **3** in moderate yields. However, the reaction is affected by the formation of other acetal regioisomers. Future optimization of this step may be achieved by performing the reaction at temperatures lower than 0 ºC. A critical step in this strategy was the cyclization of **3** into thiogalactofuranoside **4** by NIS activation, which was initially unsuccessful. The reaction was hindered by degradation of product **4** and contamination of product with succinimide. After extensive optimization of reaction conditions (reaction time, quenching method, concentration, and temperature), the current protocol deliver a high total yield of Gal*f* **4**. However, the reaction produces anomeric mixtures, reducing the yield of the **4α** anomer, and hindering subsequent protection steps. Elimination of the undesired β anomer warrants further optimization of this reaction.

The regioselective protection of galactofuranosides in the O-2 position also hampered access to the Gal*f* building block. Direct and stannyl ether-mediated acylation were both tested for regioselective protection of O-2. Direct acylation of substrates **I-33** and **4** favored the reaction in the O-2 position, but monoacylated regioisomers and diacylated products were still present. In substrate **4**, acylation with PivCl was more selective then BzCl but was affected by the anomer ratio of the starting material, with higher amounts of **4β** anomer significantly reducing reaction yield. Stannyl ether-mediated acylation also favored reactions at the O-2 position and delivered better yields then direct acylation for substrate **I-33** but did not work with thiglycoside **4**. Further optimization of stannyl ether mediated protection, and exploration of other activators (Bu_2SnO), may facilitate access to orthogonally protected galactofuranosides. The compatibility of stannyl mediators with thiogalactofuranosides should also be further investigated.

A final per-benzylation of galactofuranosides **8** and **11** could not be accomplished, regardless of the protecting group in the O-3 position (Lev or Nap). Several benzylation methods were tested, resulting in no reaction, formation of undesired products, or degradation of the starting material. Thus, acetylation was selected as the final reaction step in the synthesis of the Gal*f* building block, with no side reactions on substrate **11**. After extensive changes to the structure of the building block, **BB-1e** was attained in an overall yield of 11 %.

The synthesis of the remain building blocks was significantly more straightforward than the assembly of the Gal*f* building block. Galactopyranose building block **BB-2**, furbished with a remote participating group (Bz) in the O-4 position and a Lev group at O-6, was prepared in four steps from benzylidene protected thiogalactopyranoside **13**. Oxidative opening of benzylidene to deliver a benzoyl group in the O-4 position was tested on fully protected glycoside **14**, but failed due to oxidation of the thioethyl group. Alternatively, Lev was regioselectively installed in position O-6 of diol **17** though Steglish esterification. Benzoylation of the resulting alcohol **18** delivered **BB-2** in 37 % overall yield. The two mannose building blocks, which differed only in the protection of the O-3 position with either Nap (**BB-3**) or Bn (**BB-4**), were assembled through similar strategies. Synthesis of **BB-3** started with a regioselective installation of Nap though stannyl ether mediation, which was very effective. After benzoylation of the O-2 position and removal of benzylidene, benzylation of diol **22** was unsuccessful. Alternatively, reductive opening of the benzylidene in mannopyranoside **21** gave a substrate suitable for mono-benzylation through one-pot silylation and reductive benzylation, which delivered building block **BB-3** in good yield. The same approach to benzylation was used for **BB-4**. Notably, substrates with Bn in the O-3 position were more reactive than those with Nap, and both the reductive cleavage of benzylidene and benzylation delivered better yields.

In conclusion, four thioglycoside building blocks were synthesized. A new methodology for Gal*f* precursor synthesis was developed, which was superior to some previously reported approaches. The four building blocks will be used in the synthesis glycans moieties from *T. cruzi* and *L. major* GIPLs, to be employed in the development of new diagnostic technics for ChD and leishmaniasis.

5. Experimental Section

5.1. Equipment and Technics

Mass measurements were performed on analytical digital scales, models OHAUS Pioneer PA114 (0,0001g precision) and Sartorius CPA124s (0,0001g precision). TLC was used to verify reaction progress, performed using 0.2 mm Merk silica gel 60 F_{254} plates, visualized under UV lamp and stained by emersion in a solution of 10% H_2SO_4 (v/v) in MeOH, followed by heating to 400 ºC. When required, products were purified by normal-phase flash chromatography, using Merk silica gel 60 (0.040-0.063 mm) as stationary phase and appropriate eluents (indicated below).

NMR spectra were acquired using a Bruker Ascend 400 (400 MHz) or Bruker Avance 400 (440MHz), operating at 100.62 MHz for ^{13}C-NMR and 400.13 MHz for ^{1}H-NMR, at 25 ºC. Samples were dissolved in appropriate deuterated solvents ($CDCl_3$ or D_2O); ^{1}H-NMR spectra were calibrated with the residual solvent signals: 7.26 ppm ($CDCl_3$) and 4.79 ppm (D_2O); ^{13}C-NMR spectra were calibrated with the $CDCl_3$ carbon signal (77.16 ppm, t). Assignment of ^{1}H-NMR and ^{13}C-NMR signals was done with the assistance of 2D NMR experiments (COSY, HSQC, HMBC and NOESY). Chemical shift values (δ) are presented in ppm and coupling constants (*J*) in Hz. Optical rotation (α) of enantiomerically pure product was measured using a Perkin Elmer 343 polarimeter, at 20 ºC, with a 1 cm optical path length; concentrations (c) are presented in g/100 mL. Melting points (MP) of pure solid products were determined on a Stuart SMP 30 Melting Point Apparatus.

5.2. Synthesis and Characterization

5.2.1. Benzyl α-D-galactofuranoside (**I-5**)

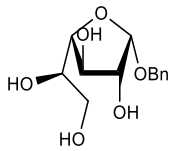

In inert atmosphere, 2.00 g (11.2 mmol) of D-Galactose were partially dissolved in 12 mL of DMPU; the mixture was cooled to 0 ºC, then 1.6 mL (13.5 mmol) of BnBr and 0.4043 g (16.8 mmol) of NaH were added. The mixture was stirred at room temperature for 40 h, then extracted 20 times with 15 mL of hexane. The resulting oil was purified by chromatography (15:1, DCM/MeOH), yielding 1.47 g (5.44 mmol, η= 49 %) of **I-5** as a white solid. R_f = 0.42 (8:1, DCM/MeOH), $[\alpha]_D^{20}$= +89º (*c*= 1.00, H_2O) (lit. +94.9º, *c*= 1.00, H_2O);[151] MP= 122-123 ºC (lit. 124-125 ºC);[151] ^{1}H-NMR spectra was in agreement with the literature.[151]

5.2.2. Benzyl 5,6-*O*-isopropylidene-α-D-galactofuranoside (**I-33**)

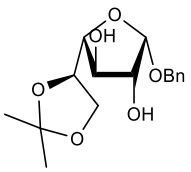

In inert atmosphere, 1.47 g (5.44 mmol) of **I-5** and 2.4 mL (19.6 mmol) of DMP were dissolved in 12 mL of acetone; the solution was cooled to 0 ºC, then 0.0249 g (0.13 mmol) of PTSA.H_2O were added. The mixture was stirred at 0 ºC for 2 h, quenched to pH= 10 with a 20 % aqueous solution of KOH, then concentrated and purified by chromatography (1:1, AcOEt/Hex), yielding 1.1262 g (3.63 mmol, η= 67 %) of **I-33** as a white solid. R_f = 0.23 (1:1, AcOEt/Hex); $[\alpha]_D^{20}$=

+69º (*c*=1.00, $CHCl_3$) (lit. +65.7, *c*= 1.00, $CHCl_3$);[151] MP= 99-101 ºC (lit. 100-101 ºC);[151] ^{1}H-NMR spectra was in agreement with the literature.[151]

5.2.3. Benzyl 5,6-*O*-isopropylidene-2-*O*-(trimethylacetyl)-α-D-galactofuranoside (**1a**)

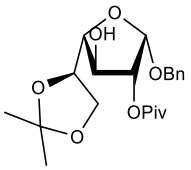

In inert atmosphere, in a round bottom flask containing freshly activated 4 Å molecular sieves, 0.1715 g (0.55 mmol) of **I-33** were dissolved in 10 mL of toluene; 0.4 mL (0.75 mmol) of $(Bu_3Sn)_2O$ were added and the mixture was refluxed (110 ºC) for 5 h 30 min, with a Dean-Stark trap, then concentrated. The resulting residue was dissolved in 1 mL of THF, cooled to 0 ºC, then 0.25 mL (1.79 mmol) of Et_3N, a catalytic amount of DMAP and 0.1 mL (0.81 mmol) of PivCl were added. The mixture was stirred for 1 h 20 min at 0 ºC, diluted with AcOEt, filtered, and sequentially washed with HCl 1 M and saturated $NaHCO_3$ solution; the resulting organic phase was dried with anhydrous Na_2SO_4, filtered, concentrated, and purified by chromatography (3:1, Hex/AcOEt), affording 0.1133 g (0.29 mmol, η= 53 %) of **1a** as a white solid. R_f = 0.49 (2:1, Hex/AcOEt); MP= 103-106 ºC; $[\alpha]_D^{20}$= +75º (*c*= 1.00, DCM); **^{1}H NMR** (400 MHz, $CDCl_3$) δ 7.34-7.24 (m, 5H, C*H* Bn), 5.27 (d, 1H, $J_{1\text{-}2}$= 4.53 Hz, H-1), 4.82-4.76 (m, 2H, H-2, CH_2 A Bn), 4.50, 4.47 (part B of AB system, 1H, $J_{A\text{-}B}$= 12.00 Hz, CH_2 B Bn), 4.31 (t, 1H, $J_{3\text{-}2}$= $J_{3\text{-}4}$= 7.20 Hz, H-3), 4.25 (q, 1H, $J_{5\text{-}6a}$= $J_{5\text{-}6b}$= $J_{4\text{-}5}$= 6.75 Hz, H-5), 4.03, 4.01 (part AX of ABX system, 1H, $J_{6a\text{-}5}$= 6.74 Hz, $J_{6a\text{-}6b}$= 8.55 Hz, H-6a), 3,96-3.90 (m, 2H, H-4, H-6b), 1,46, 1.37 (2s, 3H, CH_3 isopropylidene), 1.20 (s, 9H, CH_3 Piv); **^{13}C NMR** (100 MHz, D_2O) δ 179.32 (C=O Piv), 137.46 (qC Bn), 128.37, 127.78, 127.74 (*C*H Bn), 109.93 (qC isopropylidene), 99.66 (C-1), 82.47 (C-4), 80.14 (C-2), 77.86 (C-5), 74.00 (C-3), 69.61 (*C*H_2 Bn), 65.06 (C-6), 38.78 (qC Piv), 27.17 (*C*H_3 Piv), 26.74, 25.33 (*C*H_3 isopropylidene).

5.2.4. Benzyl 2-*O*-benzoyl-5,6-*O*-isopropylidene-α-D-galactofuranoside (**2a**)

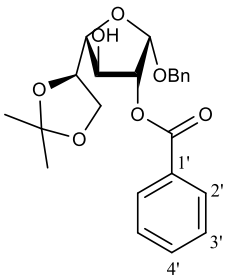

In inert atmosphere, in a round bottom flask containing freshly activated 4 Å molecular sieves, 0.1909 g (0.62 mmol) of **I-33** were dissolved in 10 mL of toluene; 0.42 mL (0.79 mmol) of $(Bu_3Sn)_2O$ were added and the mixture was refluxed (110 ºC) for 5 h with a Dean-Stark trap, then concentrated. The resulting residue was dissolved in 1 mL of THF, cooled to 0 ºC, then 0.26 mL (1.86 mmol) of Et_3N, a catalytic amount of DMAP and 0.07 mL (0.6 mol) of BzCl were added. The mixture was stirred for 30 min at 0 ºC, then 0.02 mL (0.17 mmol) of BzCl were added. After 15 h at room temperature, 0.04 mL (0.34 mmol) of BzCl were added; after another 3 h, 0.02 mL (0.17 mmol) of BzCl were added. 1 h after the last BzCl addition, the mixture was diluted with AcOEt, filtered, and sequentially washed with HCl 1 M and saturated $NaHCO_3$ solution; the resulting organic phase was dried with anhydrous Na_2SO_4, filtered, concentrated, and purified by chromatography (2.5:1, Hex/AcOEt), affording 0.1468 g (0.35 mmol, η= 57 %) of **2a** as a white solid. R_f = 0.37 (2:1,

Hex/AcOEt); MP= 116-119 ºC; $[\alpha]_D^{20}$= +62º (*c*= 1.00, DCM); **^{1}H NMR** (400 MHz, $CDCl_3$) δ 8.07 (d, 2H, $J_{2',3'}$= 7.24 Hz, H-2' Bz), 7.60 (tt, 1H, $J_{3',4'}$= 7.45 Hz, $J_{2',4'}$= 1.24 Hz, H-4' Bz), 7.45 (t, 2H, $J_{2',3'}$= $J_{3',4'}$= 7.45 Hz, H-3' Bz), 7.26 (m, 5H, C*H* Bn), 5.38 (d, 1H, $J_{1\text{-}2}$= 4.55 Hz, H-1), 5.11 (dd, 1H, $J_{2\text{-}3}$= 7.65 Hz, H-2), 4.87, 4.84, 4.58. 4.55 (2 AB systems, 2H, $J_{A\text{-}B}$= 12.09 Hz, CH_2 Bn), 4.49 (t, 1H, $J_{2\text{-}3}$= $J_{3\text{-}4}$= 7.19 Hz, H-3), 4.37 (q, 1H, $J_{5\text{-}6a}$= $J_{5\text{-}6b}$= $J_{4\text{-}5}$= 6.78 Hz, H-5), 4.08-3.94 (m, 3H, H-6, H-4), 1.49, 1.40 (2s, 3H, CH_3 isopropylidene); **^{13}C NMR** (100 MHz, D_2O) δ 167.27 (C=O Bz), 137.41 (qC Bn), 133.68 (C-4' Bz), 130,00 (C-2' Bz), 129.18 (C-1' Bz), 128.57, 128.39, 127.77, 127.66 (*C*H Bn, C-3' Bz), 109.99 (qC isopropylidene), 99.84 (C-1), 82.70 (C-4), 80.74 (C-2), 77.87 (C-5), 74.14 (C-3), 69,73 (*C*H_2 Bn), 65.10 (C-6), 26.75, 25.37 (*C*H_3 isopropylidene).

5.2.5. D-Galactose Diethyldithioacetal (**I-21**)

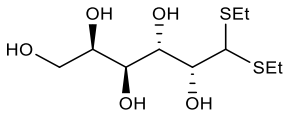

11.7 g (65 mmol) of D-Galactose were dissolved in 16 mL of HCl (fuming). The solution was cooled to 0 ºC, then 9.5 mL (0.13 mol) of EtSH were slowly added over 10 minutes; the solution was removed from the ice bath and stirred at room temperature. After 5 minutes, the mixture turned into a light pink precipitate. After 25 minutes, the solid was broken with a spatula, partially dissolved in MeOH and washed with saturated $NaHCO_3$ solution; the resulting suspension was transferred to a 1L flask and concentrated. The resulting solid was dissolved in boiling ethanol; the solution was acidified (pH=6) with 1M HCl, slowly cooled to room temperature, then chilled to 0 ºC in an ice bath, resulting in the formation of a white, crystalline solid, which was filtered and washed with small portions of 0 ºC ethanol, yielding 15,3 g (53 mmol, η=82%) of product **I-21**. R_f = 0.55 (6:1, DCM/MeOH); MP = 141-142 ºC (lit. 140-142 ºC);[158] $[\alpha]_D^{20}$= +8º (*c*= 1.00, MeOH); **^{1}H NMR** (400 MHz, D_2O) δ 4.12 (dd, 1H, $J_{2\text{-}3}$= 1.44 Hz, $J_{3\text{-}4}$= 9.36 Hz, H-3), 4.07 (d, 1H, $J_{1\text{-}2}$= 8.85 Hz, H-1), 3.95-3.88 (m, 2H, H-2, H-5), 3.66-3.59 (m, 3H, H-6, H-4), 2.76-2,59 (m, 4H, CH_2 SEt), 1.21 (t, 3H, *J*= 7.40 Hz, CH_3 SEt), 1.20 (t, 3H, *J*= 7.40 Hz, CH_3 SEt); **^{13}C NMR** (100 MHz, D_2O) δ 71.11 (C-2), 70.10 (C-2, C-5), 69.76 (C-4), 69.06 (C-3), 63.13 (C-6), 53.84 (C-1), 24.62, 24.58 (*C*H_2 SEt), 13.59, 13.54 (*C*H_3 SEt).

5.2.6. 5,6-*O*-Isopropylidene-D-Galactose Diethyldithioacetal (**3**)

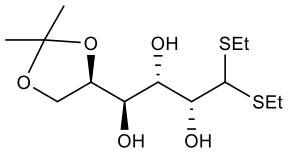

In inert atmosphere, 0.9976 g (3.48 mmol) of **I-21** were dissolved in 35 mL of DMF; the solution was cooled to 0 ºC, then 0.51 mL (4.18 mmol) of DMP and 0.03 mL (0.35 mmol) of TfOH were added. The mixture was stirred for 16 h at 0 ºC, quenched with 1 mL of Et_3N, concentrated, and purified by chromatography (1.5:1, Hex/AcOEt), yielding 0.6671 g (2.04 mmol, η=58.7 %) of **3** as a white solid. R_f = 0.62 (2:1, AcOEt/Hex); MP = 89-90 ºC (lit. 84.5 ºC);[184] $[\alpha]_D^{20}$= +56º (*c*= 1.00, DCM); **^{1}H NMR** (400 MHz, $CDCl_3$) δ 4.37 (td, 1H, $J_{5\text{-}6}$= 6.80 Hz, $J_{5\text{-}4}$=3.85 Hz, H-5), 4.10, 4.07 (part AX of ABX system, 1H, $J_{5\text{-}6a}$= 6.80 Hz, $J_{6a\text{-}6b}$= 8.20 Hz, H-6a), 4.02 (d, 1H, *J*= 9.20 Hz, H-1), 3.95-3.85 (m, 3H, H-2, H-3, H-6b), 3.57 (td, 1H, $J_{4\text{-}5}$= 3.75 Hz, $J_{3\text{-}4}$= $J_{4\text{-}OH4}$= 7.94 Hz, H-4), 3.37 (d, 1H, *J*= 1.80 Hz, O*H*-2), 2.79-2.63 (m, 4H, CH_2 SEt), 2.57 (d, 1H, *J*= 9.54 Hz, O*H*-3), 2.52 (d, 1H, *J*= 7.69 Hz, O*H*-4), 1.43, 1,38 (2s, 3H, CH_3 isopropylidene), 1.28 (t, 6H, *J*= 7.54 Hz, CH_3 SEt); **^{13}C NMR** (100 MHz, $CDCl_3$) δ 109.32 (qC isopropylidene), 75.95 (C-5), 71.77 (C-4), 71.28 (C-3), 70.14 (C-2), 66.58 (C-6),

55.87 (C-1), 26.55 (*C*H$_3$ isopropylidene), 25.78 (*C*H$_2$ SEt), 25.42 (*C*H$_3$ isopropylidene), 23.50 (*C*H$_2$ SEt), 14.74, 14.56 (*C*H$_3$ SEt).

5.2.7. Ethyl 5,6-*O*-isopropylidene-1-thio-α-D-galactofuranoside (**4α**) and Ethyl 5,6-*O*-isopropylidene-1-thio-β-D-galactofuranoside (**4β**)

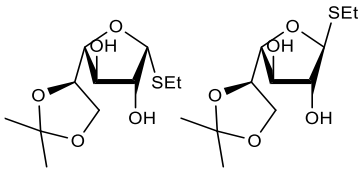

In inert atmosphere, 0.5451 g (1.67 mmol) of **3** were dissolved in 56 mL of DCM; the solution was cooled to -10 ºC in an ice and salt bath, then 0.4588 g (2.04 mmol) of NIS were added, and the resulting solution was vigorously stirred; after 5 min, 5 mL of an aqueous solution of 1M NaOH + $Na_2S_2O_3$ (saturated) was added, and the resulting heterogenous mixture was vigorously shaken, then stirred for 10 min; the aqueous phase was then removed and the organic phase concentrated; the resulting syrup was purified by chromatography (1.5:1, Hex/AcOEt, with 0.5 % Et_3N, v/v), yielding 0.3670 g (1.39 mmol, η_{total}= 83 %, η_{α}= 66 %) of **4** (1:0.25 α/β, as determined by integration of H-1 signals in ^{1}H-NMR) as a white solid. R_f = 0.43 (2:1, AcOEt/Hex); **^{1}H NMR** (400 MHz, $CDCl_3$) δ 5.34-5.30 (m, 1.25H, H-1α, H-1β), 4.36 (td, 0.25H, $J_{4\text{-}5}$= 1.79 Hz, $J_{5\text{-}6}$= 7.39Hz, H-5β), 4.28 (ddd, 1H, $J_{4\text{-}5}$= 2.78 Hz, $J_{5\text{-}6a}$= 6.90 Hz, $J_{5\text{-}6b}$= 7.97 Hz, H-5α), 4.21 (broad s, 1H, H-3α), 4.13-3.96 (m, 4.25H, H-2α, H-6α, H-2β, H-3β, H-4β, H-6β), 3.87 (t, 1H, $J_{3\text{-}4}$= $J_{4\text{-}5}$= 2.78 Hz, H-4α), 2.77-2.60 (m, 2.5 H, C*H*$_2$ SEt α, C*H*$_2$ SEt β), 1.49 (s, 3H, C*H*$_3$ isopropylidene α), 1.42 (s, 0.75H, C*H*$_3$ isopropylidene β), 1.38 (s, 3.75H, C*H*$_3$ isopropylidene α, C*H*$_3$ isopropylidene β), 1.34-1.27 (m, 3.75H, C*H*$_3$ SEt α, C*H*$_3$ SEt β); **^{13}C NMR** (100 MHz, $CDCl_3$) δ 110.42 (qC isopropylidene α), 110.22 (qC isopropylidene β), 89.87 (C-1β), 89.46 (C-1α), 84.66 (*C*H β), 84.00 (C-4α), 81.27 (*C*H β), 79.67 (*C*H β), 78.87 (C-3α), 78.78 (C-2α), 76.57 (C-5α), 75.99 (C-5β), 65.70 (C-6α, C-6β), 26.27 (*C*H$_3$ isopropylidene α), 26.02, 25.97 (*C*H$_3$ isopropylidene α, *C*H$_2$ SEt α), 25.81, 25.71, 25.08 (*C*H$_3$ isopropylidene β, *C*H$_2$ SEt β), 15.70 (*C*H$_3$ SEt α), 14.93 (*C*H$_3$ SEt β).

5.2.8. Ethyl 2-*O*-benzoyl-5,6-*O*-isopropylidene-1-thio-α-D-galactofuranoside (**5a**)

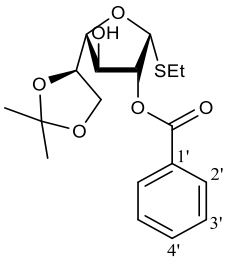

In inert atmosphere, 0.1010 g (0.38 mmol, 1α:0.12β) of **4** were dissolved in 4 mL of THF; the solution was cooled to 0 ºC, then 0.16 mL (1.15 mmol) of Et_3N, 44.5 µL (0.38 mmol) of BzCl and a catalytic amount of DMAP were added; the resulting suspension was stirred at 0 ºC for 1 h, diluted with AcOEt, sequentially washed with HCl 1 M and saturated $NaHCO_3$ solution; the resulting organic phase was dried with anhydrous Na_2SO_4, filtered, concentrated and purified by chromatography (2.5:1 Hex/AcOEt), affording 0.0579 g (0.16 mmol, η= 46 %, corrected for α portion of the starting material) of **5a** as a white solid. R_f = 0.44 (2:1, Hex/AcOEt); MP= 85-87 ºC; $[\alpha]_D^{20}$= +42º (*c*= 1.00, DCM); **^{1}H NMR** (400 MHz, $CDCl_3$) δ 8.05 (dd, 2H, $J_{2'\text{-}3'}$= 8. 40 Hz, $J_{2'\text{-}4'}$=1.30 Hz, H-2' Bz), 7.58 (tt, 1H, $J_{2'\text{-}4'}$= 1.30 Hz, $J_{3'\text{-}4'}$= 7.44 Hz, H-4' Bz), 7.44 ("t", 2H, *J*=7.84 Hz, H-3' Bz), 5.53 (d, 1H, $J_{1\text{-}2}$= 5.56 Hz, H-1), 5.30 (dd, 1H, $J_{1\text{-}2}$= 5.47 Hz, $J_{2\text{-}3}$= 4.39 Hz, H-2), 4.37 (q, 1H, $J_{4\text{-}5}$= $J_{5\text{-}6a}$= $J_{5\text{-}6b}$= 6.68 Hz, H-5), 4.27 (dd, 1H, $J_{2\text{-}3}$= 4.39 Hz, $J_{3\text{-}4}$= 6.36 Hz, H-3), 4.05, 4.03 (part AX of ABX system, 1H, $J_{6a\text{-}6b}$= 8.56 Hz,

H-6a), 3.95, 3.93 (part BX of ABX system, 1H, H-6b), 3.88 (t, 1H, $J_{3\text{-}4}$= $J_{4\text{-}5}$= 6.60 Hz, H-4), 3.50 (s, 1H, O*H*), 2.80-2.70 (m, 1H, CH_2 SEt), 1.45, 1.36 (2s, 3H, CH_3 isopropylidene), 1.28 (t, 3H, *J*= 7.45 Hz, CH_3 SEt); **^{13}C NMR** (100 MHz, $CDCl_3$) δ 166.94 (C=O Bz), 133.81 (C-4' Bz), 130.06 (C-2' Bz), 129.05 (C-1' Bz), 128.66 (C-3' Bz), 109.97 (qC isopropylidene), 85.19 (C-1), 83.85 (C-4), 82.35 (C-2), 76.87 (C-3), 76.61 (C-5), 65.31 (C-6), 26.62 (*C*H_3 isopropylidene), 25.48, 25.41 (*C*H_2 SEt, CH_3 isopropylidene), 15.02 (*C*H_3 SEt).

5.2.9. Ethyl 5,6-*O*-isopropylidene-1-thio-2-*O*-(trimethylacetyl)-α-D-galactofuranoside (**6α**)

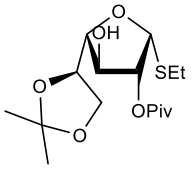

In inert atmosphere, 2.31 g (8.74 mmol, 1α:0.35β) of **4** were dissolved in 90 mL of THF; to this solution 0.3325 g (2.72 mmol) of DMAP, 1.4 mL (11.4 mmol) of PivCl and 1.9 mL (13.5 mmol) of Et_3N were added; the resulting suspension was stirred at room temperature for 4 h 30 min, 0.4 mL (3.25 mmol) of PivCl were added; after stirring for an additional 1h 30 min, the mixture was diluted with AcOEt, washed sequentially with HCl 1 M and saturated $NaHCO_3$ solution; the resulting organic phase was dried with anhydrous $MgSO_4$, filtered, concentrated and purified by chromatography (4:1 Hex/AcOEt to 100 % AcOEt), affording 1.0708 g (3.07 mmol, η= 47 %, corrected for α portion of the starting material) of product **6α** as a white solid. R_f = 0.46 (2:1, Hex/AcOEt); $[\alpha]_D^{20}$= +55º (*c*= 1.00, DCM); MP= 70-71 ºC; **^{1}H NMR** (400 MHz, $CDCl_3$) δ 5.42 (d, 1H, $J_{1\text{-}2}$= 5.50 Hz, H-1), 5.01 (dd, 1H, $J_{2\text{-}3}$=4.30 Hz, H-2), 4.35 (q, 1H, $J_{4\text{-}5}$= $J_{5\text{-}6}$= 6.60 Hz, H-5), 4.10-4.06 (m, 1H, H-3), 4.05, 4.02 (part AX of ABX system, 1H, $J_{5\text{-}6a}$= 6.70 Hz, $J_{6a\text{-}6b}$= 8.60 Hz), 3.93, 3.91 (part BX of ABX system, 1H, $J_{5\text{-}6b}$= 6.70 Hz, H-6b), 3.81 (t, 1H, $J_{3\text{-}4}$= $J_{4\text{-}5}$= 6.45 Hz, H-4), 3.12 (broad s, 1H, O*H*-3), 2.70 (q, 2H, *J*= 7.35 Hz, CH_2 SEt), 1.44, 1.36 (2s, 3H, CH_3 isopropylidene), 1.27 (t, 3H, *J*= 7.43 Hz, CH_3 SEt), 1.23 (s, 9H, CH_3 – Piv); **^{13}C NMR** (100 MHz, $CDCl_3$) δ 179.07 (C=O Piv), 109.97 (qC isopropylidene), 85.20 (C-1), 83.76 (C-4), 81.66 (C-2), 76.80 (C-3), 76.45 (C-5), 65.32 (C-6), 39.09 (qC Piv), 27.17 (*C*H_3 Piv), 26.63 (*C*H_3 isopropylidene) 25.47, 25.36 (*C*H_2 SEt, *C*H_3 isopropylidene), 15.03 (*C*H_3 SEt).

5.2.10. Ethyl 5,6-*O*-isopropylidene-3-*O*-levulinoyl-1-thio-2-*O*-(trimethylacetyl)-α-D-galactofuranoside (**7**)

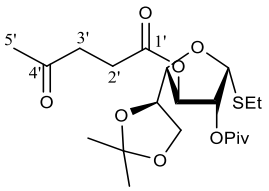

0.3401 g (0.98 mmol) of **6α** and 0.1631 g (1.40 mmol) of LevOH were dissolved in 10 mL of DCM; the solution was cooled to 0 ºC, then 0.0354 g (0.29 mmol) of DMAP and 0.2 mL (1.28 mmol) of DIC were added. The mixture was stirred at room temperature for 16 h, concentrated, and purified by chromatography (2.5:1, Hex/AcOEt), yielding 0.3862 g (0.87 mmol, η= 89%) of **7** as a syrup. R_f = 0.74 (1:1, AcOEt/Hex); **^{1}H NMR** (400 MHz, $CDCl_3$) δ 5.38 (d, 1H, $J_{1\text{-}2}$= 4.82 Hz, H-1), 5.31 (dd, 1H, $J_{1\text{-}2}$= 4.82 Hz, $J_{2\text{-}3}$= 3.10 Hz, H-2), 5.13 (dd, 1H, $J_{3\text{-}4}$= 4.55 Hz, H-3), 4.39 (q, 1H, $J_{4\text{-}5}$= $J_{5\text{-}6}$= 6.66 Hz, H-5), 4.03, 4.00 (part AX of ABX system, 1H, $J_{5\text{-}6a}$= 6.66 Hz, $J_{6a\text{-}6b}$= 8.53 Hz, H-6a), 3.90 (dd, 1H, $J_{3\text{-}4}$= 4.58 Hz, $J_{4\text{-}5}$= 6.63 Hz, H-4), 3.82, 3.80 (part BX of ABX system, 1H, $J_{5\text{-}6b}$= 6.87 Hz, H-6b), 2.84-2.66 (m, 4H, CH_2 SEt, H-3' Lev), 2.64-2.49 (m, 2H, H-2' Lev), 2.17 (s, 3H, H-5' Lev), 1.42, 1.35 (2s, 3H, CH_3 isopropylidene), 1.27 (t, 3H, *J*= 7.42 Hz, CH_3 SEt), 1.22 (s, 9H, CH_3 Piv); **^{13}C NMR** (100

MHz, $CDCl_3$) δ 206.15 (C-4' Lev), 177.11 (C=O Piv), 171.62 (C-1' Lev), 110.02 (qC isopropylidene), 86.26 (C-1), 83.12 (C-4), 77.54, 77.41 (C-2, C-3), 76.14 (C-5), 65.52 (C-6), 39.03 (qC Piv), 37.91 (C-3' Lev), 29.87 (C-5' Lev), 27.90 (C-2' Lev), 27.16 (*C*H_3 Piv), 26.59 (*C*H_3 isopropylidene), 25.72, 25.48 (*C*H_3 isopropylidene, *C*H_2 SEt), 15.11 (CH_3 SEt).

5.2.11. Ethyl 3-*O*-levulinoyl-1-thio-2-*O*-(trimethylacetyl)-α-D-galactofuranoside (**8**)

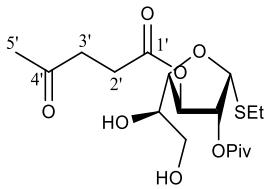

0.3862 g (0.87 mmol) of **7** was dissolved in a mixture of 6 mL AcOH and 4 mL H_2O; the mixture was stirred for 16 h at room temperature at which point TLC analysis of the reaction mixture indicated full conversion; the product was concentrated, yielding 0.3515 g (0.87 mmol, quantitative yield) of **8** as a syrup. R_f = 0.13 (1:1, AcOEt/Hex); $[\alpha]_D^{20}$= +100º (*c*= 1.00, DCM); **^{1}H NMR** (400 MHz, $CDCl_3$) δ 5.45 (d, 1H, *J*= 5.08 Hz, H-1), 5.35 (dd, 1H, $J_{2\text{-}3}$= 3.34 Hz, H-2), 5.28 (dd, 1H, $J_{3\text{-}4}$= 4.07 Hz, H-3), 4.01 (t, 1H, $J_{3\text{-}4}$=$J_{4\text{-}5}$= 4.32 Hz, H-4), 3.93-3.85 (m, 1H, H-5), 3.76-3.64 (m, 2H, H-6), 2.86-2.50 (m, 7H, H-2' Lev, H-3' Lev, C*H*$_2$ SEt, O*H*-5), 2.37-2.29 (m, 1H, O*H*-6), 2.18 (s, 3H, H-5' Lev), 1.30 (t, 3H, *J*= 7.45 Hz, C*H*$_3$ SEt), 1.22 (s, 9H, C*H*$_3$ Piv); **^{13}C NMR** (100 MHz, $CDCl_3$) δ 206.59 (C-4' Lev), 177.26 (C=O Piv), 172.18 (C-1' Lev), 86.91 (C-1), 84.16 (C-4), 77.77 (C-3), 77.28 (C-2), 70.73 (C-5), 64.09 (C-6), 39.05 (qC Piv), 37.98 (C-3' Lev), 29.91 (C-5' Lev), 27.87 (C-2' Lev), 27.16 (*C*H_3 Piv), 26.10 (*C*H_2 SEt), 15.36 (*C*H_3 SEt).

5.2.12. Ethyl 5,6-*O*-isopropylidene-3-*O*-(2-naphtylmethyl)-1-thio-2-*O*-(trimethylacetyl)-α-D-galactofuranoside (**10**)

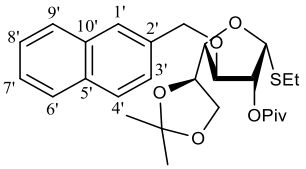

In inert atmosphere, 1.0446 g (3.0 mmol) of **6α** and 1.0754 g (4.86 mmol) of NapBr were dissolved in 30 mL of dry DMF; freshly activated 4 Å molecular sieves were added, the mixture was cooled to 0 ºC, and 0.2232 g (in mineral oil, 60 %, 5.58 mmol) of NaH were added. The mixture was stirred for 1 h at room temperature, filtered, and washed with saturated $NaHCO_3$ solution; the resulting organic phase was dried with anhydrous $MgSO_4$, filtered, concentrated, and purified by chromatography (15:1, Hex/AcOEt), affording 1.3483 g (2.76 mmol, η= 92 %) of **10** as a syrup. R_f = 0.52 (4:1, Hex/AcOEt); $[\alpha]_D^{20}$= +19º (*c*= 1.00, DCM); **^{1}H NMR** (400 MHz, $CDCl_3$) δ 7.86-7.79 (m, 3H, C*H* Nap), 7.77 (s, 1H, H-1' Nap), 7.52-7.41 (m, 3H, C*H* Nap), 5.39 (d, 1H, $J_{1\text{-}2}$= 4.49 Hz, H-1), 5.36 (dd, 1H, $J_{2\text{-}3}$= 2.54 Hz, H-2), 4.95, 4.92, 4.74, 4.72 (AB system, 1H, $J_{A\text{-}B}$= 11.77 Hz, C*H*$_2$ Nap), 4.28 (q, 1H, $J_{4\text{-}5}$= $J_{5\text{-}6a}$= $J_{5\text{-}6b}$= 6.66 Hz, H-5), 3.94 (dd, 1H, $J_{3\text{-}4}$= 5.01Hz, H-4), 3.90 (dd, 1H, $J_{2\text{-}3}$= 2.50 Hz, H-3), 3.85, 3.83, 3.79, 3.76 (ABX system, 2H, $J_{5\text{-}6a}$= 6.72 Hz, $J_{5\text{-}6b}$= 6.82 Hz , $J_{6a\text{-}6b}$= 8.50 Hz, H-6), 2.72 (q, 2H, *J*= 7.40 Hz, C*H*$_2$ SEt), 1.39, 1.33 (2s, 3H, C*H*$_3$ isopropylidene), 1.31-1.25 (m, 12H, C*H*$_3$ SEt, C*H*$_3$ Piv); **^{13}C NMR** (100 MHz, $CDCl_3$) δ 177.60 (C=O), 134.51 (C-2' Nap), 133,22, 133.17 (C-5' Nap, C-10' Nap), 128.45, 127.98, 127.80, 127.21, 126.34, 126.21, 126.00 (C-1' Nap, C-3' Nap, C-4' Nap, C-6' Nap, C-7' Nap, C-8' Nap, C-9' Nap), 109.89 (qC isopropylidene), 86.15 (C-1), 83.93 (C-4), 82.98 (C-3), 78.61 (C-2), 76.19 (C-5), 72.36 (*C*H_2 Nap), 65.36 (C-6), 39.06 (qC Piv), 27.20

(*C*H$_3$ Piv), 26.54 (*C*H$_3$ isopropylidene), 25.88 (*C*H$_2$ SEt), 25.26 (*C*H$_3$ isopropylidene), 15.15 (*C*H$_3$ SEt).

5.2.13. Ethyl 3-*O*-(2-naphtylmethyl)-1-thio-2-*O*-(trimethylacetyl)-α-D-galactofuranoside (**11**)

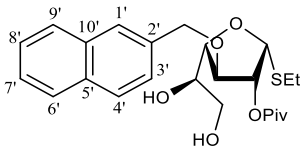

1.3313 g (2.72 mmol) of **10** was dissolved in a mixture of 15 mL of AcOH and 10 mL of H$_2$O; the mixture was stirred at 60 ºC for 2 h 30 min, then concentrated and purified by chromatography (2:1, Hex/AcOEt), yielding 1.2023 g (2.68 mmol, η= 99 %) of **11** as a syrup. R$_f$ = 0.24 (2:1, Hex/AcOEt); $[\alpha]_D^{20}$= + 44º (*c*= 1.00, DCM); **^{1}H NMR** (400 MHz, CDCl$_3$) δ 7.86-7.80 (m, 3H, C*H* Nap), 7.77 (broad s, 1H, H-1' Nap), 7.51-7.46 (m, 2H, C*H* Nap), 7.44 (dd, 1H, $J_{1'\text{-}3'}$= 1.41 Hz, $J_{3'\text{-}4'}$= 8.39 Hz, H-3' Nap), 5.48 (d, 1H, $J_{1\text{-}2}$= 5.04 Hz, H-1), 5.33 (dd, 1H, $J_{2\text{-}3}$= 3.73 Hz, H-2), 4.95, 4.92, 4.78, 4.75 (AB system, 1H, $J_{A\text{-}B}$= 11.74 Hz, C*H*$_2$ Nap), 4.22 (dd, 1H, $J_{3\text{-}4}$= 5.07 Hz, H-3), 4.05 (dd, 1H, $J_{4\text{-}5}$= 3.64 Hz, H-4), 3.77-3.70 (m, 1H, H-5), 3.69-3.62 (m, 2H, H-6a, H-6b), 2.76-2.62 (m, 3H, C*H*$_2$ SEt, O*H*-5), 2.13 (broad s, 1H, O*H*-6), 1.30 (t, 3H, *J*= 7.45 Hz, C*H*$_3$ SEt), 1.25 (s, 9H, C*H*$_3$ Piv); **^{13}C NMR** (100 MHz, CDCl$_3$) δ 177.67 (C=O Piv), 134.73 (C-2'), 133.31, 133.22 (C-5' Nap, C-10' Nap), 128.53, 128.02, 127.85 (*C*H Nap), 126.96 (C-1' Nap), 126.39, 126.24 (*C*H Nap), 125.73 (C-3' Nap), 86.98 (C-1), 84.06 (C-4), 82.76 (C-3), 78.42 (C-2), 72.67 (*C*H$_2$ - Nap), 71.07 (C-5), 64.58 (C-6), 39.04 (qC Piv), 27.20 (*C*H$_3$ Piv), 26.16 (*C*H$_2$ SEt), 15.41 (C*H*$_3$ SEt).

5.2.14. Ethyl 4,5-di-*O*-acetyl-3-*O*-(2-naphtylmethyl)-1-thio-2-*O*-(trimethylacetyl)-α-D-galactofuranoside (**BB-1e**)

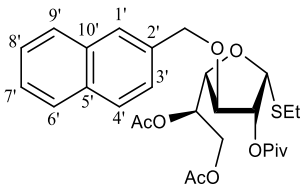

0.8614 g (1.92 mmol) of **B-10** were dissolved 19 mL of pyridine, then 0.73 mL (7.73 mmol) of Ac$_2$O and 0.1120 g (0.92 mmol) of DMAP were added. The mixture was stirred for 1 h, concentrated, and purified by chromatography (5:1, Hex/AcOEt), affording 0.9966 g (1.87 mmol, η= 97 %) of **B-12** as a syrup. R$_f$ = 0.46 (4:1, Hex/AcOEt); $[\alpha]_D^{20}$= +50º (*c*= 1.00, DCM); **^{1}H NMR** (400 MHz, CDCl$_3$) δ 7.86-7.89 (m, 3H, C*H* Nap), 7.75 (broad s, 1H, H-1' Nap), 7.51-7.45 (m, 2H, C*H* Nap), 7.42 (dd, 1H, $J_{1'\text{-}3'}$= 1.34 Hz, $J_{3'\text{-}4'}$= 3.47 Hz, H-3' Nap), 5.43 (d, 1H, $J_{1\text{-}2}$= 5.03 Hz, H-1), 5.39-5.31 (m, 2H, H-2, H-5), 4.92, 4.89, 4.74, 4.72 (AB system, 1H, $J_{A\text{-}B}$= 11.62 Hz, C*H*$_2$ Nap), 4.34, 4.31, 4.12, 4.09 (ABX system, 2H, $J_{5\text{-}6a}$= 3.81 Hz, $J_{5\text{-}6b}$= 6.87 Hz, $J_{6a\text{-}6b}$= 11.99 Hz, H-6a, H-6b), 4.07-4.03 (m, 2H, H-3, H-4), 2.66 (q, 2H, *J*= 7.40 Hz, C*H*$_2$ SEt), 1.99, 1.97 (2s, 3H, C*H*$_3$ Ac), 1.30-1.23 (m, 12H, C*H*$_3$ SEt, C*H*$_3$ Piv); **^{13}C NMR** (100 MHz, CDCl$_3$) δ 172.62 (C=O Piv), 170.67, 170.32 (C=O Ac), 134.49 (C-2'), 133.23, 133.22 (C-5' Nap, C-10' Nap), 128.57, 128.02, 127.83 (*C*H Nap), 127.15 (C-1' Nap), 126.38, 126.27 (*C*H Nap), 125.87 (C-3' Nap), 86.10 (C-1), 82.08 (C-3), 80.57 (C-4), 78.41 (C-2), 72.69 (*C*H$_2$ Nap), 70.43 (C-5), 62.78 (C-6), 39.01 (qC Piv), 27.22 (*C*H$_3$ Piv), 25.60 (*C*H$_2$ SEt), 20.97, 20.82 (*C*H$_3$ Ac), 15.16 (*C*H$_3$ SEt).

5.2.15. Ethyl 2,3-di-*O*-benzyl-4,6-*O*-benzylidene-1-thio-β-D-galactopyranoside (**14**)

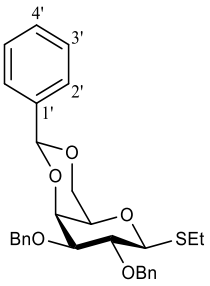

In inert atmosphere, 1,994 g (6.38 mmol) of **13** were dissolved in 60 mL of DMF; the solution was cooled to 0 ºC, then 2.4 mL (20.1 mmol) of BnBr and 0.4578 g (19.1 mmol) of NaH were added. The mixture was stirred at room temperature for 17 h, then diluted with DCM and washed with saturated $NaHCO_3$ solution; the resulting aqueous phase was back-extracted with DCM twice; the combined organic phases were then dried with anhydrous Na_2SO_4, filtered, concentrated, and purified by chromatography (2.5:1, Hex/AcOEt), affording 1.8694 g (3.79 mmol, η= 60 %) of **14** as a syrup. R_f = 0.27 (3:1, Hex/AcOEt); **^{1}H NMR** (400 MHz, $CDCl_3$) δ 7.58 (dd, 2H, $J_{2'\text{-}4'}$= 1.39 Hz, $J_{2'\text{-}3'}$= 7.83 Hz, H-2' benzylidene, H-6' benzylidene), 7.48 – 7.28 (m, 13H, H-4´ benzylidene, C*H* Bn2, C*H* Bn3), 5.50 (s, 1H, C*H* benzylidene), 4.94, 4.92, 4.89, 4.86 (AB system , 2H, $J_{A\text{-}B}$=10.16 Hz, CH_2 Bn2), 4.79 (s, 2H, CH_2 Bn3), 4.47 (d, 1H, $J_{1\text{-}2}$= 9.64 Hz, H-1), 4.34, 4.31 (part AX of ABX system, 1H, $J_{6a\text{-}6b}$= 12.36 Hz, $J_{6a\text{-}5}$= 1,00 Hz, H-6a), 4.17 (d, 1H, $J_{3\text{-}4}$= 3.45 Hz, H-4), 4.01-3.88 (m, 2H, H-2, H-6b), 3.62 (dd, 1H, $J_{2\text{-}3}$= 9.19 Hz, H-3), 3.35 (s, 1H, H-5), 2.96-2.73 (m, 2H, CH_2 SEt), 1.36 (t, 3H, *J*= 7.42 Hz, CH_3 SEt); **^{13}C NMR** (100 MHz, $CDCl_3$) δ 138.41, 138.31, 137.97 (C-1' benzylidene, qC Bn2, qC Bn3), 129.10, 128.46, 128.38, 128.26, 127.82, 127.80,126.62 (C-2' benzylidene, C-3' benzylidene, C-4' benzylidene, *C*H Bn2, *C*H Bn3), 101.52 (*C*H benzylidene), 84.42 (C-1), 81.08 (C-3), 76.91 (C-2), 75.78 (*C*H_2 Bn2), 73.97 (C-4), 71.79 (*C*H_2 Bn3), 69.78 (C-5), 69.45 (C-6), 23.86 (*C*H_2 SEt), 15.16 (*C*H_3 SEt).

5.2.16. Ethyl 2,3-di-*O*-benzyl-1-thio-β-D-galactopyranoside (**17**)

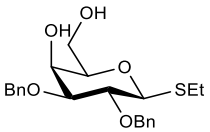

1.2536 g (2.54 mmol) of **14** and 0.2416 g (1.33 mmol) of PTSA were dissolved in a mixture of 12 mL of MeOH and 3 mL DCM. The mixture was stirred at 40 ºC for 24 h, quenched with 0.5 g of $NaHCO_3$, concentrated, dissolved in DCM and washed with brine; the resulting aqueous phase was back-extracted 3 times with DCM; the combined organic phases were then dried with anhydrous Na_2SO_4, filtered, concentrated and purified by chromatography (1.5:1, AcOEt/Hex), affording 0.8628 g (2.13 mmol, η= 84%) of **17** as a white solid. R_f = 0.24 (1:1, Hex/AcOEt); $[\alpha]_D^{20}$= +4º (*c*= 1.00, DCM); MP= 93-94 ºC; **^{1}H NMR** (400 MHz, $CDCl_3$) δ 7.43-7.27 (m, 10H, C*H* Bn2, C*H* Bn3), 4.90, 4.88, 4.79, 4.76 (AB system, 2H, $J_{A\text{-}B}$=10.25 Hz, CH_2 Bn2), 4.73 (s, 2H, CH_2 Bn3), 4.44 (d, 1H, $J_{1\text{-}2}$= 9.72 Hz, H-1), 4.06 (broad s, 1H, H-4), 3.96, 3.93 (part AXY of ABXY system, 1H, $J_{6a\text{-}OH6}$= 4.37 Hz, $J_{5\text{-}6a}$= 6.45 Hz, $J_{6a\text{-}6b}$= 11.48 Hz, H-6a), 3.81, 3.78 (part BXY of ABXY system, 1H, $J_{5\text{-}6b}$= 4.66 Hz, $J_{6b\text{-}OH6}$= 8.06, H-6b), 3.68 (t, 1H, $J_{1\text{-}2}$= $J_{2\text{-}3}$= 9.46 Hz, H-2), 3.55 (dd, 1H, $J_{3\text{-}4}$=3.28 Hz, H-3), 3.47 (broad t, 1H, *J*=5.59 Hz, H-5), 2.85-2.69 (m, 3H, CH_2 SEt, O*H*-4), 2.49 (dd, 1H, O*H*-6), 1.32 (t, 3H, *J*=7.42 Hz, CH_3 SEt); **^{13}C NMR** (100 MHz, $CDCl_3$) δ 138.14 (qC Bn3), 137.70 (qC Bn2), 128.65, 128.46, 128.43, 128.13, 127.96, 127.93(*C*H Bn2, C*H* Bn3), 85.25 (C-1), 82.25 (C-3), 77.91 (C-5), 77.84 (C-2), 75.91 (*C*H_2 Bn2), 72.27 (*C*H_2 Bn3), 67.41 (C-4), 62.69 (C-6), 24.95 (*C*H_2 SEt), 15.21 (*C*H_3 SEt).

5.2.17. Ethyl 2,3-di-*O*-benzyl-6-*O*-levulinoyl-1-thio-β-D-galactopyranoside (**18a**)

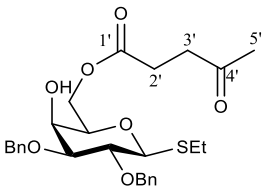

In inert atmosphere, 1.6585 g (4.10 mmol) of **17**, 0.4771 g (4.11 mmol) of LevOH and 0.1621 g (1.33 mmol) of DMAP were dissolved in 40 mL of DCM; 1.4 mL (4.34 mmol) of DIC were added, and the solution was stirred at room temperature for 2 h 30 min, then concentrated and purified by chromatography (2:1, Hex/AcOEt), affording 1.3589 g (2.70 mmol, η= 66%) of **C-6** as a syrup. R_f = 0.30 (1.5:1, Hex/AcOEt); $[\alpha]_D^{20}$= +14º (*c*= 1.00, DCM); **^{1}H NMR** (400 MHz, $CDCl_3$) δ 7.42-7.27 (m, 10H, C*H* Bn2, C*H* Bn3), 4.88, 4.86, 4.77, 4.75 (AB system, 2H, $J_{A\text{-}B}$= 10.26 Hz, CH_2 Bn2), 4.73 (s, 2H, CH_2 Bn3), 4.43 (d, 1H, $J_{1\text{-}2}$= 9.66 Hz, H-1), 4.37, 4.34, 4.32, 4.29 (ABX system, 2H, $J_{5\text{-}6a}$= 5.83 Hz, $J_{5\text{-}6b}$= 6.84 Hz, $J_{6a\text{-}6b}$= 11.45 Hz, H-6), 4.02 (broad s, 1H, H-4), 3.68-3.54 (m, 3H, H-2, H-3, H-5), 2.84-2.67 (m, 4H, CH_2 SEt, H-3' Lev), 2.61-2.55 (m, 2H, H-2' Lev), 2.48 (d, 1H, $J_{4\text{-}OH4}$= 1.52 Hz, O*H*-4), 2.19 (s, 3H, H-5' Lev), 1.32 (t, 3H, *J*= 7.44 Hz, CH_3 SEt); **^{13}C NMR** (100 MHz, $CDCl_3$) δ 206.69 (C-4' Lev), 172.77 (C-1' Lev), 138.15 (qC Bn2), 137.71 (qC Bn3), 128.66, 128.46, 128.44, 128.14, 128.01, 127.94 (*C*H Bn2, *C*H Bn3), 85.21 (C-1), 82.11 (C-3), 77.80 (C-2), 75.92 (*C*H_2 Bn2), 75.50 (C-5), 72.28 (*C*H_2 Bn3), 66.55 (C-4), 63.36 (C-6), 38.01 (C-3' Lev), 29.98 (C-5' Lev), 27.95 (C-2' Lev), 25.03 (*C*H_2 SEt), 15.24 (*C*H_3 SEt).

5.2.18. Ethyl 4-*O*-benzoyl-2,3-di-*O*-benzyl-6-*O*-levulinoyl-1-thio-β-D-galactopyranoside (**BB-2**)

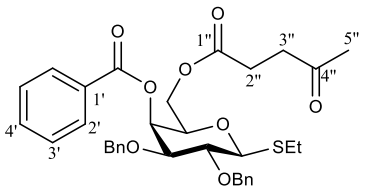

In inert atmosphere, 1.1254 g (2.24 mmol) of **18a** and 0.0848 g (0.69 mmol) DMAP were dissolve in 15 mL of THF; 0.4 mL (3.44 mmol) of BzCl and 1 mL (7.17 mmol) of Et_3N were added, and the mixture was refluxed 3 h, then diluted with DCM, and washed sequentially with HCl 1 M and saturated $NaHCO_3$ solution; the resulting organic phase was dried with anhydrous $MgSO_4$, filtered, concentrated and purified by chromatography (2.5:1, Hex/AcOEt), affording 1.1777 g (1.94 mmol, η= 87 %) of **C-7** as a syrup. R_f = 0.26 (2.5:1, Hex/AcOEt); $[\alpha]_D^{20}$= +29º (*c*= 1.00, DCM); **^{1}H NMR** (400 MHz, $CDCl_3$) δ 8.10 (d, 2H, $J_{2',4'}$= 1.30 Hz, $J_{2',3'}$= 8.46 Hz, H-2' Bz), 7.60 (tt, 1H, $J_{2',4'}$= 1.20 Hz, $J_{3',4'}$=7.34 Hz, H-4' Bz), 7.47 (t, 2H, *J*= 7.83 Hz, H-3' Bz), 7.38-7.32 (m, 10H, C*H* Bn2, C*H* Bn3), 5.81 (d, 1H, *J*= 2.90 Hz, H-4), 4.86, 4.83 (part A of AB system, 1H, $J_{A\text{-}B}$= 11.47, CH_2 A Bn3), 4.83, 4.81, 4.77, 4.74 (AB system, 2H, $J_{A\text{-}B}$= 10.26 Hz, CH_2 Bn2), 4.59, 4.56 (part B of AB system, 1H, CH_2 B Bn3), 4.55 (d, 1H, $J_{1\text{-}2}$= 9.17 Hz , H-1), 4.30, 4.27, 4.15, 4.12 (ABX system, 2H, $J_{5\text{-}6a}$= 6.90 Hz, $J_{5\text{-}6b}$= 6.33 Hz $J_{6a\text{-}6b}$= 11.30 Hz, H-6), 3.90 (t, 1H, $J_{4\text{-}5}$= $J_{5\text{-}6}$= 6.60 Hz, H-5), 3.75 (dd, 1H, $J_{3\text{-}4}$= 3.20 Hz, $J_{2\text{-}3}$= 9.16 Hz, H-3), 3.68 (t, 1H, $J_{1\text{-}2}$= $J_{2\text{-}3}$= 9.30 Hz, H-2), 2.87-2.72 (m, 4H, CH_2 SEt, H-3'' Lev), 2.59-2.53 (m, 2H, H-2'' Lev), 2.19 (s, 3H, H-5'' Lev), 1.36 (t, 3H, *J*= 7.45 Hz, CH_3 SEt); **^{13}C NMR** (100 MHz, $CDCl_3$) δ 206.68 (C-4'' Lev), 172.46 (C-1'' Lev), 165.83 (C=O Bz), 138.13, 137.73 (qC Bn2, qC Bn3), 133.45 (C-4' Bz), 130.11 (C-2' Bz), 129.69, 128.60, 128.52, 128.43, 128.42, 128.26, 127.91, 127.84 (*C*H Bn2, *C*H Bn3, C-1' Bz, C-3' Bz), 85.62 (C-1), 81.00 (C-3), 77.72 (C-2), 76.00 (*C*H_2 Bn2),

74.52 (C-5), 71.93 (*C*H$_2$ Bn3), 67.32 (C-4), 62.56 (C-6), 38.04 (C-3'' Lev), 29.95 (C-5'' Lev), 27.98 (C-2'' Lev), 25.18 (*C*H$_2$ SEt), 15.25 (*C*H$_3$ SEt).

5.2.19. Ethyl 4,6-*O*-benzylidene-3-*O*-(2-naphtylmethyl)-1-thio-α-D-mannopyranoside (**20**)

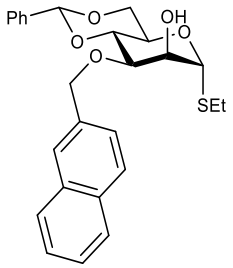

2.33 g (7.46 mmol) of commercially available **19** were dissolved in 150 mL of toluene; 5.15 mL (9.69 mmol) of $(Bu_3Sn)_2O$ and freshly activated 4 Å molecular sieves were added; the mixture was refluxed for 6 h (110 ºC), with a Dean-Stark trap, then cooled to room temperature; 2.14 g (9.69 mmol) of NapBr and 3.58 g (9.69 mmol) of TBAI were added, and the mixture was refluxed for 24 h, then diluted with DCM, filtered, washed with water, dried with anhydrous Na_2SO_4, filtered, concentrated and partially purified by chromatography (3:1, Hex/AcOEt), yielding 3.16 g of contaminated **20**, as a syrup. R_f = 0.48 (2:1, Hex/AcOEt).

5.2.20. Ethyl 2-*O*-benzoyl-4,6-*O*-benzylidene-3-*O*-(2-naphtylmethyl)-1-thio-α-D-mannopyranoside (**21**)

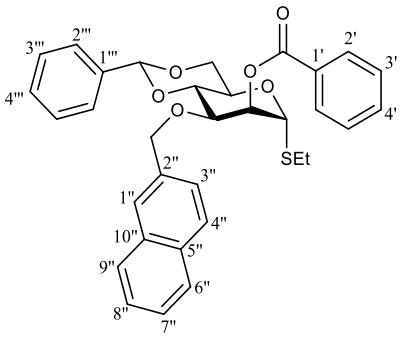

In inert atmosphere, 3.16 g of contaminated **20** was dissolved in 55 mL THF, then 0.3029 g (2.48 mmol) of DMAP, 1.5 mL of BzCl (contaminated with BzOH) and 3.5 mL (25.0 mmol) of Et_3N were added. The mixture was refluxed for 3 h, then diluted with DCM, and washed sequentially with HCl 2 M and saturated $NaHCO_3$ solution; the resulting organic phase was dried with anhydrous $MgSO_4$, filtered, concentrated and purified by chromatography (9:1, Hex/AcOEt), affording two fraction: 2.02 g of **21** contaminated with BzOH, as a syrup, and 1.4926 g of pure **21**, as a white solid. R_f = 0.74 (2:1, Hex/AcOEt); $[\alpha]_D^{20}$= +24º (*c*= 1.00, DCM); **^{1}H NMR** (400 MHz, $CDCl_3$) δ 8.14 (dd, 2H, $J_{2',4'}$= 1.34 Hz, $J_{2',3'}$= 8.45 Hz, H-2' Bz), 7.81-7.76 (m, 2H, H-1'' Nap, H-4''' benzylidene), 7.73 (d, 1H, $J_{3'',4''}$= 8.43 Hz, H-4'' Nap), 7.63-7.37 (m, 12H, H-3' Bz, H-4' Bz, H-3'' Nap, H-6'' Nap, H-7'' Nap, H-8'' Nap, H-9'' Nap, H-2''' benzylidene, H-3''' benzylidene), 5.75 (dd, 1H, J_{1-2}= 1.22 Hz, J_{2-3}= 3.30 Hz, H-2), 5.72 (s, 1H, C*H* benzylidene), 5.43 (d, 1H, J_{1-2}= 0.99 Hz, H-1), 4.91, 4.88, 4.85, 4.82 (AB system, 2H, J_{A-B}= 12.74 Hz, CH_2 Nap), 4.36-4.23 (m, 3H, H-6a, H-4, H-5), 4.13 (dd, 1H, J_{2-3} = 3.40 Hz, J_{3-4}= 9.27 Hz, H-3), 3.98-3.91 (m, 1H, H-6b), 2.74-2.56 (m, 2H, CH_2 SEt), 1.30 (t, 3H, *J*= 7.40 Hz, CH_3 SEt); **^{13}C NMR** (100 MHz, $CDCl_3$) δ 165.87 (C=O Bz), 137.55 (C-1''' benzylidene), 135.40 (C-2'' Nap), 133.53 (C-1' Bz), 133.35, 133.04, 130.10, 129.83, 129.15, 128.62, 128.38, 128.15, 128.09, 127.71, 126.38, 126.01, 125.86, 125.62 (C-2' Bz, C-3' Bz, C-4' Bz, C-5' Bz, C-6' Bz, C-1''Nap, C-3'' Nap, C-4'' Nap, C-5'' Nap, C-6'' Nap, C-7'' Nap, C-8'' Nap, C-9'' Nap, C-10''

Nap, C-2''' benzylidene, C-3''' benzylidene, C-4''' benzylidene), 101.92 (*C*H benzylidene), 83.67 (C-1), 79.02 (C-4), 74.45 (C-3), 72.11, 71.97 (C-2, *C*H_2 Nap), 68.80 (C-6), 64.70 (C-5), 25.76 (*C*H_2 SEt), 15.06 (*C*H_3 SEt).

5.2.21. Ethyl 2-*O*-benzoyl-3-*O*-(2-naphtylmethyl)-1-thio-α-D-mannopyranoside (**22**)

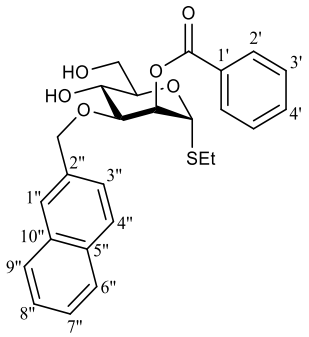

Both fractions from the previous synthesis of **21** and 0.6864 of PTSA.H_2O (3.60 mmol) were dissolved in a mixture of 40 mL of MeOH and 10 mL DCM. The reaction mixture was stirred at 40 ºC for 1h 30 min, then quenched with 0.86 g of $NaHCO_3$. The mixture was then concentrated, dissolved in DCM and washed with brine; the resulting aqueous phase was back-extracted 3 times with DCM; the combined organic phases were dried with anhydrous $MgSO_4$, filtered, concentrated and purified by chromatography (1.5:1, Hex/AcOEt), affording 2.5811 g (5.51 mmol, η= 74% over 3 steps) of **22** as a syrup. R_f = 0.23 (1.5:1, Hex/AcOEt); $[\alpha]_D^{20}$= +9º (*c*= 1.00, DCM); **^{1}H NMR** (400 MHz, $CDCl_3$) δ 8.08 (dd, 2H, $J_{2',4'}$= 1.25 Hz $J_{2',3'}$= 8.41 Hz, H-2' Bz), 7.80-7.67 (m, 4H, H-4'' Nap, H-1'' Nap, C*H* Nap), 7.59 (t, 1H, $J_{2',4'}$= 1.16 Hz, $J_{3',4'}$= 7.48 Hz, H-4' Bz), 7.49.7.41 (m, 4H, H-3' Bz, C*H* Nap), 7.37 (dd, 1H, *J*= 1.10 Hz, *J*= 8.36 Hz, H-3'' Nap), 5.73 (dd, 1H, J_{1-2}= 1.47 Hz, J_{2-3}= 2.92 Hz, H-2), 5.43 (d, 1H, H-1), 4.91, 4.89, 4.65, 4.62 (AB system, 2H, J_{A-B}= 11.50 Hz, CH_2 Nap), 4.19-4.06 (m, 2H, H-4, H-5), 3.96-3.85 (m, 3H, H-3, H-6), 2.72-2.56 (m, 2H, CH_2 SEt), 2.34 (broad s, 2H, O*H*-5, O*H*-6), 1.30 (t, 3H, *J*= 7.42 Hz, CH_3 SEt); **^{13}C NMR** (100 MHz, $CDCl_3$) δ 165.79 (C=O Bz), 134.78 (C-2'' Nap), 133.54, 133.27, 133.14, 130.00, 129.71, 128.65, 128.50, 128.01, 127.77, 127.21, 126.26, 126.15, 125.91 (C-1' Bz, C-2' Bz, C-3' Bz, C-4' Bz, C-1''Nap, C-3'' Nap, C-4'' Nap, C-5'' Nap, C-6'' Nap, C-7'' Nap, C-8'' Nap, C-9'' Nap, C-10'' Nap), 82.75 (C-1), 78.12 (C-3), 72.43 (C-4), 71.56 (C-6), 70.26 (C-2), 67.41 (C-5), 62.60 (CH_2 Nap), 25.74 (*C*H_2 SEt), 14.97 (*C*H_3 SEt).

5.2.22. Ethyl 2-*O*-benzoyl-4-*O*-benzyl-3-*O*-(2-naphtylmethyl)-1-thio-α-D-mannopyranoside (**23**)

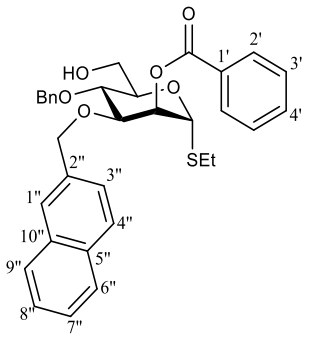

In inert atmosphere, 2.0134 g (3.62 mmol) of **21** were dissolved in 36 mL of DCM; 18 mL (18 mmol) of 1 M BH_3.THF solution and 0.1 mL (5.53 mmol) of TMSOTf were added; the mixture was stirred 2 h, then quenched, first with 1 mL Et_3N, then with small additions of HCl 2M until no H_2

evolution was visible; the resulting organic phase was washed with saturated $NaHCO_3$ solution, dried with anhydrous $MgSO_4$, filtered, concentrated and purified by chromatography (3:1, Hex/AcOEt), yielding 1.5859 g (2.84 mmol, η= 78 %) of **23** as a syrup. R_f = 0.30 (3:1, Hex/AcOEt); $[\alpha]_D^{20}$= +14º (*c*= 1.00, DCM); **^{1}H NMR** (400 MHz, $CDCl_3$) δ 8.11 (dd, 2H, $J_{2'\text{-}4'}$= 1.28 Hz, $J_{2'\text{-}3'}$= 8.45 Hz, H-2' Bz), 7.82-7.71 (m, 3H, C*H* Bn/Nap), 7.69-7.57 (m, 2H, C*H* Bn/Nap, H-4' Bz), 7.54-7.38 (m, 5H, C*H* Bn/Nap, H-3' Bz), 7.36-7.27 (m, 5H, C*H* Bn/Nap), 5.76 (t, 1H, $J_{1\text{-}2}$= $J_{2\text{-}3}$= 1.90 Hz, H-2), 5.41 (d, 1H, H-1), 4.98, 4.95 (part A of AB system, 1H, $J_{A\text{-}B}$= 11.00 Hz, CH_2 A Bn4), 4.94, 4.91 (part A of AB system, 1H, $J_{A\text{-}B}$= 11.63 Hz, CH_2 A Nap), 4.75, 4.72 (part B of AB system, 1H, CH_2 B Nap), 4.72, 4.69 (part B of AB system, 1H, CH_2 B Bn4), 4.16-4.02 (m, 3H, H-3, H-4, H-5), 3.88 (broad s, 2H, H-6), 2.73-2.56 (m, 2H, CH_2 SEt), 1.90 (broad s, 1H, O*H*-6), 1.29 (t, 3H, *J*= 7.37 Hz, CH_3 SEt); **^{13}C NMR** (100 MHz, $CDCl_3$) δ 165.80 (C=O Bz), 138.30 (qC Bn), 135.27 (C-2'' Nap), 133.48, 133.33, 133.08, 130.04, 129.94, 128.66, 128.55, 128.22, 128.04, 127.93, 127.74, 126.97, 126.12, 126.09, 125.97 (*C*H - Bn ,C-1' Bz, C-2' Bz, C-3' Bz, C-4' Bz, C-1''Nap, C-3'' Nap, C-4'' Nap, C-5'' Nap, C-6'' Nap, C-7'' Nap, C-8'' Nap, C-9'' Nap, C-10'' Nap), 82.68 (C-1), 78.70 (C-3), 75.38 (*C*H_2 Bn), 74.23 (C-4), 72.41 (C-5), 71.72 (*C*H_2 Nap), 71.07 (C-2), 62.20 (C-6), 25.75 (*C*H_2 SEt), 15.02 (*C*H_3 SEt).

5.2.23. Ethyl 2-*O*-benzoyl-4,6-di-*O*-benzyl-3-*O*-(2-naphtylmethyl)-1-thio-α-D-mannopyranoside (**BB-3**)

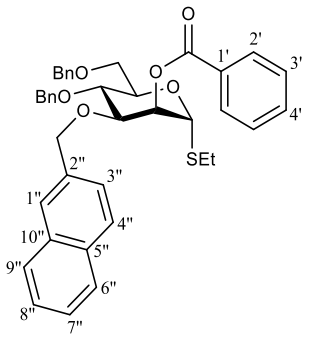

0.2921 g (0.52 mmol) of **23** were dissolved in 1 mL of DCM, then 0.16 mL (0.77 mmol) of HMDS (0.48 mmol) and 0.02 mL (0.11 mmol) of TMSOTf were added, and the resulting suspension was stirred for 1 h at room temperature, then concentrated. In inert atmosphere, the resulting residue was redissolved in 5 mL of DCM, and cooled to 0 ºC; freshly activated 4 Å molecular sieves, 0.03 mL (0.16 mmol) of TMSOTf and 0.11 mL (1.08 mmol) of PhCHO were added; the mixture was stirred at 0 ºC for 1 h, then 0.17 mL (1.06 mmol) of TES were added; the mixture was stirred for 1 h at 0 ºC, then diluted with DCM, filtered, washed with saturated $NaHCO_3$ solution, dried with anhydrous $MgSO_4$, filtered, concentrated, and purified by chromatography (13:1, Hex/AcOEt), affording 0.2414 g (0.37 mmol, η= 71 %) of **BB-3** as a syrup. R_f = 0.20 (13:1, Hex/AcOEt), $[\alpha]_D^{20}$= +12º (*c*= 1.00, DCM), **^{1}H NMR** (400 MHz, $CDCl_3$) δ 8.11 (dd, 2H, $J_{2'\text{-}4'}$= 1.15 Hz, $J_{2'\text{-}3'}$= 8.40 Hz, H-2' Bz), 7.81-7.62 (m, 4H, C*H* Bn/Nap), 7.57 (tt, 1H, $J_{3'\text{-}4'}$= 7.43 Hz, H-4' Bz), 7.47-7.24 (m, 13H, H-3' Bz, C*H* Bn), 7.23-7.17 (m, 2H, C*H* Bn, C*H* Nap), 5.79 (dd, 1H, $J_{1\text{-}2}$= 1.74 Hz, $J_{2\text{-}3}$= 2.60 Hz, H-2), 5.47 (d, 1H, H-1), 4.95, 4.92 (part A of AB system, 1H, $J_{A\text{-}B}$= 11.41 Hz, CH_2 Nap), 4.93, 4.90 (part A of AB system, 1H, $J_{A\text{-}B}$= 10.66 Hz, CH_2 Bn4), 4.77,4.74 (part A of AB system, 1H, $J_{A\text{-}B}$= 11.63 Hz, CH_2 Bn6), 4.74, 4.71 (part B of AB system, 1H, CH_2 Nap), 4.58, 4.55 (part B of AB system, 1H, CH_2 Bn4), 4.55, 4.52 (part B of AB system, 1H, CH_2 Bn6), 4.25 (ddd, 1H, $J_{4\text{-}5}$= 9.30 Hz, $J_{5\text{-}6a}$= 3.71 Hz, $J_{5\text{-}6b}$= 1.66 Hz, H-5), 4.18 (t, 1H, $J_{3\text{-}4}$= $J_{4\text{-}5}$= 9.30 Hz, H-4), 4.09 (dd, 1H, $J_{2\text{-}3}$= 3.01 Hz, H-3), 3.96, 3.94, 3.79, 3.77 (ABX system, 1H, $J_{6a\text{-}6b}$= 10.87 Hz, H-6), 2.75-2.57 (m, 2H, CH_2 SEt), 1.30 (t, 3H, *J*= 7.50 Hz, CH_3 SEt); **^{13}C NMR** (100 MHz, $CDCl_3$) δ 165.84 (C=O Bz), 138.49 (qC Bn 4/6), 135.33 (C-1''

Nap), 133.35, 133.31, 133.09, 130.12, 130.02, 128.56, 128.46, 128.45, 128.21, 128.06, 128.04, 127.74, 127.66, 127.63, 127.02, 126.21, 126.06, 125.94 (*C*H Bn ,C-1' Bz, C-2' Bz, C-3' Bz, C-4' Bz, C-1''Nap, C-3'' Nap, C-4'' Nap, C-5'' Nap, C-6'' Nap, C-7'' Nap, C-8'' Nap, C-9'' Nap, C-10'' Nap), 82.71 (C-1), 78.81 (C-3), 75.41 (*C*H_2 Bn4), 74.60 (C-4), 73.53 (*C*H_2 Bn6), 72.09 (C-5), 71.72 (*C*H_2 Nap), 70.94 (C-2), 69.11 (C-6), 25.77 (*C*H_2 SEt), 15.12 (*C*H_3 SEt).

5.2.24. Ethyl 2-*O*-benzoyl-3-*O*-benzyl-4,6-*O*-benzylidene-1-thio-α-D-mannopyranoside (**25**)

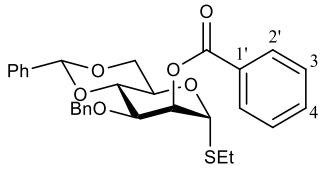

In inert atmosphere, 1.8872 g (4.67 mmol) of **24** were dissolved in 20 mL of THF; 0.82 mL of BzCl (7.06 mmol), 2 mL (14.3 mmol) of Et_3N and a catalytic amount of DMAP were added; the mixture was refluxed for 28 h, diluted with DCM, and sequentially washed with HCl 1 M and saturated $NaHCO_3$ solution; the resulting organic phase was dried with anhydrous Na_2SO_4, filtered, concentrated and purified by chromatography (15:1, Hex/AcOEt), yielding 1.8437 g (3.64 mmol, η= 78 %) of **25** as a syrup. R_f = 0.20 (15:1, Hex/AcOEt); $[\alpha]_D^{20}$= +24º (*c*=1.00, DCM); **^{1}H NMR** (400 MHz, $CDCl_3$) δ 8.13 (dd, 2H,, $J_{2'\text{-}4'}$= 1.34 Hz, $J_{2'\text{-}3'}$= 8.45 Hz, H-2' Bz), 7.61 (tt, 1H, $J_{3'\text{-}4'}$= 7.51 Hz, H-4' Bz), 7.56-7.23 (m, 12H, H-3' Bz, C*H* Ph benzylidene, C*H* Bn), 5.70 (s, 1H, C*H* benzylidene), 5.67 (dd, 1H, $J_{1\text{-}2}$= 1.27 Hz, $J_{2\text{-}3}$= 3.36 Hz, H-2), 5.42 (d, 1H, H-1), 4.76, 4.73, 4.71, 4.68 (AB system, 2H, $J_{A\text{-}B}$= 12.24 Hz, CH_2 Bn), 4.36-4.20 (m, 3H, H-4, H-5, H-6a), 4.08 (dd, 1H, $J_{3\text{-}4}$= 9.65 Hz, H-3), 4.00-3.93 (m, 1H, H-6b), 2.75-2.58 (m, 2H, CH_2 SEt), 1.31 (t, 3H, *J*= 7.44 Hz, CH_3 SEt); **^{13}C NMR** (100 MHz, $CDCl_3$) δ 165.84 (C=O Bz), 137.87 (qC Bn), 137.50 (qC benzylidene), 133.48 (C-4' Bz), 130.06 (C-2' Bz), 129.82, 129.09, 128.58, 128.44, 128.32, 127.79, 127.77, 126.26 (*C*H Bn, C-1' Bz, C-3' Bz, *C*H Ph benzylidene), 101.78 (*C*H benzylidene), 83.66 (C-1), 79.03 (C-4), 74.39 (C-3), 72.24, 72.19 (C-2, *C*H_2 Bn), 68.77 (C-6), 64.71 (C-5), 25.77 (*C*H_2 SEt), 15.08 (*C*H_3 SEt).

5.2.25. Ethyl 2-*O*-benzoyl-3,5-di-*O*-benzyl-1-thio-α-D-mannopyranoside (**26**)

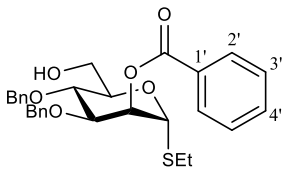

In inert atmosphere, 1.4531 g (2.87 mmol) of **25** were dissolved in 28 mL of DCM; 12 mL (12 mmol) of 1 M BH_3.THF solution and 0.1 mL (5.53 mmol) of TMSOTf were added; the mixture was stirred for 2 h, then quenched first with 1 mL Et_3N, then with small additions of HCl 2M until no H_2 evolution was visible; the resulting organic phase was diluted with AcOEt, washed with saturated $NaHCO_3$ solution, dried with anhydrous $MgSO_4$, filtered, concentrated and purified by chromatography (3:1, Hex/AcOEt), yielding 1.3917 g (2.74 mmol, η= 95 %) of **26** as a syrup. R_f = 0.31 (3:1, Hex/AcOEt); $[\alpha]_D^{20}$= +52º (*c*=1.00, DCM); **^{1}H NMR** (400 MHz, $CDCl_3$) δ 8.09 (dd, 2H, $J_{2'\text{-}4'}$= 1.31 Hz, $J_{2'\text{-}3'}$= 8.41 Hz, H-2' Bz), 7.61 (tt, 1H, $J_{3'\text{-}4'}$= 7.50 Hz, H-4' Bz), 7.48 (broad t, 2H, *J*= 7.79 Hz, H-3' Bz), 7.39-7.23 (m, 10H, C*H* Bn), 5.68 (dd, 1H, $J_{1\text{-}2}$= 1.63 Hz, $J_{2\text{-}3}$= 2.51 Hz, H-2), 5.39 (d, 1H, H-1), 4.95, 4.92 (part A of AB system, 1H, $J_{A\text{-}B}$= 10.97 Hz, CH_2 A Bn4), 4.78, 4.75 (part A of AB system, 1H, $J_{A\text{-}B}$= 11.42 Hz, CH_2 A Bn3), 4.69, 4.66 (part B of AB system, 1H, CH_2 B Bn4), 4.59, 4.56 (part B of AB system, 1H, CH_2 B Bn3), 4.13.3,99 (m, 3H, H-3, H-4, H-5), 3.89-3.82 (m, 2H, H-6), 2.72-2.55 (m, 2H, CH_2 SEt), 1.88 (t, 1H, $J_{6\text{-}OH}$= 6.58 Hz, O*H*-6), 1.29 (t, 3H, *J*= 7.42 Hz, CH_3 SEt); **^{13}C NMR** (100 MHz, $CDCl_3$) δ 165.75 (C=O Bz), 138.29 (qC Bn 4), 137.78 (qC Bn 3), 133.44 (C-4'

Bz), 130.01, 129.94 (C-1' Bz, C-3' Bz), 128.64, 128.54, 128.49, 128.27, 128.19, 127.95, 127.87 (*C*H - Bn, C-2' Bz), 82.68 (C-1), 78.65 (C-3), 75.38 (*C*H_2 Bn 4), 74.24 (C-4), 72.40 (C-5), 71.71 (*C*H_2 Bn 3), 71.09 (C-2), 62.20 (C-6), 25.76 (*C*H_2 SEt), 15.03 (*C*H_3 SEt).

5.2.26. Ethyl 2-*O*-benzoyl-3,5,6-tri-*O*-benzyl-1-thio-α-D-mannopyranoside (**BB-4**)

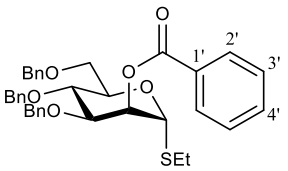

In inert atmosphere, in a round bottom flask containing freshly activated 4 Å molecular sieves, 1.3711 g (2.70 mmol) of **26** were dissolved in 27 mL of THF; the solution was cooled to 0 ºC, then 0.24 mL (1.33 mmol) of TMSOTf and 3.4 mL (24.5 mmol) of HMDSO were added; the mixture was stirred for 1 h at 0 ºC, then 0.82 mL (8.07 mmol) of PhCHO were added, and the mixture was again stirred for 1 h at 0 ºC, after which 1.3 mL (8.14 mmol) of TES were added; the reaction mixture was stirred for 4 h 30 min, then diluted with AcOEt, filtered, washed with saturated $NaHCO_3$ solution, dried with anhydrous $MgSO_4$, filtered, concentrated and purified by chromatography (12:1 Hex/AcOEt to 10:1 Hex/AcOEt), yielding 1.2440 g (2.08 mmol, η= 77 %) of **BB-4** as a syrup. R_f = 0.34 (10:1, Hex/AcOEt); $[\alpha]_D^{20}$= +47º (*c*=1.00, DCM); **^{1}H NMR** (400 MHz, $CDCl_3$) δ 8.09 (dd, 2H, $J_{2'\text{-}4'}$=1.29 Hz, $J_{2'\text{-}3'}$= 8.41 Hz, C-2' Bz), 7.57 (tt, 1H, $J_{3'\text{-}4'}$= 7.43 Hz, H-4' Bz), 7.43-7.18 (m, 17H, H-3' Bz, C*H* Bn3, C*H* Bn4, C*H* Bn6), 5.72 (dd, 1H, $J_{1\text{-}2}$= 1.77 Hz, $J_{2\text{-}3}$= 2.94 Hz, H-2), 5.45 (d, 1H, H-1), 4.90, 4.87 (part A of AB system, 1H, $J_{A\text{-}B}$= 10.80 Hz, CH_2 A Bn4), 4.79,4.76 (part A of AB system, 1H, $J_{A\text{-}B}$= 11.41 Hz, CH_2 A Bn3), 4.76, 4.73 (part A of AB system, 1H, $J_{A\text{-}B}$= 11.92 Hz, CH_2 B Bn6), 4.58,4.55 (part B of AB system, 1H, CH_2 B BN3), 4.55, 4.53 (part B of AB system, 1H, CH_2 B Bn4), 4.54, 4.51 (part B of AB system, 1H, CH_2 B Bn6), 4.23 (ddd, $J_{4\text{-}5}$= 9.30 Hz, $J_{6a\text{-}5}$= 3.71 Hz, $J_{6b\text{-}5}$= 1.65 Hz, H-5), 4.15 (t, 1H, $J_{3\text{-}4}$= $J_{4\text{-}5}$= 9.30 Hz, H-4), 4.03 (dd, 1H, H-3), 3.95, 3.92, 3.78, 3.76 (ABX system, 2H, $J_{6a\text{-}6b}$= 10.87 Hz, H-6), 2.76-2.56 (m, 2H, CH_2 SEt), 1.30 (t, 3H, J= 7.40 Hz, CH_3 SEt); **^{13}C NMR** (100 MHz, $CDCl_3$) δ 165.79 (C=O), 138.49, 138.47, 137.83 (qC Bn 3/4/6), 133.28 (C-4' Bz), 130.09, 130.01, 128.53, 128.47, 128.46, 128.44, 128.27, 128.08, 127.85, 127.77, 127.65, 127.63 (*C*H Bn, C-1' Bz, C-2' Bz, C-3' Bz), 82.70 (C-1), 78.77 (C-3), 75.41 (*C*H_2 Bn4), 74.60 (C-4), 73.52 (*C*H_2 Bn6), 72.07 (C-5), 71.71 (*C*H_2 Bn3), 70.95 (C-2), 69.10 (C-6), 25.77 (*C*H_2 SEt), 15.13 (*C*H_3 SEt).

6. References

(1) D'avila-Levy, C. M.; Boucinha, C.; Kostygov, A.; Santos, H. L. C.; Morelli, K. A.; Grybchuk-Ieremenko, A.; Duval, L.; Votýpka, J.; Yurchenko, V.; Grellier, P.; et al. Exploring the Environmental Diversity of Kinetoplastid Flagellates in the High-Throughput DNA Sequencing Era. *Mem. Inst. Oswaldo Cruz* **2015**, *110* (8), 956–965.

(2) World Health Organization. Neglected tropical diseases https://www.who.int/health-topics/neglected-tropical-diseases#tab=tab_1 (accessed 19 July, 2021).

(3) Lidani, K. C. F.; Andrade, F. A.; Bavia, L.; Damasceno, F. S.; Beltrame, M. H.; Messias-Reason, I. J.; Sandri, T. L. Chagas Disease: From Discovery to a Worldwide Health Problem. *J. Phys. Oceanogr.* **2019**, *49* (6), 1–13.

(4) Pérez-Molina, J. A.; Molina, I. Chagas Disease. *Lancet* **2018**, *391* (10115), 82–94.

(5) World Health Organization. Chagas disease (also known as American trypanosomiasis) https://www.who.int/news-room/fact-sheets/detail/chagas-disease-(american-trypanosomiasis) (accessed July 19, 2021).

(6) de Lana, M.; de Menezes Machado, E. M. Biology of *Trypanosoma Cruzi* and Biological Diversity. In *American Trypanosomiasis Chagas Disease: One Hundred Years of Research (Second Edition)*; Telleria, J., Tibayrenc, M., Eds.; Elsevier Inc., 2017; pp 345–369.

(7) Center for Disease Control and Prevention. American Trypanosomiasis https://www.cdc.gov/dpdx/trypanosomiasisamerican/index.html (accessed January 23, 2022).

(8) Cardoso, M. S.; Reis-Cunha, J. L.; Bartholomeu, D. C. Evasion of the Immune Response by *Trypanosoma Cruzi* during Acute Infection. *Front. Immunol.* **2016**, *6* (JAN), 1–15.

(9) Ropert, C.; Gazzinelli, R. T. Signaling of Immune System Cells by Glycosylphosphatidylinositol (GPI) Anchor and Related Structures Derived from Parasitic Protozoa. *Curr. Opin. Microbiol.* **2000**, *3* (4), 395–403.

(10) Bern, C.; Martin, D. L.; Gilman, R. H. Acute and Congenital Chagas Disease. In *Advances in Parasitology*; Weiss, L. M., Tanowitz, H. B., Kirchhoff, L. V., Eds.; Elsevier Ltd., 2011; Vol. 75, pp 19–47.

(11) Bern, C. Chagas' Disease. *N. Engl. J. Med.* **2015**, *373* (5), 456–466.

(12) Bonney, K. M.; Luthringer, D. J.; Kim, S. A.; Garg, N. J.; Engman, D. M. Pathology and Pathogenesis of Chagas Heart Disease. *Annu. Rev. Pathol. Mech. Dis.* **2019**, *14*, 421–447.

(13) Zingales, B. *Trypanosoma Cruzi* Genetic Diversity: Something New for Something Known about Chagas Disease Manifestations, Serodiagnosis and Drug Sensitivity. *Acta Trop.* **2018**, *184* (April 2017), 38–52.

(14) Urbina, J. A. Specific Chemotherapy of Chagas Disease: Relevance, Current Limitations and New Approaches. *Acta Trop.* **2010**, *115* (1–2), 55–68.

(15) Bern, C. Antitrypanosomal Therapy for Chronic Chagas' Disease. *N. Engl. J. Med.* **2011**, *364* (26), 2527–2534.

(16) Beaumier, C. M.; Gillespie, P. M.; Strych, U.; Hayward, T.; Hotez, P. J.; Bottazzi, M. E. Status of Vaccine Research and Development of Vaccines for Chagas Disease. *Vaccine* **2016**, *34* (26), 2996–3000.

(17) Dumonteil, E.; Herrera, C. The Case for the Development of a Chagas Disease Vaccine: Why? How? When? *Trop. Med. Infect. Dis.* **2021**, *6* (16), 1–14.

(18) Lascano, F.; García Bournissen, F.; Altcheh, J. Review of Pharmacological Options for the Treatment of Chagas Disease. *Br. J. Clin. Pharmacol.* **2020**, No. September 2020.

(19) Matsuda, N. M.; Miller, S. M.; Evora, P. R. B. The Chronic Gastrointestinal Manifestations of Chagas Disease. *Clinics* **2009**, *64* (12), 1219–1224.

(20) Nunes, M. C. P.; Dones, W.; Morillo, C. A.; Encina, J. J.; Ribeiro, A. L. Chagas Disease: An Overview of Clinical and Epidemiological Aspects. *J. Am. Coll. Cardiol.* **2013**, *62* (9), 767–776.

(21) Nunes, M. C. P.; Beaton, A.; Acquatella, H.; Bern, C.; Bolger, A. F.; Echeverría, L. E.; Dutra, W. O.; Gascon, J.; Morillo, C. A.; Oliveira-Filho, J.; et al. Chagas Cardiomyopathy: An Update of Current Clinical Knowledge and Management: A Scientific Statement From the American Heart Association. *Circulation* **2018**, *138* (12), e169–e209.

(22) Burza, S.; Croft, S. L.; Boelaert, M. Leishmaniasis. *Lancet* **2018**, *392* (10151), 951–970.
(23) Beattie, L.; Kaye, P. M. *Leishmania*-Host Interactions: What Has Imaging Taught Us? *Cell. Microbiol.* **2011**, *13* (11), 1659–1667.
(24) Center for Disease Control and Prevention. Leishmaniasis https://www.cdc.gov/dpdx/leishmaniasis/index.html (accessed January 23, 2022).
(25) World Health Organization. Leishmaniasis https://www.who.int/news-room/fact-sheets/detail/leishmaniasis (accessed 19 July, 2021).
(26) Hartley, M. A.; Drexler, S.; Ronet, C.; Beverley, S. M.; Fasel, N. The Immunological, Environmental, and Phylogenetic Perpetrators of Metastatic Leishmaniasis. *Trends Parasitol.* **2014**, *30* (8), 412–422.
(27) Reithinger, R.; Dujardin, J. C.; Louzir, H.; Pirmez, C.; Alexander, B.; Brooker, S. Cutaneous Leishmaniasis. *Lancet Infect. Dis.* **2007**, *7* (9), 581–596.
(28) Saporito, L.; Giammanco, G. M.; De Grazia, S.; Colomba, C. Visceral Leishmaniasis: Host-Parasite Interactions and Clinical Presentation in the Immunocompetent and in the Immunocompromised Host. *Int. J. Infect. Dis.* **2013**, *17* (8), 1–5.
(29) Poulaki, A.; Piperaki, E. T.; Voulgarelis, M. Effects of Visceralising Leishmania on the Spleen, Liver, and Bone Marrow: A Pathophysiological Perspective. *Microorganisms* **2021**, *9* (4).
(30) Chappuis, F.; Sundar, S.; Hailu, A.; Ghalib, H.; Rijal, S.; Peeling, R. W.; Alvar, J.; Boelaert, M. Visceral Leishmaniasis: What Are the Needs for Diagnosis, Treatment and Control? *Nat. Rev. Microbiol.* **2007**, *5* (11), 873–882.
(31) Ponte-Sucre, A.; Gamarro, F.; Dujardin, J. C.; Barrett, M. P.; López-Vélez, R.; García-Hernández, R.; Pountain, A. W.; Mwenechanya, R.; Papadopoulou, B. Drug Resistance and Treatment Failure in Leishmaniasis: A 21st Century Challenge. *PLoS Negl. Trop. Dis.* **2017**, *11* (12), 1–24.
(32) Ghorbani, M.; Farhoudi, R. Leishmaniasis in Humans: Drug or Vaccine Therapy? *Drug Des. Devel. Ther.* **2018**, *12*, 25–40.
(33) Akilov, O. E.; Khachemoune, A.; Hasan, T. Clinical Manifestations and Classification of Old World Cutaneous Leishmaniasis. *Int. J. Dermatol.* **2007**, *46* (2), 132–142.
(34) Scorza, B. M.; Carvalho, E. M.; Wilson, M. E. Cutaneous Manifestations of Human and Murine Leishmaniasis. *Int. J. Mol. Sci.* **2017**, *18* (6).
(35) Srivastava, S.; Shankar, P.; Mishra, J.; Singh, S. Possibilities and Challenges for Developing a Successful Vaccine for Leishmaniasis. *Parasites and Vectors* **2016**, *9* (1), 1–15.
(36) Zutshi, S.; Kumar, S.; Chauhan, P.; Bansode, Y.; Nair, A.; Roy, S.; Sarkar, A.; Saha, B. Anti-Leishmanial Vaccines: Assumptions, Approaches, and Annulments. *Vaccines* **2019**, *7* (4), 1–33.
(37) Sasidharan, S.; Saudagar, P. Leishmaniasis: Where Are We and Where Are We Heading? *Parasitol. Res.* **2021**, *120* (5), 1541–1554.
(38) Ikezawa, H. Glycosylphosphatidylinositol (GPI)-Anchored Proteins. *Biol. Pharm. Bull.* **2002**, *25* (4), 409–417.
(39) Borges, A. R.; Link, F.; Engstler, M.; Jones, N. G. The Glycosylphosphatidylinositol Anchor: A Linchpin for Cell Surface Versatility of Trypanosomatids. *Front. Cell Dev. Biol.* **2021**, *9* (November), 1–30.
(40) Brimacombe, J. S.; Cottaz, S.; Field, R. A.; Homans, S. W.; McConville, M. J.; Mehlert, A.; Milne, K. G.; Ralton, J. E.; Roy, Y. A.; Schneider, P.; et al. Glycosyl-Phosphatidylinositol Molecules of the Parasite and the Host. *Parasitology* **1994**, *108* (S1), S45–S54.
(41) Almeida, I. C.; Camargo, M. M.; Procópio, D. O.; Silva, L. S.; Mehlert, A.; Travassos, L. R.; Gazzinelli, R. T.; Ferguson, M. A. J. Highly Purified Glycosylphosphatidylinositols from *Trypanosoma Cruzi* Are Potent Proinflammatory Agents. *EMBO J.* **2000**, *19* (7), 1476–1485.
(42) Peltier, P.; Euzen, R.; Daniellou, R.; Nugier-Chauvin, C.; Ferrières, V. Recent Knowledge and Innovations Related to Hexofuranosides: Structure, Synthesis and Applications. *Carbohydr. Res.* **2008**, *343* (12), 1897–1923.
(43) Latge, J. P. Galactofuranose Containing Molecules in *Aspergillus Fumigatus*. *Med. Mycol.* **2009**, *47* (SUPPL. 1), 104–109.
(44) Tanner, J. J.; Boechi, L.; Andrew McCammon, J.; Sobrado, P. Structure, Mechanism, and Dynamics of UDP-Galactopyranose Mutase. *Arch. Biochem. Biophys.* **2014**, *544*, 128–141.

(45) Tefsen, B.; Ram, A. F. J.; Van Die, I.; Routier, F. H. Galactofuranose in Eukaryotes: Aspects of Biosynthesis and Functional Impact. *Glycobiology* **2012**, *22* (4), 456–469.
(46) Pedersen, L. L.; Turco, S. J. Galactofuranose Metabolism: A Potential Target for Antimicrobial Chemotherapy. *Cell. Mol. Life Sci.* **2003**, *60* (2), 259–266.
(47) Kremer, L.; Dover, L. G.; Morehouse, C.; Hitchin, P.; Everett, M.; Morris, H. R.; Dell, A.; Brennan, P. J.; McNeil, M. R.; Flaherty, C.; et al. Galactan Biosynthesis in *Mycobacterium Tuberculosis*: Identification of a Bifunctional UDP-Galactofuranosyltransferase. *J. Biol. Chem.* **2001**, *276* (28), 26430–26440.
(48) Completo, G. C.; Lowary, T. L. Synthesis of Galactofuranose-Containing Acceptor Substrates for Mycobacterial Galactofuranosyltransferases. *J. Org. Chem.* **2008**, *73* (12), 4513–4525.
(49) Baldoni, L.; Marino, C. Synthetic Tools for the Characterization of Galactofuranosyl Transferases: Glycosylations via Acylated Glycosyl Iodides. *Carbohydr. Res.* **2013**, *374*, 75–81.
(50) Richards, M. R.; Lowary, T. L. Chemistry and Biology of Galactofuranose-Containing Polysaccharides. *ChemBioChem* **2009**, *10* (12), 1920–1938.
(51) Giorgi, M. E.; de Lederkremer, R. M. The Glycan Structure of *T. Cruzi* Mucins Depends on the Host. Insights on the Chameleonic Galactose. *Molecules* **2020**, *25* (17).
(52) Campetella, O.; Buscaglia, C. A.; Mucci, J.; Leguizamón, M. S. Parasite-Host Glycan Interactions during *Trypanosoma Cruzi* Infection: Trans-Sialidase Rides the Show. *Biochim. Biophys. Acta - Mol. Basis Dis.* **2020**, *1866* (5), 165692.
(53) Cavalcante, T.; Medeiros, M. M.; Mule, S. N.; Palmisano, G.; Stolf, B. S. The Role of Sialic Acids in the Establishment of Infections by Pathogens, With Special Focus on *Leishmania*. *Front. Cell. Infect. Microbiol.* **2021**, *11* (May), 1–13.
(54) Zingales, B.; Miles, M. A.; Campbell, D. A.; Tibayrenc, M.; Macedo, A. M.; Teixeira, M. M. G.; Schijman, A. G.; Llewellyn, M. S.; Lages-Silva, E.; Machado, C. R.; et al. The Revised *Trypanosoma Cruzi* Subspecific Nomenclature: Rationale, Epidemiological Relevance and Research Applications. *Infect. Genet. Evol.* **2012**, *12* (2), 240–253.
(55) Cámara, M. de los M.; Balouz, V.; Cameán, C. C.; Cori, C. R.; Kashiwagi, G. A.; Gil, S. A.; Macchiaverna, N. P.; Cardinal, M. V.; Guaimas, F.; Lobo, M. M.; et al. *Trypanosoma Cruzi* Surface Mucins Are Involved in the Attachment to the *Triatoma Infestans* Rectal Ampoule. *PLoS Negl. Trop. Dis.* **2019**, *13* (5), 1–23.
(56) De Lederkremer, R. M.; Alves, M. J. M.; Fonseca, G. C.; Colli, W. A Lipopeptidophosphoglycan from *Trypanosoma Cruzi* (Epimastigote): Isolation, Purification and Carbohydrate Composition. *Biochem. Biophys. Acta* **1976**, *444*, 85–96.
(57) Golgher, D. B.; Colli, W.; Souto-Padrón, T.; Zingales, B. Galactofuranose-Containing Glycoconjugates of Epimastigote and Trypomastigote Forms of *Trypanosoma Cruzi*. *Mol. Biochem. Parasitol.* **1993**, *60* (2), 249–264.
(58) Suzuki, E.; Mortara, R. A.; Takahashi, H. K.; Straus, A. H. Reactivity of MEST-1 (Antigalactofuranose) with *Trypanosoma Cruzi* Glycosylinositol Phosphorylceramides (GIPCs): Immunolocalization of GIPCs in Acidic Vesicles of Epimastigotes. *Clin. Diagn. Lab. Immunol.* **2001**, *8* (5), 1031–1035.
(59) De Lederkremer, R. M.; Lima, C.; Ramirez, M. I.; Ferguson, M. A. J.; Homans, S. W.; Thomas-Oates, J. Complete Structure of the Glycan of Lipopeptidophosphoglycan from *Trypanosoma Cruzi* Epimastigotes. *J. Biol. Chem.* **1991**, *266* (35), 23670–23675.
(60) Carreira, J. C.; Jones, C.; Wait, R.; Previato, J. O.; Mendonça-Previato, L. Structural Variation in the Glycoinositolphospholipids of Different Strains of *Trypanosoma Cruzi*. *Glycoconj. J.* **1996**, *13* (6), 955–966.
(61) Nakayasu, E. S.; Yashunsky, D. V.; Nohara, L. L.; Torrecilhas, A. C. T.; Nikolaev, A. V.; Almeida, I. C. GPIomics: Global Analysis of Glycosylphosphatidylinositol-Anchored Molecules of *Trypanosoma Cruzi*. *Mol. Syst. Biol.* **2009**, *5* (261), 1–17.
(62) De Lederkremer, R. M.; Lima, C. E.; Ramirez, M. I.; Gonçalvez, M. F.; Colli, W. Hexadecylpalmitoyglycerol or Ceramide Is Linked to Similar Glycophosphoinositol Anchor-like Structures in *Trypanosoma Cruzi*. *Eur. J. Biochem.* **1993**, *218* (3), 929–936.
(63) Salto, M. L.; Bertello, L. E.; Vieira, M.; Docampo, R.; Moreno, S. N. J.; De Lederkremer, R. M. Formation and Remodeling of Inositolphosphoceramide during Differentiation of

Trypanosoma Cruzi from Trypomastigote to Amastigote. *Eukaryot. Cell* **2003**, *2* (4), 756–768.
(64) Nogueira, N. F. S.; Gonzalez, M. S.; Gomes, J. E.; de Souza, W.; Garcia, E. S.; Azambuja, P.; Nohara, L. L.; Almeida, I. C.; Zingales, B.; Colli, W. *Trypanosoma Cruzi*: Involvement of Glycoinositolphospholipids in the Attachment to the Luminal Midgut Surface of Rhodnius Prolixus. *Exp. Parasitol.* **2007**, *116* (2), 120–128.
(65) de Arruda, M. V.; Calli, W.; Zingales, B. Terminal B-D-galactofuranosyl Epitopes Recognized by Antibodies That Inhibit *Trypanosoma Cruzi* Internalization into Mammalian Cells. *Eur. J. Biochem.* **1989**, *182* (2), 413–421.
(66) Freire-De-Lima, C. G.; Nunes, M. P.; Corte-Real, S.; Soares, M. P.; Previato, J. O.; Mendonça-Previato, L.; DosReis, G. A. Proapoptotic Activity of a *Trypanosoma Cruzi* Ceramide-Containing Glycolipid Turned on in Host Macrophages by IFN-γ. *J. Immunol.* **1998**, *161* (9), 4909–49016.
(67) DosReis, G. A.; Peçanha, L. M. T.; Bellio, M.; Previato, J. O.; Mendonça-Previato, L. Glycoinositol Phospholipids from *Trypanosoma Cruzi* Transmit Signals to the Cells of the Host Immune System through Both Ceramide and Glycan Chains. *Microbes Infect.* **2002**, *4* (9), 1007–1013.
(68) Brodskyn, C.; Patricio, J.; Oliveira, R.; Lobo, L.; Arnholdt, A.; Mendonça-Previato, L.; Barral, A.; Barral-Netto, M. Glycoinositolphospholipids from *Trypanosoma Cruzi* Interfere with Macrophages and Dendritic Cell Responses. *Infect. Immun.* **2002**, *70* (7), 3736–3743.
(69) Gomes, N. A.; Previato, J. O.; Zingales, B.; Mendonça-Previato, L.; DosReis, G. A. Down-Regulation of T Lymphocyte Activation *In Vitro* and *In Vivo* Induced by Glycoinositolphospholipids from *Trypanosoma Cruzi*: Assignment of the T Cell-Suppressive Determinant to the Ceramide Domain. *J. Immunol.* **1996**, *156* (2), 628–635.
(70) Oliveira, A.C.; Peixoto, J. R.; de Arruda, L. B.; Campos, M. A.; Gazzinelli, R. T.; Golenbock, D. T.; Akira, S.; Previato, J. O.; Mendonça-Previato, L.; Nobrega, A.; et al. Expression of Functional TLR4 Confers Proinflammatory Responsiveness to *Trypanosoma Cruzi* Glycoinositolphospholipids and Higher Resistance to Infection with *T. Cruzi*. *J. Immunol.* **2004**, *173* (9), 5688–5696.
(71) Medeiros, M. M.; Peixoto, J. R.; Oliveira, A.-C.; Cardilo-Reis, L.; Koatz, V. L. G.; Van Kaer, L.; Previato, J. O.; Mendonça-Previato, L.; Nobrega, A.; Bellio, M. Toll-like Receptor 4 (TLR4)-Dependent Proinflammatory and Immunomodulatory Properties of the Glycoinositolphospholipid (GIPL) from *Trypanosoma Cruzi*. *J. Leukoc. Biol.* **2007**, *82* (3), 488–496.
(72) Campos, M. A. S.; Almeida, I. C.; Takeuchi, O.; Akira, S.; Valente, E. P.; Procópio, D. O.; Travassos, L. R.; Smith, J. A.; Golenbock, D. T.; Gazzinelli, R. T. Activation of Toll-Like Receptor-2 by Glycosylphosphatidylinositol Anchors from a Protozoan Parasite. *J. Immunol.* **2001**, *167* (1), 416–423.
(73) Umezawa, E. S.; Shikanai-Yasuda, M. A.; Gruber, A.; Pereira-Chioccola, V. L.; Zingales, B. *Trypanosoma Cruzi* Defined Antigens in the Serological Evaluation of an Outbreak of Acute Chagas Disease in Brazil (Catolé Do Rocha, Paraíba). *Mem. Inst. Oswaldo Cruz* **1996**, *91* (1), 87–93.
(74) Turco, S. J.; Descoteaux, A. The Lipophosphoglycan of *Leishmania* Parasites. *Annu. Rev. Microbiol* **1992**, *46*, 65–94.
(75) Forestier, C. L.; Gao, Q.; Boons, G. J. *Leishmania* Lipophosphoglycan: How to Establish Structure-Activity Relationships for This Highly Complex and Multifunctional Glycoconjugate? *Front. Cell. Infect. Microbiol.* **2014**, *4* (January), 1–7.
(76) De Assis, R. R.; Ibraim, I. C.; Nogueira, P. M.; Soares, R. P.; Turco, S. J. Glycoconjugates in New World Species of *Leishmania*: Polymorphisms in Lipophosphoglycan and Glycoinositolphospholipids and Interaction with Hosts. *Biochim. Biophys. Acta - Gen. Subj.* **2012**, *1820* (9), 1354–1365.
(77) Dostálová, A.; Volf, P. *Leishmania* Development in Sand Flies: Parasite-Vector Interactions Overview. *Parasit. Vectors* **2012**, *276*, 1–12.
(78) Moradin, N.; Descoteaux, A. *Leishmania* Promastigotes: Building a Safe Niche within Macrophages. *Front. Cell. Infect. Microbiol.* **2012**, *2* (September), 121.
(79) Turco, S. J.; Späth, G. F.; Beverley, S. M. Is Lipophophoglycan a Virulence Factor? A

Surprising Diversity between *Leishmania* Species. *Trends Parasitol.* **2001**, *17* (5), 223–226.
(80) Ibraim, I. C.; De Assis, R. R.; Pessoa, N. L.; Campos, M. A.; Melo, M. N.; Turco, S. J.; Soares, R. P. Two Biochemically Distinct Lipophosphoglycans from *Leishmania Braziliensis* and *Leishmania Infantum* Trigger Different Innate Immune Responses in Murine Macrophages. *Parasites and Vectors* **2013**, *6* (1), 1–11.
(81) Späth, G. F.; Epstein, L.; Leader, B.; Singer, S. M.; Avila, H. A.; Turco, S. J.; Beverley, S. M. Lipophosphoglycan Is a Virulence Factor Distinct from Related Glycoconjugates in the Protozoan Parasite *Leishmania Major*. *Proc. Natl. Acad. Sci. U. S. A.* **2000**, *97* (16), 9258–9263.
(82) Ilg, T. Lipophosphoglycan Is Not Required for Infection of Macrophages or Mice by *Leishmania Mexicana*. *EMBO J.* **2000**, *19* (9), 1953–1962.
(83) Cardoso, C. A.; Araujo, G. V.; Sandoval, C. M.; Nogueira, P. M.; Zúniga, C.; Sosa-Ochoa, W. H.; Laurenti, M. D.; Soares, R. P. Lipophosphoglycans from Dermotropic *Leishmania Infantum* Are More Pro-Inflammatory Than Those from Viscerotropic Strains. *Mem. Inst. Oswaldo Cruz* **2020**, *115* (8), 1–6.
(84) Schneider, P.; Schnur, L. F.; Jaffe, C. L.; Ferguson, M. A. J.; McConville, M. J. Glycoinositol-Phospholipid Profiles of Four Serotypically Distinct Old World *Leishmania* Strains. *Biochem. J.* **1994**, *304* (2), 603–609.
(85) McConville, M. J.; Homans, S. W.; Thomas-Oates, J. E.; Dell, A.; Bacic, A. Structures of the Glycoinositolphospholipids from *Leishmania Major*. A Family of Novel Galactofuranose-Containing Glycolipids. *J. Biol. Chem.* **1990**, *265* (13), 7385–7394.
(86) McConville, M. J.; Collidge, T. A. C.; Ferguson, M. A. J.; Schneider, P. The Glycoinositol Phospholipids of *Leishmania Mexicana* Promastigotes. Evidence for the Presence of Three Distinct Pathways of Glycolipid Biosynthesis. *J. Biol. Chem.* **1993**, *268* (21), 15595–15604.
(87) Winter, G.; Fuchs, M.; McConville, M. J.; Stierhof, Y. D.; Overath, P. Surface Antigens of *Leishmania Mexicana* Amastigotes: Characterization of Glycoinositol Phospholipids and a Macrophage-Derived Glycosphingolipid. *J. Cell Sci.* **1994**, *107* (9), 2471–2482.
(88) Assis, R. R.; Ibraim, I. C.; Noronha, F. S.; Turco, S. J.; Soares, R. P. Glycoinositolphospholipids from *Leishmania Braziliensis* and *L. Infantum*: Modulation of Innate Immune System and Variations in Carbohydrate Structure. *PLoS Negl. Trop. Dis.* **2012**, *6* (2), 1–11.
(89) Zawadzki, J.; Scholz, C.; Currie, G.; Coombs, G. H.; McConville, M. J. The Glycoinositolphospholipids from *Leishmania Panamensis* Contain Unusual Glycan and Lipid Moieties. *J. Mol. Biol.* **1998**, *282* (2), 287–299.
(90) McConville, M. J.; Thomas-Oates, J. E.; Ferguson, M. A. J.; Homans, S. W. Structure of the Lipophosphoglycan from *Leishmania Major*. *J. Biol. Chem.* **1990**, *265* (32), 19611–19623.
(91) Schneider, P.; Rosat, J. P.; Ransijn, A.; Ferguson, M. A. J.; McConville, M. J. Characterization of Glycoinositol Phospholipids in the Amastigote Stage of the Protozoan Parasite *Leishmania Major*. *Biochem. J.* **1993**, *295* (2), 555–564.
(92) Rosen, G.; Londner, M. V.; Sevlever, D.; Greenblatt, C. L. *Leishmania Major*: Glycolipid Antigens Recognized by Immune Human Sera. *Mol. Biochem. Parasitol.* **1988**, *27*, 93–100.
(93) Avila, J. L.; Rojas, M.; Acosta, A. Glycoinositol Phospholipids from American *Leishmania* and *Trypanosoma* spp.: Partial Characterization of the Glycan Cores and the Human Humoral Immune Response to Them. *J. Clin. Microbiol.* **1991**, *29* (10), 2305–2312.
(94) Suzuki, E.; Tanaka, A. K.; Toledo, M. S.; Takahashi, H. K.; Straus, A. H. Role of β-D-Galactofuranose in *Leishmania Major* Macrophage Invasion. *Infect. Immun.* **2002**, *70* (12), 6592–6596.
(95) Proudfoot, L.; O'Donnell, C. A.; Liew, F. Y. Glycoinositolphospholipids of *Leishmania Major* Inhibit Nitric Oxide Synthesis and Reduce Leishmanicidal Activity in Murine Macrophages. *Eur. J. Immunol* **1995**, *25*, 745–750.
(96) Kleczka, B.; Lamerz, A. C.; Van Zandbergen, G.; Wenzel, A.; Gerardy-Schahn, R.; Wiese, M.; Routier, F. H. Targeted Gene Deletion of *Leishmania Major* UDP-Galactopyranose Mutase Leads to Attenuated Virulence. *J. Biol. Chem.* **2007**, *282* (14), 10498–10505.
(97) Zufferey, R.; Allen, S.; Barron, T.; Sullivan, D. R.; Denny, P. W.; Almeida, I. C.; Smith, D. F.; Turco, S. J.; Ferguson, M. A. J.; Beverley, S. M. Ether Phospholipids and

Glycosylinositolphospholipids Are Not Required for Amastigote Virulence or for Inhibition of Macrophage Activation by *Leishmania Major*. *J. Biol. Chem.* **2003**, *278* (45), 44708–44718.
(98) Guo, Z.; Bishop, L. Chemical Synthesis of GPIs and GPI-Anchored Glycopeptides. *European J. Org. Chem.* **2004**, No. 17, 3585–3596.
(99) Nikolaev, A. V.; Al-Maharik, N. Synthetic Glycosylphosphatidylinositol (GPI) Anchors: How These Complex Molecules Have Been Made. *Nat. Prod. Rep.* **2011**, *28* (5), 970–1020.
(100) Swarts, B. M.; Guo, Z. Chemical Synthesis of Glycosylphosphatidylinositol Anchors. In *Advances in Carbohydrate Chemistry and Biochemistry*; Horton, D., Ed.; Elsevier Inc., 2012; Vol. 67, pp 137–219.
(101) Tsai, Y. H.; Götze, S.; Vilotijevic, I.; Grube, M.; Silva, D. V.; Seeberger, P. H. A General and Convergent Synthesis of Diverse Glycosylphosphatidylinositol Glycolipids. *Chem. Sci.* **2013**, *4* (1), 468–481.
(102) Swarts, B. M. Recent Advances in the Chemical Synthesis of Glycosylphosphatidylinositols (GPIs): Expanding Synthetic Versatility for Investigating GPI Biology. *J. Carbohydr. Chem.* **2013**, *32* (5–6), 275–300.
(103) Hederos, M.; Konradsson, P. Synthesis of the Trypanosoma Cruzi LPPG Heptasaccharyl *Myo*-Inositol. *J. Am. Chem. Soc.* **2006**, *128* (10), 3414–3419.
(104) Ruda, K.; Lindberg, J.; Garegg, P. J.; Oscarson, S.; Konradsson, P. Synthesis of the *Leishmania* LPG Core Heptasaccharyl *Myo*-Inositol. *J. Am. Chem. Soc.* **2000**, *122* (45), 11067–11072.
(105) Ding, N.; Li, X.; Chinoy, Z. S.; Boons, G. J. Synthesis of a Glycosylphosphatidylinositol Anchor Derived from *Leishmania Donovani* That Can Be Functionalized by Cu-Catalyzed Azide-Alkyne Cycloadditions. *Org. Lett.* **2017**, *19* (14), 3827–3830.
(106) Lee, B. Y.; Seeberger, P. H.; Varon Silva, D. Synthesis of Glycosylphosphatidylinositol (GPI)-Anchor Glycolipids Bearing Unsaturated Lipids. *Chem. Commun.* **2016**, *52* (8), 1586–1589.
(107) Malik, A.; Seeberger, P. H.; Varón Silva, D. Advances in the Chemical Synthesis of Carbohydrates and Glycoconjugates. In *Advances in Biochemical Engineering/Biotechnology*; 2021; Vol. 175, pp 201–230.
(108) Ranade, S. C.; Demchenko, A. V. Mechanism of Chemical Glycosylation: Focus on the Mode of Activation and Departure of Anomeric Leaving Groups. *J. Carbohydr. Chem.* **2013**, *32* (1), 1–43.
(109) Adero, P. O.; Amarasekara, H.; Wen, P.; Bohé, L.; Crich, D. The Experimental Evidence in Support of Glycosylation Mechanisms at the S_N1-S_N2 Interface. *Chem. Rev.* **2018**, *118* (17), 8242–8284.
(110) Chatterjee, S.; Moon, S.; Hentschel, F.; Gilmore, K.; Seeberger, P. H. An Empirical Understanding of the Glycosylation Reaction. *J. Am. Chem. Soc.* **2018**, *140* (38), 11942–11953.
(111) Nigudkar, S. S.; Demchenko, A. V. Stereocontrolled 1,2-*Cis* Glycosylation as the Driving Force of Progress in Synthetic Carbohydrate Chemistry. *Chem. Sci.* **2015**, *6* (5), 2687–2704.
(112) Guo, J.; Ye, X. S. Protecting Groups in Carbohydrate Chemistry: Influence on Stereoselectivity of Glycosylations. *Molecules* **2010**, *15* (10), 7235–7265.
(113) Komarova, B. S.; Tsvetkov, Y. E.; Nifantiev, N. E. Design of α-Selective Glycopyranosyl Donors Relying on Remote Anchimeric Assistance. *Chem. Rec.* **2016**, *16* (1), 488–506.
(114) Hettikankanamalage, A. A.; Lassfolk, R.; Ekholm, F. S.; Leino, R.; Crich, D. Mechanisms of Stereodirecting Participation and Ester Migration from near and Far in Glycosylation and Related Reactions. *Chem. Rev.* **2020**, *120* (15), 7104–7151.
(115) Elferink, H.; Severijnen, M. E.; Martens, J.; Mensink, R. A.; Berden, G.; Oomens, J.; Rutjes, F. P. J. T.; Rijs, A. M.; Boltje, T. J. Direct Experimental Characterization of Glycosyl Cations by Infrared Ion Spectroscopy. *J. Am. Chem. Soc.* **2018**, *140* (19), 6034–6038.
(116) Marianski, M.; Mucha, E.; Greis, K.; Moon, S.; Pardo, A.; Kirschbaum, C.; Thomas, D. A.; Meijer, G.; von Helden, G.; Gilmore, K.; et al. Remote Participation during Glycosylation Reactions of Galactose Building Blocks: Direct Evidence from Cryogenic Vibrational Spectroscopy. *Angew. Chemie - Int. Ed.* **2020**, *59* (15), 6166–6171.
(117) Hansen, T.; Elferink, H.; van Hengst, J. M. A.; Houthuijs, K. J.; Remmerswaal, W. A.; Kromm, A.; Berden, G.; van der Vorm, S.; Rijs, A. M.; Overkleeft, H. S.; et al. Characterization of Glycosyl Dioxolenium Ions and Their Role in Glycosylation Reactions.

Nat. Commun. **2020**, *11* (1), 1–9.
(118) Crich, D. En Route to the Transformation of Glycoscience: A Chemist's Perspective on Internal and External Crossroads in Glycochemistry. *J. Am. Chem. Soc.* **2021**, *143* (1), 17–34.
(119) Baek, J. Y.; Kwon, H. W.; Myung, S. J.; Park, J. J.; Kim, M. Y.; Rathwell, D. C. K.; Jeon, H. B.; Seeberger, P. H.; Kim, K. S. Directing Effect by Remote Electron-Withdrawing Protecting Groups at O-3 or O-4 Position of Donors in Glucosylations and Galactosylations. *Tetrahedron* **2015**, *71* (33), 5315–5320.
(120) Demchenko, A. V.; Rousson, E.; Boons, G. J. Stereoselective 1,2-*Cis*-Galactosylation Assisted by Remote Neighboring Group Participation and Solvent Effects. *Tetrahedron Lett.* **1999**, *40* (36), 6523–6526.
(121) Ding, Y.; Vara Prasad, C. V. N. S.; Wang, B. Glycosylation on Unprotected or Partially Protected Acceptors. *European J. Org. Chem.* **2020**, *2020* (12), 1784–1801.
(122) Wen, L.; Edmunds, G.; Gibbons, C.; Zhang, J.; Gadi, M. R.; Zhu, H.; Fang, J.; Liu, X.; Kong, Y.; Wang, P. G. Toward Automated Enzymatic Synthesis of Oligosaccharides. *Chem. Rev.* **2018**, *118* (17), 8151–8187.
(123) Kulkarni, S. S.; Wang, C. C.; Sabbavarapu, N. M.; Podilapu, A. R.; Liao, P. H.; Hung, S. C. "One-Pot" Protection, Glycosylation, and Protection-Glycosylation Strategies of Carbohydrates. *Chem. Rev.* **2018**, *118* (17), 8025–8104.
(124) Panza, M.; Pistorio, S. G.; Stine, K. J.; Demchenko, A. V. Automated Chemical Oligosaccharide Synthesis: Novel Approach to Traditional Challenges. *Chem. Rev.* **2018**, *118* (17), 8105–8150.
(125) Guberman, M.; Seeberger, P. H. Automated Glycan Assembly: A Perspective. *J. Am. Chem. Soc.* **2019**, *141* (14), 5581–5592.
(126) Yu, Y.; Kononov, A.; Delbianco, M.; Seeberger, P. H. A Capping Step During Automated Glycan Assembly Enables Access to Complex Glycans in High Yield. *Chem. - A Eur. J.* **2018**, *24* (23), 6075–6078.
(127) Le Mai Hoang, K.; Pardo-Vargas, A.; Zhu, Y.; Yu, Y.; Loria, M.; Delbianco, M.; Seeberger, P. H. Traceless Photolabile Linker Expedites the Chemical Synthesis of Complex Oligosaccharides by Automated Glycan Assembly. *J. Am. Chem. Soc.* **2019**, *141* (22), 9079–9086.
(128) Hahm, H. S.; Hurevich, M.; Seeberger, P. H. Automated Assembly of Oligosaccharides Containing Multiple *Cis*-Glycosidic Linkages. *Nat. Commun.* **2016**, *7*, 2–9.
(129) Zhu, Y.; Delbianco, M.; Seeberger, P. H. Automated Assembly of Starch and Glycogen Polysaccharides. *J. Am. Chem. Soc.* **2021**, *143* (26), 9758–9768.
(130) Joseph, A. A.; Pardo-Vargas, A.; Seeberger, P. H. Total Synthesis of Polysaccharides by Automated Glycan Assembly. *J. Am. Chem. Soc.* **2020**, *142* (19), 8561–8564.
(131) Schmidt, D.; Schuhmacher, F.; Geissner, A.; Seeberger, P. H.; Pfrengle, F. Automated Synthesis of Arabinoxylan-Oligosaccharides Enables Characterization of Antibodies That Recognize Plant Cell Wall Glycans. *Chem. - A Eur. J.* **2015**, *21* (15), 5709–5713.
(132) Dallabernardina, P.; Ruprecht, C.; Smith, P. J.; Hahn, M. G.; Urbanowicz, B. R.; Pfrengle, F. Automated Glycan Assembly of Galactosylated Xyloglucan Oligosaccharides and Their Recognition by Plant Cell Wall Glycan-Directed Antibodies. *Org. Biomol. Chem.* **2017**, *15* (47), 9996–10000.
(133) Marino, C.; Baldoni, L. Synthesis of D-Galactofuranose-Containing Molecules: Design of Galactofuranosyl Acceptors. *ChemBioChem* **2014**, *15* (2), 189–204.
(134) Angyal, S. J. The Composition of Reducing Sugars in Solution. In *Advances in Carbohydrate Chemistry and Biochemistry*; Tipson, R. S., Horton, D., Eds.; Academic Press, 1984; Vol. 42, pp 15–68.
(135) Paez, M.; Martínez-Castro, I.; Sanz, J.; Olano, A.; Garcia-Raso, A.; Saura-Calixto, F. Identification of the Components of Aldoses in a Tautomeric Equilibrium Mixture as Their Trimethylsilyl Ethers by Capillary Gas Chromatography. *Chromatographia* **1987**, *23* (1), 43–46.
(136) Morgenlie, S. Isopropylidene Derivatives of α-D-Galactofuranose. *Acta Chem. Scand.* **1973**, *27*, 3609–3610.
(137) Cattiaux, L.; Sendid, B.; Collot, M.; MacHez, E.; Poulain, D.; Mallet, J. M. Synthetic

Biotinylated Tetra β(1→5) Galactofuranoside for *in Vitro* Aspergillosis Diagnosis. *Bioorganic Med. Chem.* **2011**, *19* (1), 547–555.
(138) Ota, R.; Okamoto, Y.; Vavricka, C. J.; Oka, T.; Matsunaga, E.; Takegawa, K.; Kiyota, H.; Izumi, M. Chemo-Enzymatic Synthesis of *p*-Nitrophenyl β-D-Galactofuranosyl Disaccharides from *Aspergillus* Sp. Fungal-Type Galactomannan. *Carbohydr. Res.* **2019**, *473* (December 2018), 99–103.
(139) Gallo-rodriguez, C.; Varela, O.; Lederkremer, R. M. De. One-Pot Synthesis of β-D-Gal*f*(1→4)[β-D-Gal*p*(1→6)]-D-GlcNAc, a "core" Trisaccharide Linked *O*-Glycosidically in Glycoproteins of Trypanosoma Cruzi. *Carbohydr. Res.* **1998**, *305*, 163–170.
(140) Baldoni, L.; Marino, C. Facile Synthesis of Per-O-Tert-Butyldimethylsilyl-β-D-Galactofuranose and Efficient Glycosylation via the Galactofuranosyl Iodide. *J. Org. Chem.* **2009**, *74* (5), 1994–2003.
(141) Dureau, R.; Legentil, L.; Daniellou, R.; Ferrières, V. Two-Step Synthesis of Per-*O*-Acetylfuranoses: Optimization and Rationalization. *J. Org. Chem.* **2012**, *77* (3), 1301–1307.
(142) Baldoni, L.; Marino, C. Synthesis of S- and C-Galactofuranosides via a Galactofuranosyl Iodide. Isolable 1-Galactofuranosylthiol Derivative as a New Glycosyl Donor. *Carbohydr. Res.* **2012**, *362*, 70–78.
(143) Arasappan, A.; Fraser-Reid, B. *N*-Pentenyl Furanosides: Synthesis and Glycosidation Reactions of Some Galacto Derivatives. *Tetrahedron Lett.* **1995**, *36* (44), 7967–7970.
(144) Velty, R.; Benvegnu, T.; Gelin, M.; Privat, E.; Plusquellec, D. A Convenient Synthesis of Disaccharides Containing Furanoside Units. *Carbohydr. Res.* **1997**, *299* (1–2), 7–14.
(145) Ferrières, V.; Bertho, J. N.; Plusquellec, D. A New Synthesis of *O*-Glycosides from Totally *O*-Unprotected Glycosyl Donors. *Tetrahedron Lett.* **1995**, *36* (16), 2749–2752.
(146) Ferrières, V.; Bertho, J. N.; Plusquellec, D. A Convenient Synthesis of Alkyl D-Glycofuranosiduronic Acids and Alkyl D-Glycofuranosides from Unprotected Carbohydrates. *Carbohydr. Res.* **1998**, *311* (1–2), 25–35.
(147) Lubineau, A.; Fischer, J. C. High-Yielding One-Step Conversion of D-Glucose and D-Galactose to the Corresponding α and β Methyl-D-Glucofuranosides and Galactofuranosides. *Synth. Commun.* **1991**, *21* (6), 815–818.
(148) Masui, S.; Manabe, Y.; Hirao, K.; Shimoyama, A.; Fukuyama, T.; Ryu, I.; Fukase, K. Kinetically Controlled Fischer Glycosidation under Flow Conditions: A New Method for Preparing Furanosides. *Synlett* **2019**, *30* (4), 397–400.
(149) Klotz, W.; Schmidt, R. R. Anomeric *O*-Alkylation of *O*-Unprotected Hexoses and Pentoses – Convenient Synthesis of Decyl, Benzyl, and Allyl Glycosides. *Liebigs Ann. der Chemie* **1993**, 683–690.
(150) Gola, G.; Libenson, P.; Gandolfi-Donadío, L.; Gallo-Rodriguez, C. Synthesis of 2,3,5,6-Tetra-*O*-Benzyl-D-Galactofuranose for α-Glycosidation. *Arkivoc* **2006**, *2005* (12), 234–242.
(151) Kashiwagi, G. A.; Mendoza, V. M.; De Lederkremer, R. M.; Gallo-Rodriguez, C. Synthesis of the O-Linked Hexasaccharide Containing β-D-Galf- (1→2)-β-D-Gal*f* in *Trypanosoma Cruzi* Mucins. *Org. Biomol. Chem.* **2012**, *10* (31), 6322–6332.
(152) Thomann, J. S.; Monneaux, F.; Creusat, G.; Spanedda, M. V.; Heurtault, B.; Habermacher, C.; Schuber, F.; Bourel-Bonnet, L.; Frisch, B. Novel Glycolipid TLR2 Ligands of the Type Pam_2Cys-α-Gal: Synthesis and Biological Properties. *Eur. J. Med. Chem.* **2012**, *51*, 174–183.
(153) Rauter, A. P.; Ramôa-Ribeiro, F.; Fernandes, A. C.; Figueiredo, J. A. A New Method of Acetonation with the Zeolite HY as Catalyst. Synthesis of *O*-Isopropylidene Sugar Derivatives. *Tetrahedron* **1995**, *51* (23), 6529–6540.
(154) Wang, H.; Zhang, G.; Ning, J. First Synthesis of β-D-Gal*f*-(1→3)-D-Gal*p* - The Repeating Unit of the Backbone Structure of the O-Antigenic Polysaccharide Present in the Lipopolysaccharide (LPS) of the Genus *Klebsiella*. *Carbohydr. Res.* **2003**, *338* (10), 1033–1037.
(155) Wang, H.; Ning, J. A One-Pot Strategy for Synthesis of 5-O-(α-D-Arabinofuranosyl)-6-O-(β-D-Galactofuranosyl)-D-Galactofuranose Present in Motif E of the *Mycobacterium Tuberculosis* Cell Wall. *J. Org. Chem.* **2003**, *68* (6), 2521–2524.
(156) Lemieux, R. U.; Stick, R. V. 1,2:5,6-Di-*O*-Isopropylidene-α-D-Galactofuranose. *Aust. J. Chem.* **1975**, *28*, 1799–1801.

(157) Sato, K. I.; Akai, S.; Sakuma, M.; Kojima, M.; Suzuki, K. J. Practical Synthesis of [1-^{13}C]- and [6-^{13}C]-D-Galactose. *Tetrahedron Lett.* **2003**, *44* (26), 4903–4907.
(158) Horton, D.; Norris, P. Dialkyl Dithioacetals of Sugars. In *Preparative Carbohydrate Chemistry*; Hanessian, S., Ed.; Marcel Dekker, Inc: New York, 1997; pp 35–52.
(159) Lerner, L. M. The Acetolysis of D-Galactose Diethyl Dithioacetal. *Carbohydr. Res.* **1996**, *282* (1), 189–192.
(160) Wolfrom, M. L.; Yosizawa, Z.; Juliano, B. O. Ethyl 1-Thio-α-D-Galactofuranoside. *J. Org. Chem* **1959**, *24* (10), 1529–1530.
(161) Wolfrom, M. L.; McWain, P.; Pagnucco, R.; Thompson, A. Hexofuranosyl Nucleosides from Sugar Dithioacetals. *J. Org. Chem.* **1964**, *29* (2), 454–457.
(162) De Talancé, V. L.; Thiery, E.; Eppe, G.; Bkassiny, S. El; Mortier, J.; Vincent, S. P. A Simple Synthesis of D-Galactono-1,4-Lactone and Key Building Blocks for the Preparation of Galactofuranosides. *J. Carbohydr. Chem.* **2011**, *30* (7–9), 605–617.
(163) Choudhury, A. K.; Roy, N. Synthesis of Some Galactofuranosyl Disaccharides Using a Galactofuranosyl Trichloroacetimidate as Donor. *Carbohydr. Res.* **1998**, *308* (1–2), 207–211.
(164) Misra, A. K.; Mukherjee, C. Glycosylation and Pyranose-Furanose Isomerization of Carbohydrates Using $HClO_4$-SiO_2: Synthesis of Oligosaccharides Containing Galactofuranose. *Synthesis (Stuttg).* **2007**, *5*, 683–692.
(165) Krylov, V. B.; Argunov, D. A.; Vinnitskiy, D. Z.; Verkhnyatskaya, S. A.; Gerbst, A. G.; Ustyuzhanina, N. E.; Dmitrenok, A. S.; Huebner, J.; Holst, O.; Siebert, H. C.; et al. Pyranoside-into-Furanoside Rearrangement: New Reaction in Carbohydrate Chemistry and Its Application in Oligosaccharide Synthesis. *Chem. - A Eur. J.* **2014**, *20* (50), 16516–16522.
(166) Krylov, V. B.; Argunov, D. A.; Vinnitskiy, D. Z.; Gerbst, A. G.; Ustyuzhanina, N. E.; Dmitrenok, A. S.; Nifantiev, N. E. The Pyranoside-into-Furanoside Rearrangement of Alkyl Glycosides: Scope and Limitations. *Synlett* **2016**, *27* (11), 1659–1664.
(167) Verkhnyatskaya, S. A.; Krylov, V. B.; Nifantiev, N. E. Pyranoside-into-Furanoside Rearrangement of 4-Pentenyl Glycosides in the Synthesis of a Tetrasaccharide-Related to Galactan I of *Klebsiella Pneumoniae*. *European J. Org. Chem.* **2017**, *2017* (3), 710–718.
(168) Argunov, D. A.; Krylov, V. B.; Nifantiev, N. E. Convergent Synthesis of Isomeric Heterosaccharides Related to the Fragments of Galactomannan from *Aspergillus Fumigatus*. *Org. Biomol. Chem.* **2015**, *13* (11), 3255–3267.
(169) Johnston, B. D.; Pinto, B. M. Use of a Phenyl 1-Selenogalactofuranoside as a Glycosyl Donor for the Synthesis of Galactofuranosyl-Containing Disaccharides. *Carbohydr. Res.* **1999**, *315* (3–4), 355–360.
(170) Randell, K. D.; Johnston, B. D.; Brown, P. N.; Pinto, B. M. Synthesis of Galactofuranosyl-Containing Oligosaccharides Corresponding to the Glycosylinositolphospholipid of *Trypanosoma Cruzi*. *Carbohydr. Res.* **2000**, *325* (4), 253–264.
(171) Gallo-Rodriguez, C.; Gandolfi, L.; De Lederkremer, R. M. Synthesis of β-D-Gal*f*-(1-3)-D-GlcNAc by the Trichloroacetamidate Method and of β-D-Gal*f*-(1-6)-D-GlcNAc by $SnCl_4$-Promoted Glycosylation. *Org. Lett.* **1999**, *1* (2), 245–247.
(172) Morris, P. E.; Kiely, D. E. Ruthenium Tetraoxide Phase-Transfer-Promoted Oxidation of Secondary Alcohols to Ketones. *J. Org. Chem.* **1987**, *52* (6), 1149–1152.
(173) Gandolfi-Donadio, L.; Gallo-Rodriguez, C.; De Lederkremer, R. M. Synthesis of α-D-Gal*p*-(1→3)-β-D-Gal*f*-(1→3)-D-Man, a Terminal Trisaccharide of Leishmania Type-2 Glycoinositolphospholipids. *J. Org. Chem.* **2002**, *67*, 4430–4435.
(174) Fleet, G. W. J.; Son, J. C. Polyhydroxylated Pyrrolidines from Sugar Lactones: Synthesis of 1,4-Dideoxy-1,4-Imino-D-Glucitol from D-Galactonolactone and Syntheses of 1,4-Dideoxy-1,4-Imino-D-Allitol, 1,4-Dideoxy-1,4-Imino-D-Ribitol, and (2S,3R,4S)-3,4-Dihydroxyproline from D-Gulonola. *Tetrahedron* **1988**, *44* (9), 2637–2647.
(175) Argunov, D. A.; Krylov, V. B.; Nifantiev, N. E. The Use of Pyranoside-into-Furanoside Rearrangement and Controlled O(5) → O(6) Benzoyl Migration as the Basis of a Synthetic Strategy to Assemble (1→5)- and (1→6)-Linked Galactofuranosyl Chains. *Org. Lett.* **2016**, *18* (21), 5504–5507.
(176) Iniguez, E.; Schocker, N. S.; Subramaniam, K.; Portillo, S.; Montoya, A. L.; Al-Salem, W. S.; Torres, C. L.; Rodriguez, F.; Moreira, O. C.; Acosta-Serrano, A.; et al. An α-Gal-Containing

Neoglycoprotein-Based Vaccine Partially Protects against Murine Cutaneous Leishmaniasis Caused by *Leishmania Major*. *PLoS Negl. Trop. Dis.* **2017**, *11* (10), 1–25.
(177) Montoya, A. L.; Austin, V. M.; Portillo, S.; Vinales, I.; Ashmus, R. A.; Estevao, I.; Jankuru, S. R.; Alraey, Y.; Al-Salem, W. S.; Acosta-Serrano, Á.; et al. Reversed Immunoglycomics Identifies α-Galactosyl-Bearing Glycotopes Specific for *Leishmania Major* Infection. *JACS Au* **2021**, *1* (8), 1275–1287.
(178) Neises, B.; Steglich, W. Simple Method for the Esterification of Carboxylic Acids. *Angew. Chemie Int. Ed. English* **1978**, *17* (7), 522–524.
(179) Horton, D.; Nakadate, M.; Tronchet, J. M. J. 1,2:3,4-Di-*O*-Isopropylidene-α-D-Galacto-Hexodialdo-1,5-Pyranose and Its 6-Aldehydrol. *Carbohydr. Res.* **1968**, *7*, 56–65.
(180) Gelin, M.; Ferrières, V.; Lefeuvre, M.; Plusquellec, D. First Intramolecular Aglycon Delivery onto a D-Fucofuranosyl Entity for the Synthesis of α-D-Fucofuranose-Containing Disaccharides. *European J. Org. Chem.* **2003**, *2* (7), 1285–1293.
(181) Lawandi, J.; Rocheleau, S.; Moitessier, N. Regioselective Acylation, Alkylation, Silylation and Glycosylation of Monosaccharides. *Tetrahedron* **2016**, *72* (41), 6283–6319.
(182) Grindley, T. B. Applications of Tin-Containing Intermediates to Carbohydrate Chemistry. In *Advances in Carbohydrate Chemistry and Biochemistry*; Horton, D., Ed.; Academic Press, 1998; Vol. 53, pp 17–142.
(183) Holzapfel, C. W.; Koekemoer, J. M.; Marais, C. F. Benzoylation of Carbohydrate Derivatives Containing Regioselectively Activated Secondary Hydroxyl Groups. *South African J. Chem.* **1984**, *37* (July 1983), 19–26.
(184) Grindley, T. B.; Cote, C. J. P.; Wickramage, C. Kinetic Cyclohexylidenation and Isopropylidenation of Aldose Diethyl Dithioacetals. *Carbohydr. Res.* **1985**, *140*, 215–238.
(185) Grindley, T. B.; Wickramage, C. The Rearrangement of Mono-*O*-Isopropylidene Derivates of Aldose Diethyl Dithioacetals. *Carbohydr. Res.* **1987**, *167*, 105–121.
(186) Adibekian, A.; Bindschädler, P.; Timmer, M. S. M.; Noti, C.; Schützenmeister, N.; Seeberger, P. H. De Novo Synthesis of Uronic Acid Building Blocks for Assembly of Heparin Oligosaccharides. *Chem. - A Eur. J.* **2007**, *13* (16), 4510–4522.
(187) Bindschädler, P.; Adibekian, A.; Grünstein, D.; Seeberger, P. H. De Novo Synthesis of Differentially Protected L-Iduronic Acid Glycosylating Agents. *Carbohydr. Res.* **2010**, *345* (7), 948–955.
(188) Song, W. S.; Liu, S. X.; Chang, C. C. Synthesis of L-Deoxyribonucleosides from D-Ribose. *J. Org. Chem.* **2018**, *83* (24), 14923–14932.
(189) Durón, S. G.; Polat, T.; Wong, C. H. N-(Phenylthio)-ε-Caprolactam: A New Promoter for the Activation of Thioglycosides. *Org. Lett.* **2004**, *6* (5), 839–841.
(190) Peng, W.; Jayasuriya, A. B.; Imamura, A.; Lowary, T. L. Synthesis of the 6-O-Methyl-D-Glycero-α-L-Gluco-Heptopyranose Moiety Present in the Capsular Polysaccharide from *Campylobacter Jejuni* NCTC 11168. *Org. Lett.* **2011**, *13* (19), 5290–5293.
(191) Cyr, N.; Perlin, A. S. The Conformations of Furanosides. A ^{13}C Nuclear Magnetic Resonance Study. *Can. J. Chem.* **1979**, *57*, 2504–2511.
(192) Deng, L. M.; Liu, X.; Liang, X. Y.; Yang, J. S. Regioselective Glycosylation Method Using Partially Protected Arabino- and Galactofuranosyl Thioglycosides as Key Glycosylating Substrates and Its Application to One-Pot Synthesis of Oligofuranoses. *J. Org. Chem.* **2012**, *77* (7), 3025–3037.
(193) Iversen, T.; Bundle, D. K. Benzyl Trichloroacetimidate, a Versatile Reagent for Acid-Catalysed Benzylation of Hydroxy-Groups. *J. Chem. Soc. Chem. Commun.* **1981**, No. 23, 1240–1241.
(194) Gathirwa, J. W.; Maki, T. Benzylation of Hydroxy Groups with Tertiary Amine as a Base. *Tetrahedron* **2012**, *68* (1), 370–375.
(195) Wang, L.; Hashidoko, Y.; Hashimoto, M. Cosolvent-Promoted *O*-Benzylation with Silver(I) Oxide: Synthesis of 1′-Benzylated Sucrose Derivatives, Mechanistic Studies, and Scope Investigation. *J. Org. Chem.* **2016**, *81* (11), 4464–4474.
(196) Yamada, K.; Fujita, H.; Kunishima, M. A Novel Acid-Catalyzed *O*-Benzylating Reagent with the Smallest Unit of Imidate Structure. *Org. Lett.* **2012**, *14* (19), 5026–5029.
(197) Zhang, Z.; Ollmann, I. R.; Ye, X.; Wischnat, R.; Baasov, T.; Wong, C. Programmable One-Pot

Oligosaccharide Synthesis. *J. Am. Chem. Soc.* **1999**, *121* (4), 734–753.
(198) D'Accorso, N. B.; Thiel, I. M. E.; Schüller, M. Proton and C-13 Nuclear Magnetic Resonance Spectra of Some Benzoylated Aldohexoses. *Carbohydr. Res.* **1983**, *124* (2), 177–184.
(199) Marino, C.; Mariño, K.; Miletti, L.; Alves, M. J. M.; Colli, W.; De Lederkremer, R. M. 1-Thio-β-D-Galactofuranosides: Synthesis and Evaluation as β-D-Galactofuranosidase Inhibitors. *Glycobiology* **1998**, *8* (9), 901–904.
(200) Mariño, K.; Marino, C. Synthesis of Heteroaryl 1-Thio-β-D-Galactofuranosides and Evaluation of Their Inhibitory Activity towards a β-D-Galactofuranosidase. *Arkivoc* **2005**, *2005* (12), 341–351.
(201) Wang, S.; Meng, X.; Huang, W.; Yang, J. S. Influence of Silyl Protections on the Anomeric Reactivity of Galactofuranosyl Thioglycosides and Application of the Silylated Thiogalactofuranosides to One-Pot Synthesis of Diverse β-D-Oligogalactofuranosides. *J. Org. Chem.* **2014**, *79* (21), 10203–10217.
(202) Zhu, S. Y.; Yang, J. S. Synthesis of Tetra- and Hexasaccharide Fragments Corresponding to the O-Antigenic Polysaccharide of *Klebsiella Pneumoniae*. *Tetrahedron* **2012**, *68* (20), 3795–3802.
(203) He, P.; Li, X. H.; Chen, Q. H.; Yang, J. S.; Wang, F. P. Total Synthesis of Fuzinoside. *Tetrahedron* **2014**, *70* (26), 4022–4030.
(204) Vatèle, J. M. Regioselective Oxidative Cleavage of Benzylidene Acetals of Glycopyranosides with Periodic Acid Catalyzed by Tetrabutylammonium Bromide. *Synlett* **2014**, *25* (1), 115–119.
(205) Fukase, K.; Fukase, Y.; Oikawa, M.; Liu, W. C.; Suda, Y.; Kusumoto, S. Divergent Synthesis and Biological Activities of Lipid A Analogues of Shorter Acyl Chains. *Tetrahedron* **1998**, *54* (16), 4033–4050.
(206) Wang, C. C.; Lee, J. C.; Luo, S. Y.; Kulkarni, S. S.; Huang, Y. W.; Lee, C. C.; Chang, K. L.; Hung, S. C. Regioselective One-Pot Protection of Carbohydrates. *Nature* **2007**, *446* (7138), 896–899.
(207) Joseph, A. A.; Verma, V. P.; Liu, X. Y.; Wu, C. H.; Dhurandhare, V. M.; Wang, C. C. TMSOTf-Catalyzed Silylation: Streamlined Regioselective One-Pot Protection and Acetylation of Carbohydrates. *European J. Org. Chem.* **2012**, No. 4, 744–753.
(208) Ohlin, M.; Johnsson, R.; Ellervik, U. Regioselective Reductive Openings of 4,6-Benzylidene Acetals: Synthetic and Mechanistic Aspects. *Carbohydr. Res.* **2011**, *346* (12), 1358–1370.
(209) Daragics, K.; Fügedi, P. Regio- and Chemoselective Reductive Cleavage of 4,6-O-Benzylidene-Type Acetals of Hexopyranosides Using BH_3.THF-TMSOTf. *Tetrahedron Lett.* **2009**, *50* (24), 2914–2916.

Appendix

Content

List of Appendix Figures

A. NMR Spectra

A.1. 1,2:5,6-Di-*O*-isoprolylidine-α-D-galactopyranose (**I-10)**

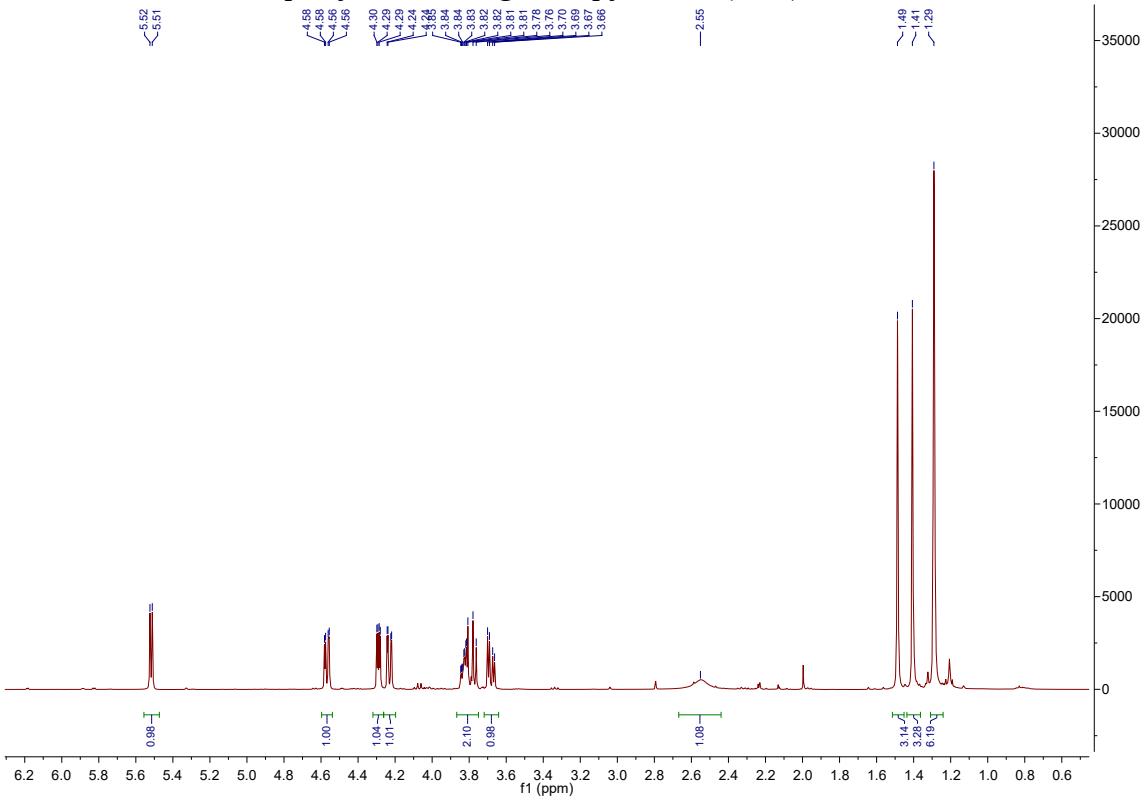

Figure A.1: ^{1}H NMR spectrum of **I-10**, in $CDCl_3$

A.2. Contaminated 1,2:5,6-Di-*O*-isoprolylidine-α-D-galactofuranose (**I-9)**

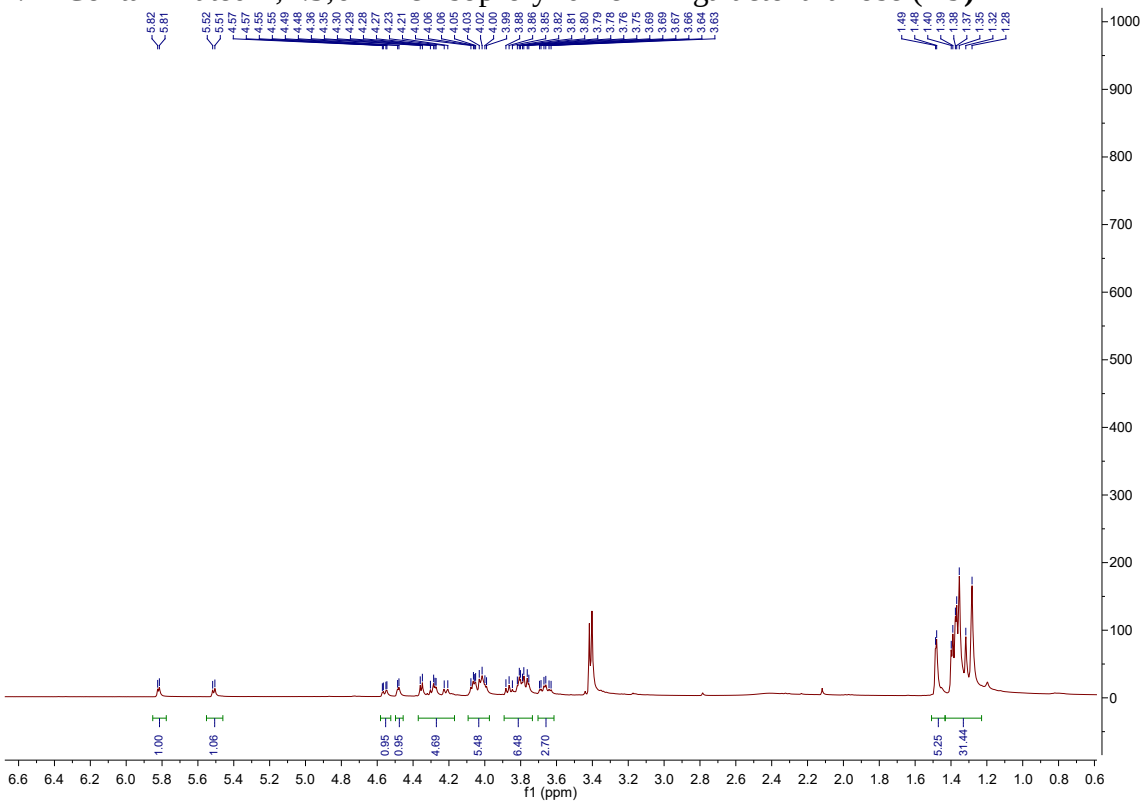

Figure A.2: ^{1}H NMR spectrum of contaminated **I-9**, in $CDCl_3$.

A.3. Benzyl α-D-galactofuranoside (**I-5**)

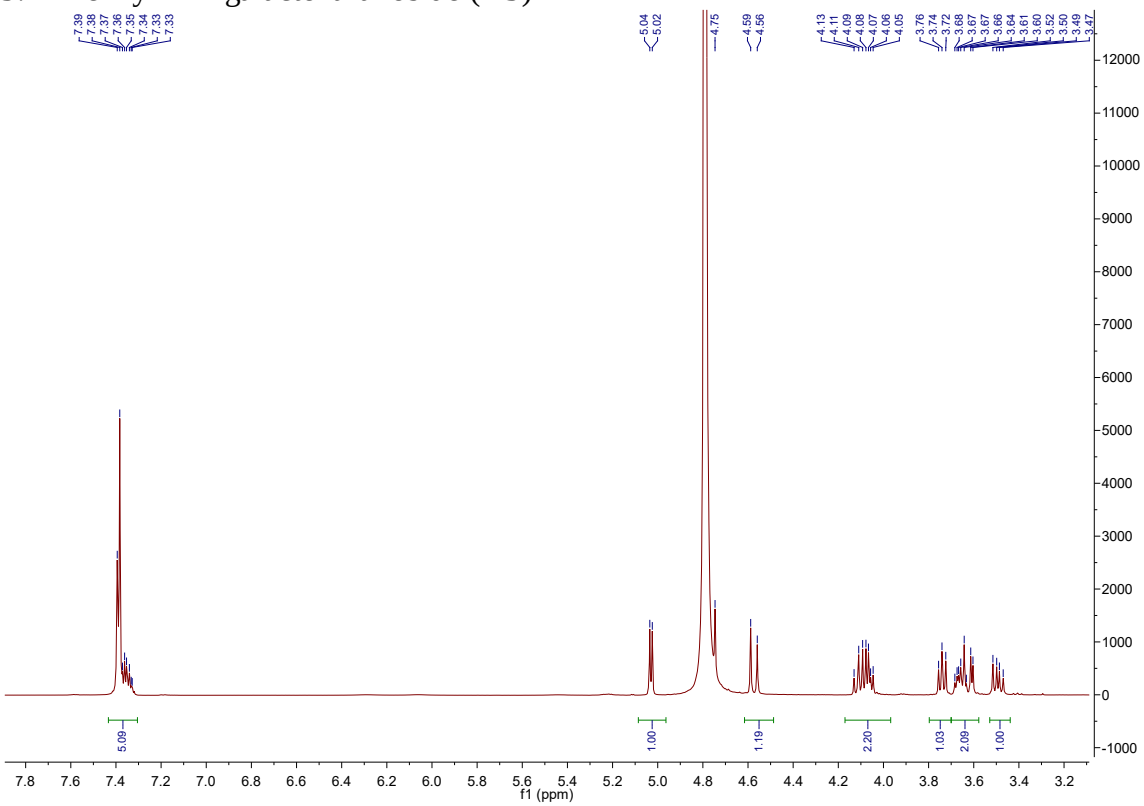

Figure A.3: ^{1}H NMR spectrum of **I-5**, in D_2O.

A.4. Benzyl 5,6-O-isopropylidene-α-D-galactofuranoside (**I-33**), contaminated with DMPU

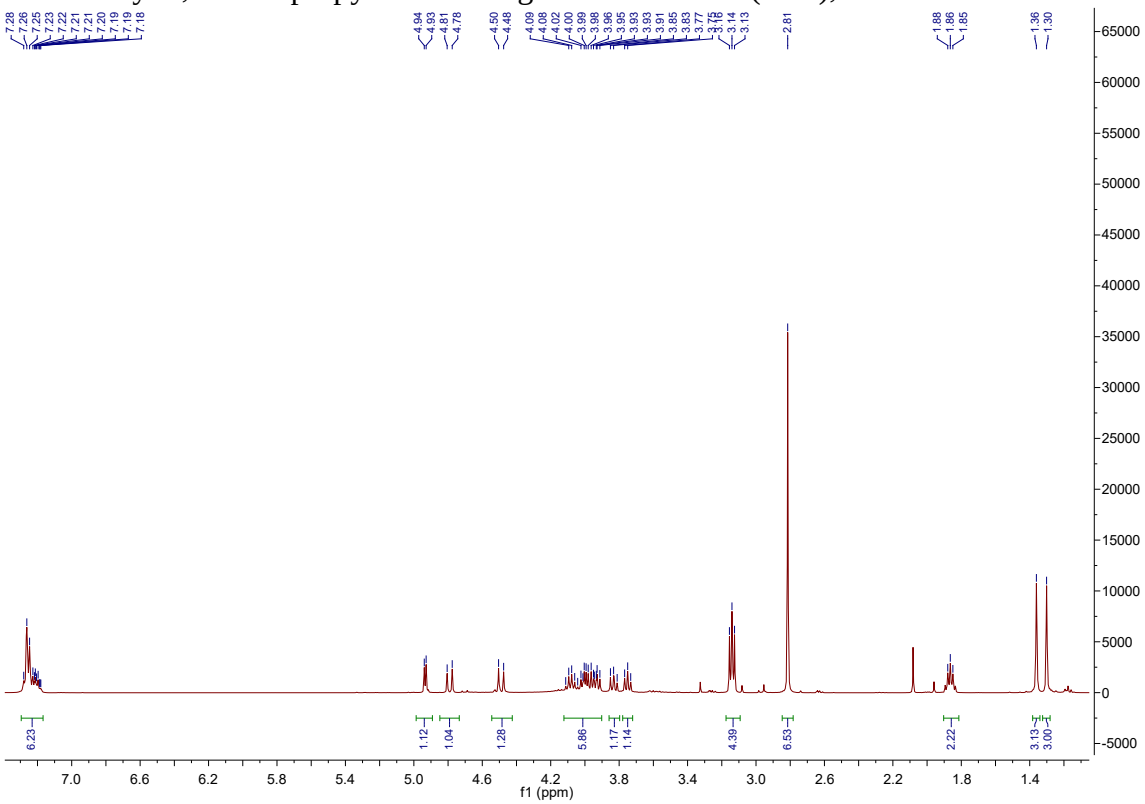

Figure A.4: ^{1}H NMR spectrum of **I-33** and DMPU, in $CDCl_3$.

A.5. Benzyl 5,6-*O*-isopropylidene-2-*O*-(trimethylacetyl)-α-D-galactofuranoside (**1a**)

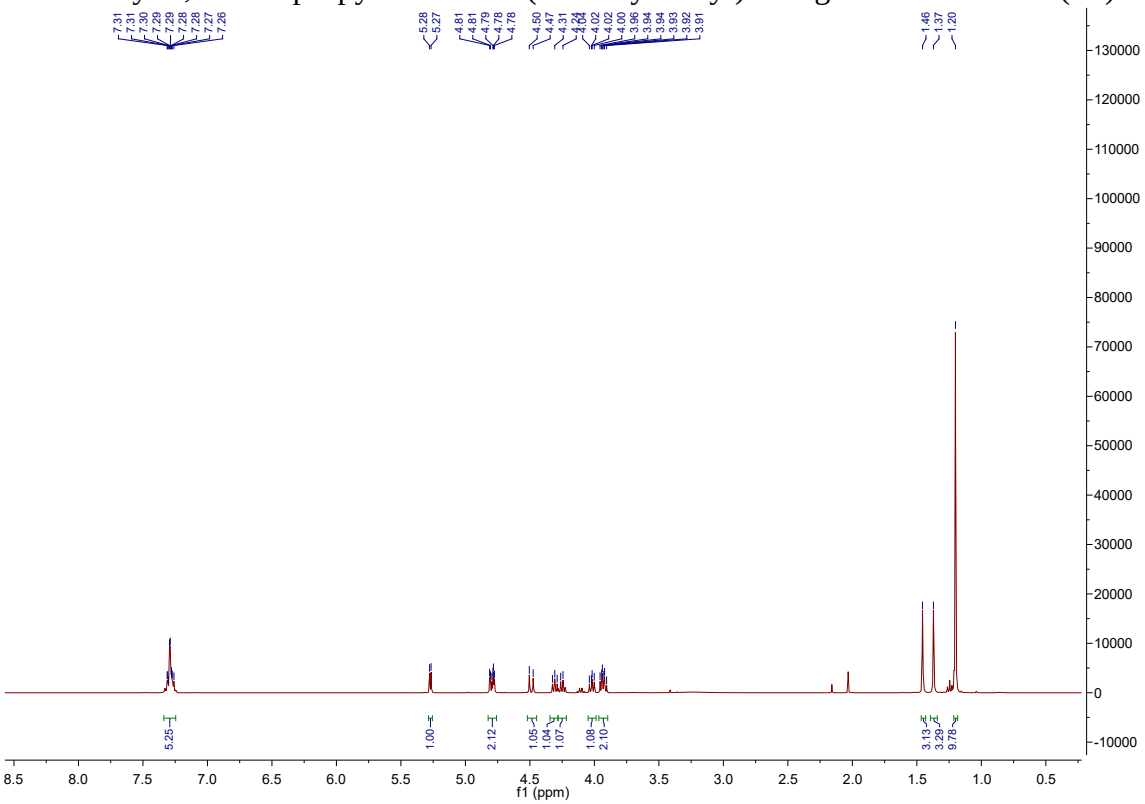

Figure A.5: ^{1}H NMR spectrum of **1a**, in $CDCl_3$.

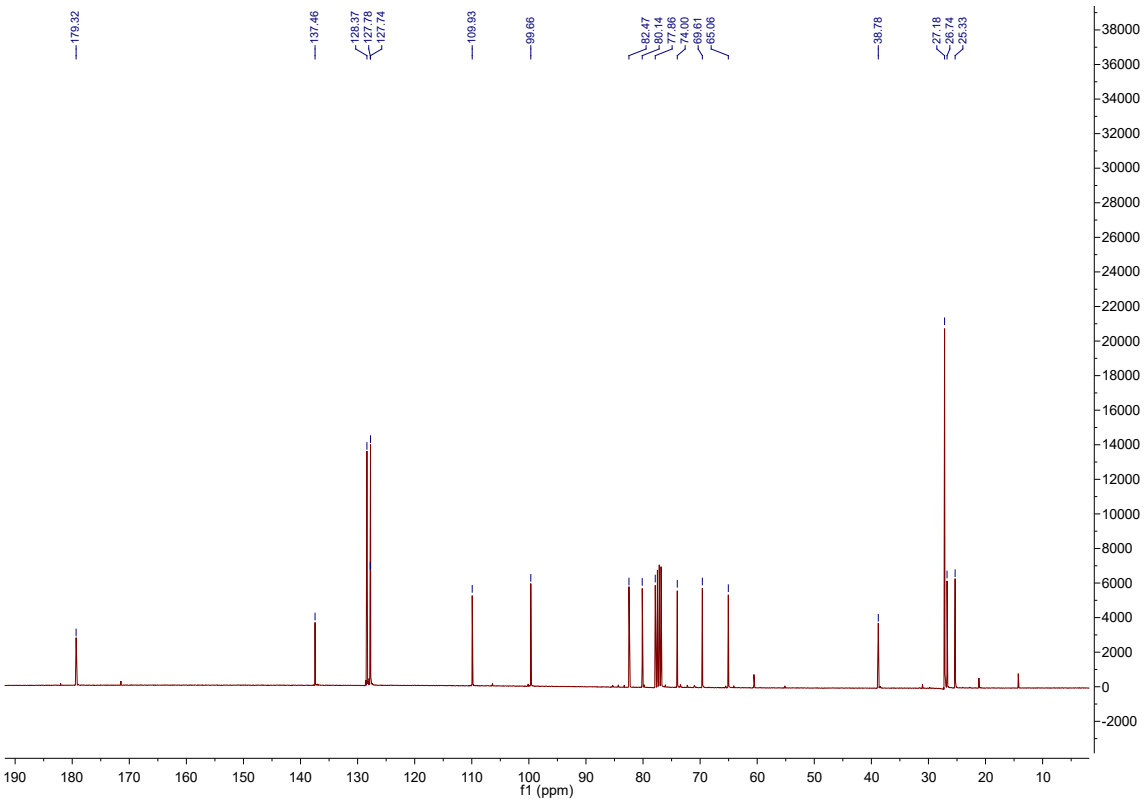

Figure A.6: ^{13}C NMR spectrum of **1a**, in $CDCl_3$.

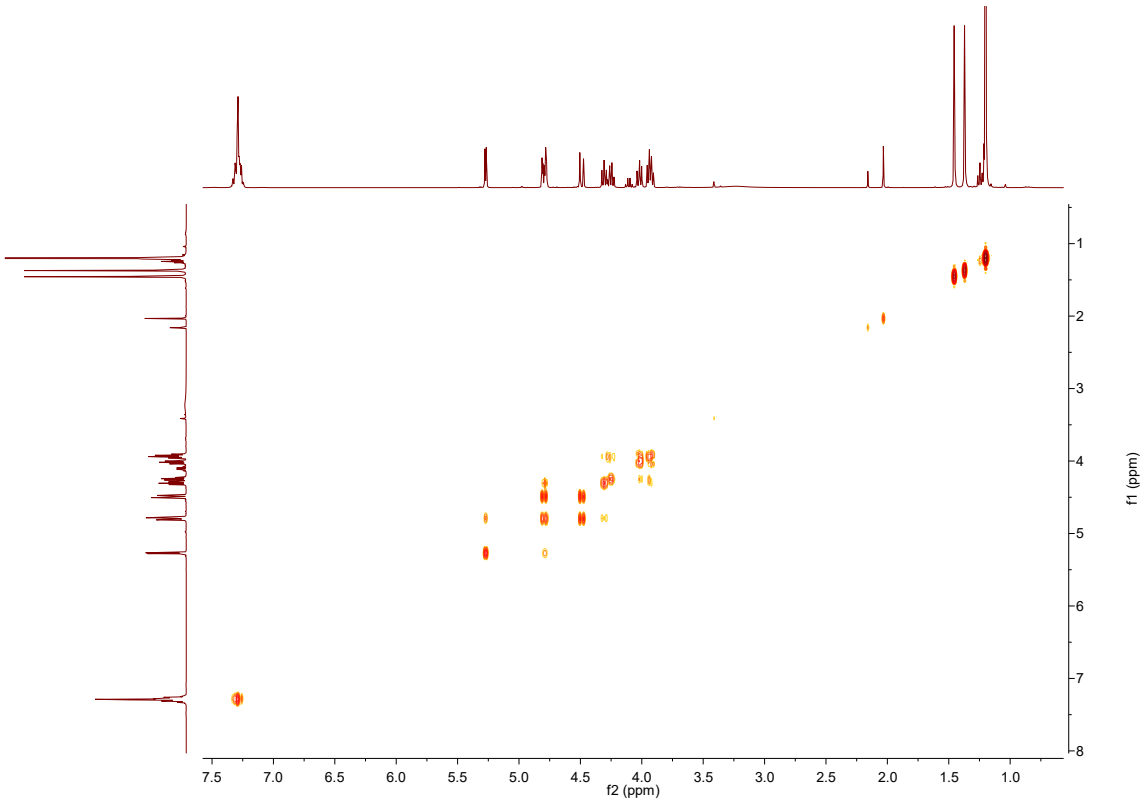

Figure A.7: COSY spectrum of **1a**, in $CDCl_3$.

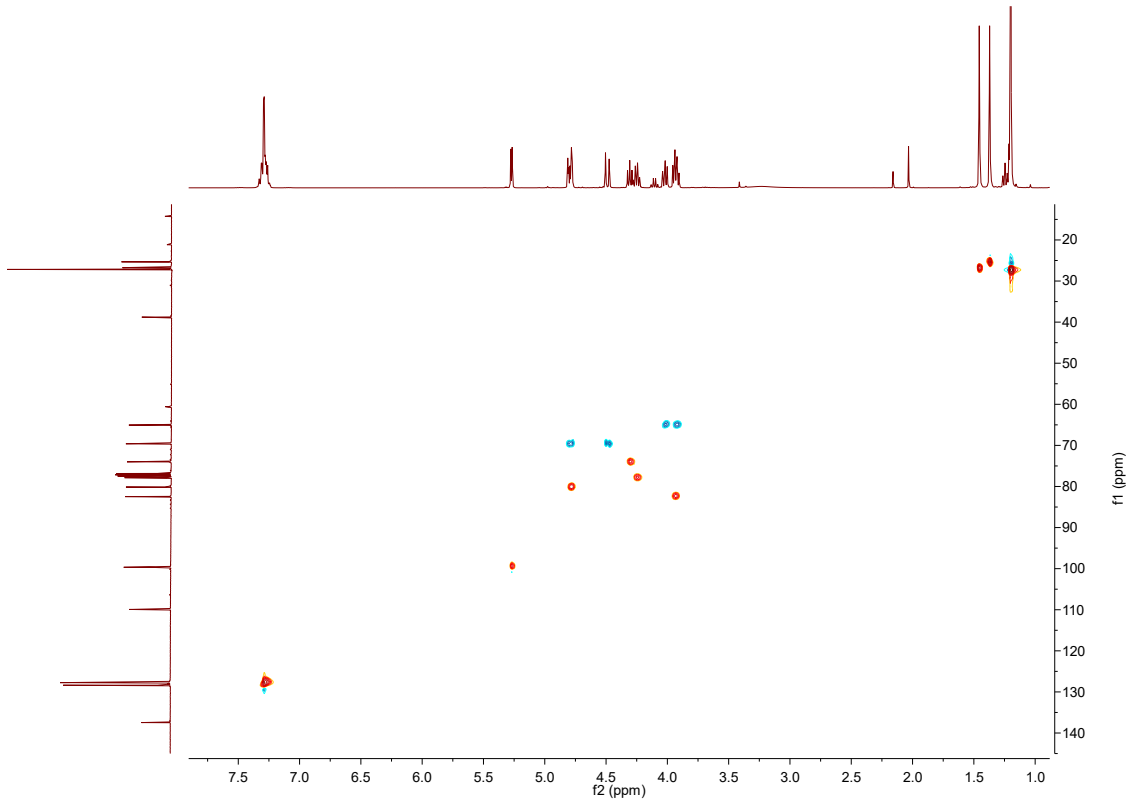

Figure A.8: HSQC spectrum of **1a**, in $CDCl_3$.

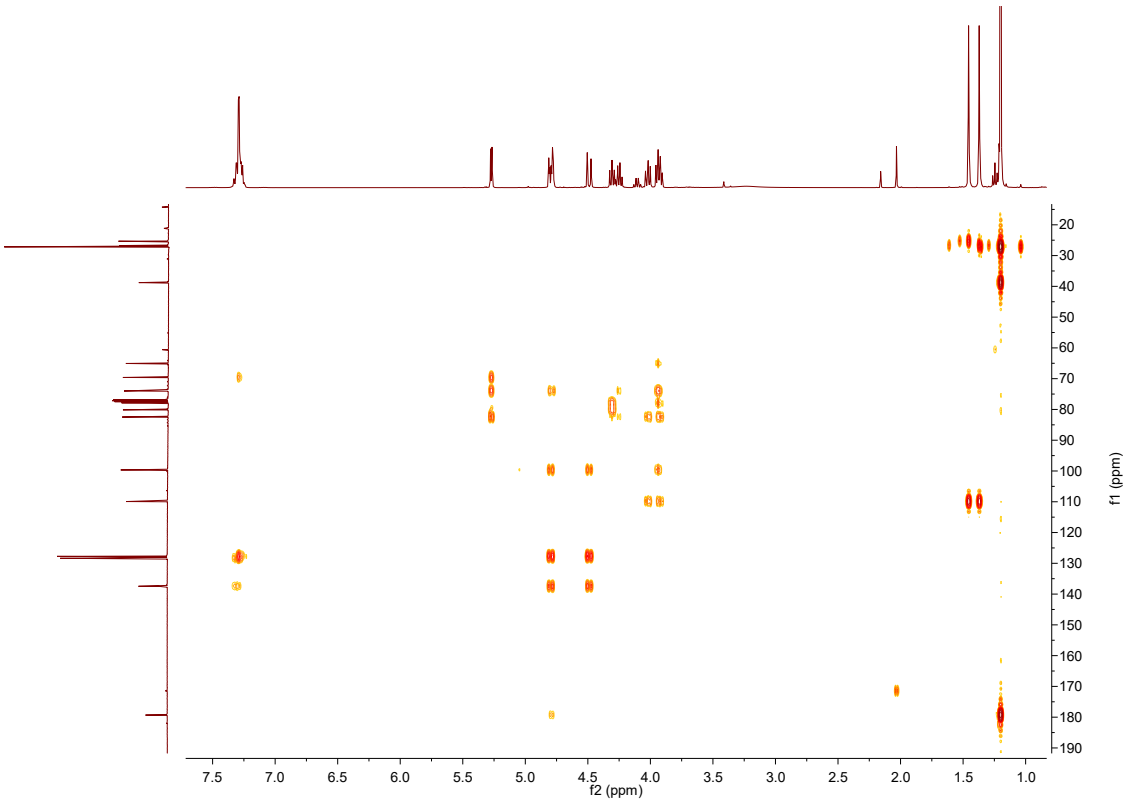

Figure A.9: HMBC spectrum of **1a**, in $CDCl_3$.

A.6. Benzyl 2-*O*-benzoyl-5,6-*O*-isopropylidene-α-D-galactofuranoside (**2a**)

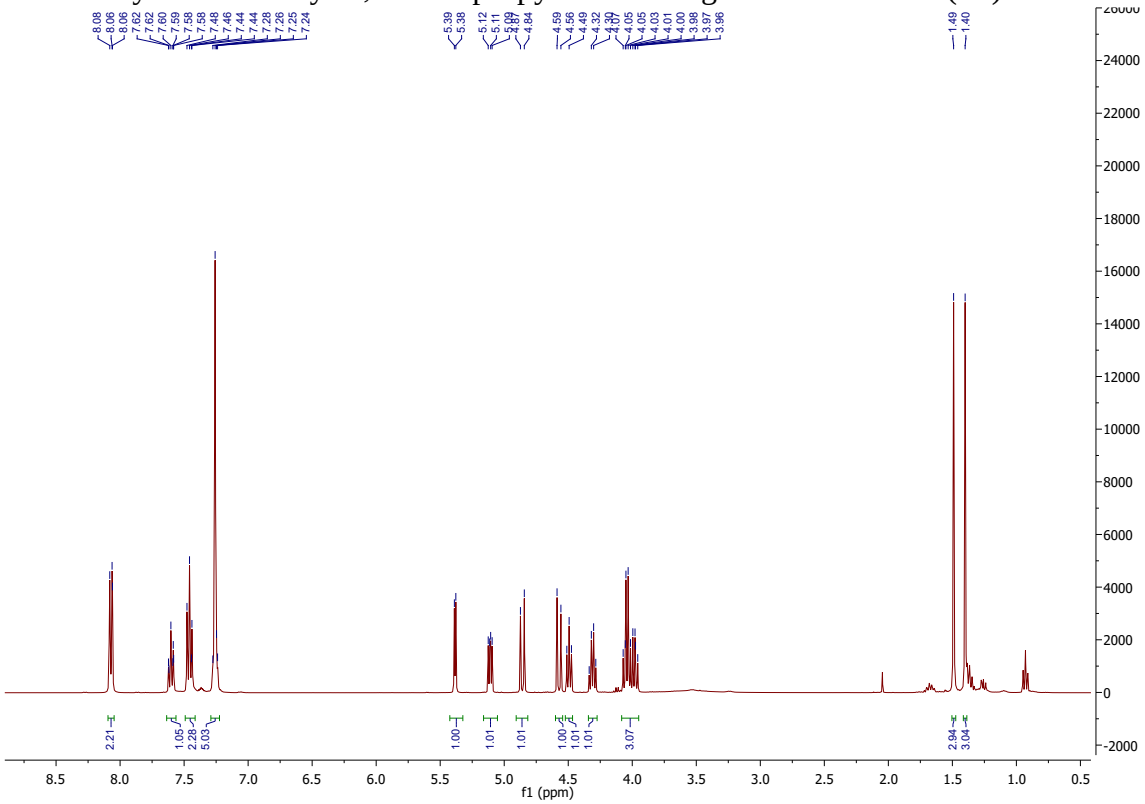

Figure A.10: ^{1}H NMR spectrum of **2a**, in $CDCl_3$.

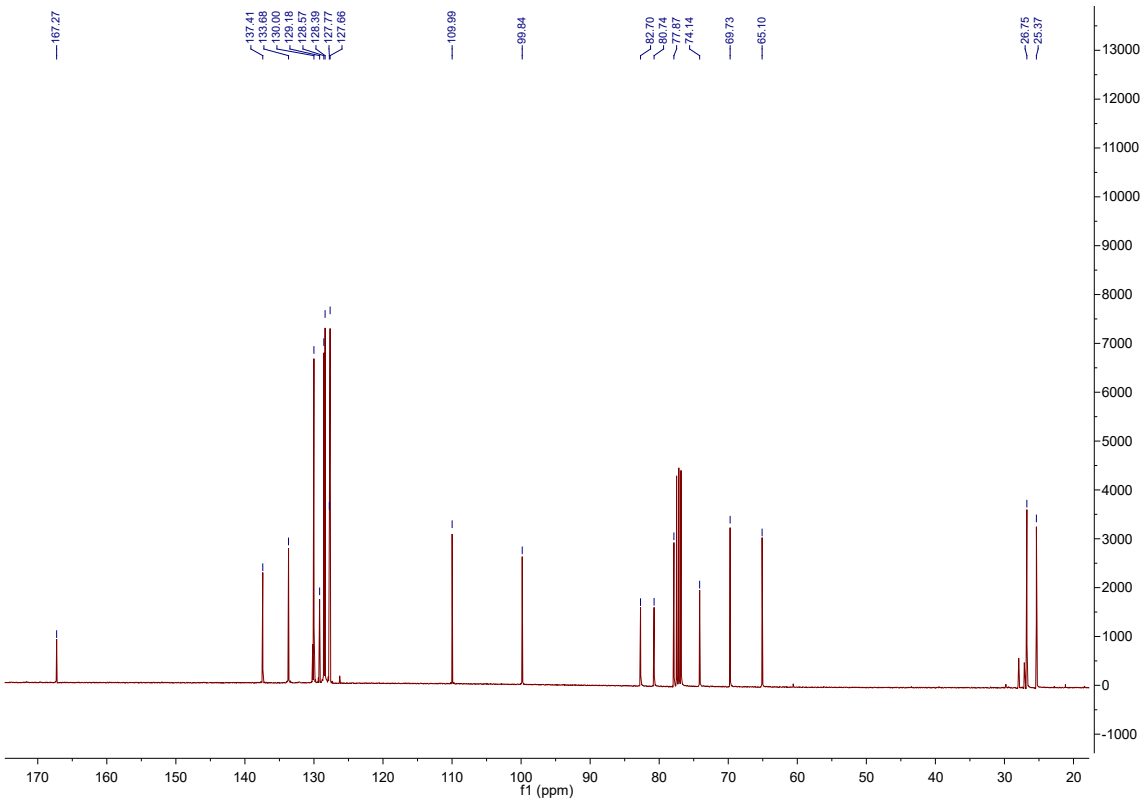

Figure A.11: ^{13}C NMR spectrum of **2a**, in $CDCl_3$.

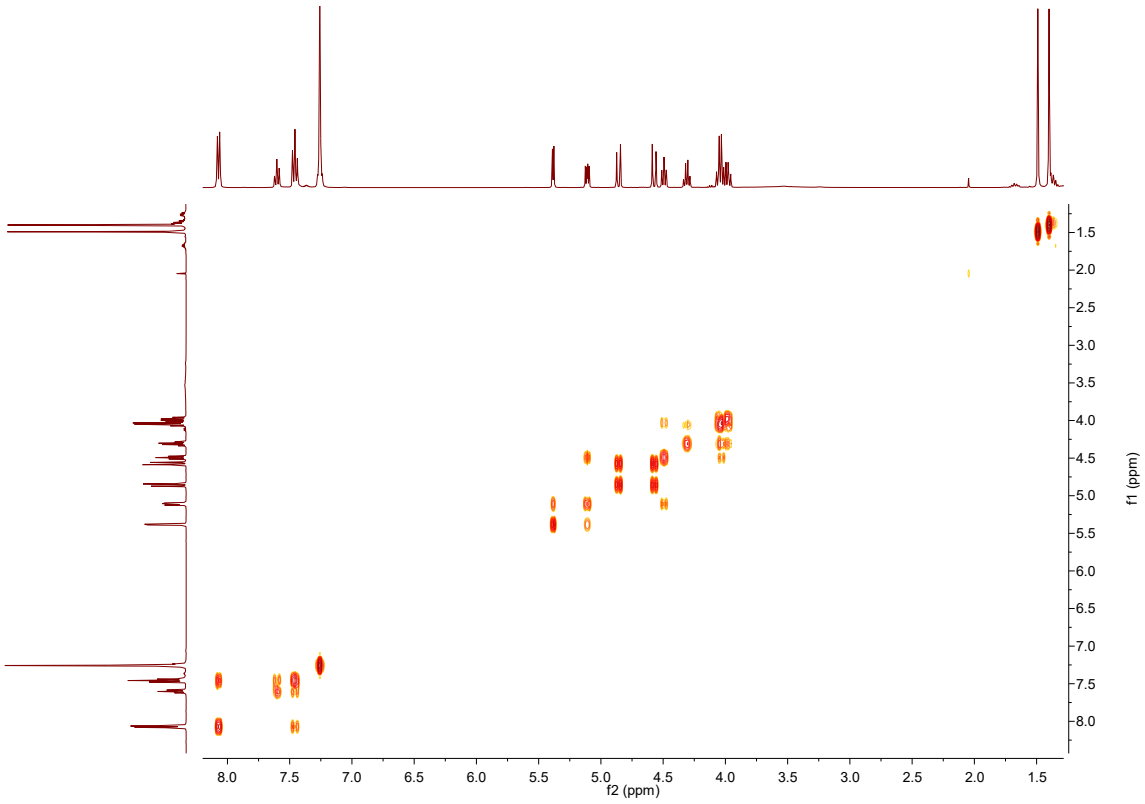

Figure A.12: COSY spectrum of **2a**, in $CDCl_3$.

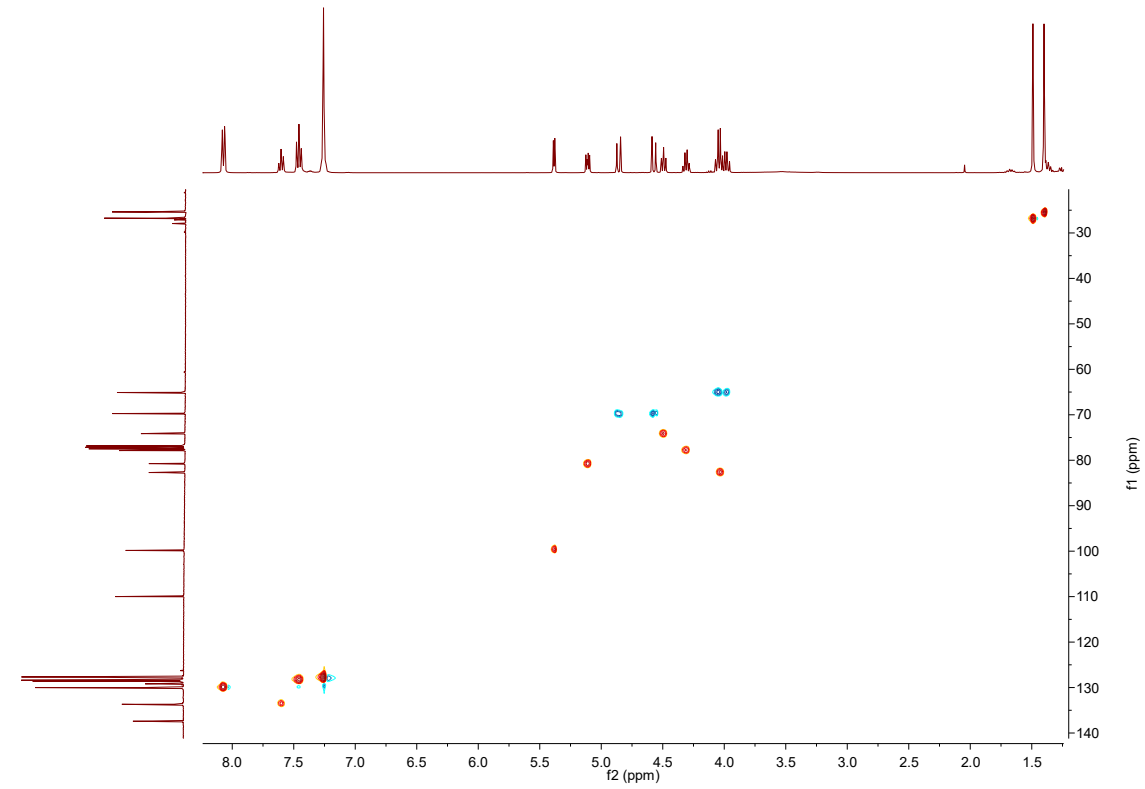

Figure A.13: HSQC spectrum of **2a**, in $CDCl_3$.

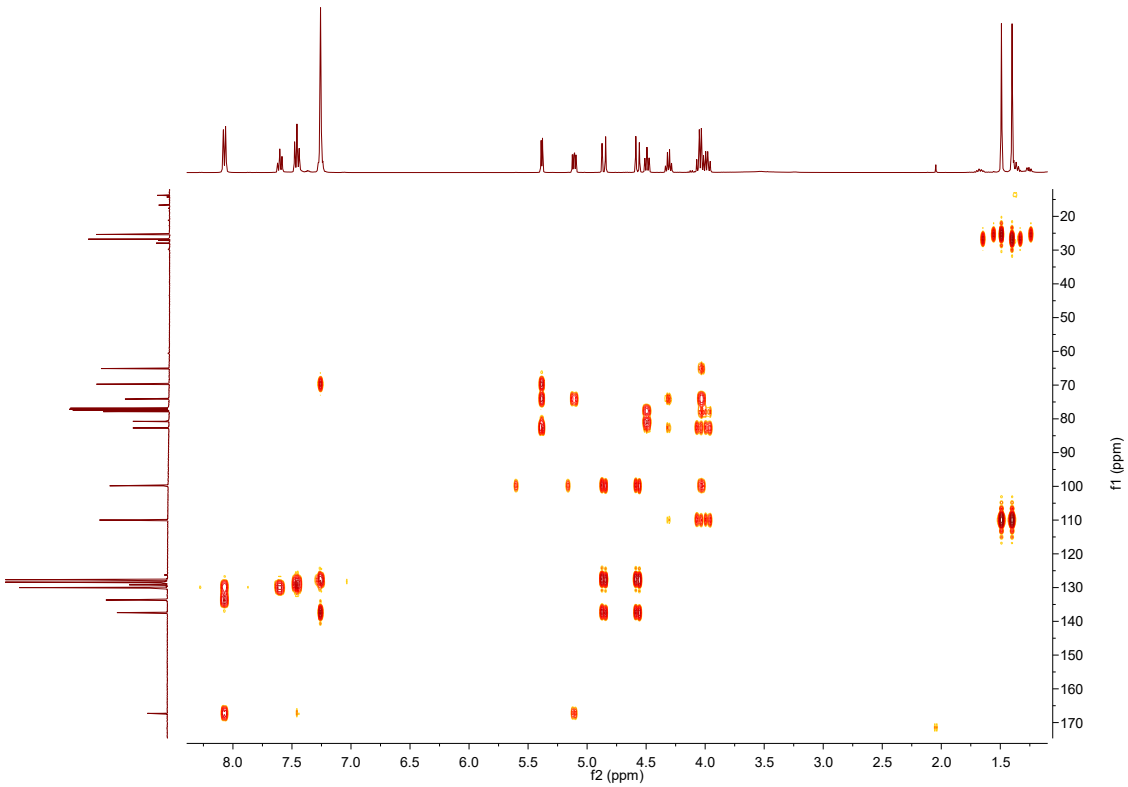

Figure A.14: HMBC spectrum of **2a**, in $CDCl_3$.

A.7. D-Galactose Diethyldithioacetal (**I-21**)

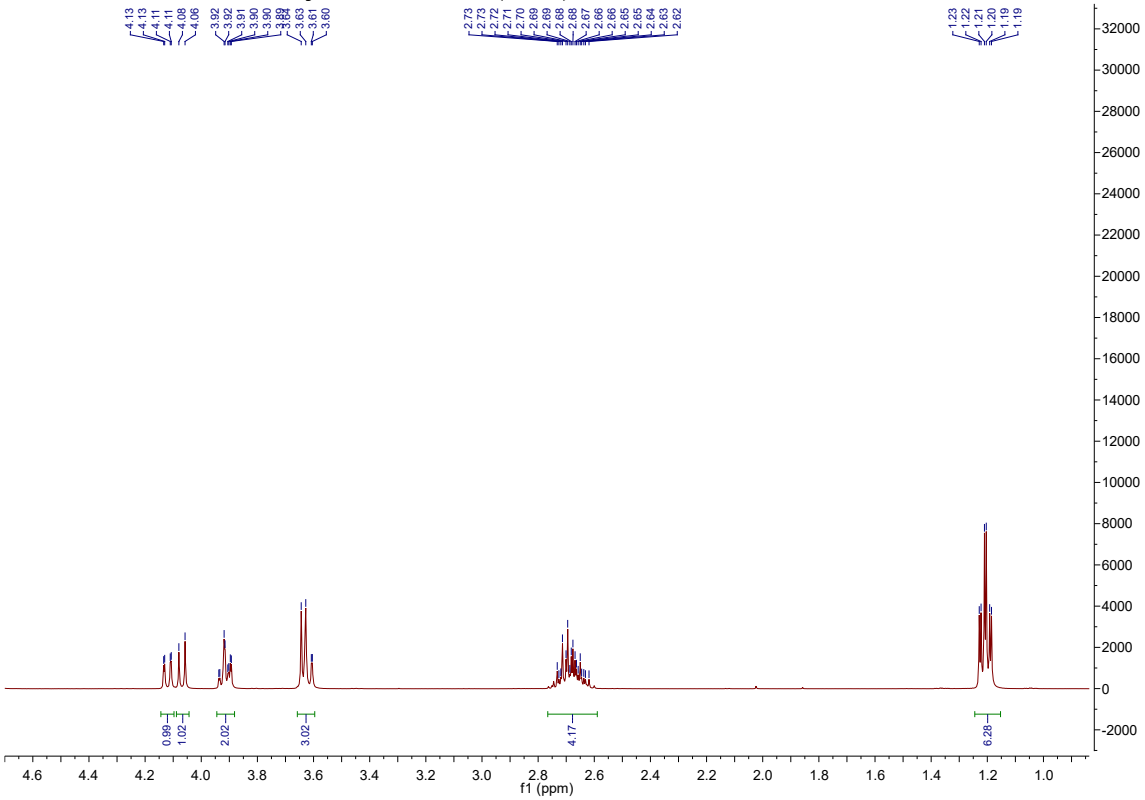

Figure A.15: ^{1}H NMR spectrum of **I-21**, in D_2O.

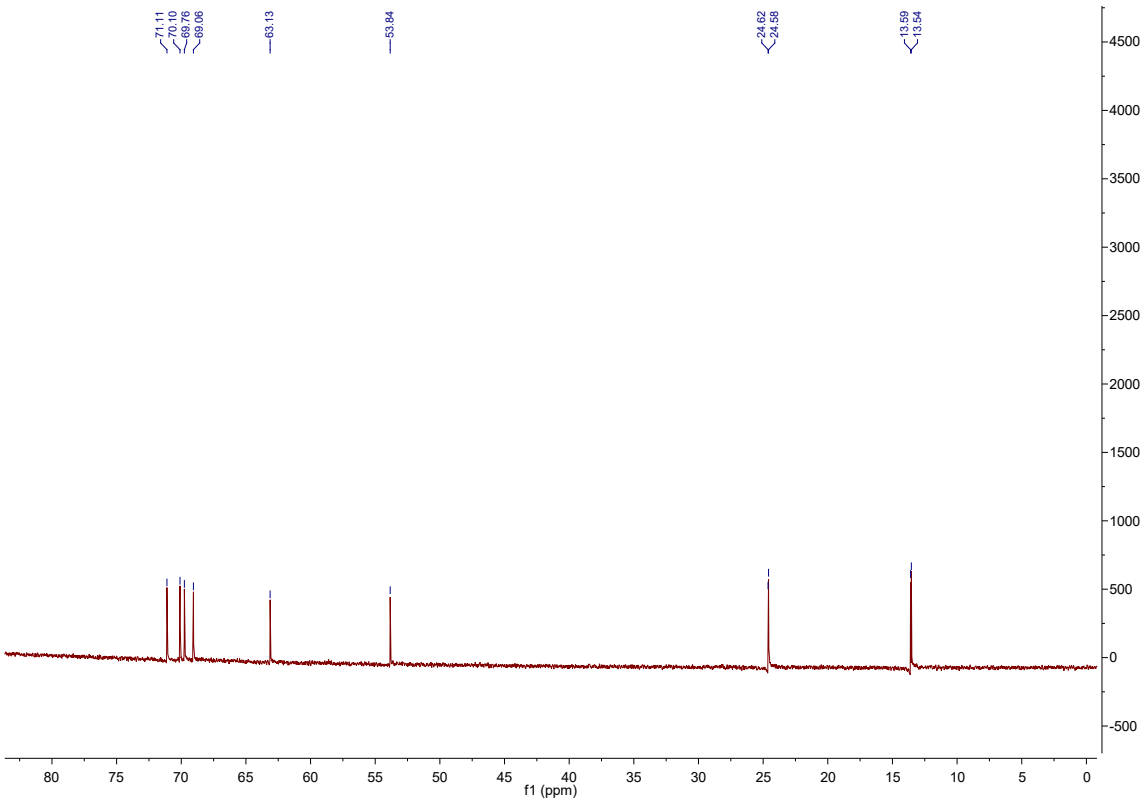

Figure A.16: ^{13}C NMR spectrum of **I-21**, in D_2O.

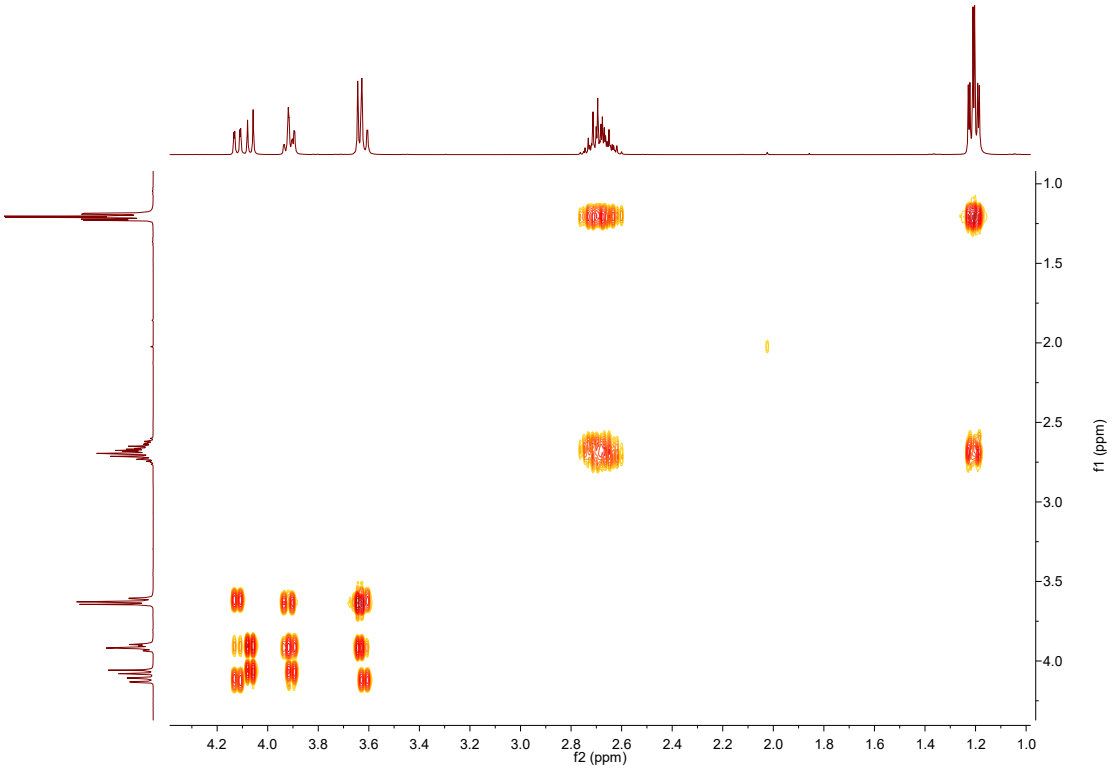

Figure A.17: COSY spectrum of **I-21**, in D_2O.

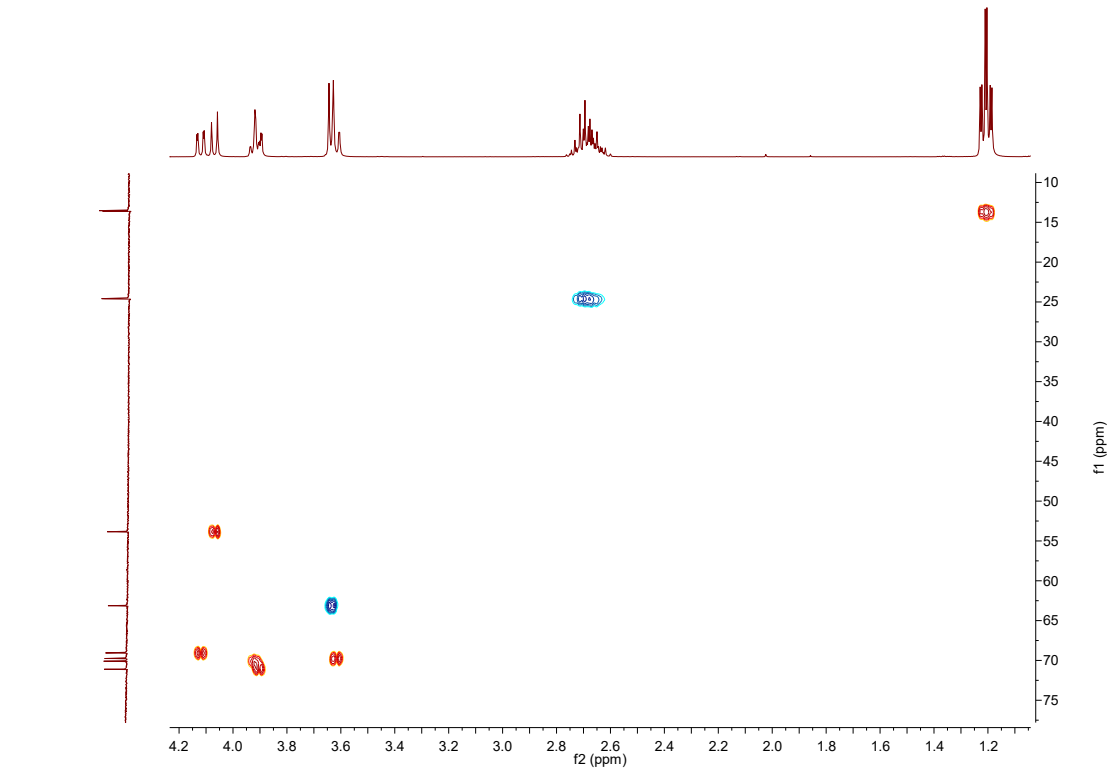

Figure A.18: HSQC spectrum of **I-21**, in D_2O.

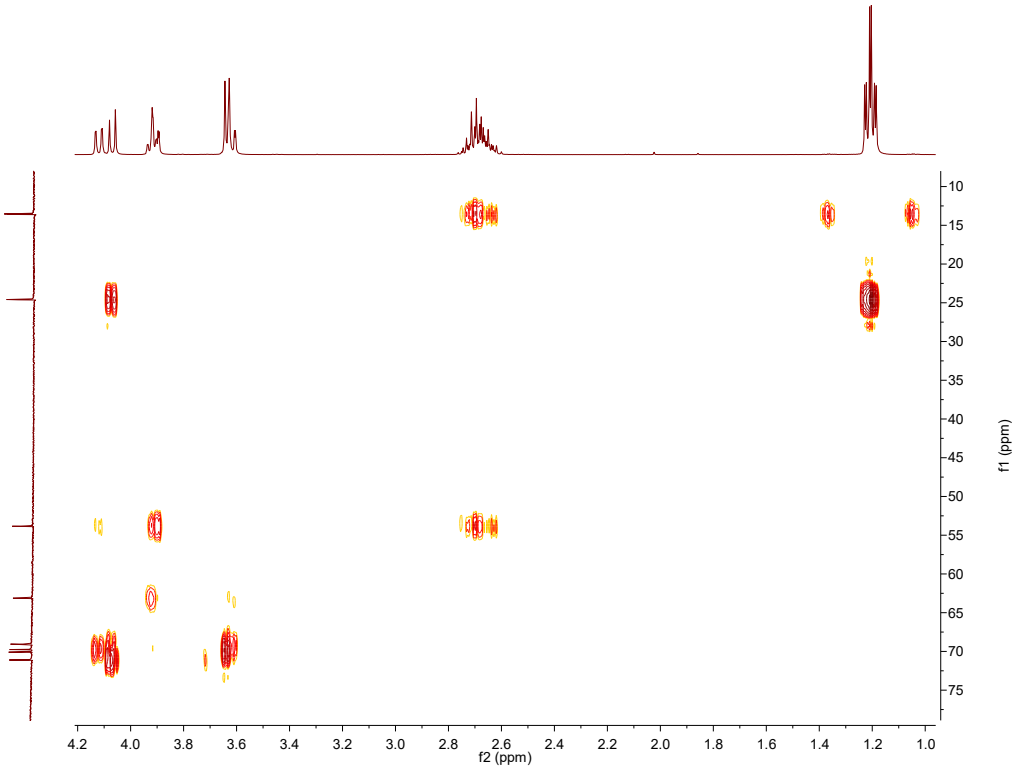

Figure A.19: HMBC spectrum of **I-21**, in D_2O.

A.8. 5,6-*O*-isopropylidene-D-Galactose Diethyldithioacetal (**3**)

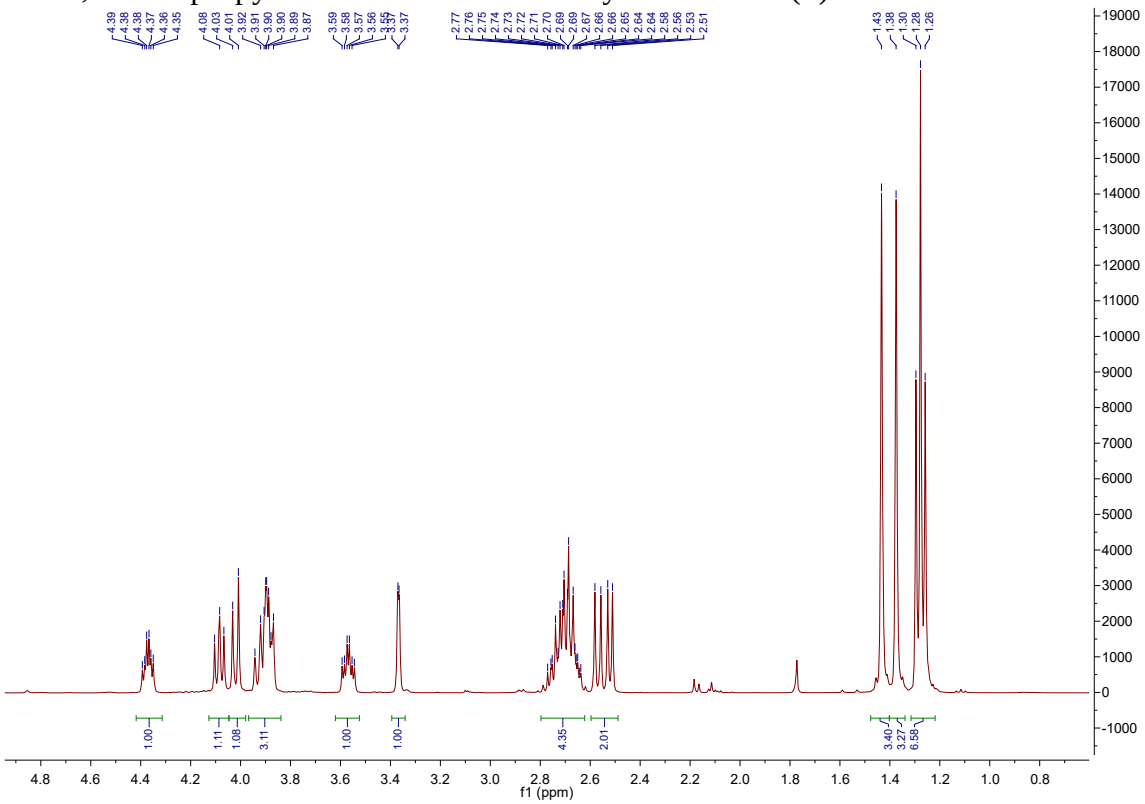

Figure A.20: ^{1}H NMR spectrum of **3**, in $CDCl_3$.

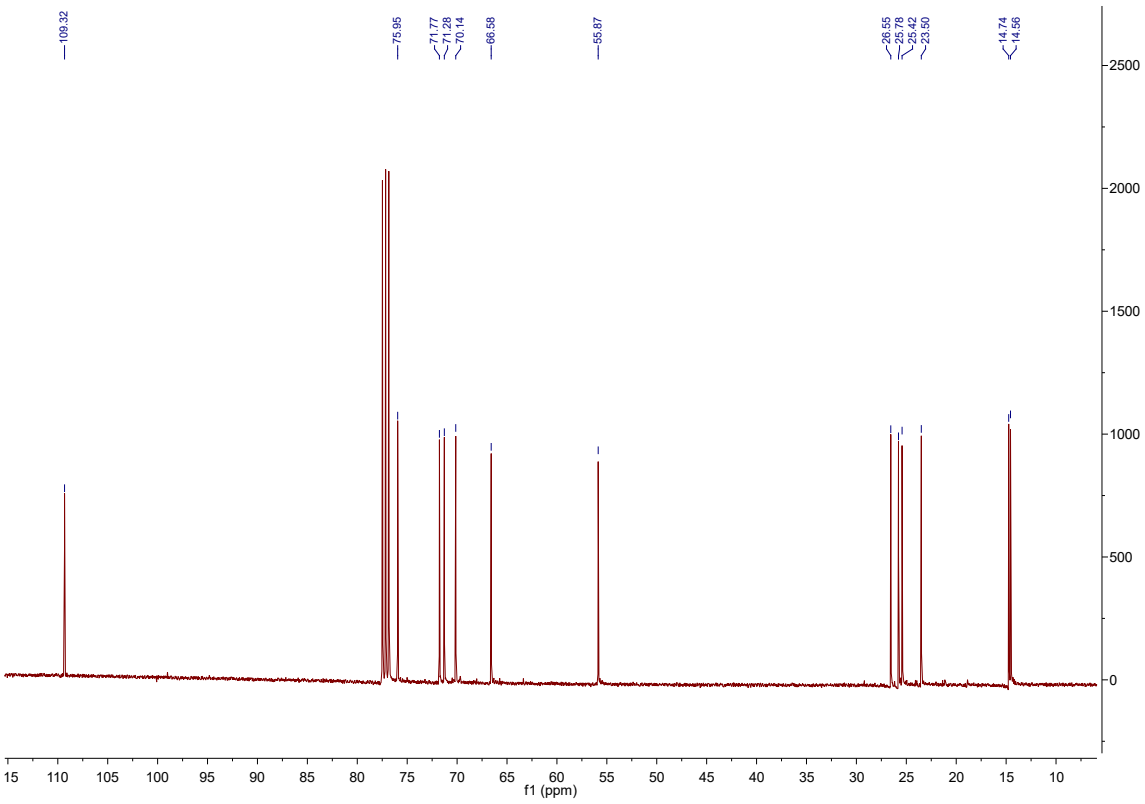

Figure A.21: ^{13}C NMR spectrum of **3**, in $CDCl_3$.

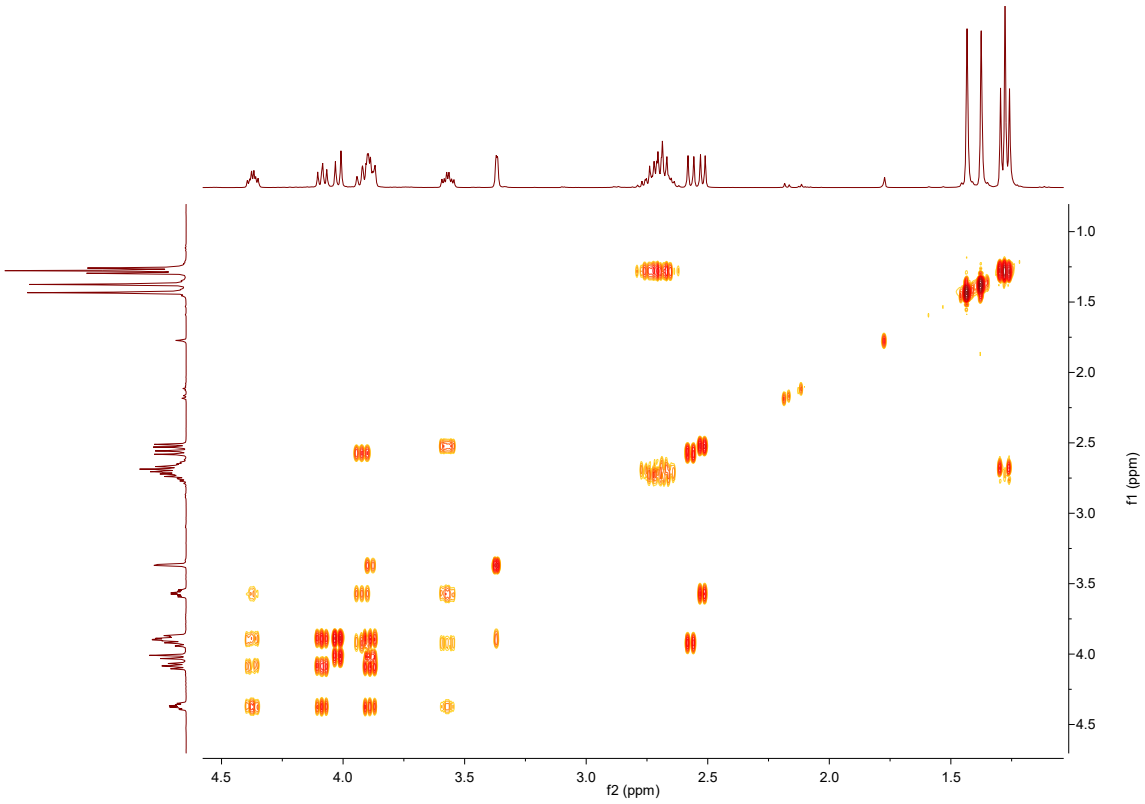

Figure A.22: COSY spectrum of **3**, in $CDCl_3$.

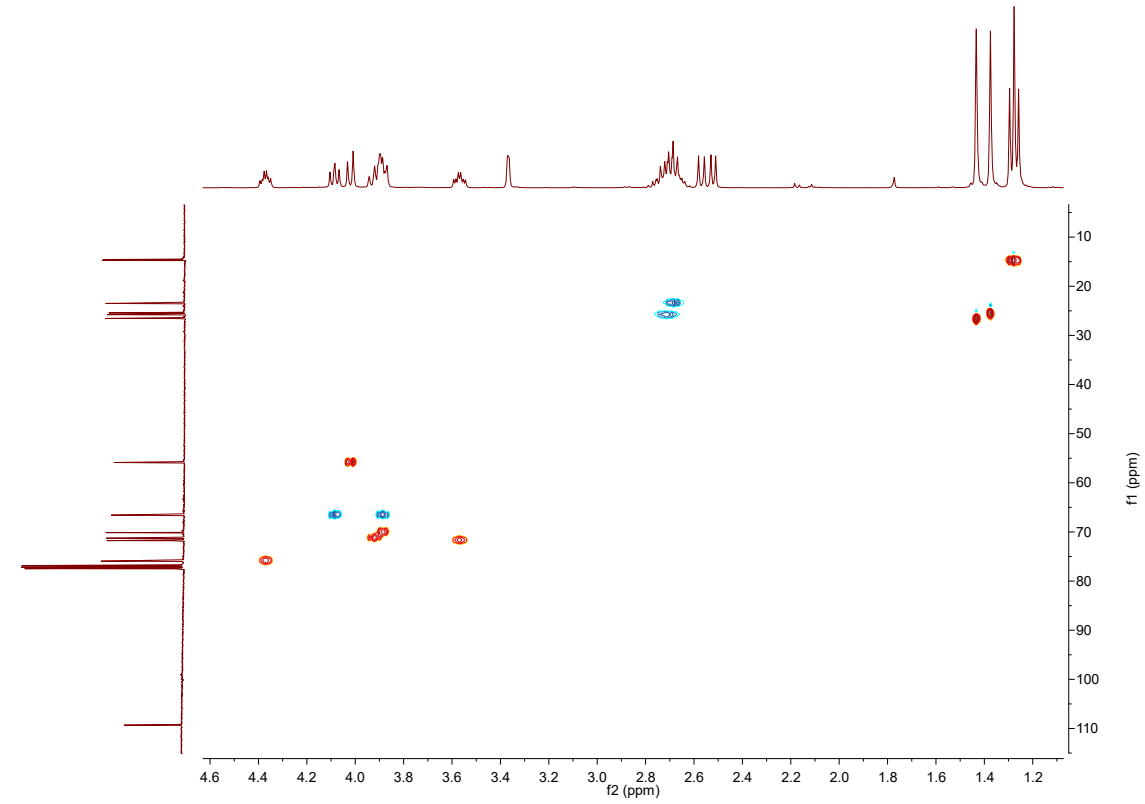

Figure A.23: HSQC spectrum of **3**, in $CDCl_3$.

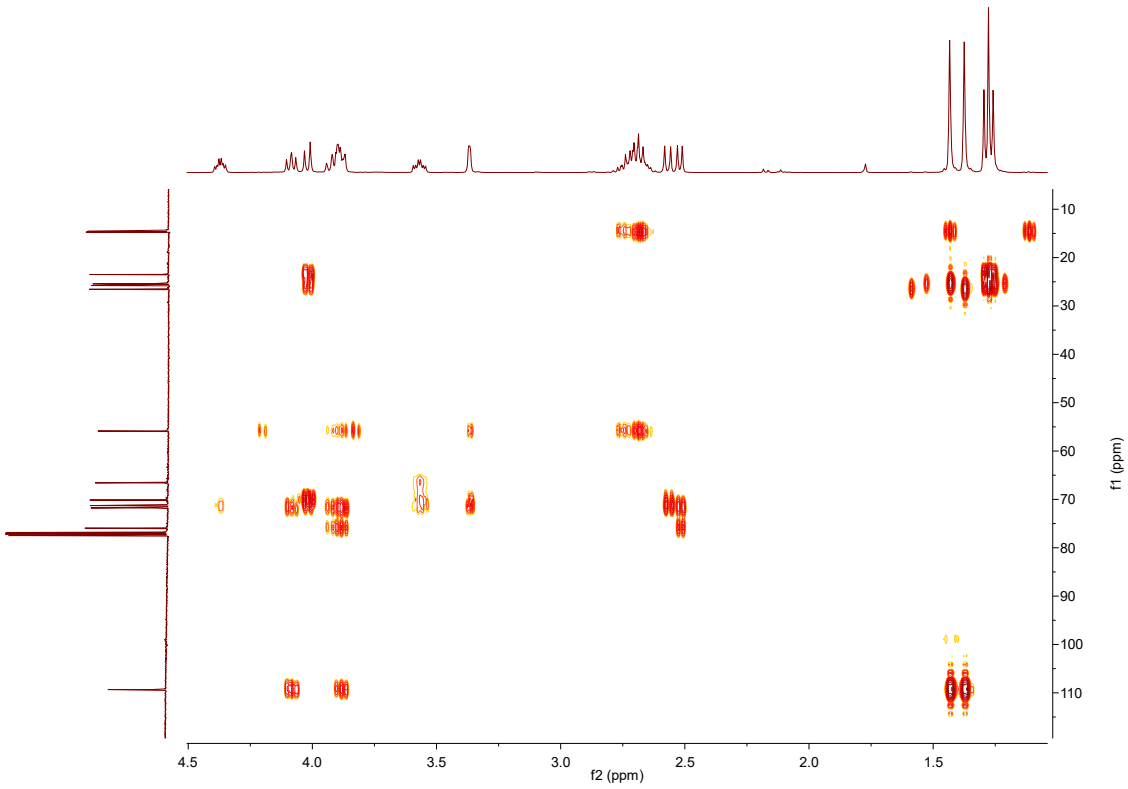

Figure A.24: HMBC spectrum of **3**, in $CDCl_3$.

A.9. Ethyl 5,6-*O*-isopropylidene-1-thio-α-D-galactofuranoside (**4α**) and Ethyl 5,6-*O*-isopropylidene-1-thio-β-D-galactofuranoside (**4β**)

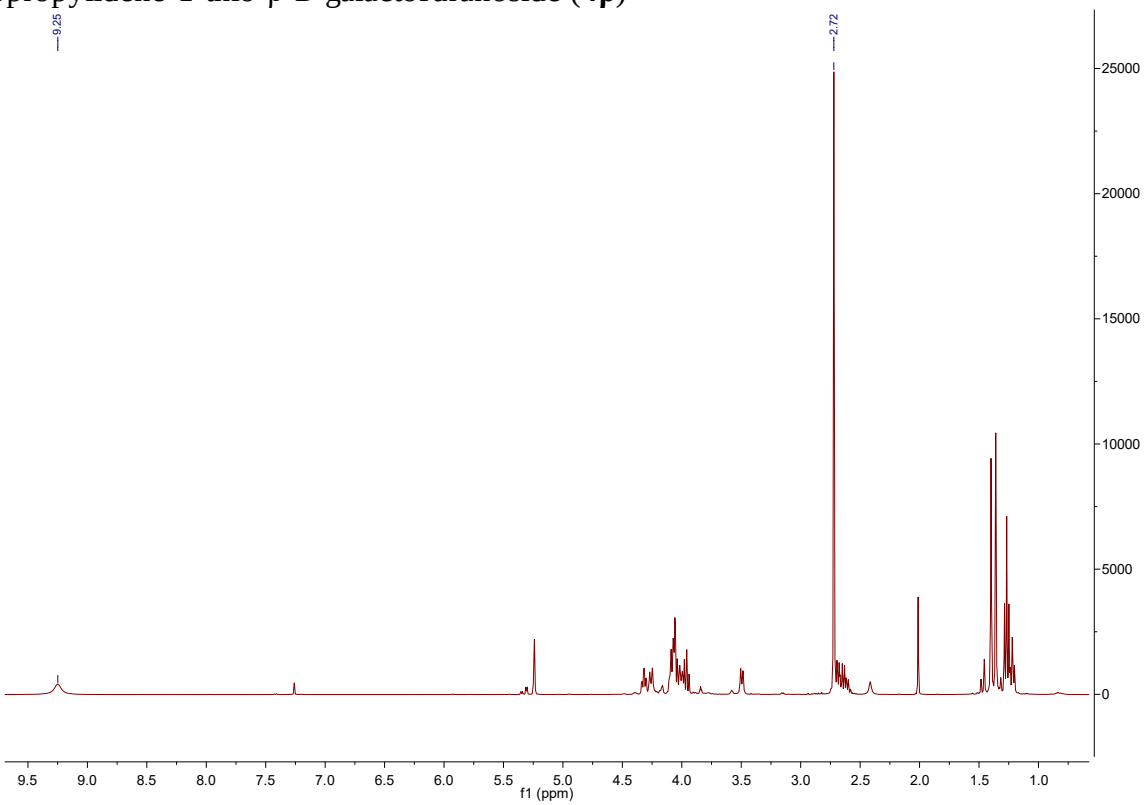

Figure A.25: ^{1}H NMR spectrum of **4** contaminated with succinimide, in $CDCl_3$.

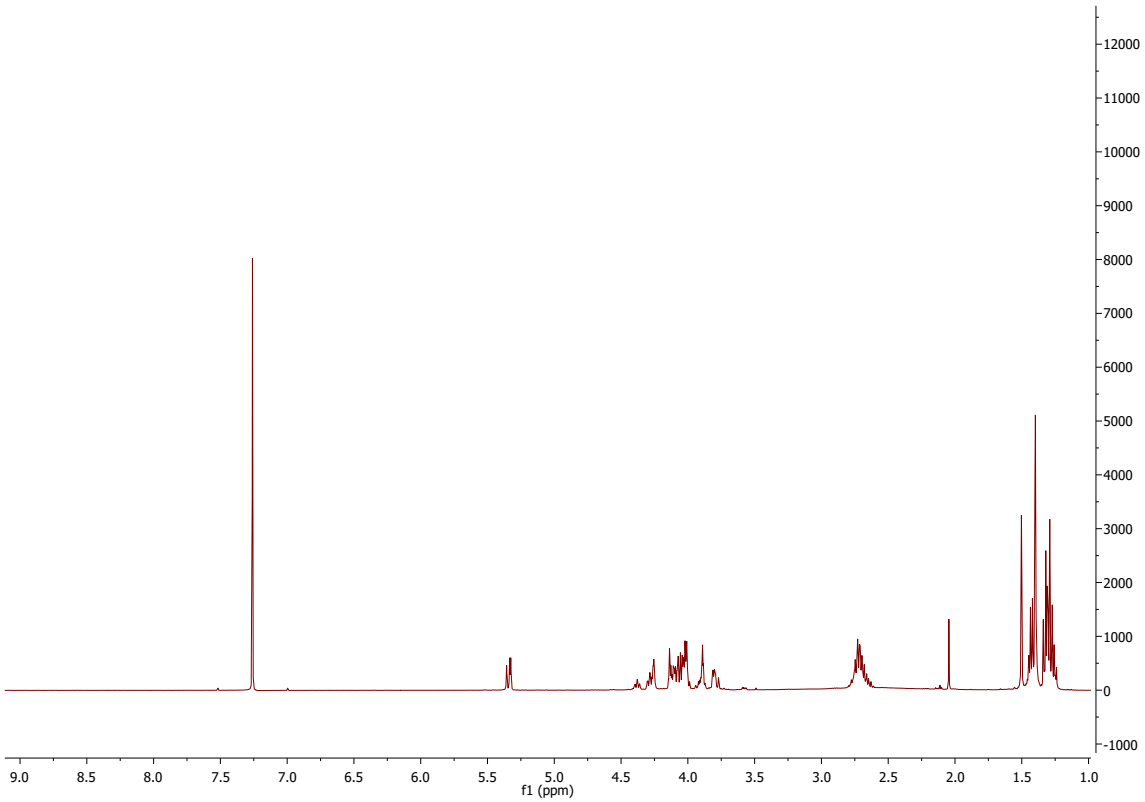

Figure A.26: ^{1}H NMR spectrum of crude **4** after quenching with $H_2S_2O_3$ and NaOH, in $CDCl_3$.

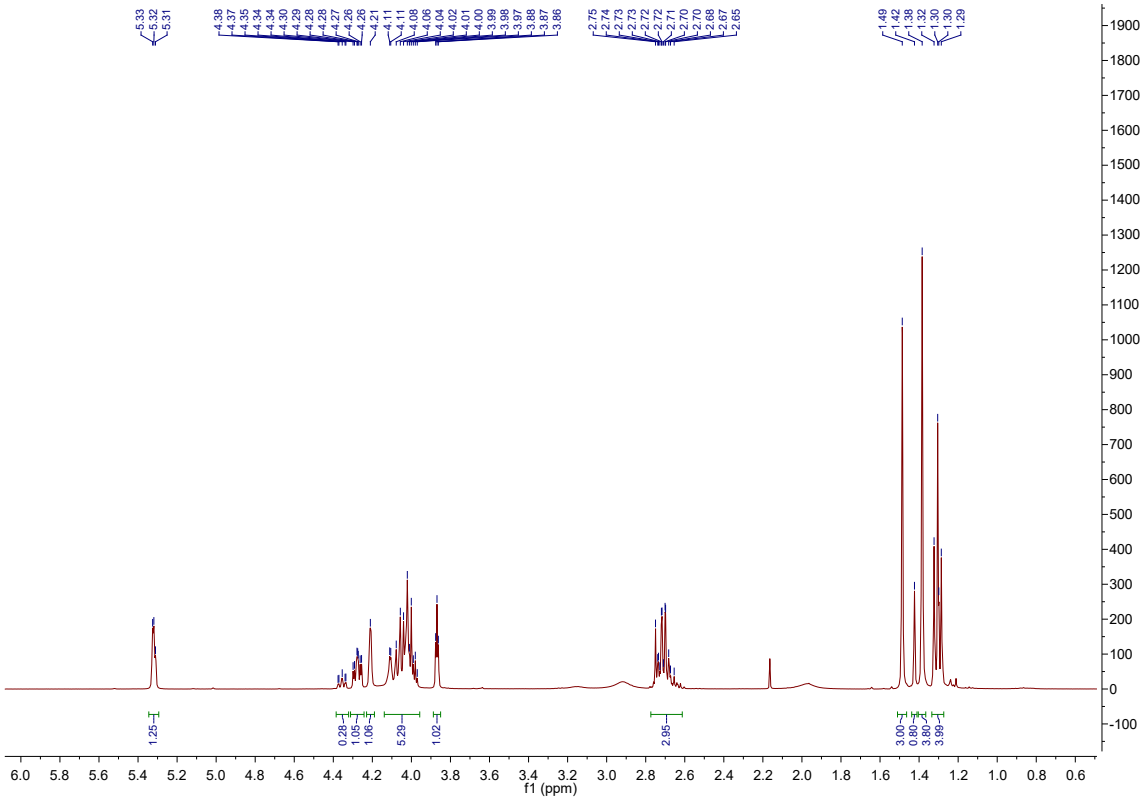

Figure A.27: ^{1}H NMR spectrum of **4**, in $CDCl_3$.

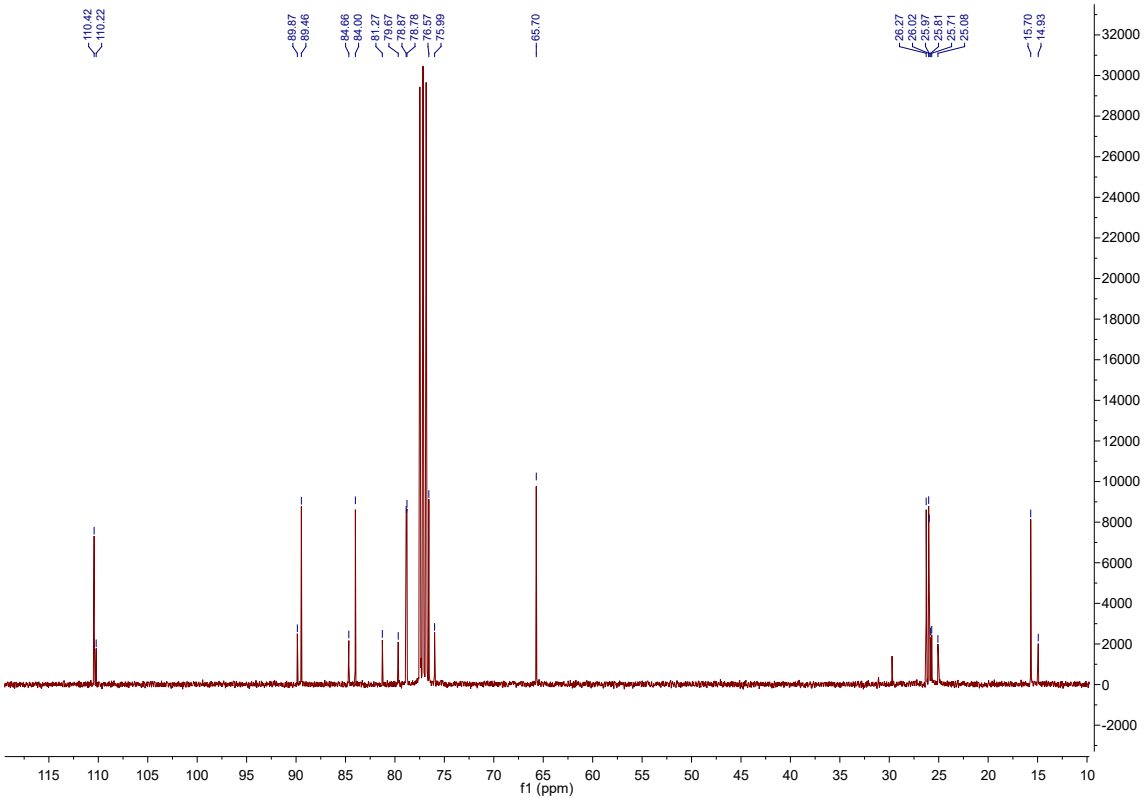

Figure A.28: ^{13}C NMR spectrum of **4**, in $CDCl_3$.

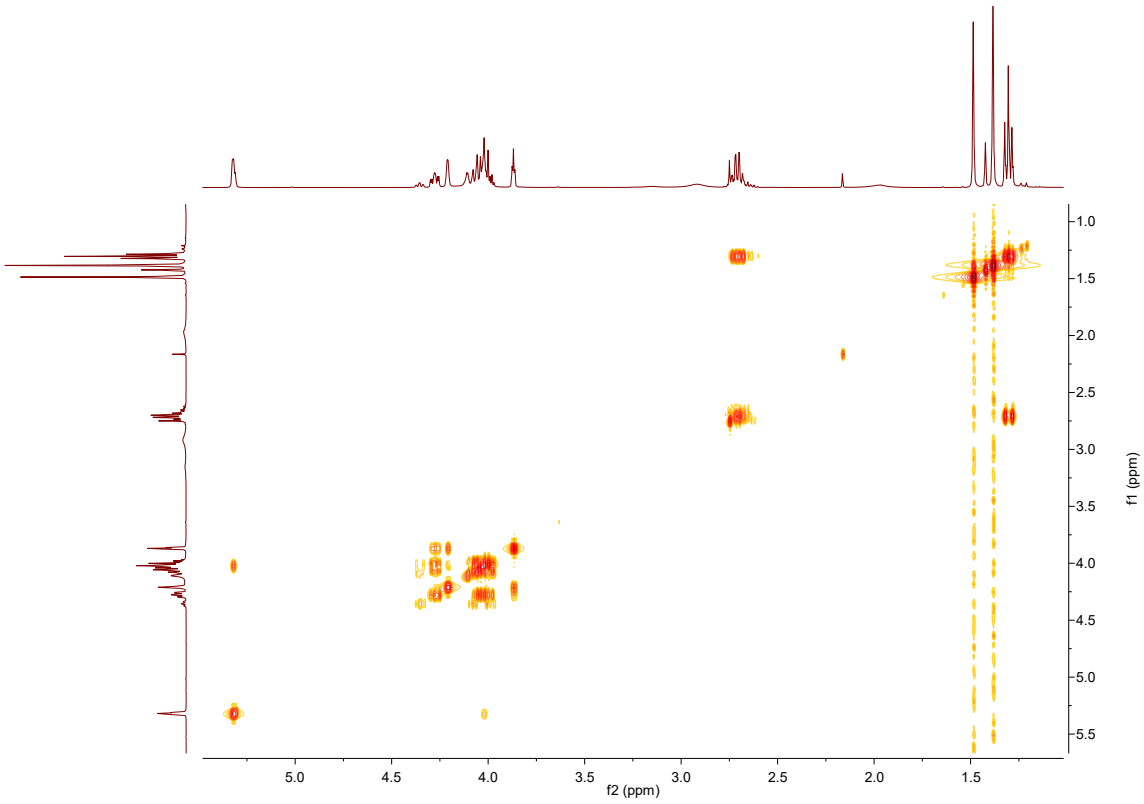

Figure A.29: COSY spectrum of **4**, in $CDCl_3$.

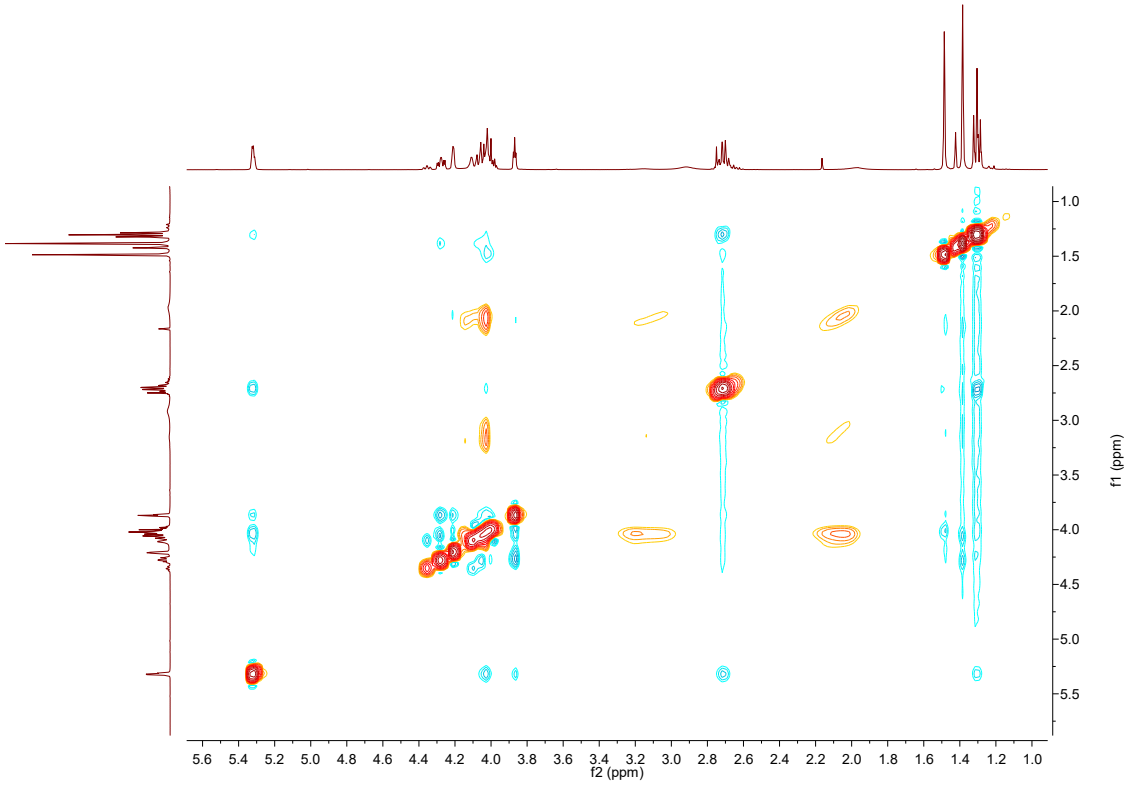

Figure A.30: NOESY spectrum of **4**, in $CDCl_3$.

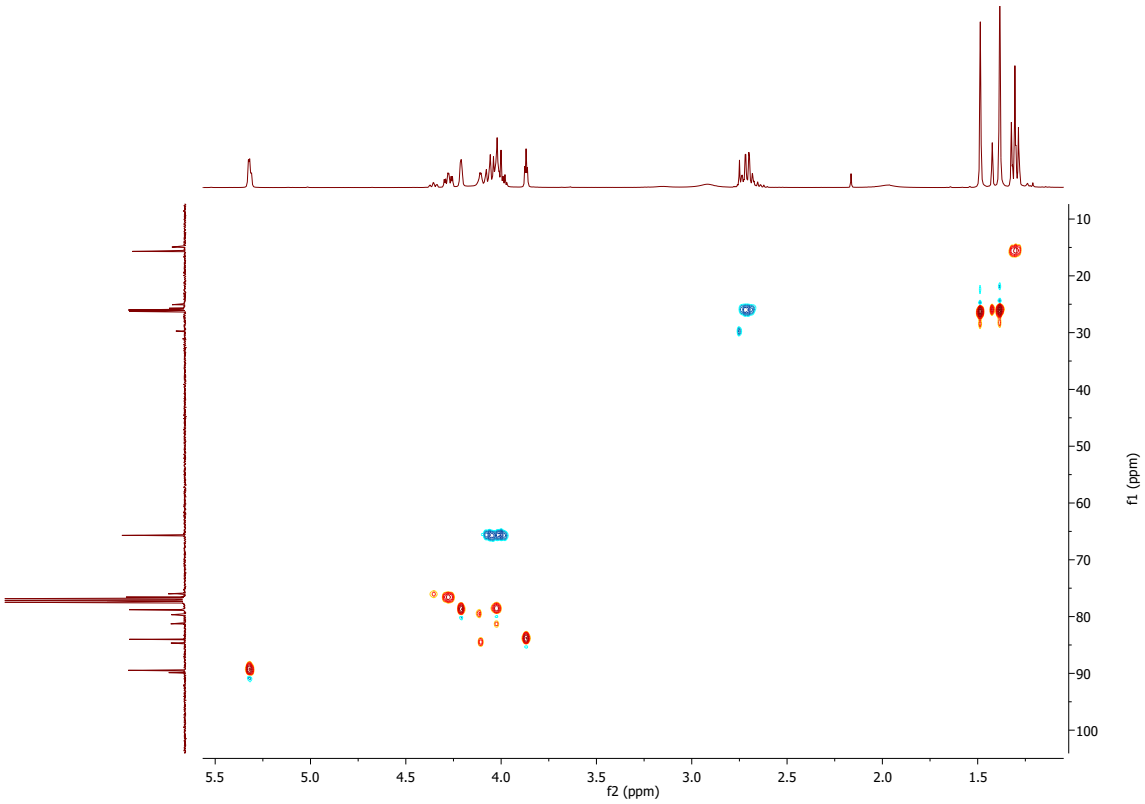

Figure A.31: HSQC spectrum of **4**, in $CDCl_3$.

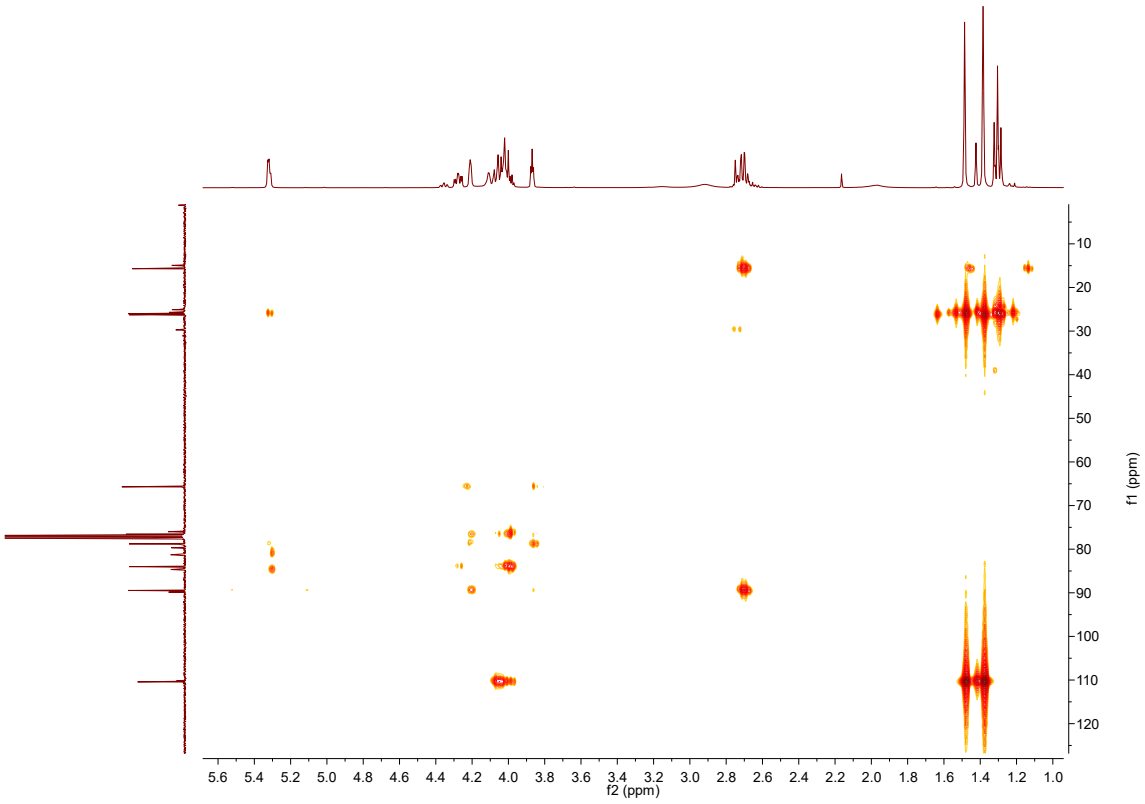

Figure A.32: HMBC spectrum of **4**, in $CDCl_3$.

A.10. Ethyl 2-*O*-benzoyl-5,6-*O*-isopropylidene-1-thio-α-D-galactofuranoside (**5a**)

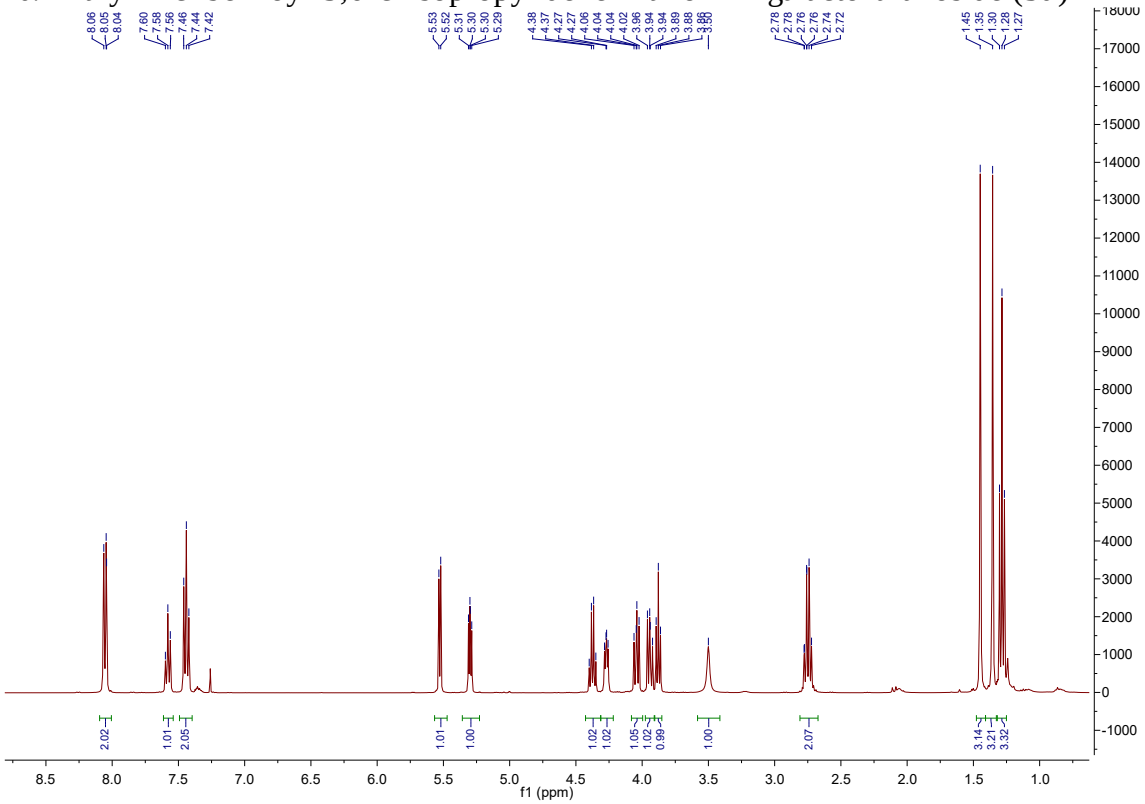

Figure A.33: ^{1}H NMR spectrum of **5a**, in $CDCl_3$.

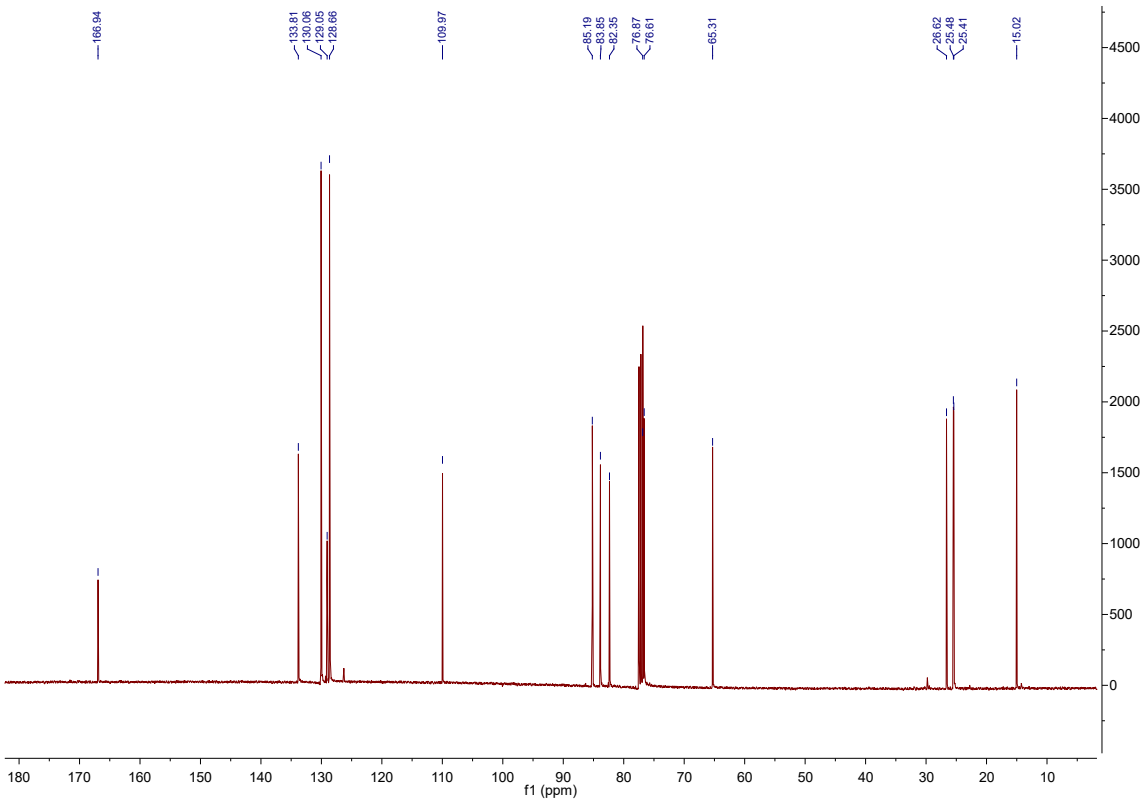

Figure A.34: ^{13}C NMR spectrum of **5a**, in $CDCl_3$.

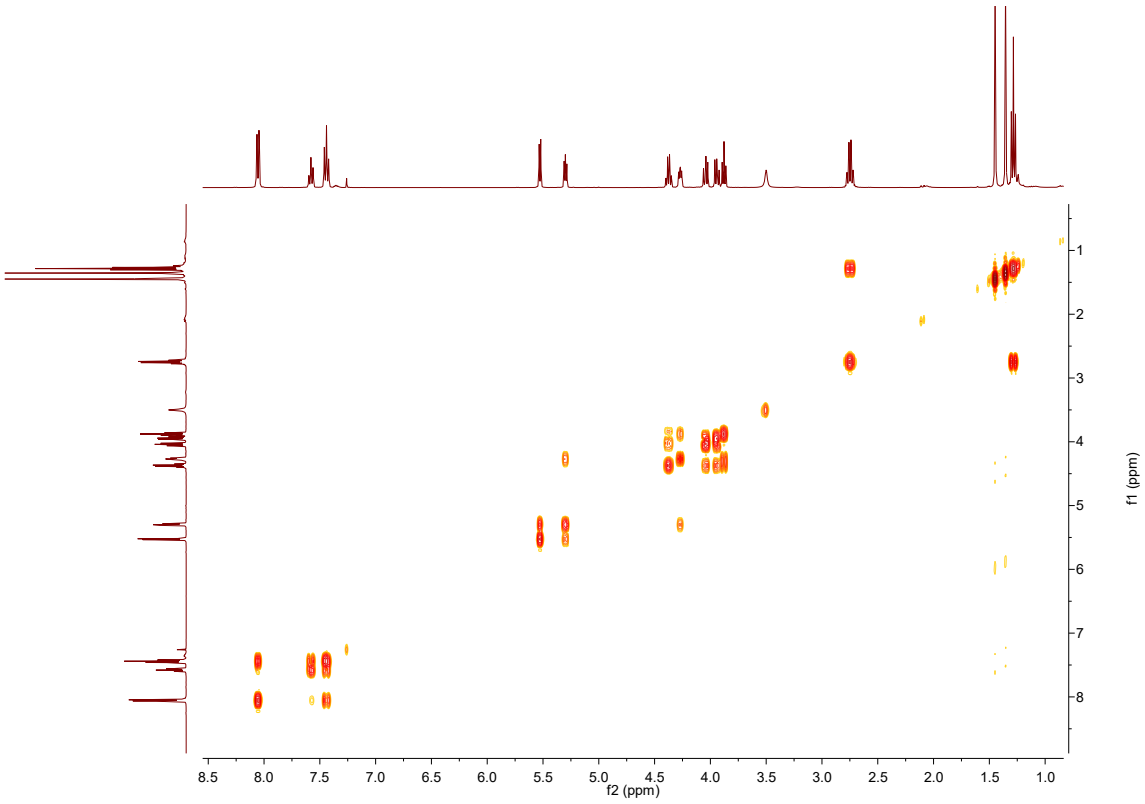

Figure A.35: COSY spectrum of **5a**, in $CDCl_3$.

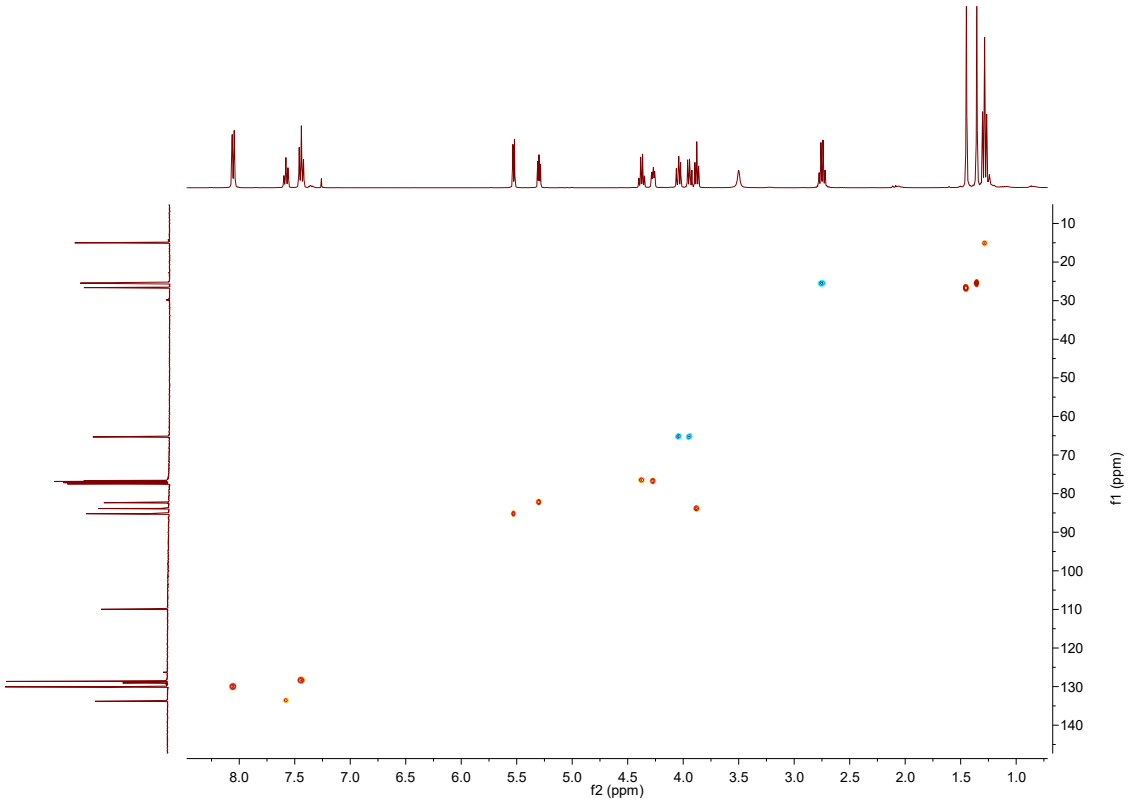

Figure A.36: HSQC spectrum of **5a**, in $CDCl_3$.

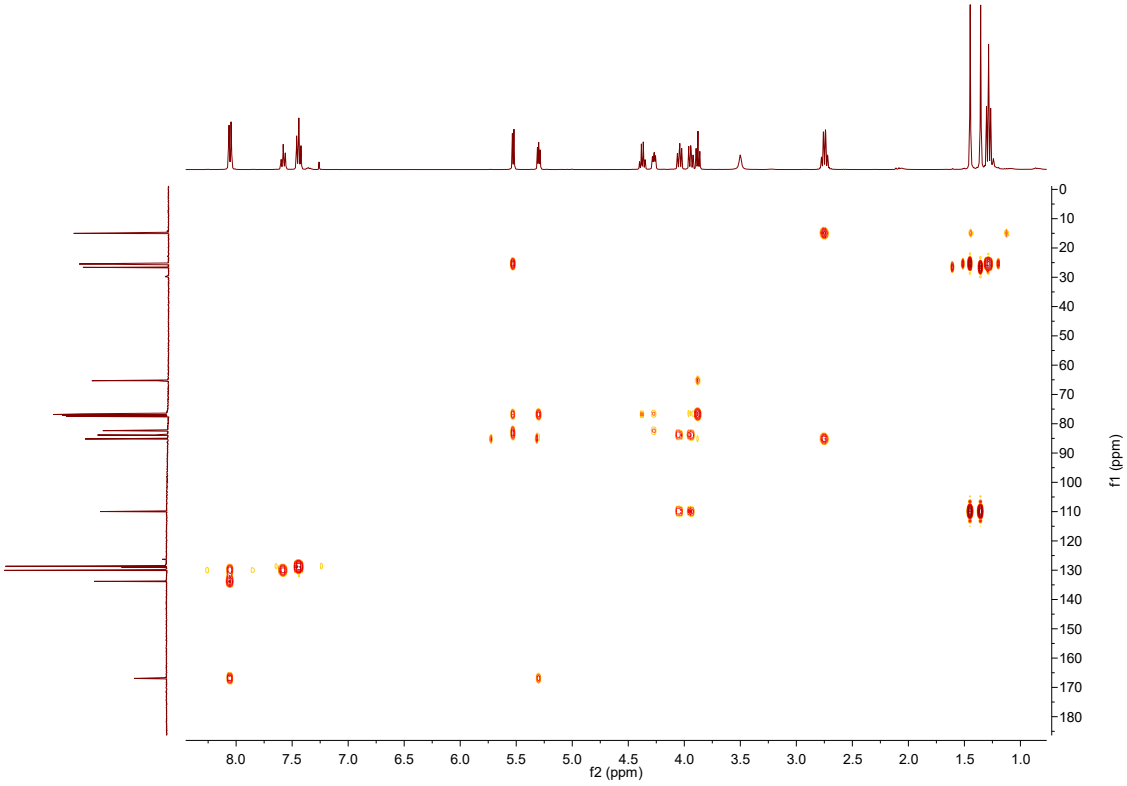

Figure A.37: HMBC spectrum of **5a**, in $CDCl_3$.

A.11. Ethyl 5,6-*O*-isopropylidene-1-thio-2-*O*-(trimethylacetyl)-α-D-galactofuranoside (**6α**)

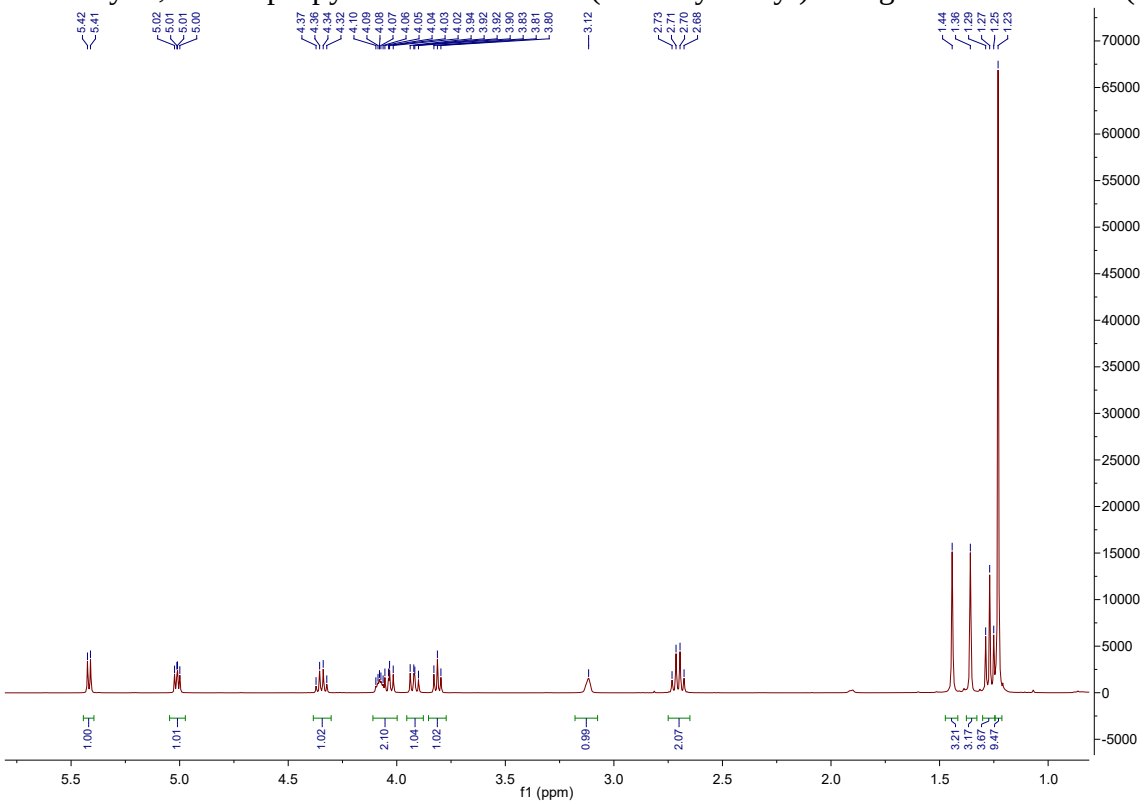

Figure A.38: ^{1}H NMR spectrum of **6α**, in $CDCl_3$.

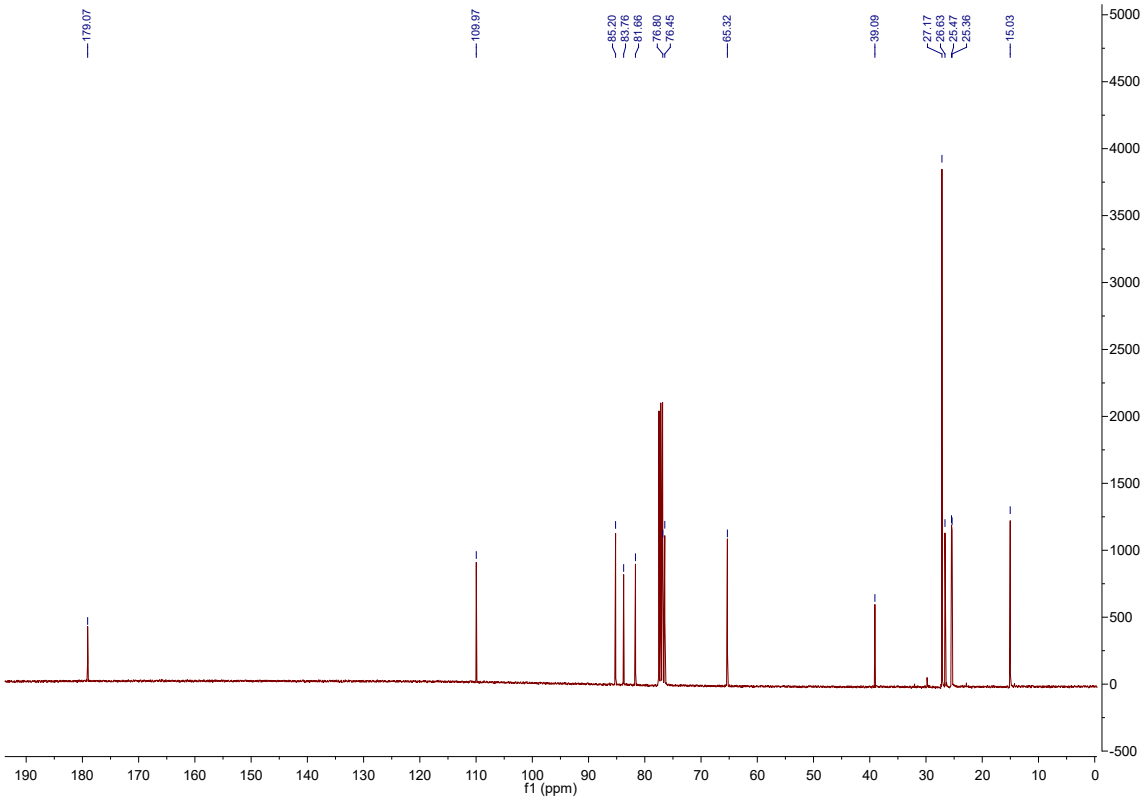

Figure A.39: ^{13}C NMR spectrum of **6α**, in $CDCl_3$.

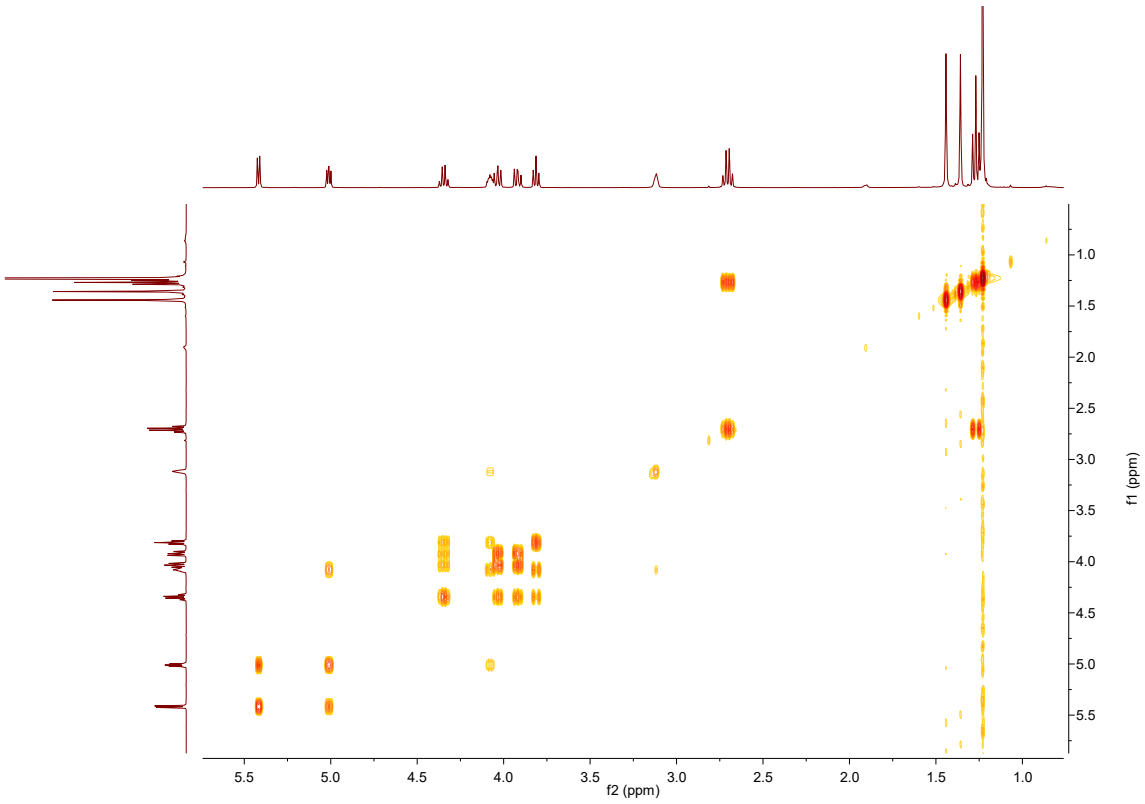

Figure A.40: COSY spectrum of **6*α***, in $CDCl_3$.

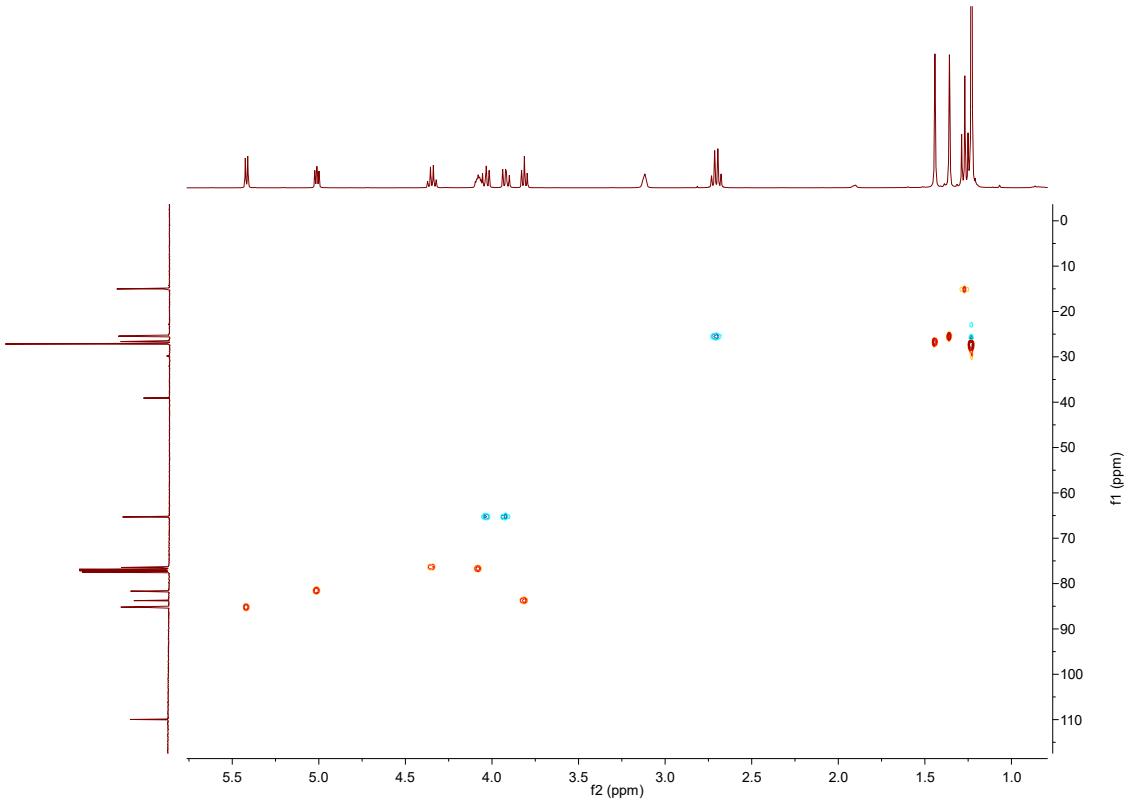

Figure A.41: HSQC spectrum of **6*α***, in $CDCl_3$.

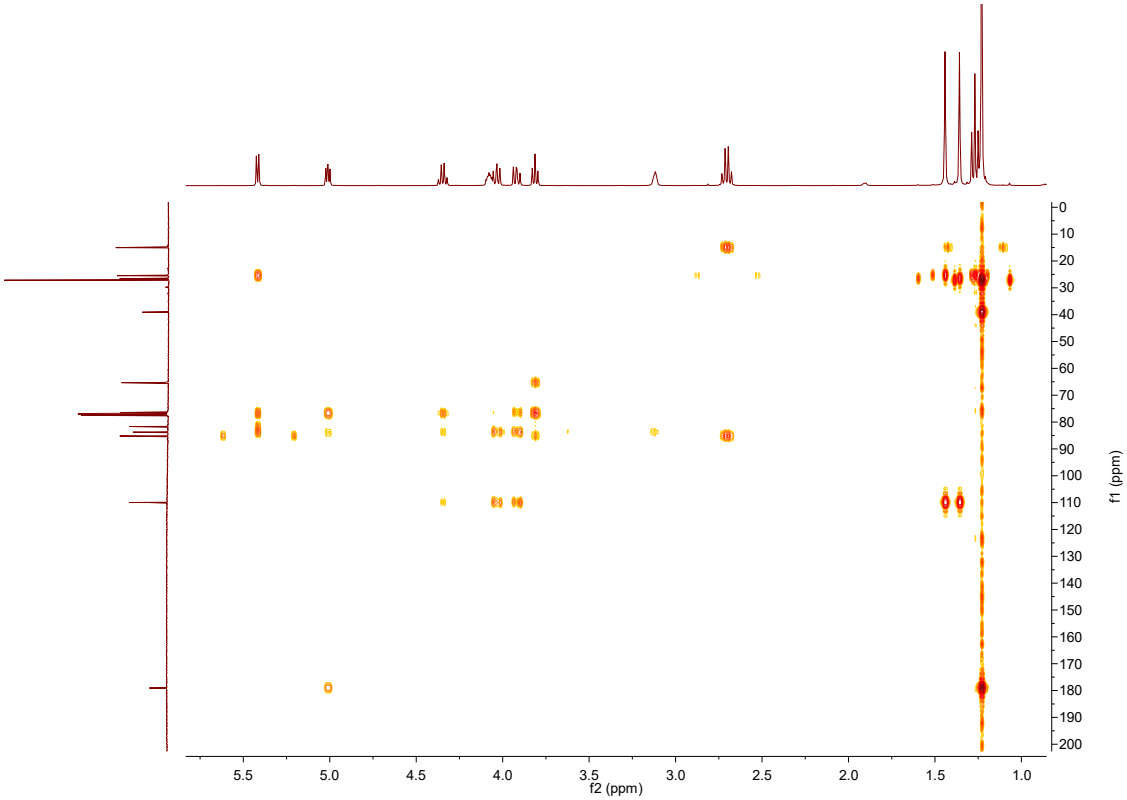

Figure A.42: HMBC spectrum of **6*α***, in $CDCl_3$.

A.12. Ethyl 5,6-*O*-isopropylidene-3-*O*-levulinoyl-1-thio-2-*O*-(trimethylacetyl)-α-D-galactofuranoside (**7**)

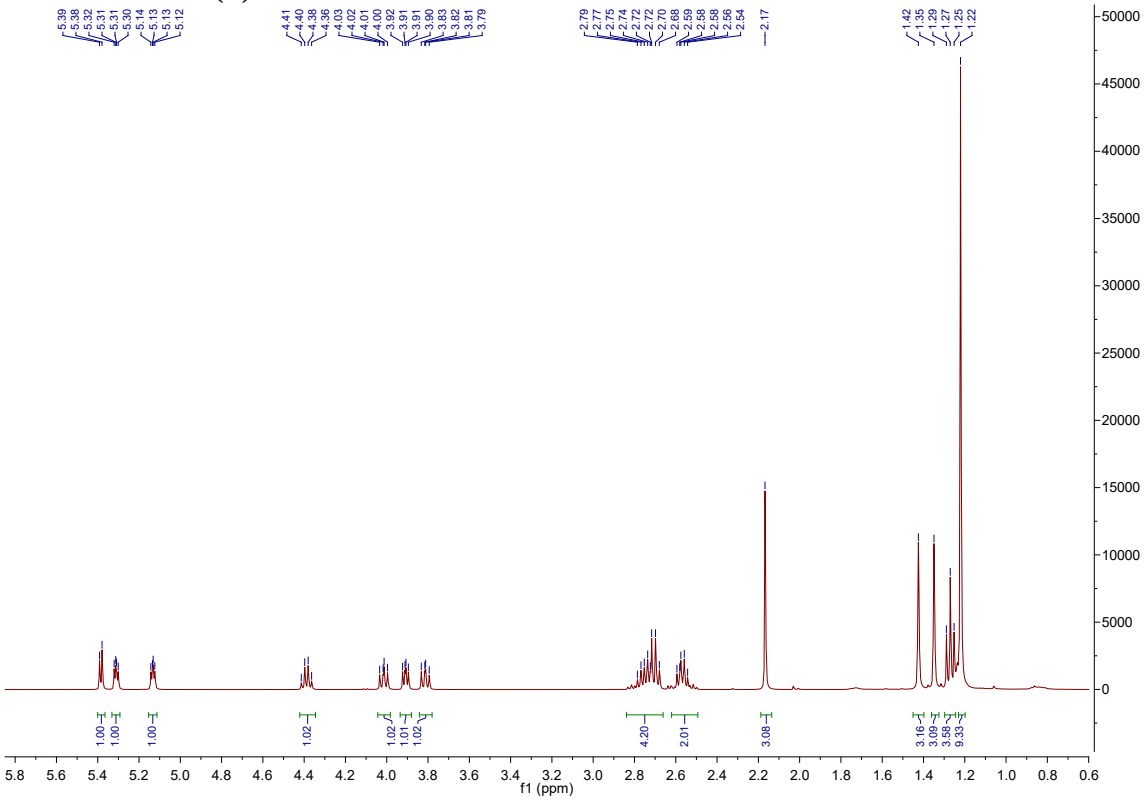

Figure A.43: ^{1}H NMR spectrum of **7**, in $CDCl_3$.

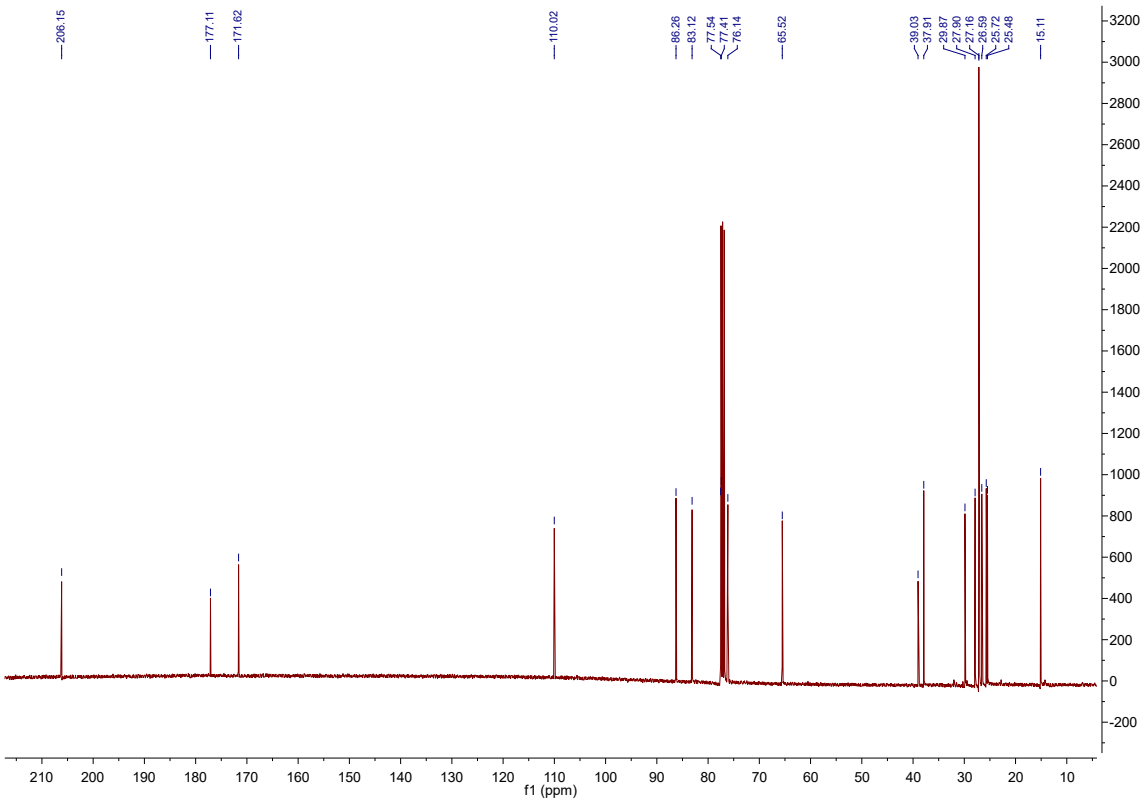

Figure A.44: ^{13}C NMR spectrum of **7**, in $CDCl_3$.

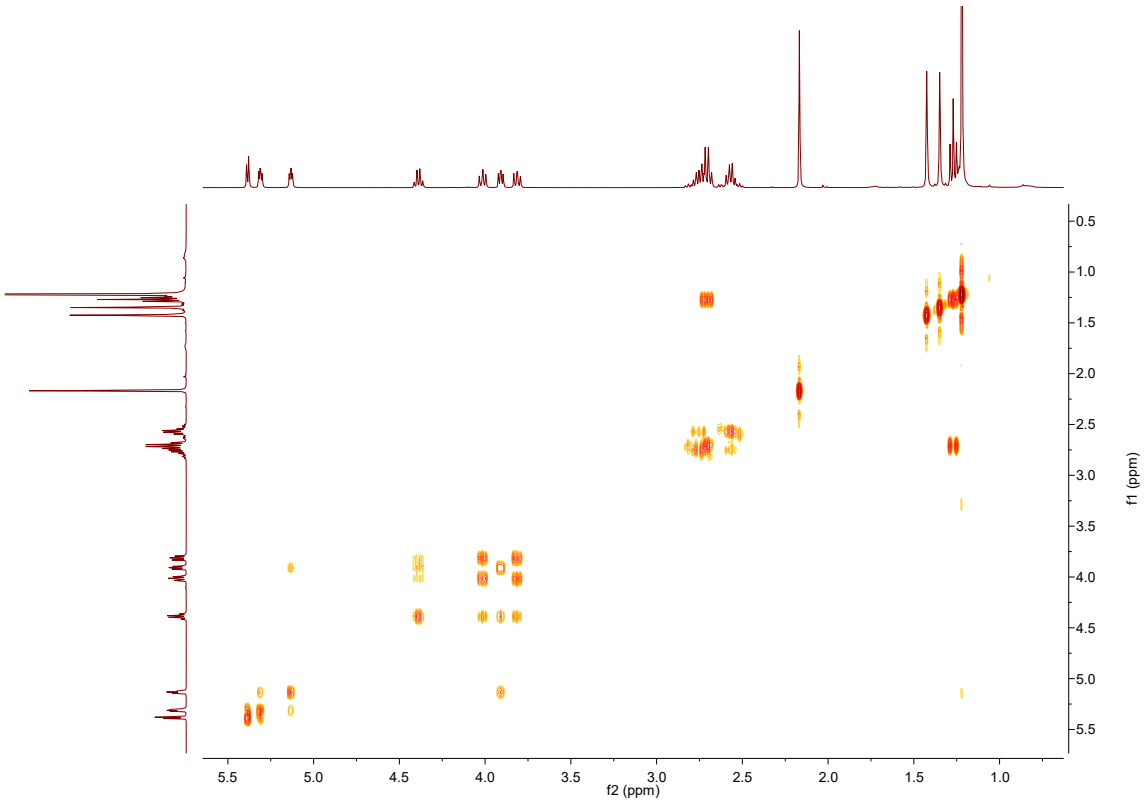

Figure A.45: COSY spectrum of **7**, in $CDCl_3$.

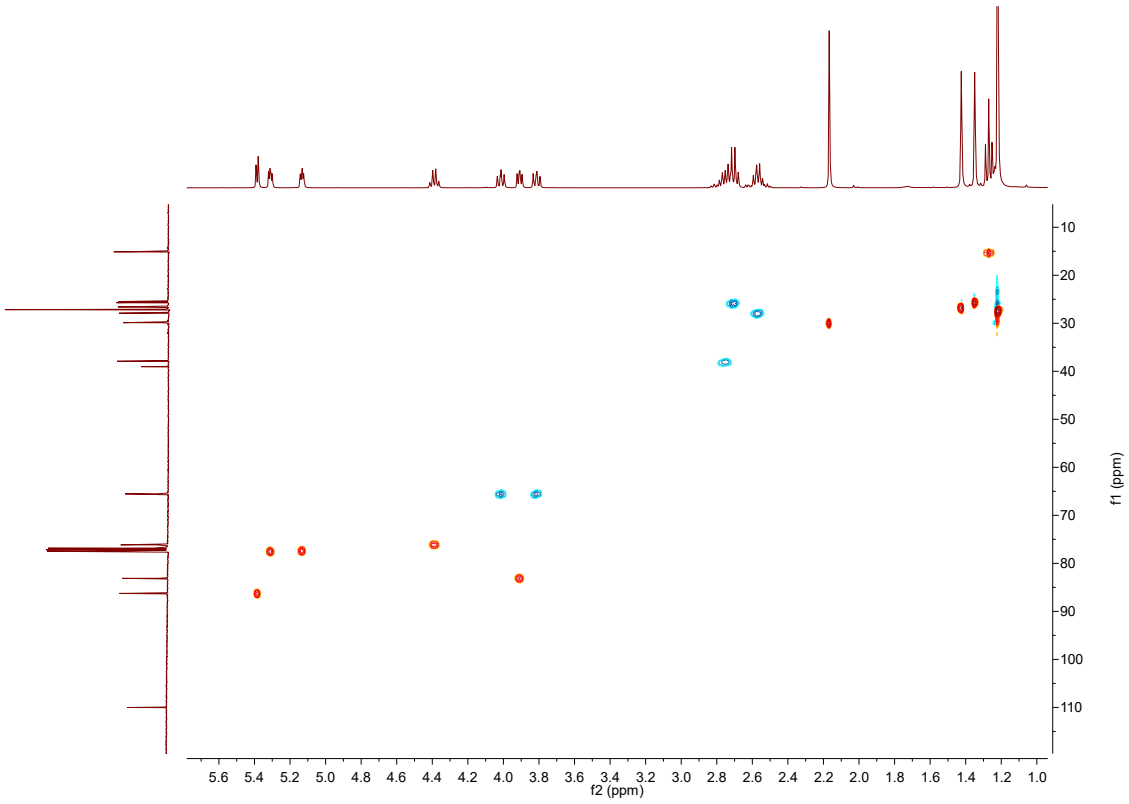

Figure A.46: HSQC spectrum of **7**, in $CDCl_3$.

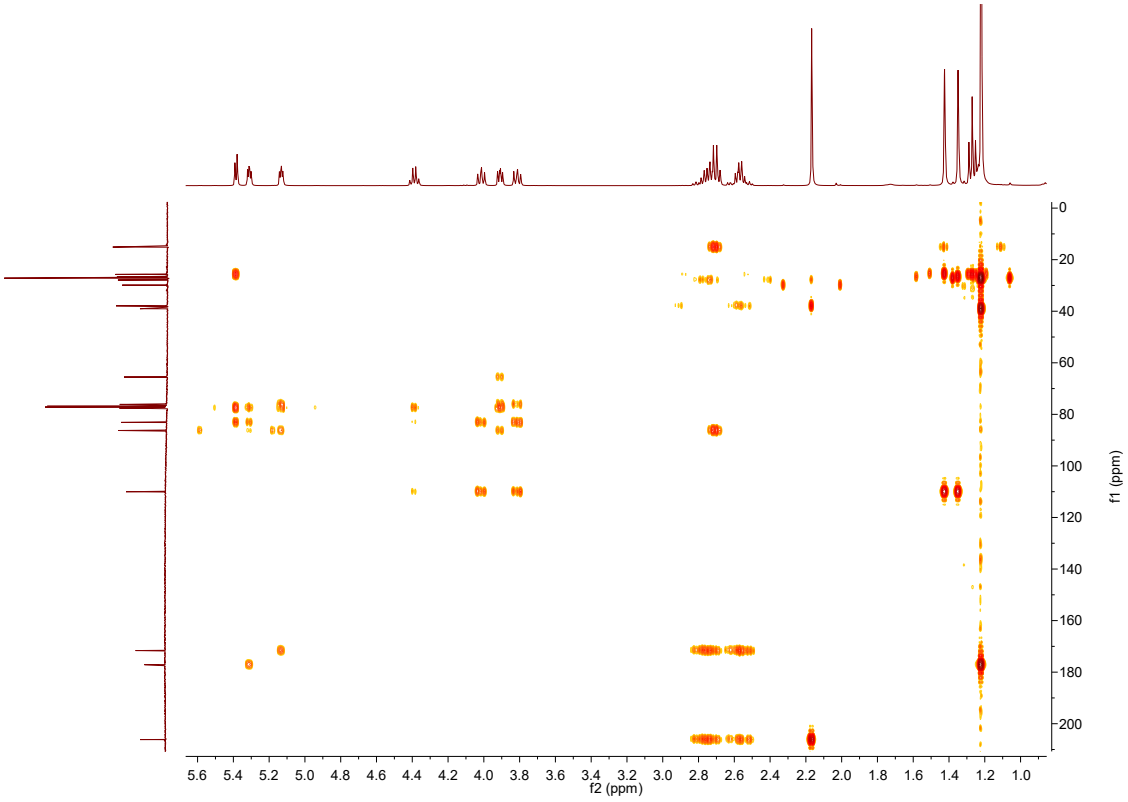

Figure A.47: HMBC spectrum of **7**, in $CDCl_3$.

A.13. Ethyl 3-*O*-levulinoyl-1-thio-2-*O*-(trimethylacetyl)-α-D-galactofuranoside (**8**)

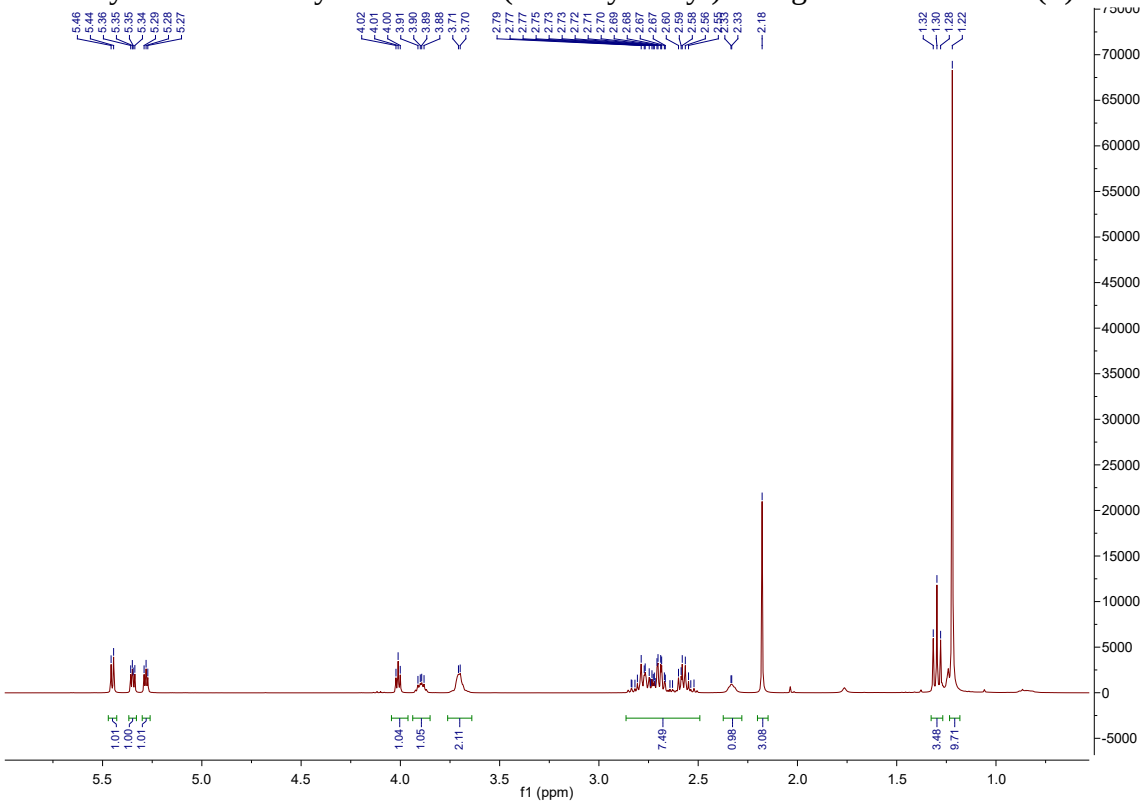

Figure A.48: ^{1}H NMR spectrum of **8**, in $CDCl_3$.

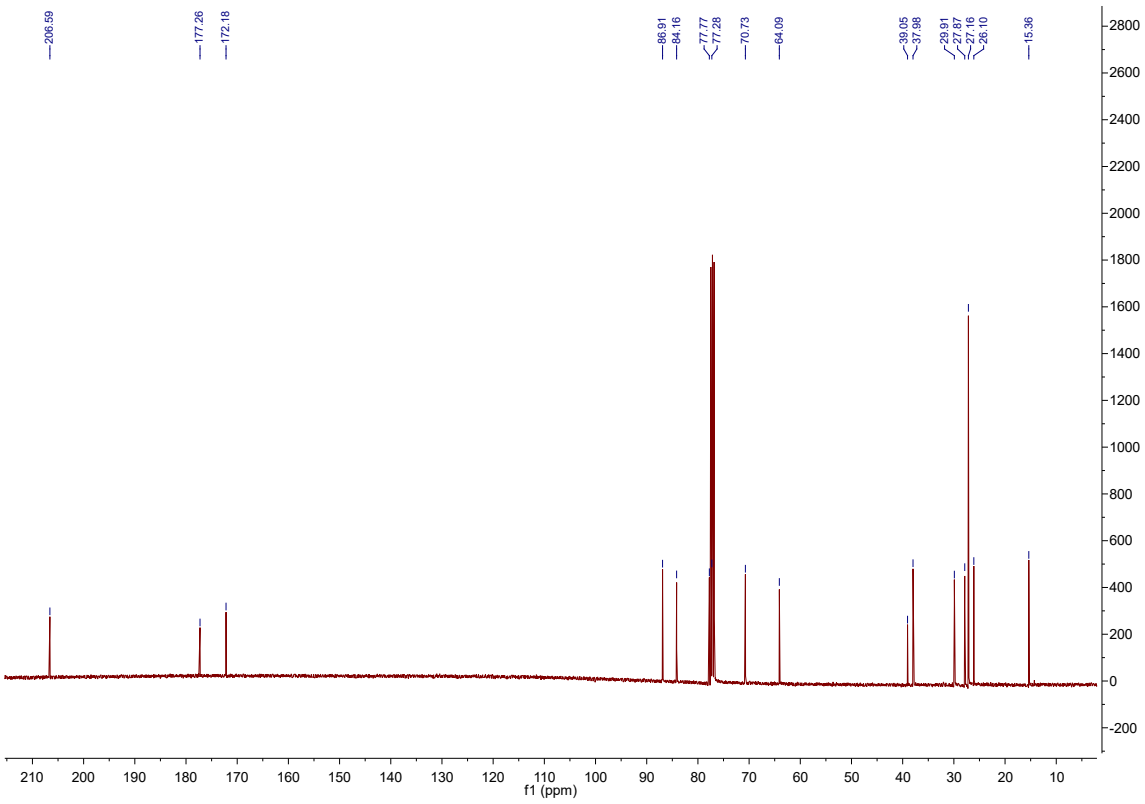

Figure A.49: ^{13}C NMR spectrum of **8**, in $CDCl_3$.

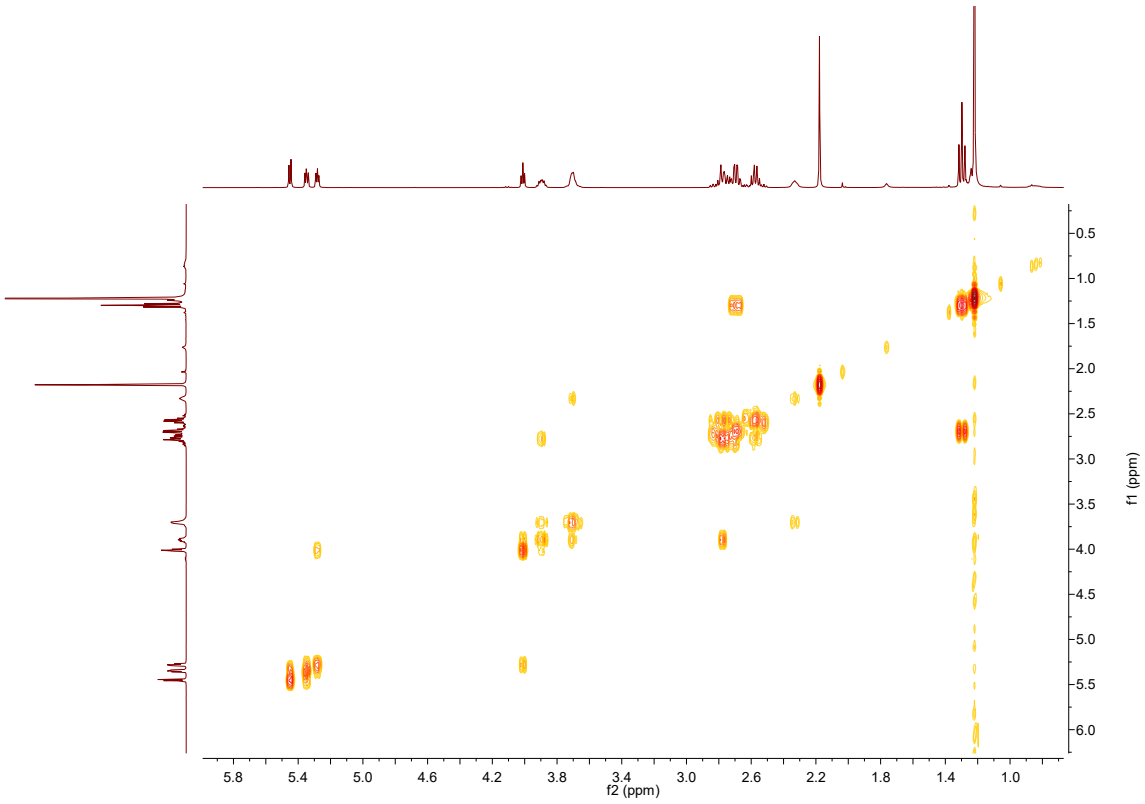

Figure A.50: COSY spectrum of **8**, in $CDCl_3$.

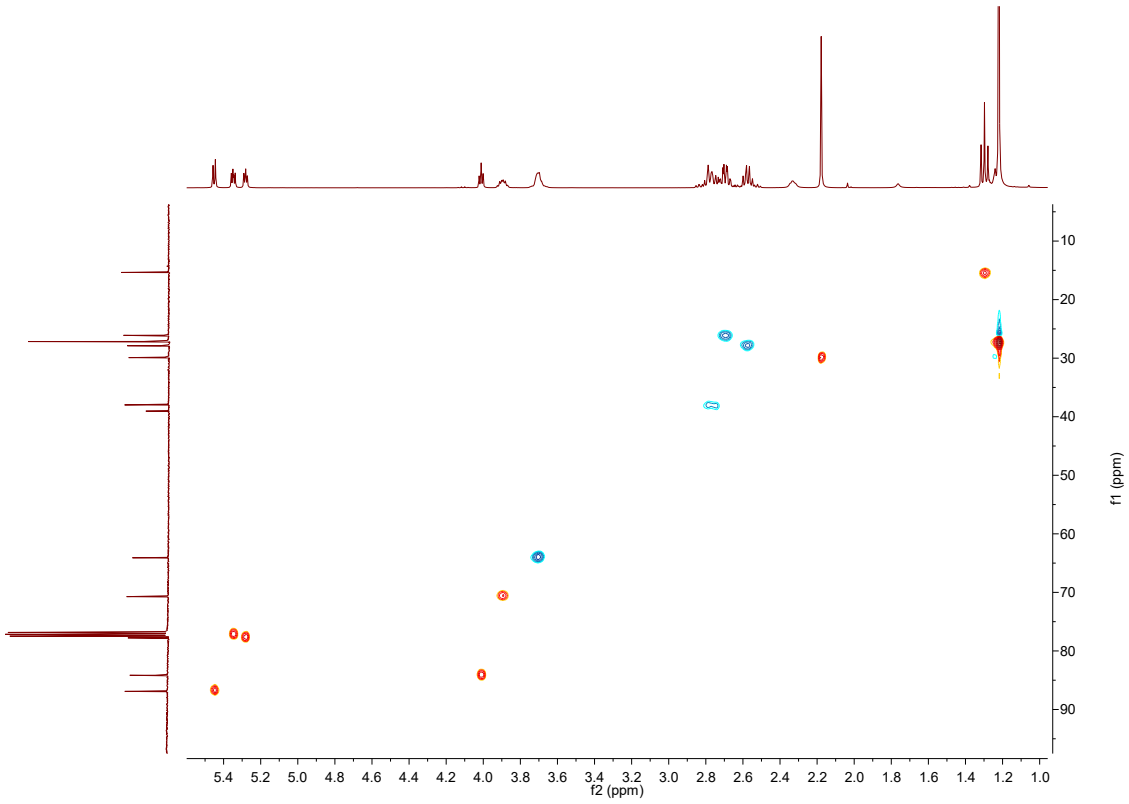

Figure A.51: HSQC spectrum of **8**, in $CDCl_3$.

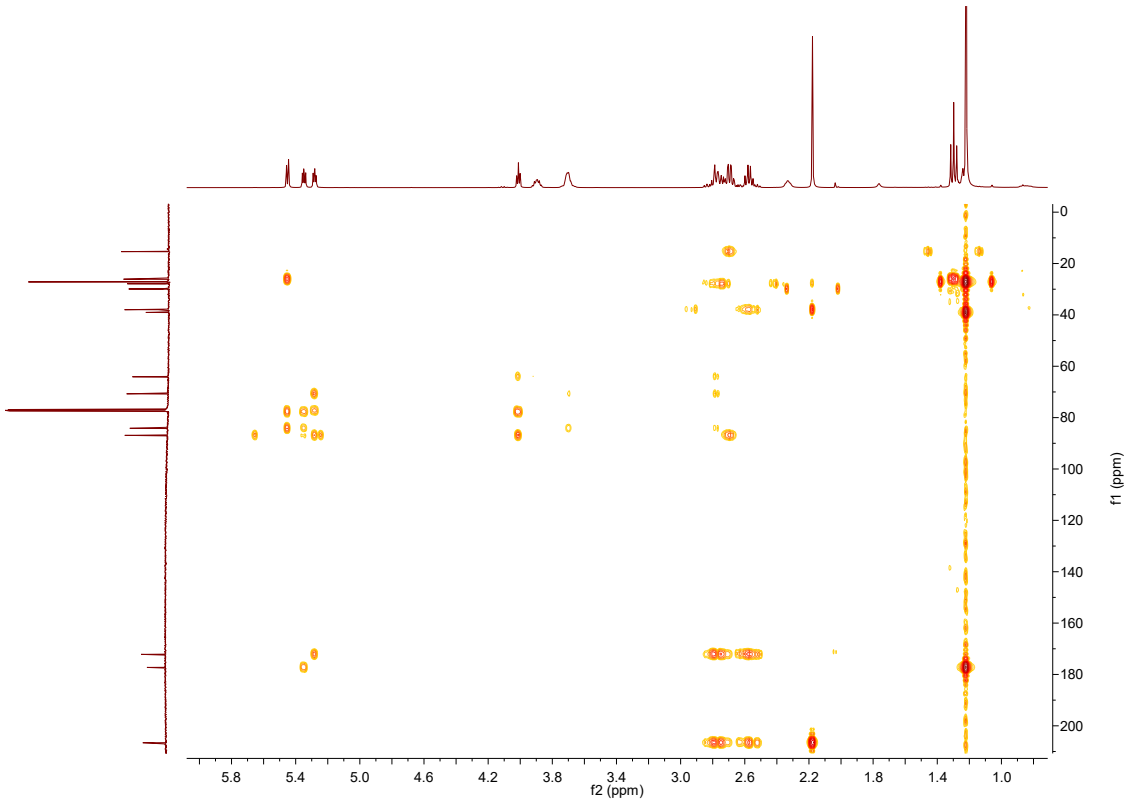

Figure A.52: HMBC spectrum of **8**, in $CDCl_3$.

A.14. Ethyl 3-*O*-benzyl-6-*O*-levulinoyl-1-thio-2-*O*-(trimethylacetyl)-α-D-galactofuranoside (**9**)

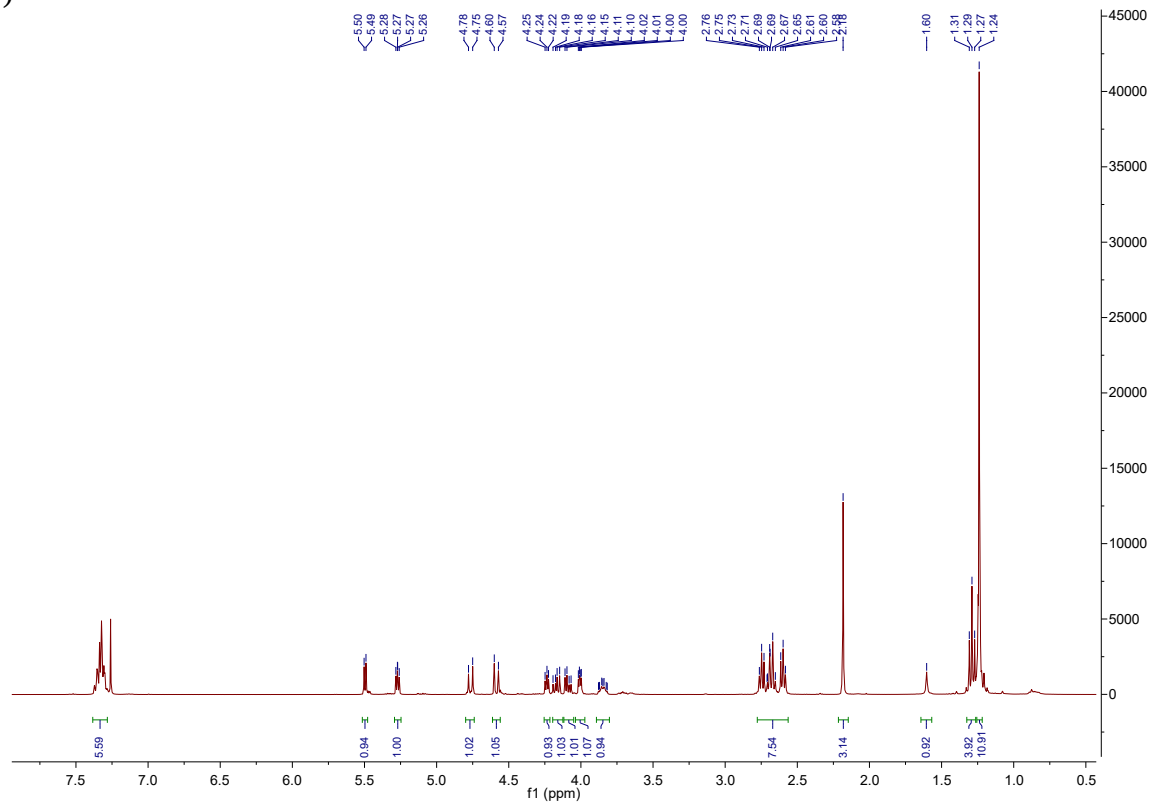

Figure A.53: ^{1}H NMR spectrum of **9**, in $CDCl_3$.

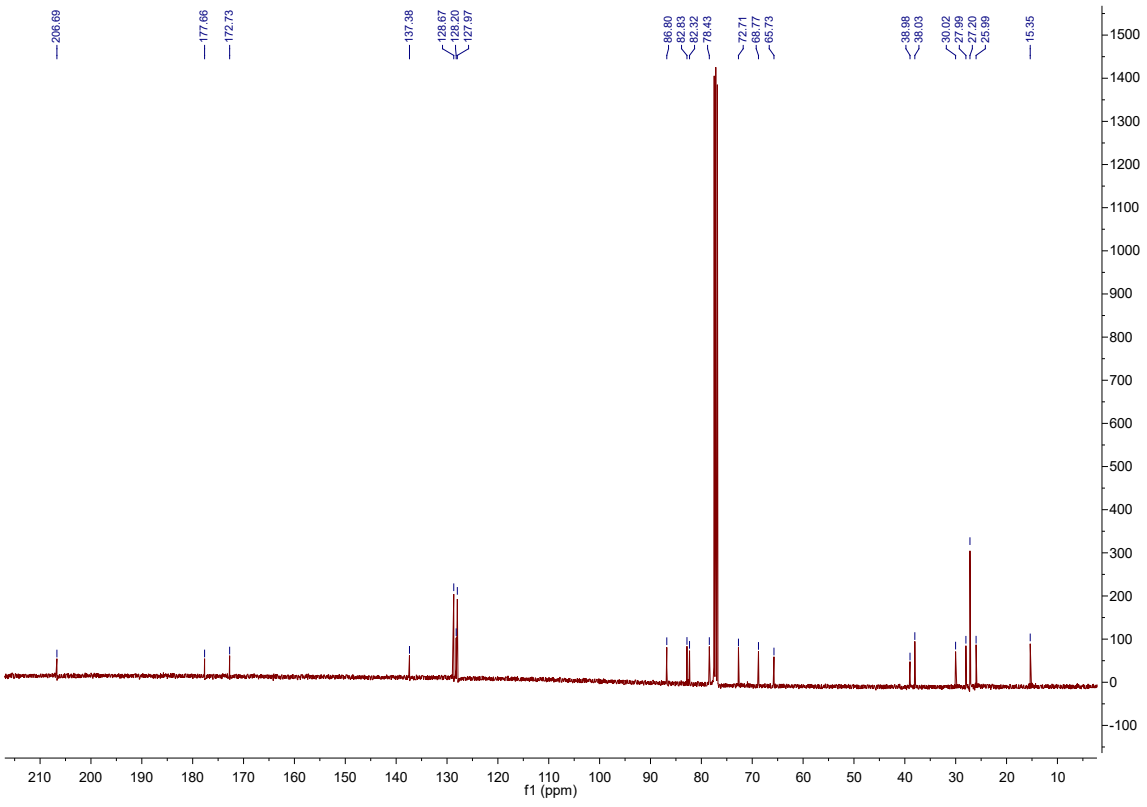

Figure A.54: ^{13}C NMR spectrum of **9**, in $CDCl_3$.

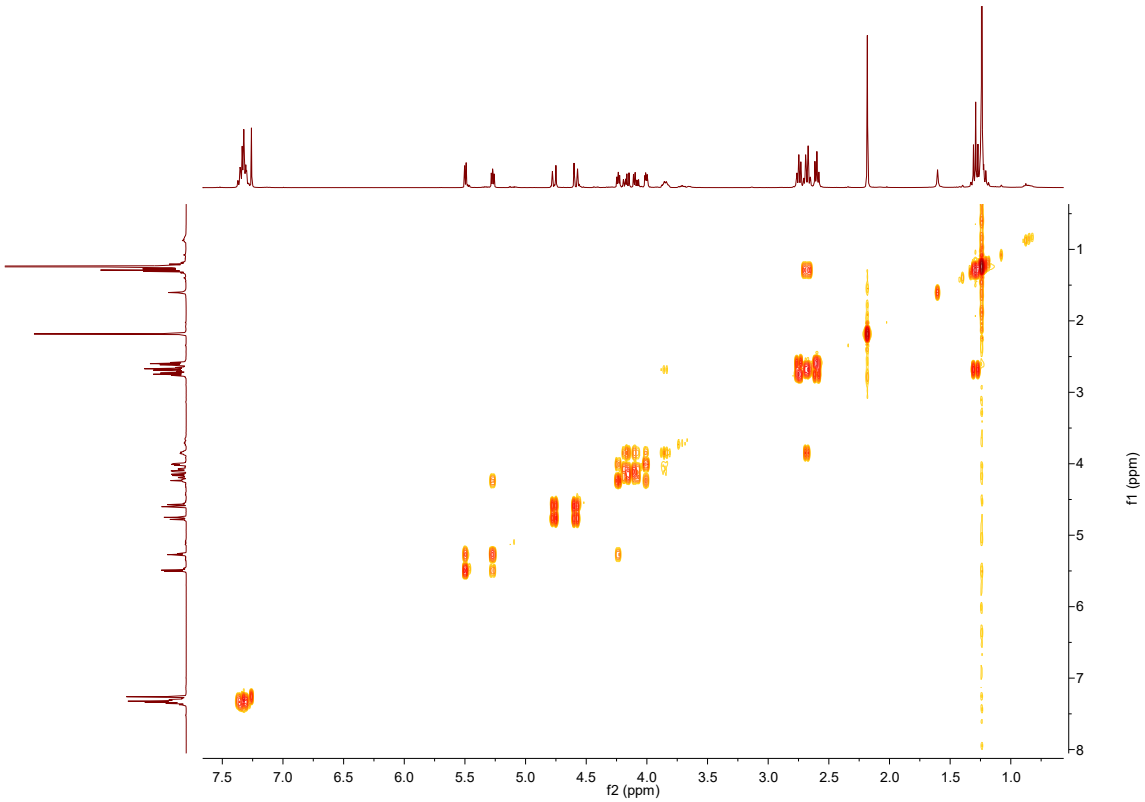

Figure A.55: COSY spectrum of **9**, in $CDCl_3$.

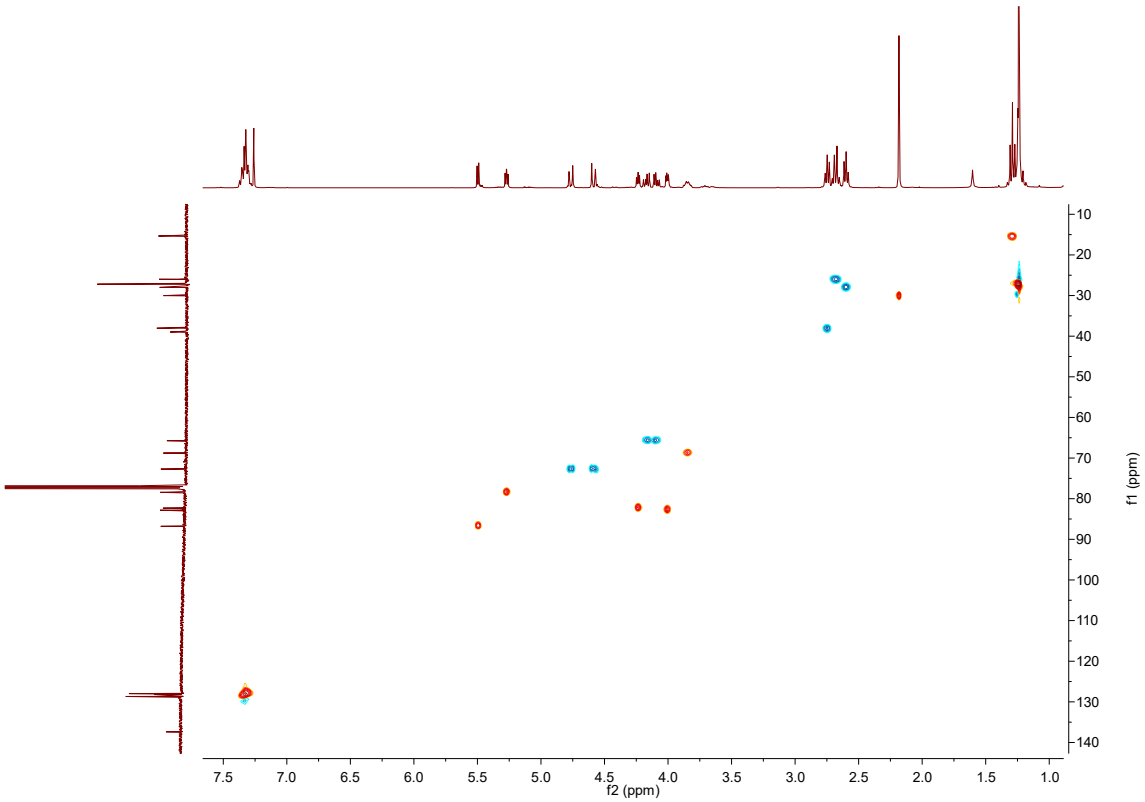

Figure A.56: HSQC spectrum of **9**, in $CDCl_3$.

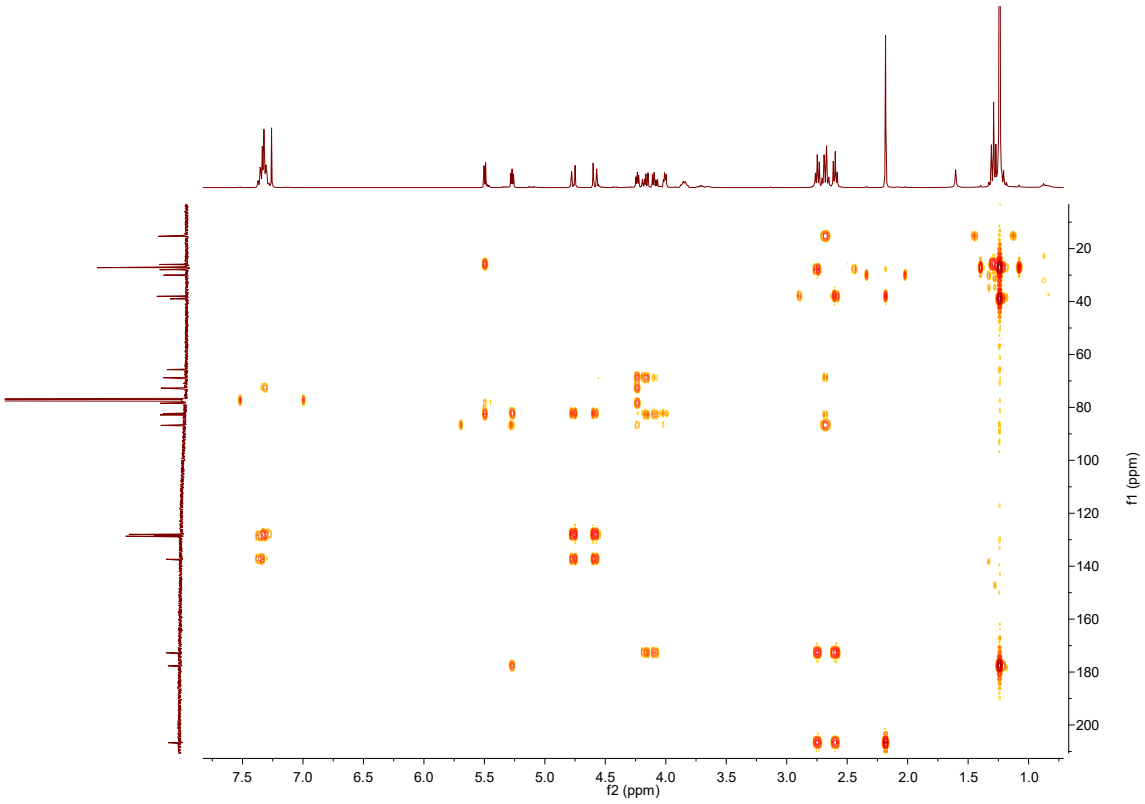

Figure A.57: HMBC spectrum of **9**, in $CDCl_3$.

A.15. Ethyl 5,6-*O*-isopropylidene-3-*O*-(2-naphtylmethyl)-1-thio-2-*O*-(trimethylacetyl)-α-D-galactofuranoside (**10**)

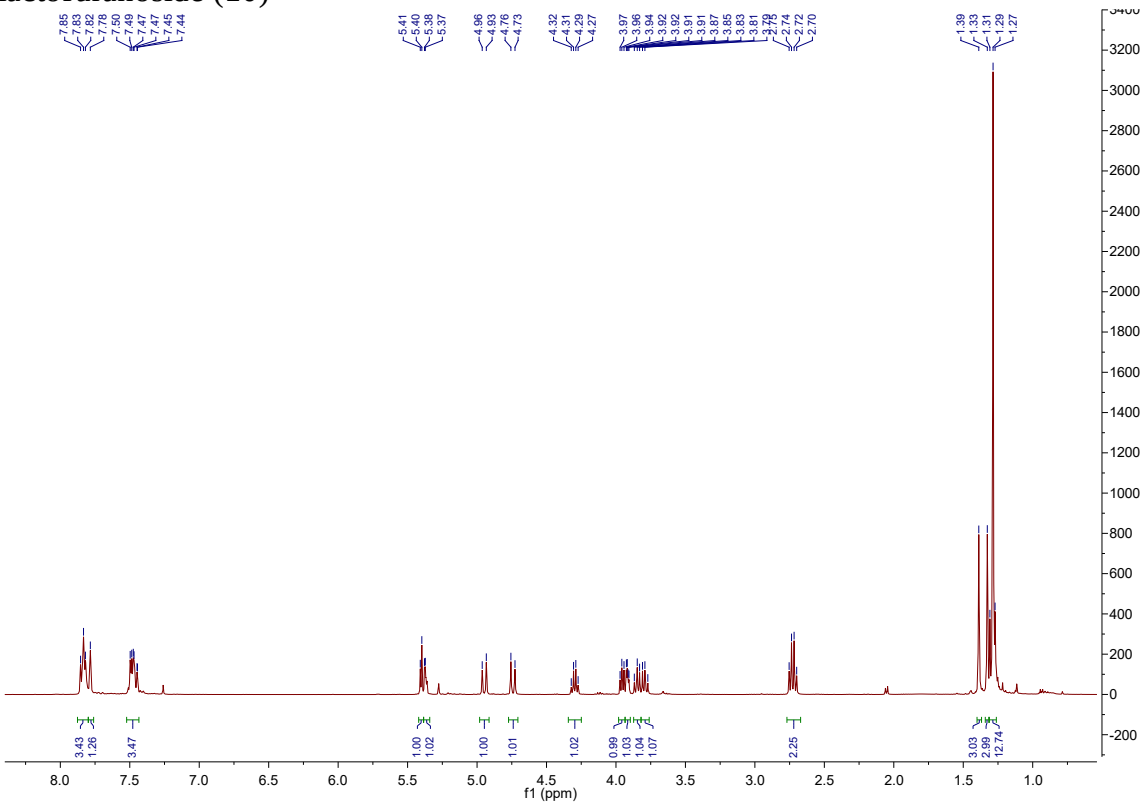

Figure A.58: ^{1}H NMR spectrum of **10**, in $CDCl_3$.

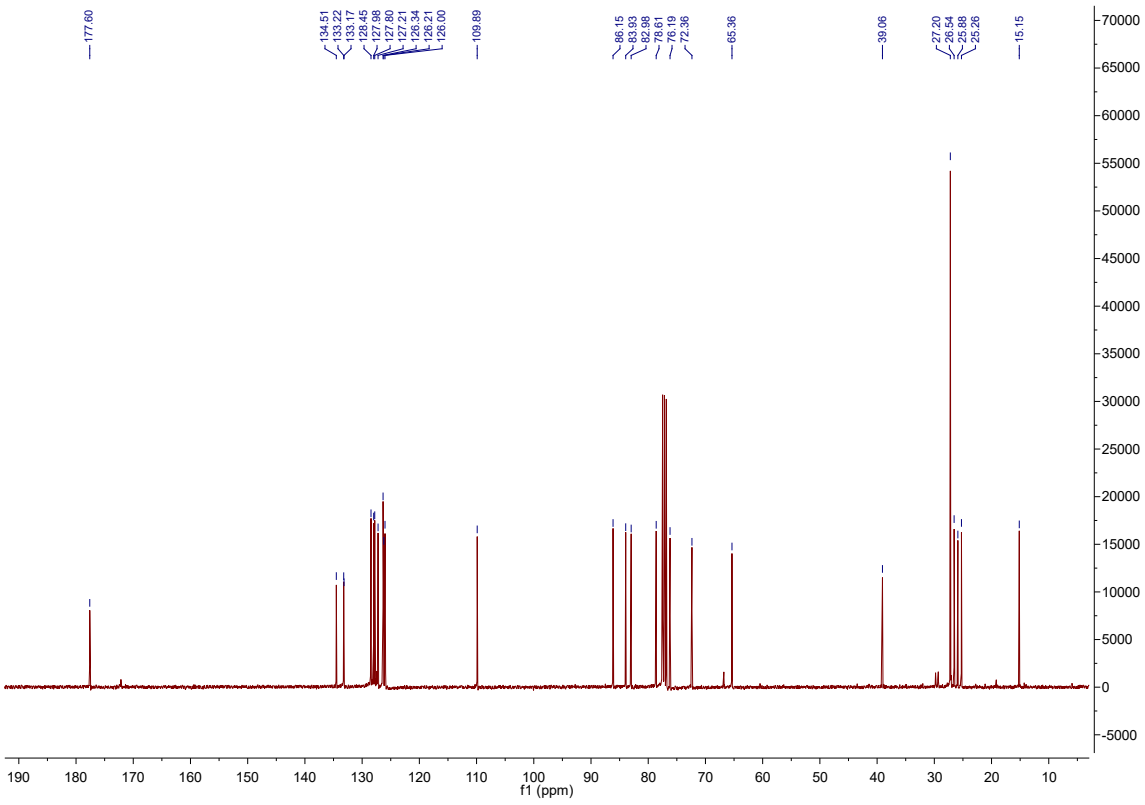

Figure A.59: ^{13}C NMR spectrum of **10**, in $CDCl_3$.

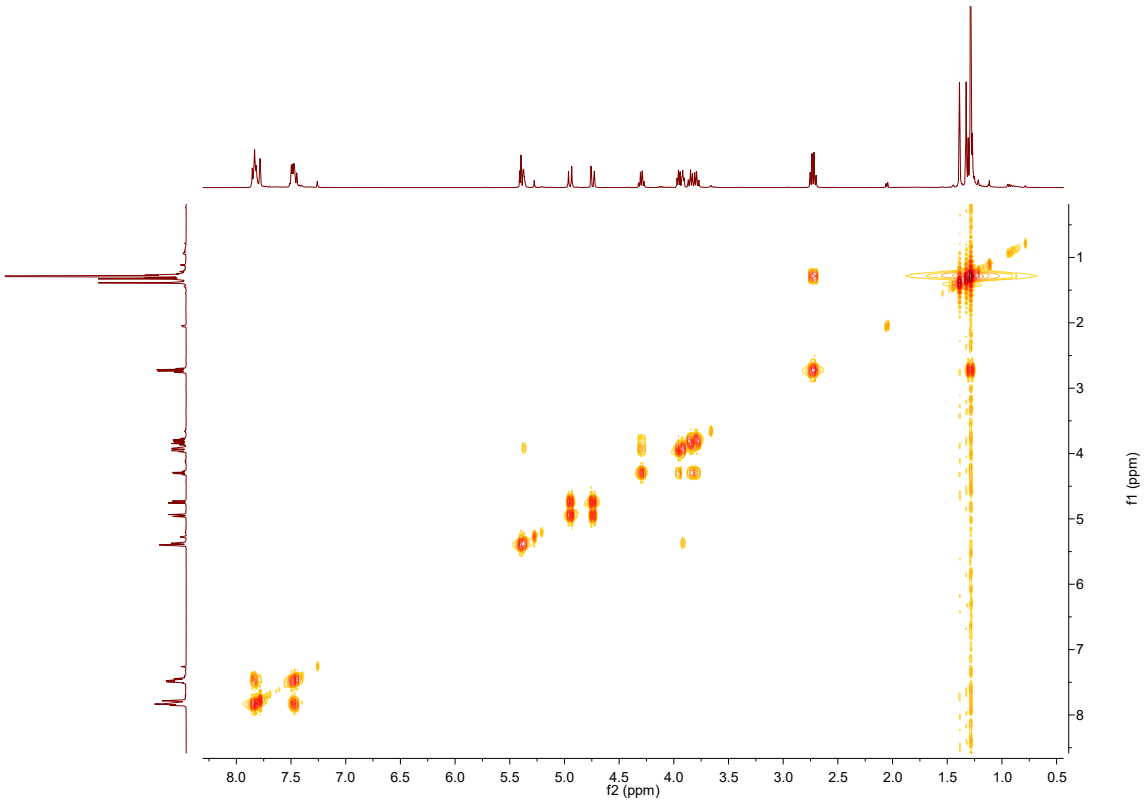

Figure A.60: COSY spectrum of **10**, in $CDCl_3$.

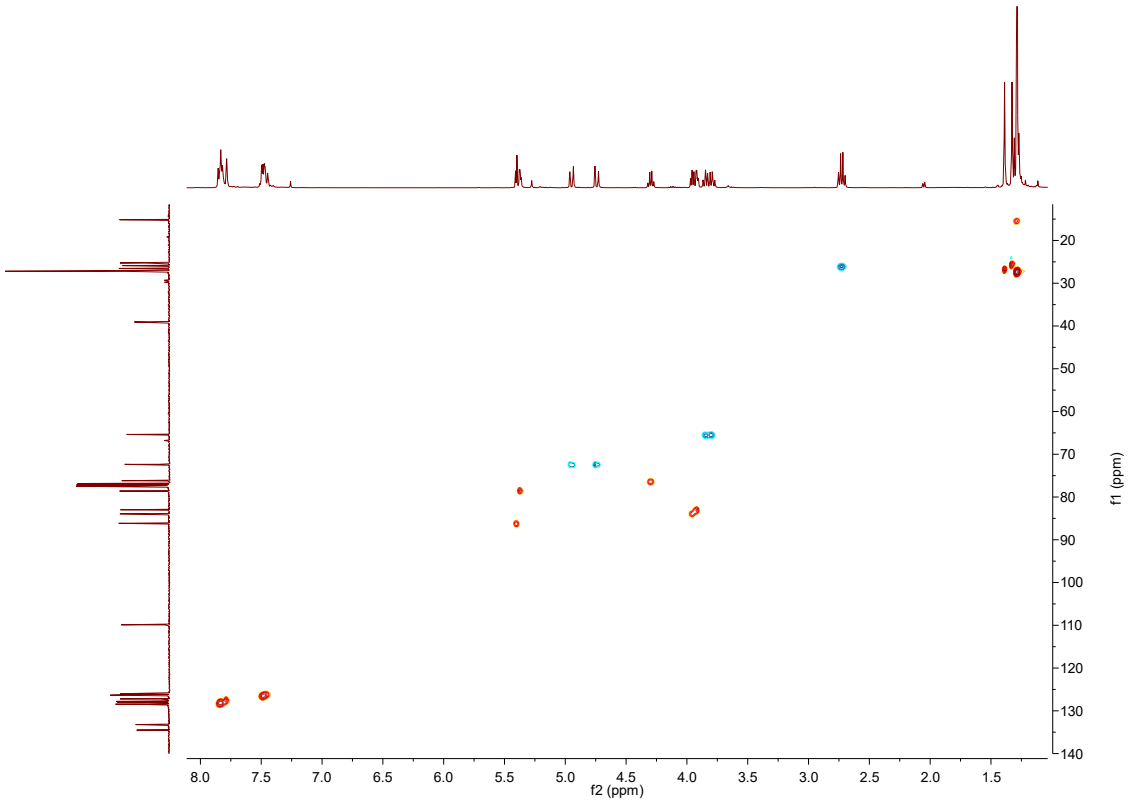

Figure A.61: HSQC spectrum of **10**, in $CDCl_3$.

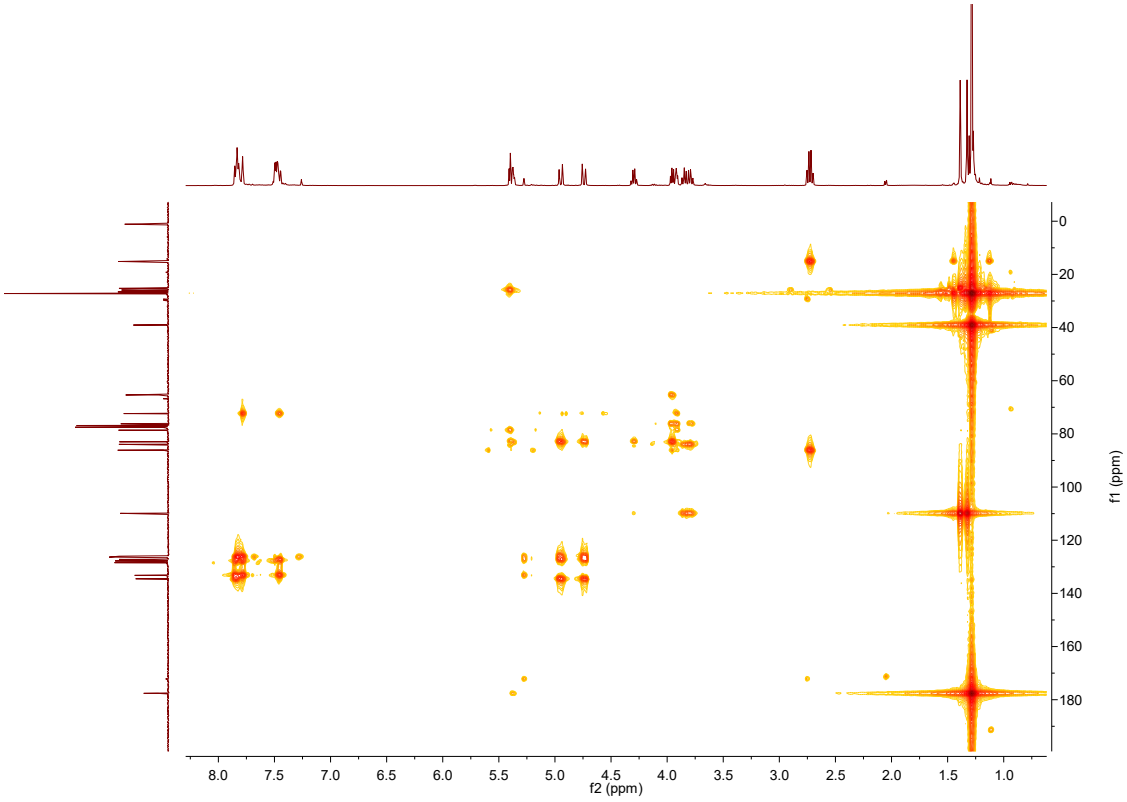

Figure A.62: HMBC spectrum of **10**, in $CDCl_3$.

A.16. Ethyl 3-*O*-(2-naphtylmethyl)-1-thio-2-*O*-(trimethylacetyl)-α-D-galactofuranoside (**11**)

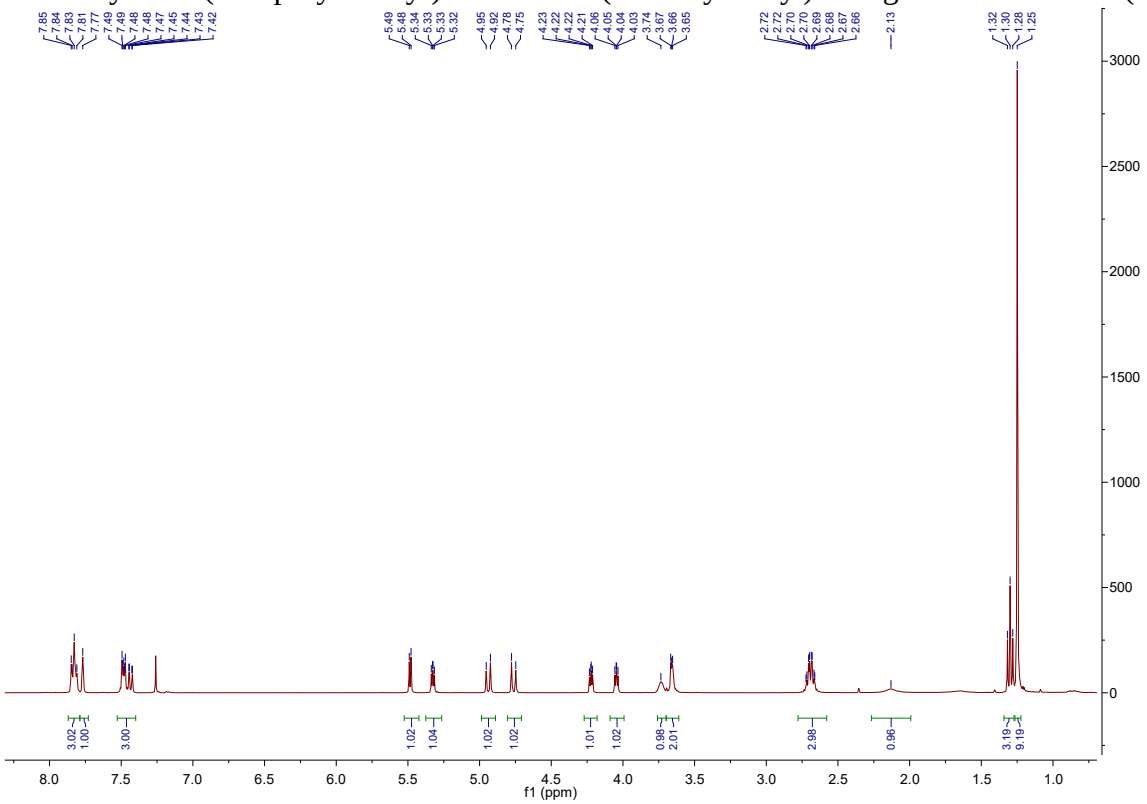

Figure A.63: ^{1}H NMR spectrum of **11**, in $CDCl_3$.

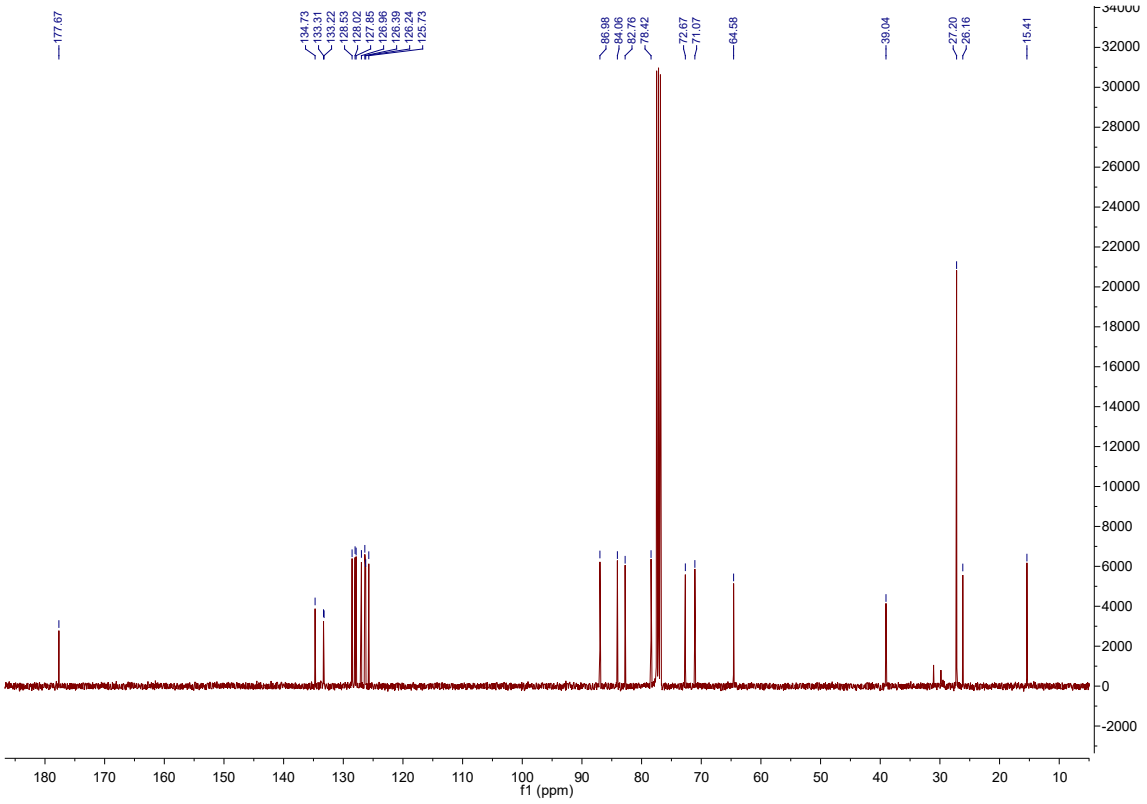

Figure A.64: ^{13}C NMR spectrum of **11**, in $CDCl_3$.

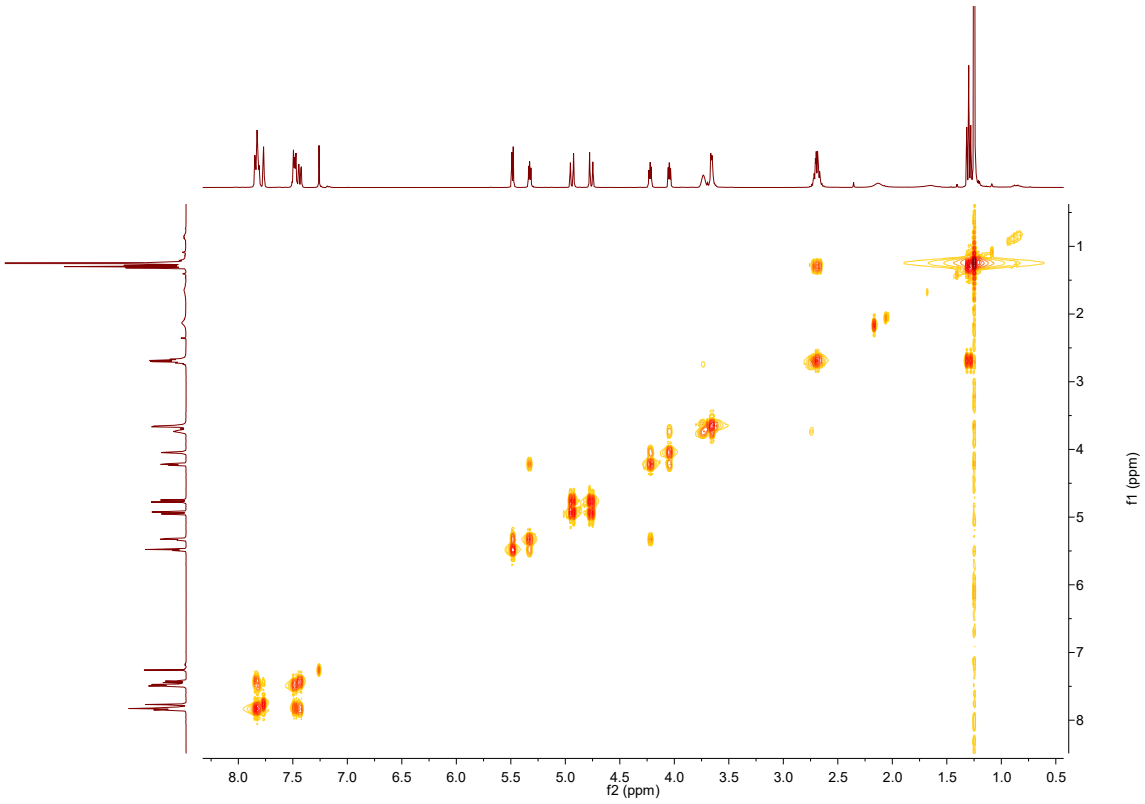

Figure A.65: COSY spectrum of **11**, in $CDCl_3$.

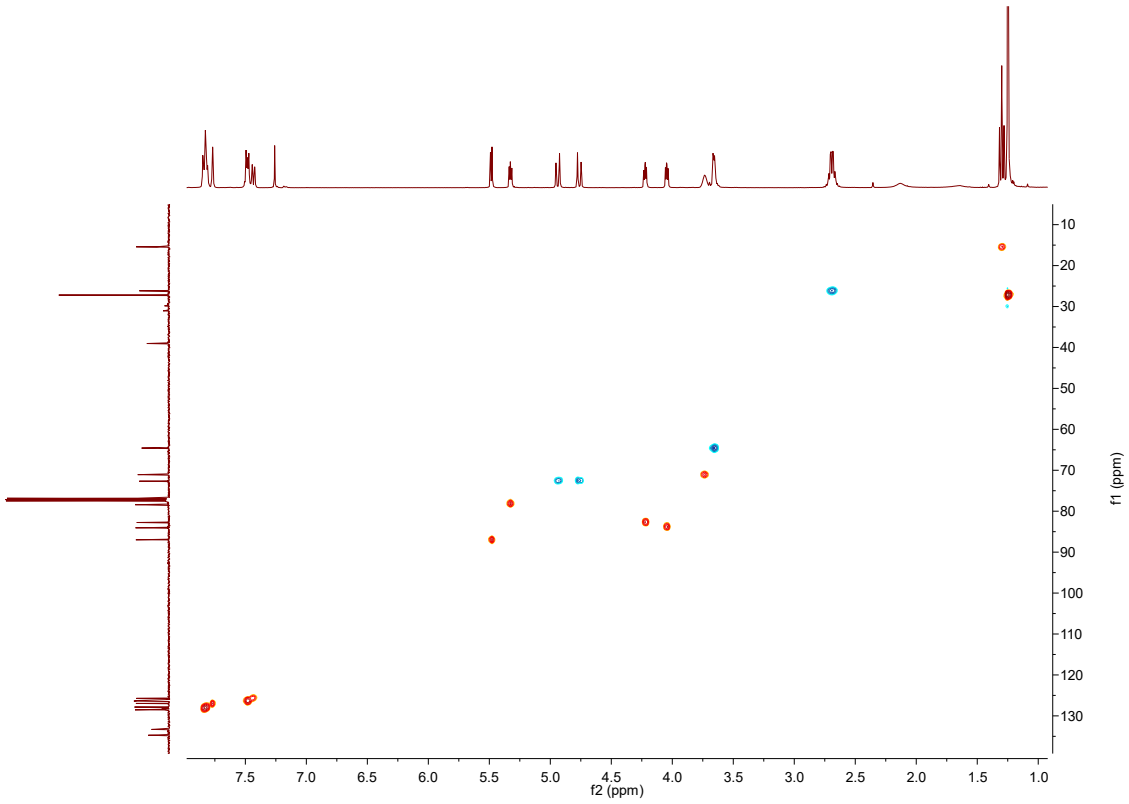

Figure A.66: HSQC spectrum of **11**, in $CDCl_3$.

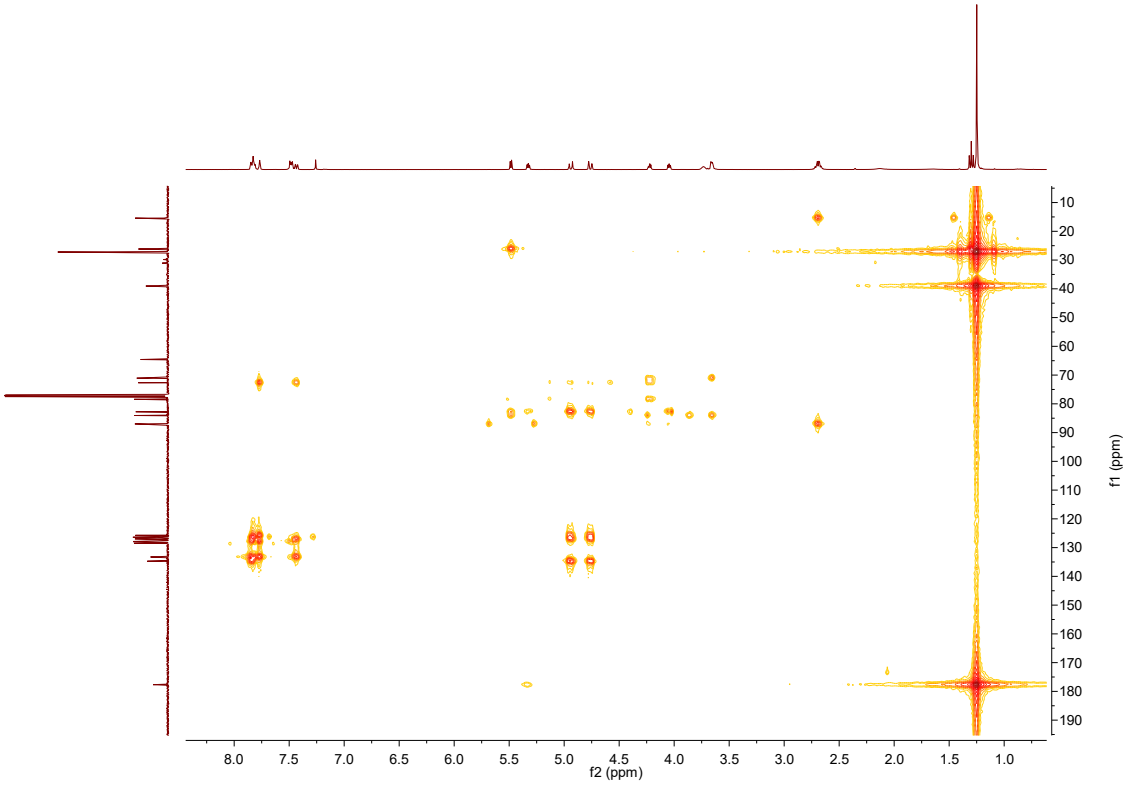

Figure A.67: HMBC spectrum of **11**, in $CDCl_3$.

A.17. Failed basic benzylation of **11** into **BB-1d**

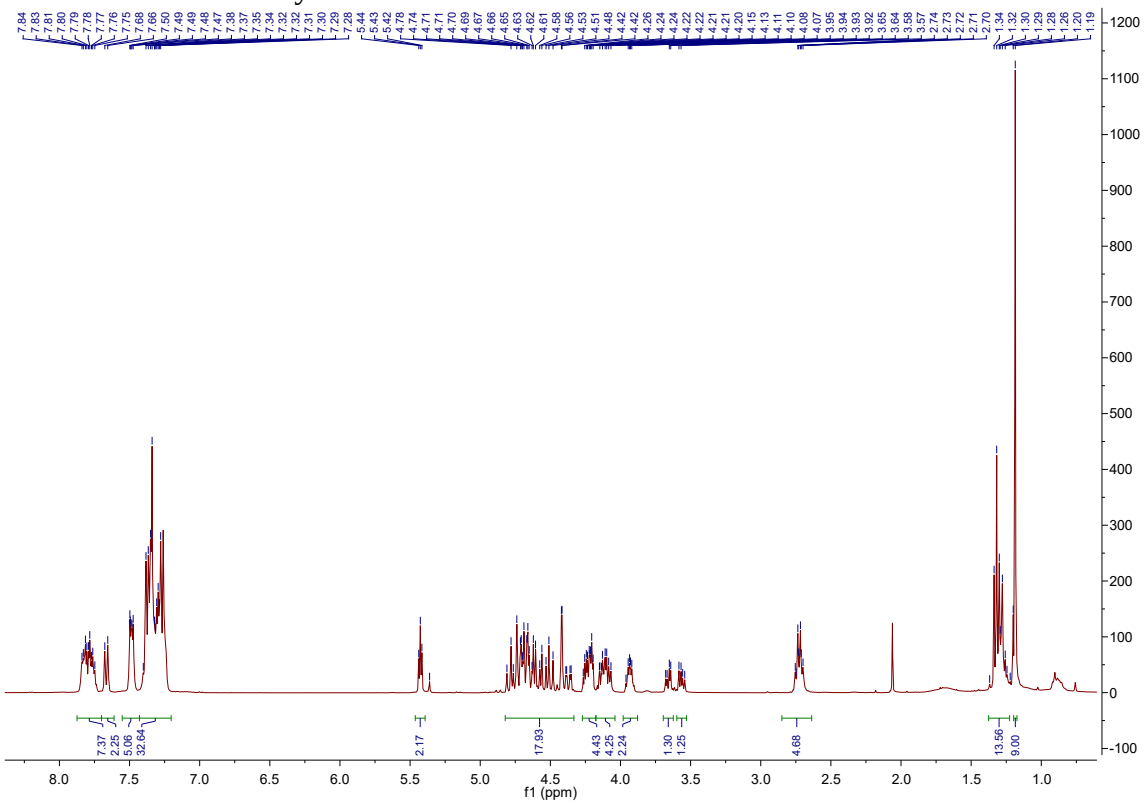

Figure A.68: ^{1}H NMR spectrum of product mixture from benzylation of **11**, in $CDCl_3$.

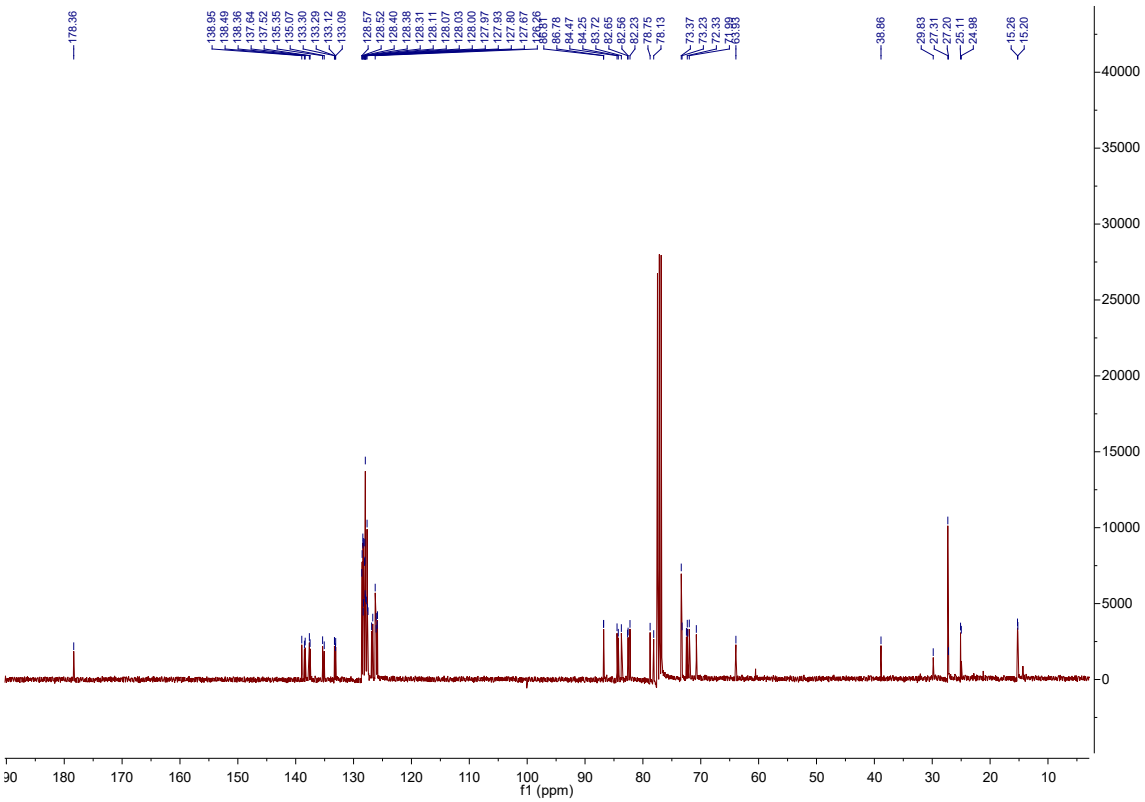

Figure A.69: ^{13}C NMR spectrum of product mixture from benzylation of **11**, in $CDCl_3$.

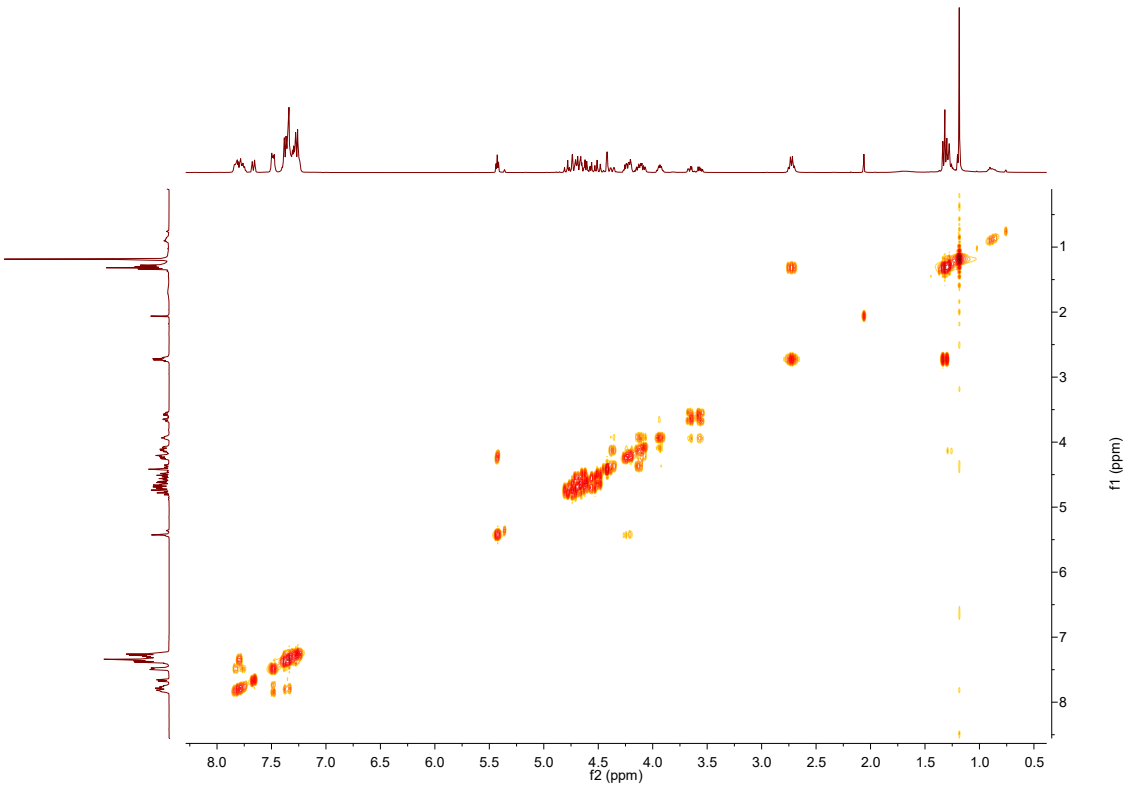

Figure A.70: COSY spectrum of product mixture from benzylation of **11**, in $CDCl_3$.

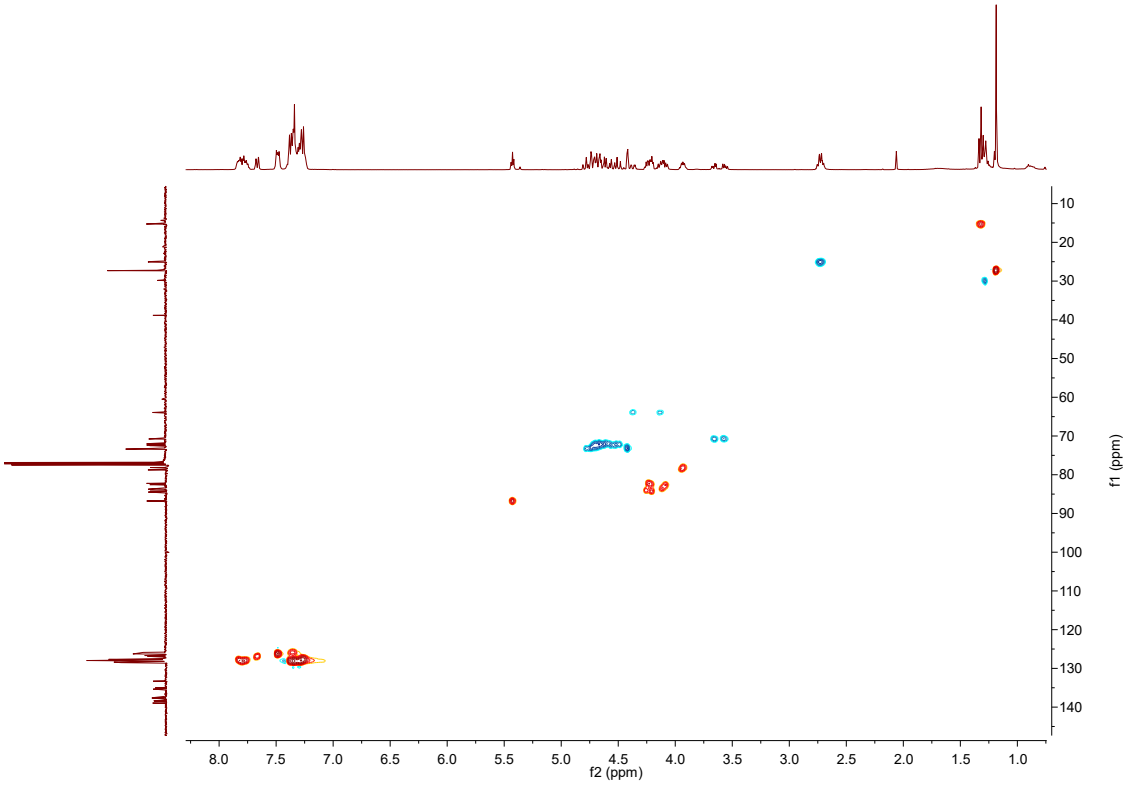

Figure A.71: HSQC spectrum of product mixture from benzylation of **11**, in $CDCl_3$.

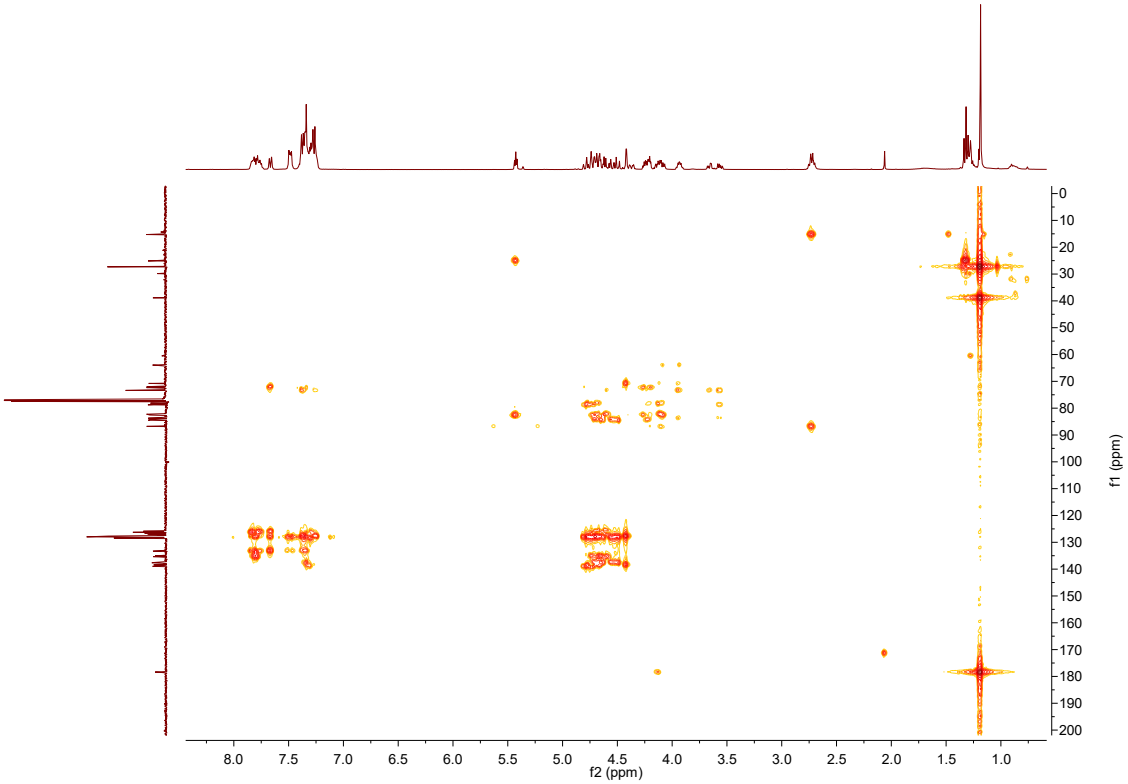

Figure A.72: HMBC spectrum of product mixture from benzylation of **11**, in $CDCl_3$.

A.18. Ethyl 5,6-*O*-benzylidene-3-*O*-(2-naphtylmethyl)-1-thio-2-*O*-(trimethylacetyl)-α-D-galactofuranoside (**12**)

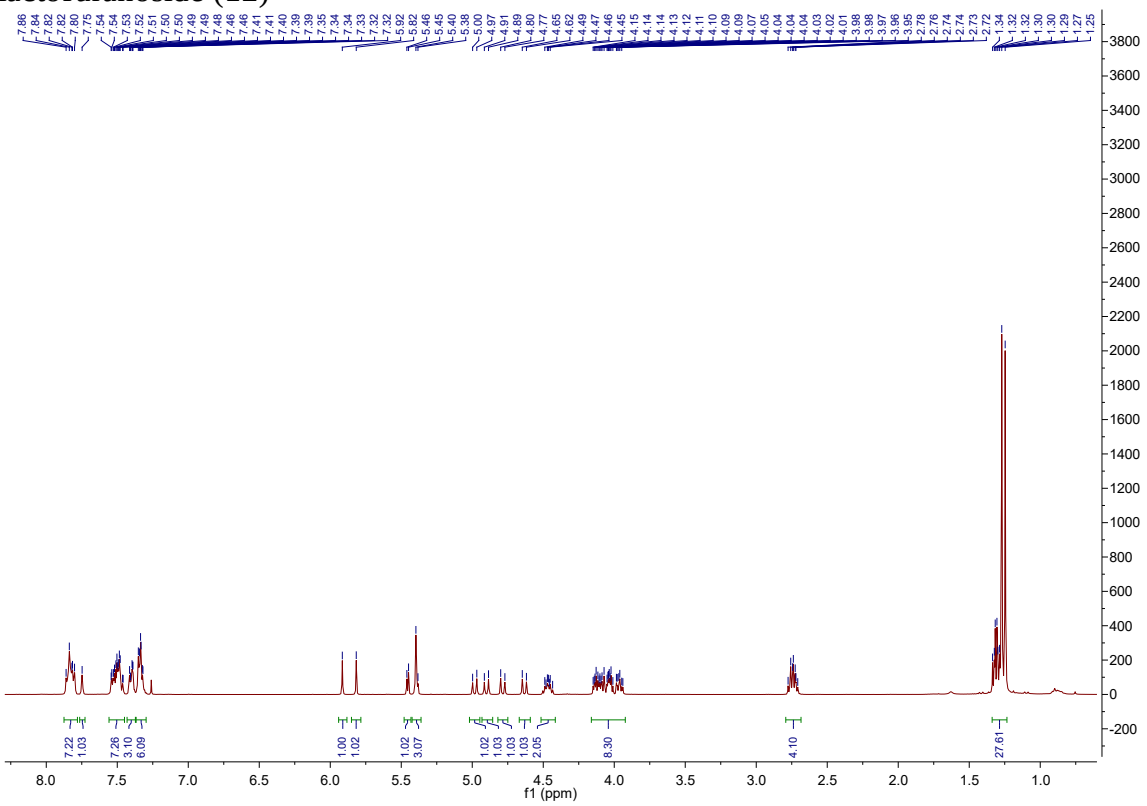

Figure A.73: ^{1}H NMR spectrum of **12**, in $CDCl_3$.

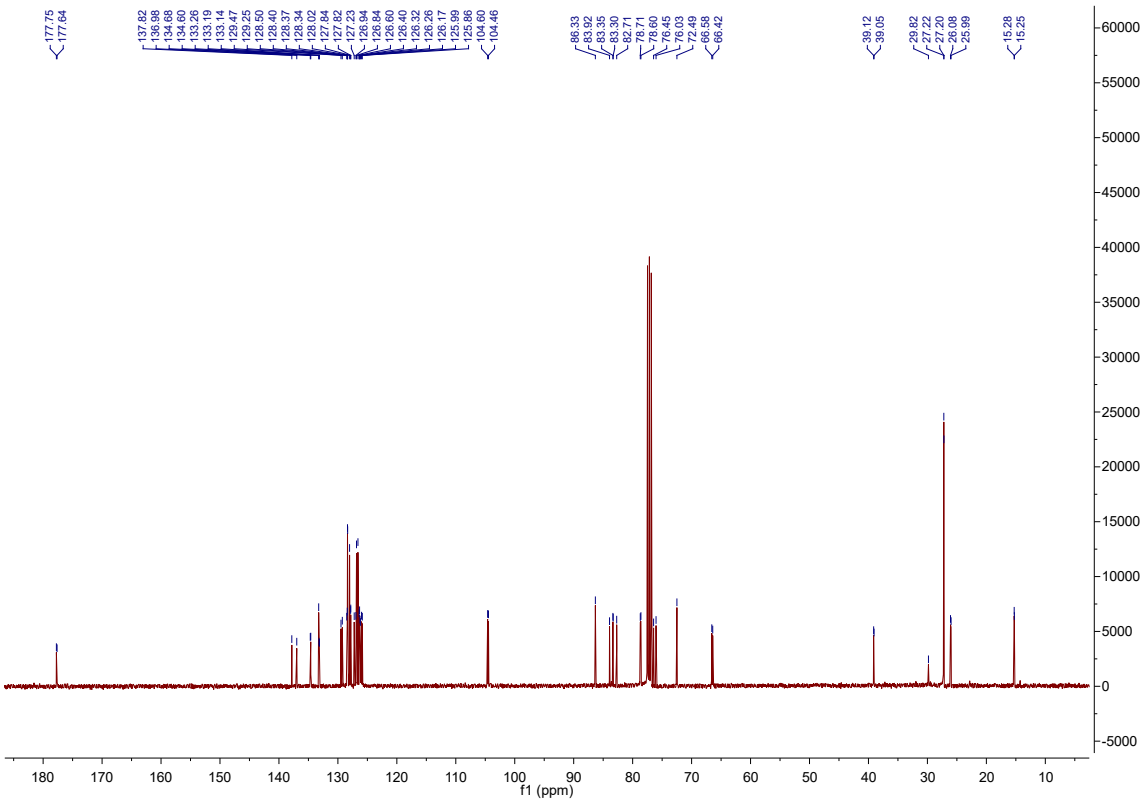

Figure A.74: ^{13}C NMR spectrum of **12**, in $CDCl_3$.

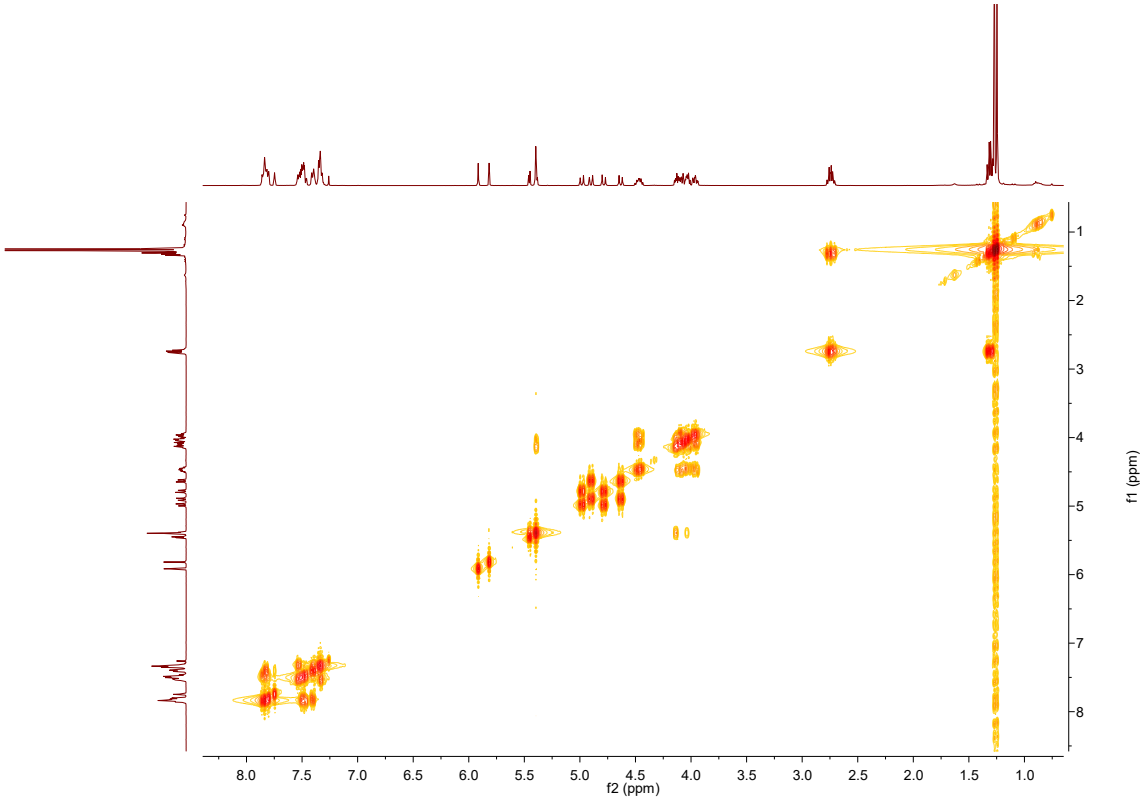

Figure A.75: COSY spectrum of **12**, in $CDCl_3$.

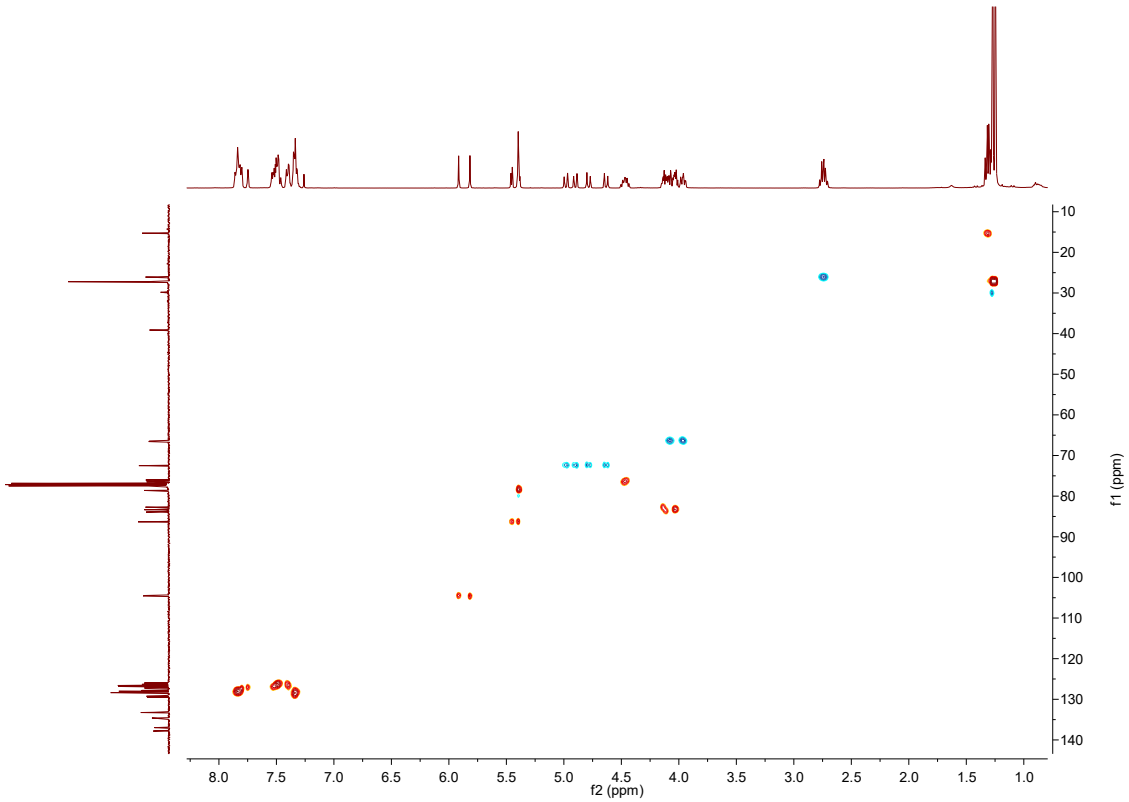

Figure A.76: HSQC spectrum of **12**, in $CDCl_3$.

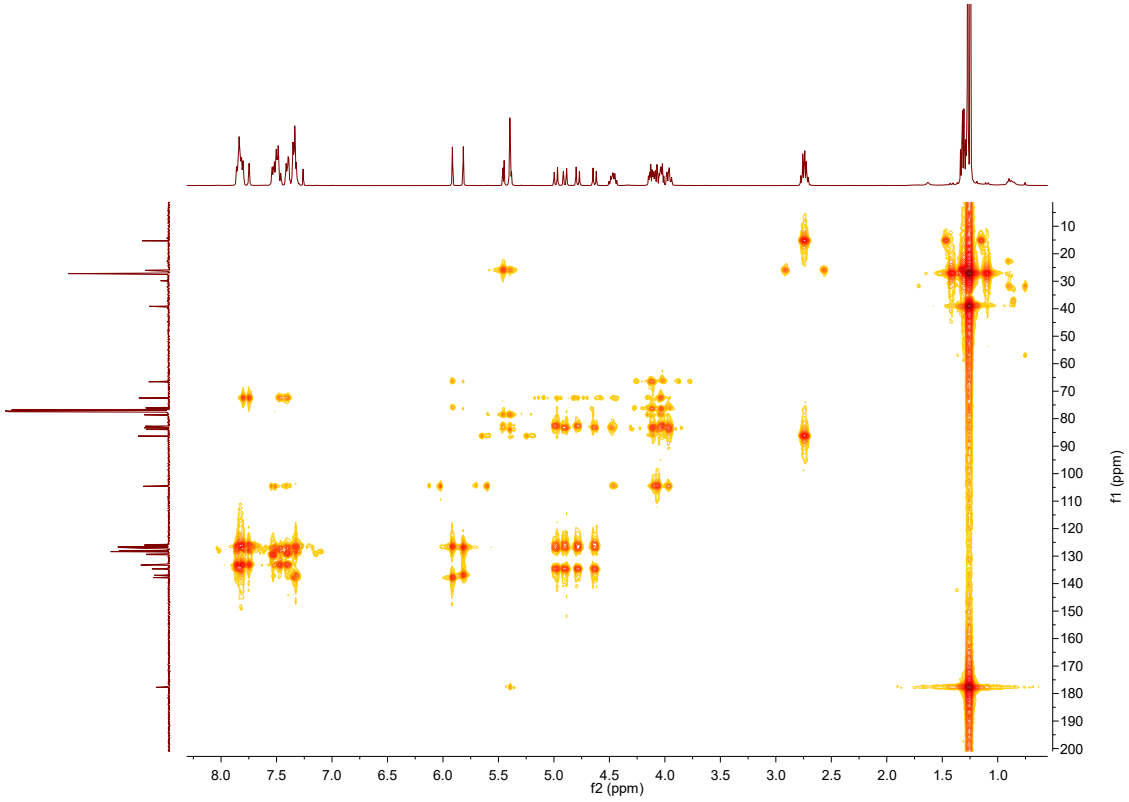

Figure A.77: HMBC spectrum of **12**, in $CDCl_3$.

A.19. Ethyl 5,6-di-*O*-acetyl-3-*O*-(2-naphtylmethyl)-1-thio-2-*O*-(trimethylacetyl)-α-D-galactofuranoside (**BB-1e**)

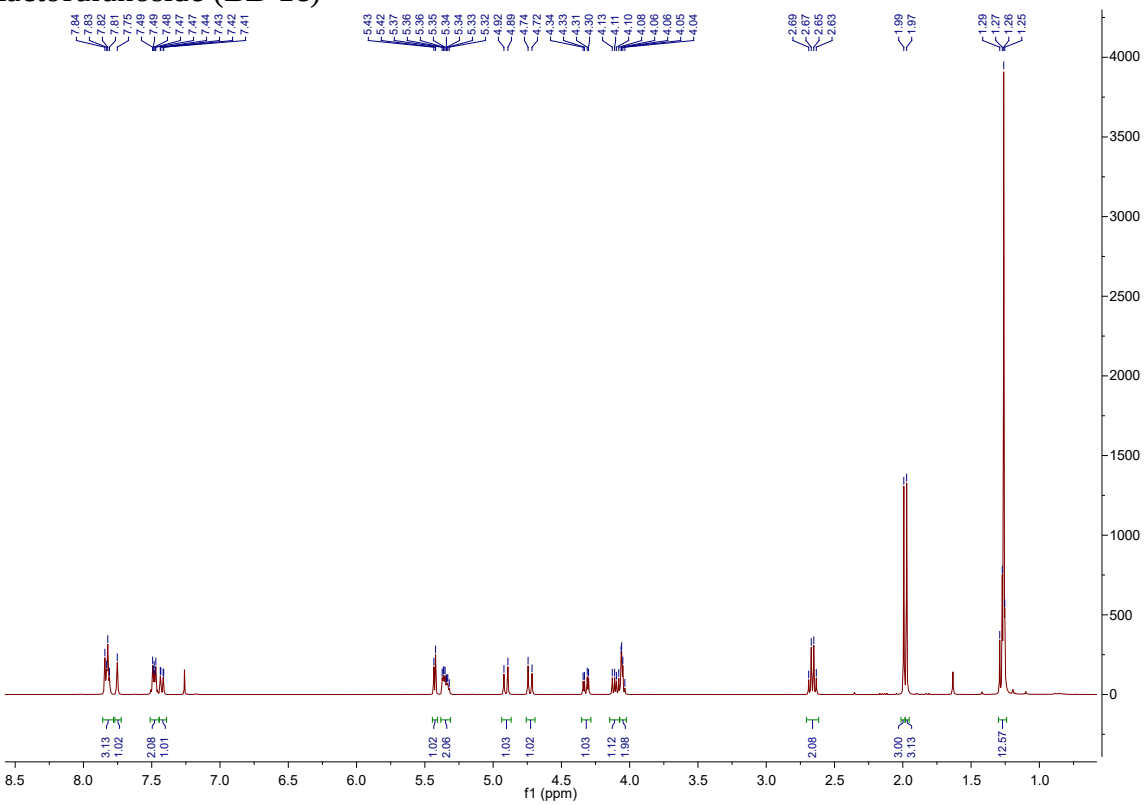

Figure A.78: ^{1}H NMR spectrum of **BB-1e**, in $CDCl_3$.

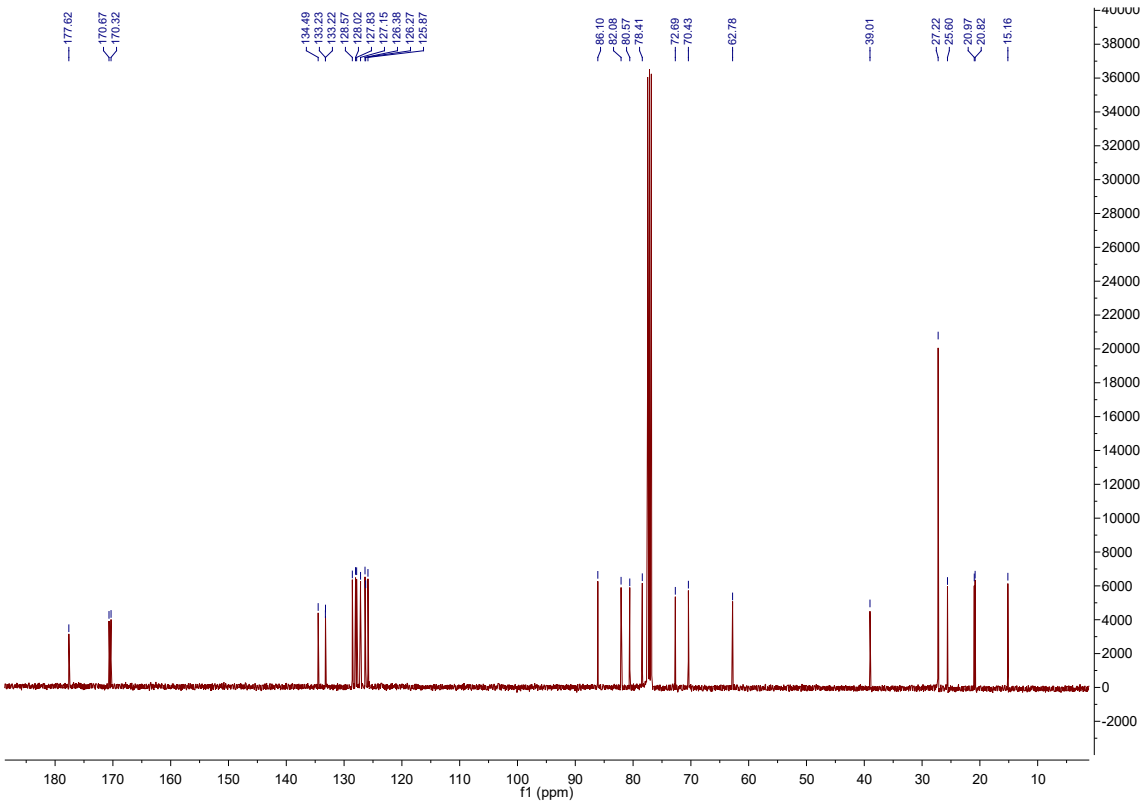

Figure A.79: ^{13}C NMR spectrum of **BB-1e**, in $CDCl_3$.

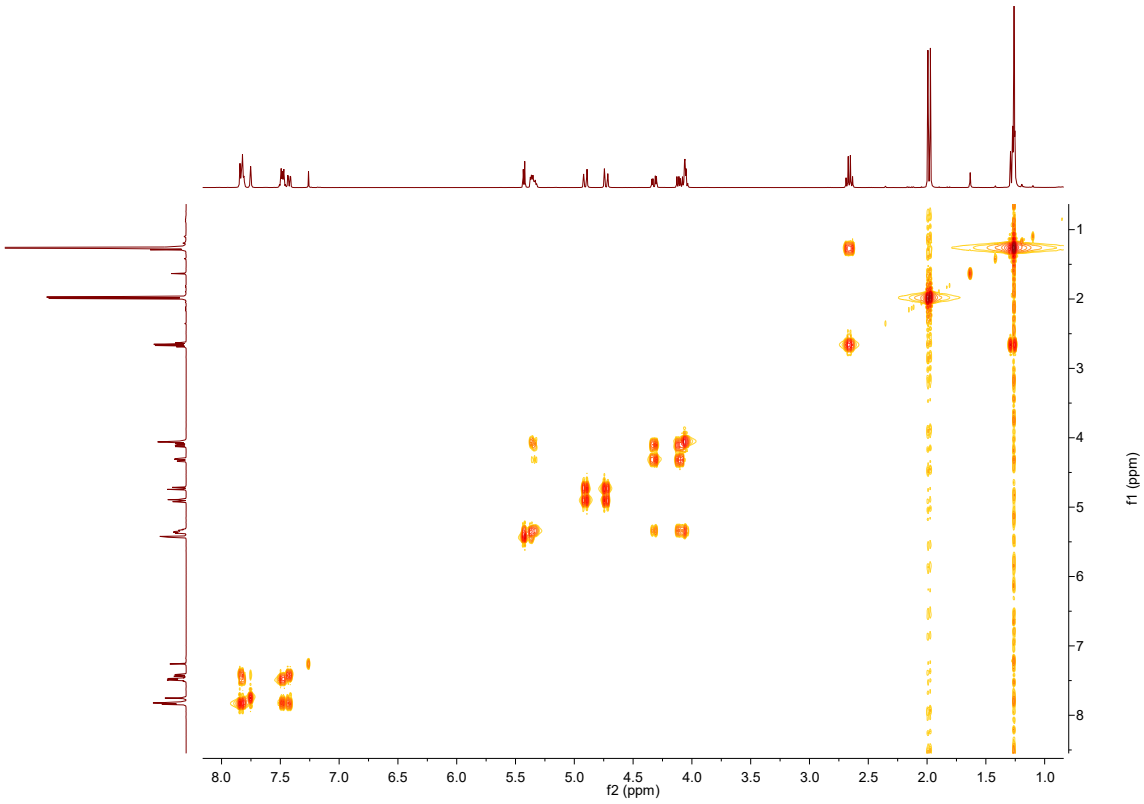

Figure A.80: COSY spectrum of **BB-1e**, in $CDCl_3$.

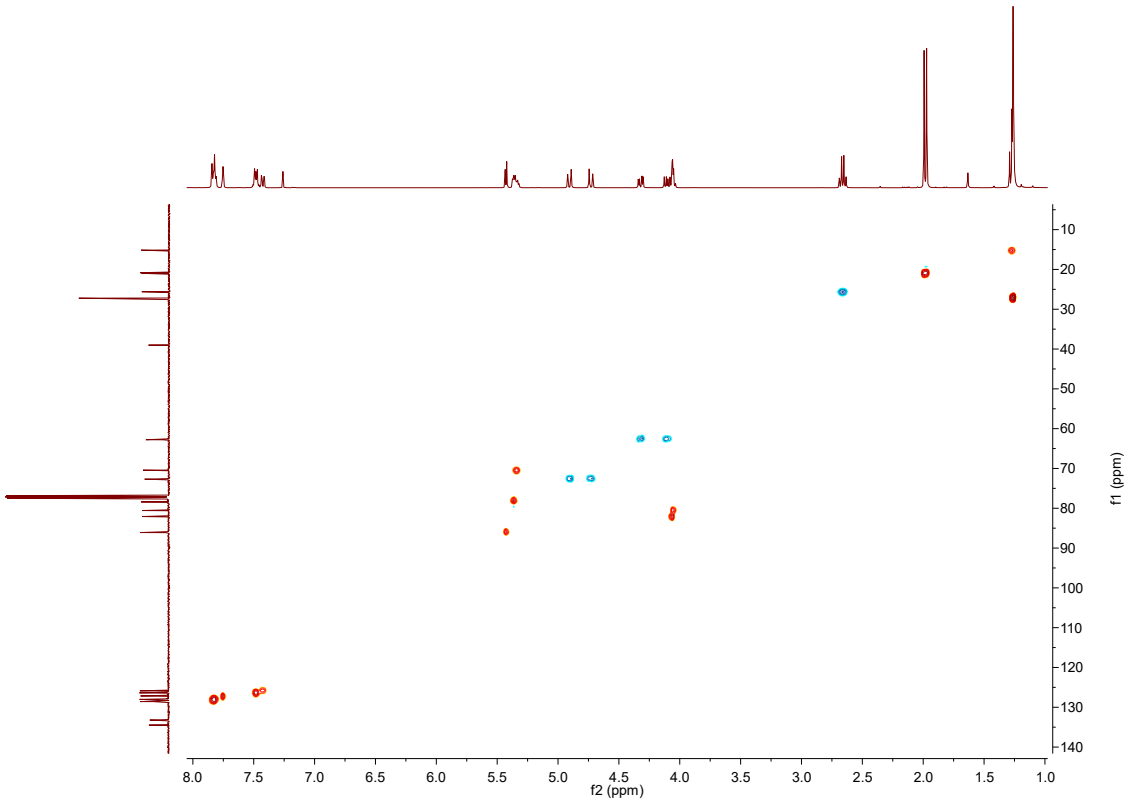

Figure A.81: HSQC spectrum of **BB-1e**, in $CDCl_3$.

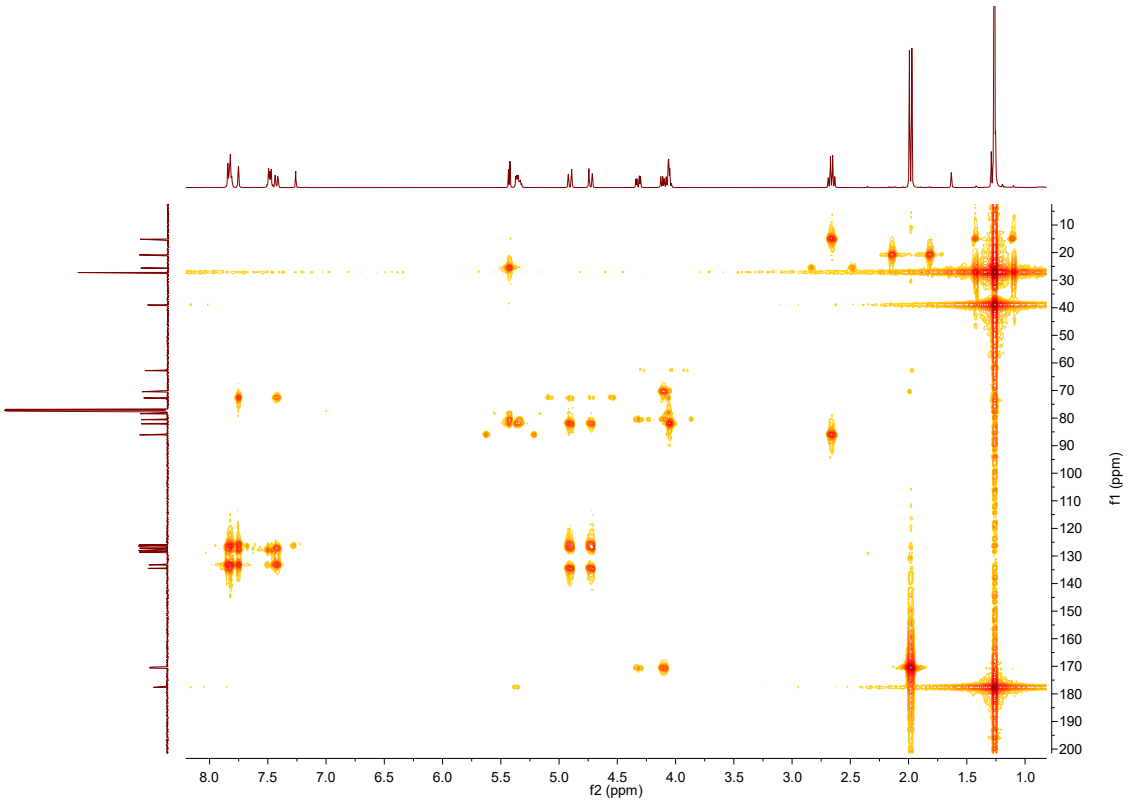

Figure A.82: HMBC spectrum of **BB-1e**, in $CDCl_3$.

A.20. Ethyl 2,3-di-*O*-benzyl-4,6-*O*-benzylidene-1-thio-β-D-galactopyranoside (**14**)

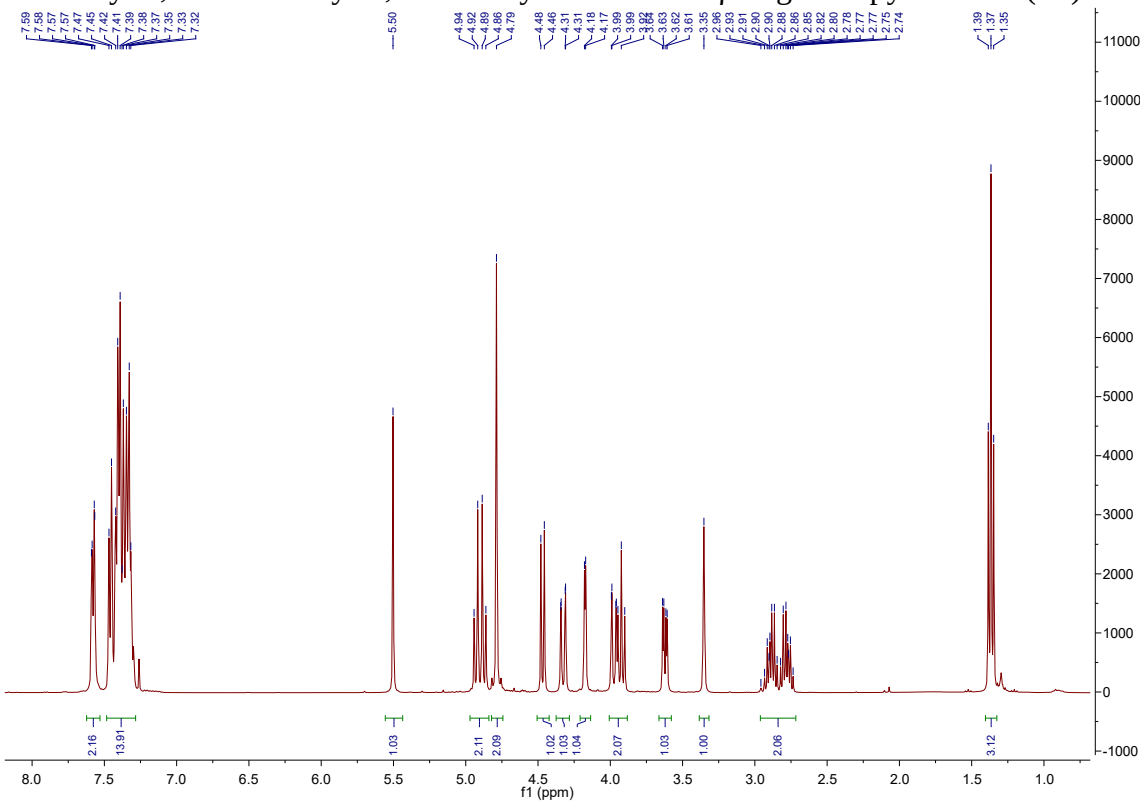

Figure A.83: ^{1}H NMR spectrum of **14**, in $CDCl_3$.

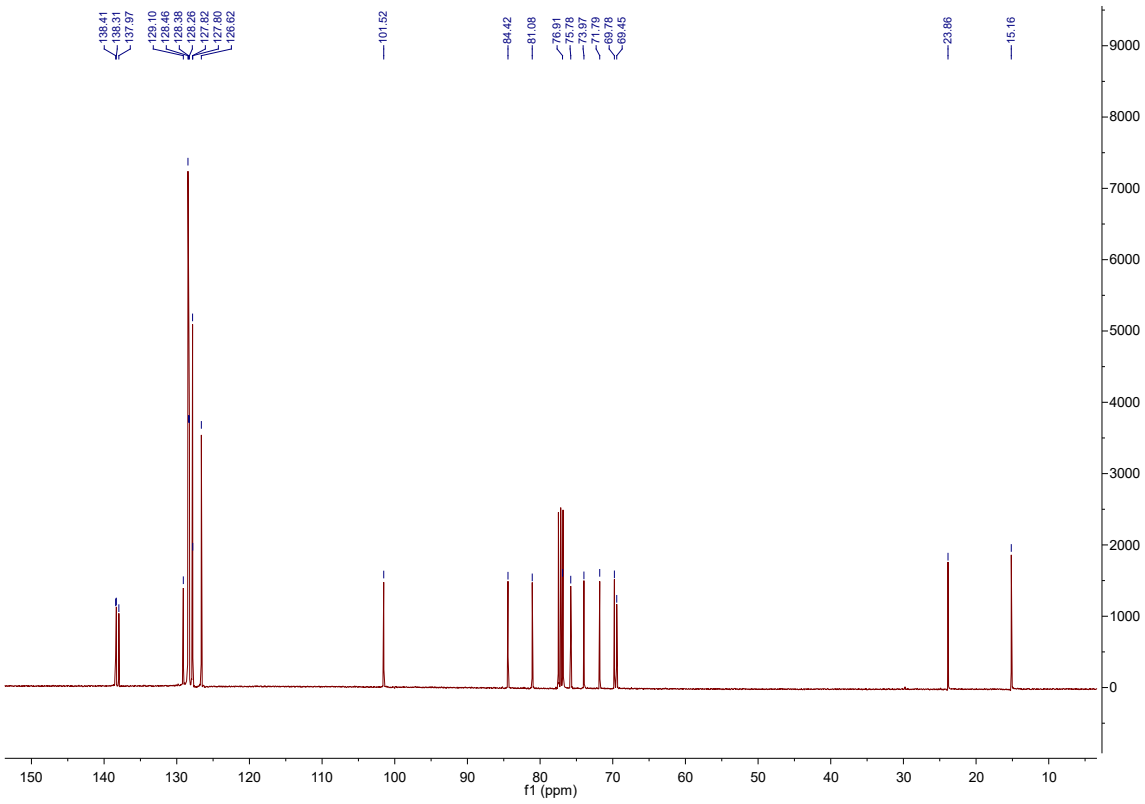

Figure A.84: ^{13}C NMR spectrum of **14**, in $CDCl_3$.

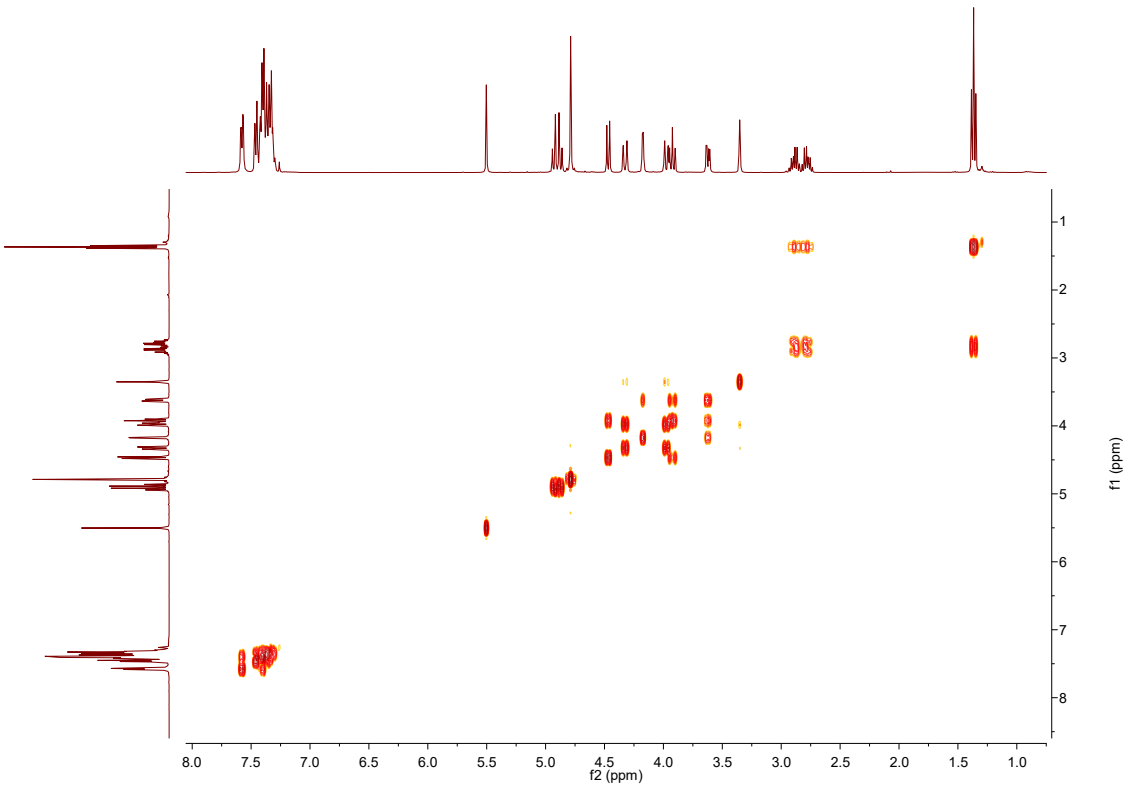

Figure A.85: COSY spectrum of **14**, in $CDCl_3$.

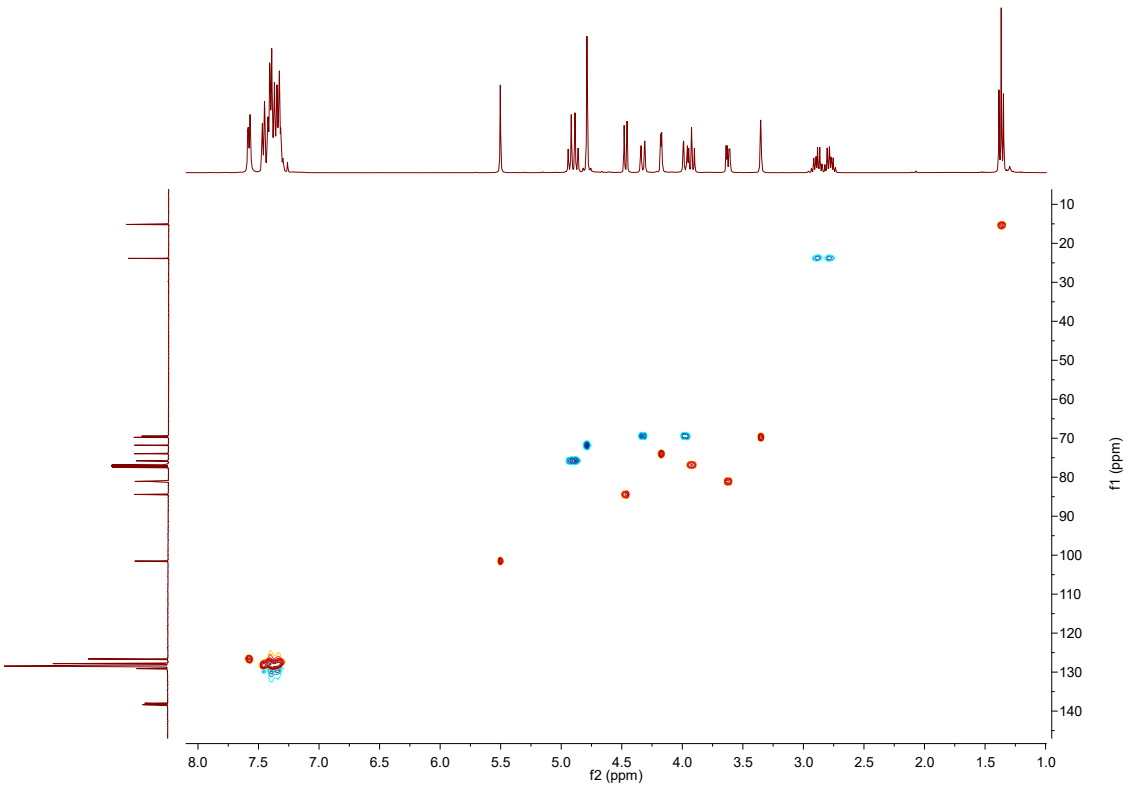

Figure A.86: HSQC spectrum of **14**, in $CDCl_3$.

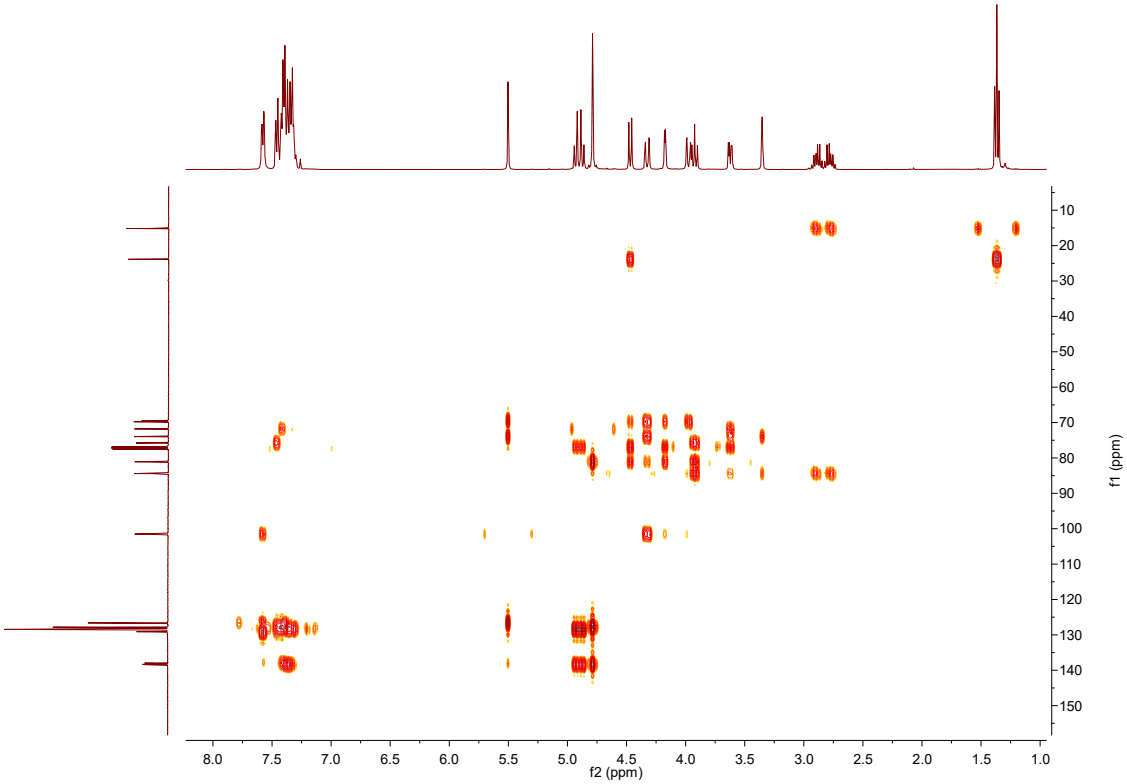

Figure A.87: HMBC spectrum of **14**, in $CDCl_3$.

A.21. Failed oxidative cleavage of **14**

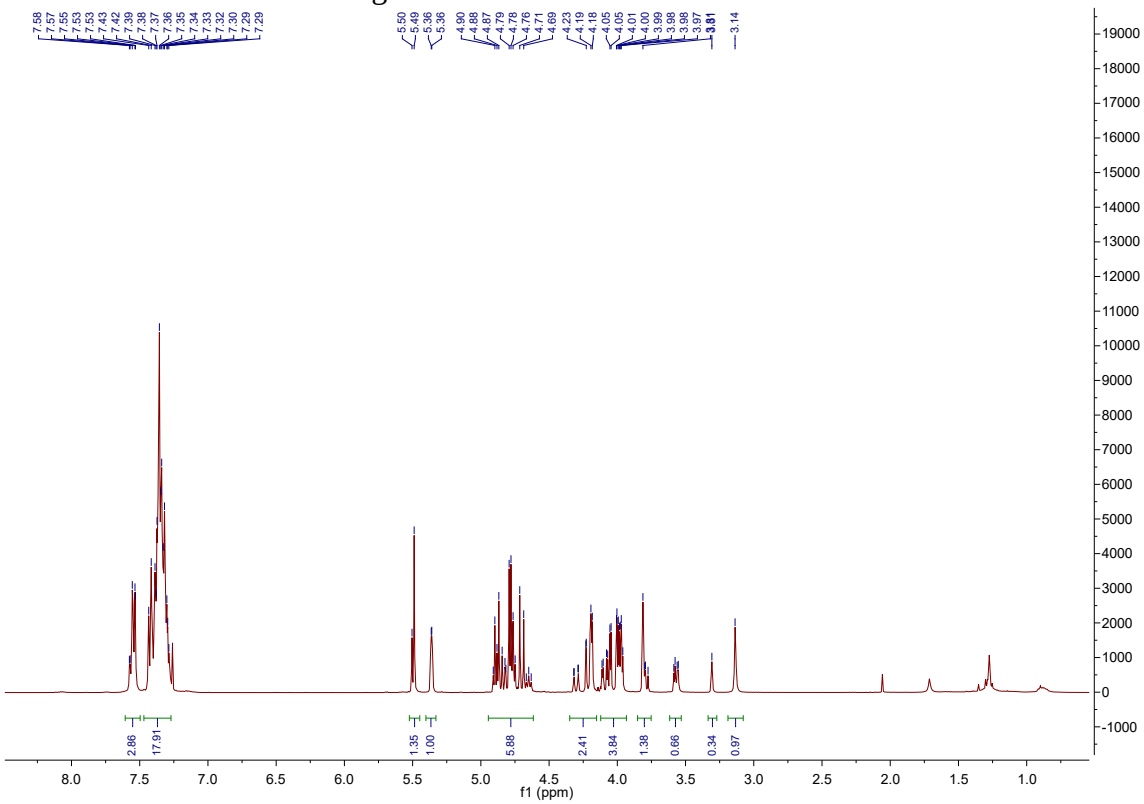

Figure A.88: ^{1}H NMR spectrum of product mixture from oxidative cleavage of **14**, in $CDCl_3$.

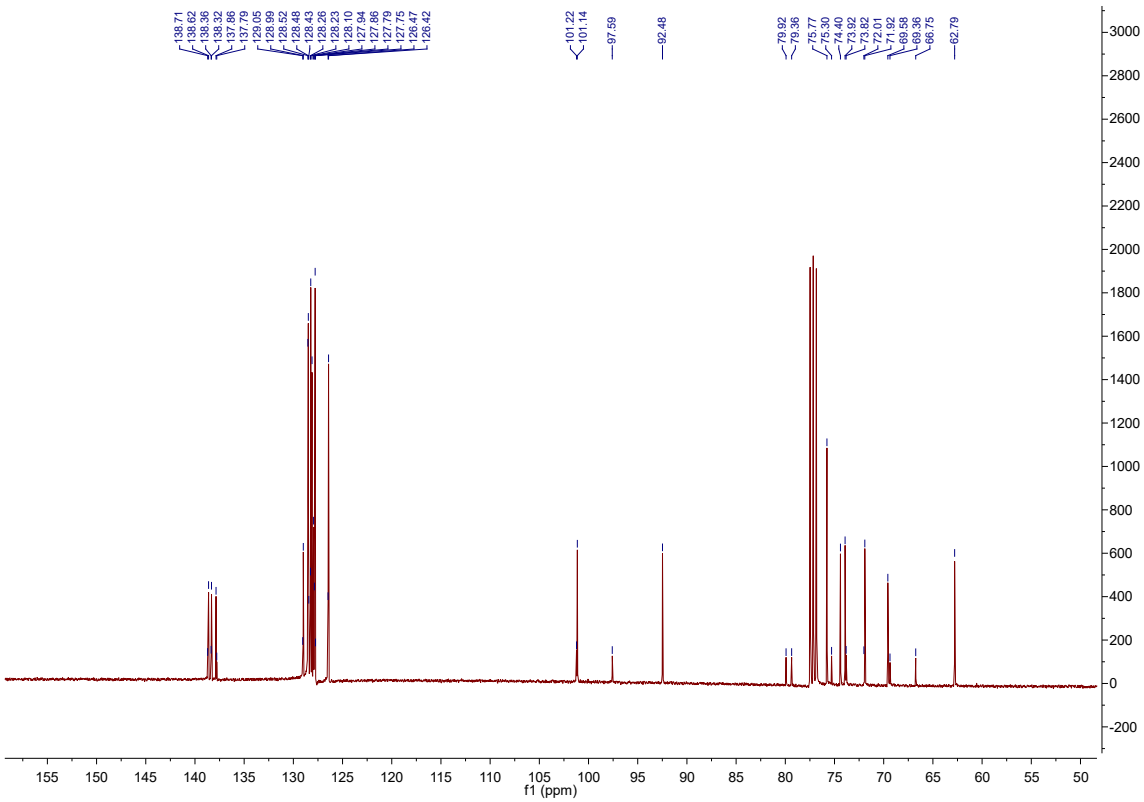

Figure A.89: ^{13}C NMR spectrum of product mixture from oxidative cleavage of **14**, in $CDCl_3$.

A.22. Ethyl 2,3-di-*O*-benzyl-1-thio-β-D-galactopyranoside (**17**)

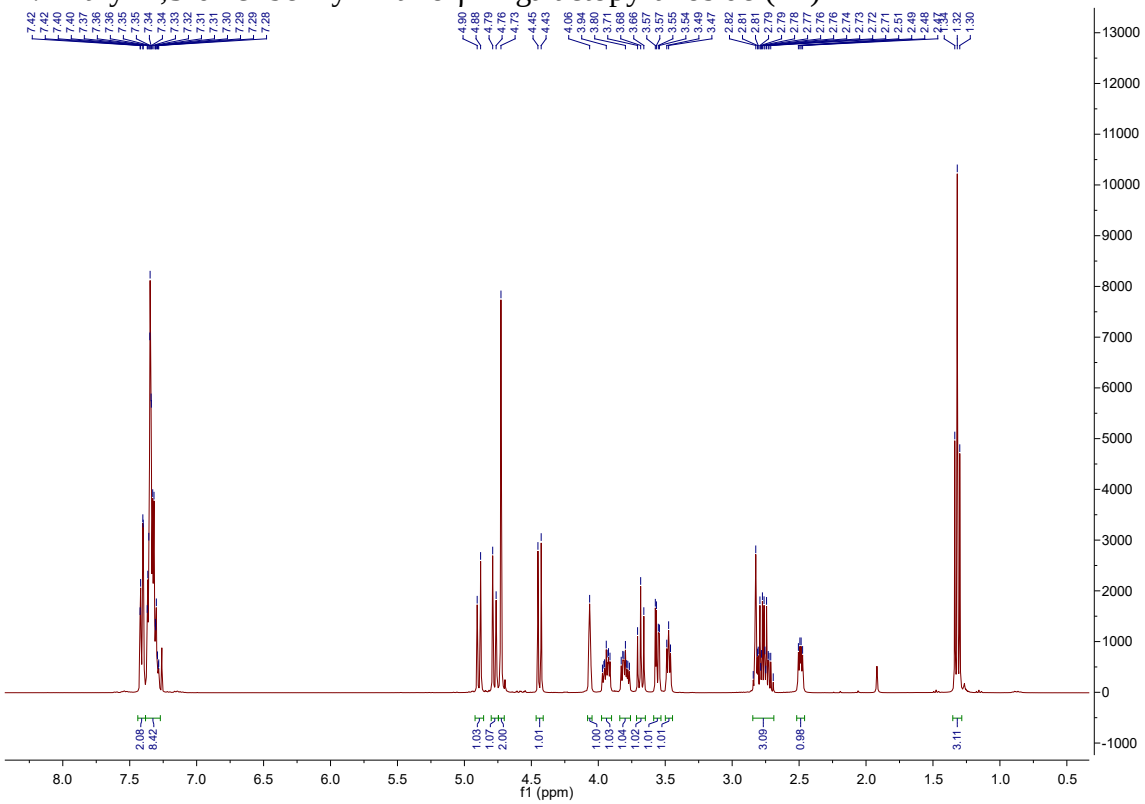

Figure A.90: ^{1}H NMR spectrum of **17**, in $CDCl_3$.

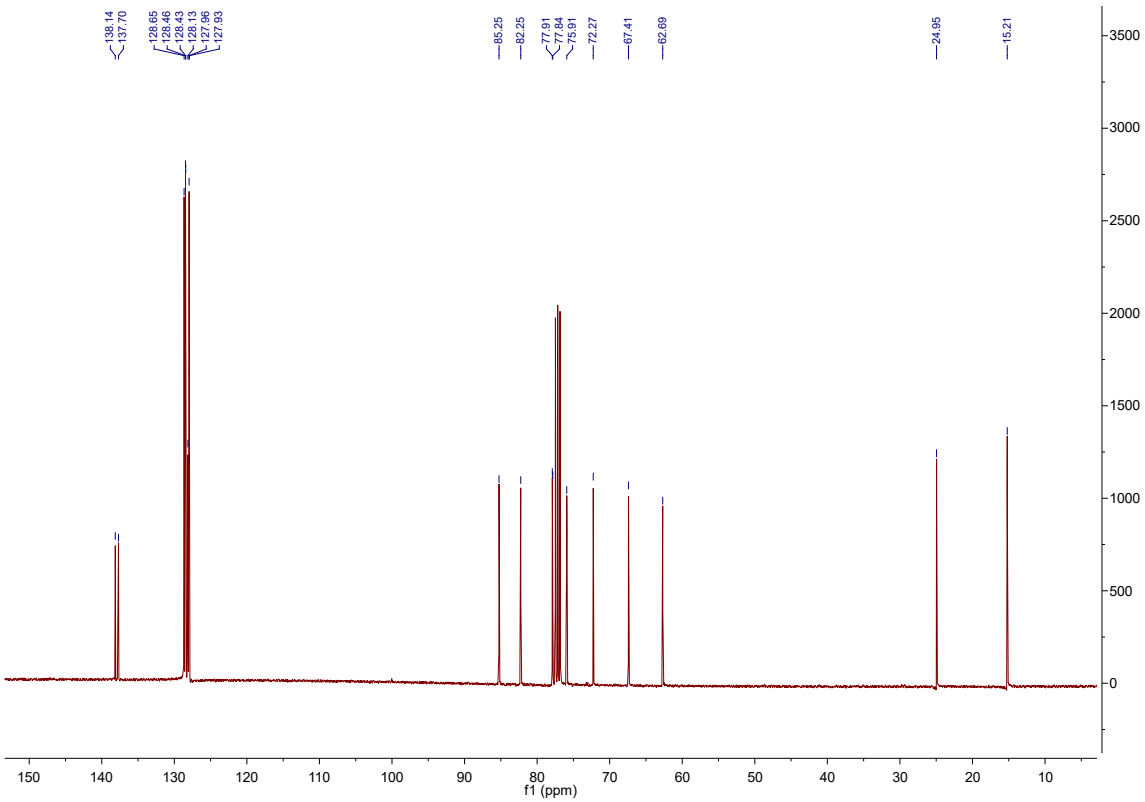

Figure A.91: ^{13}C NMR spectrum of **17**, in $CDCl_3$.

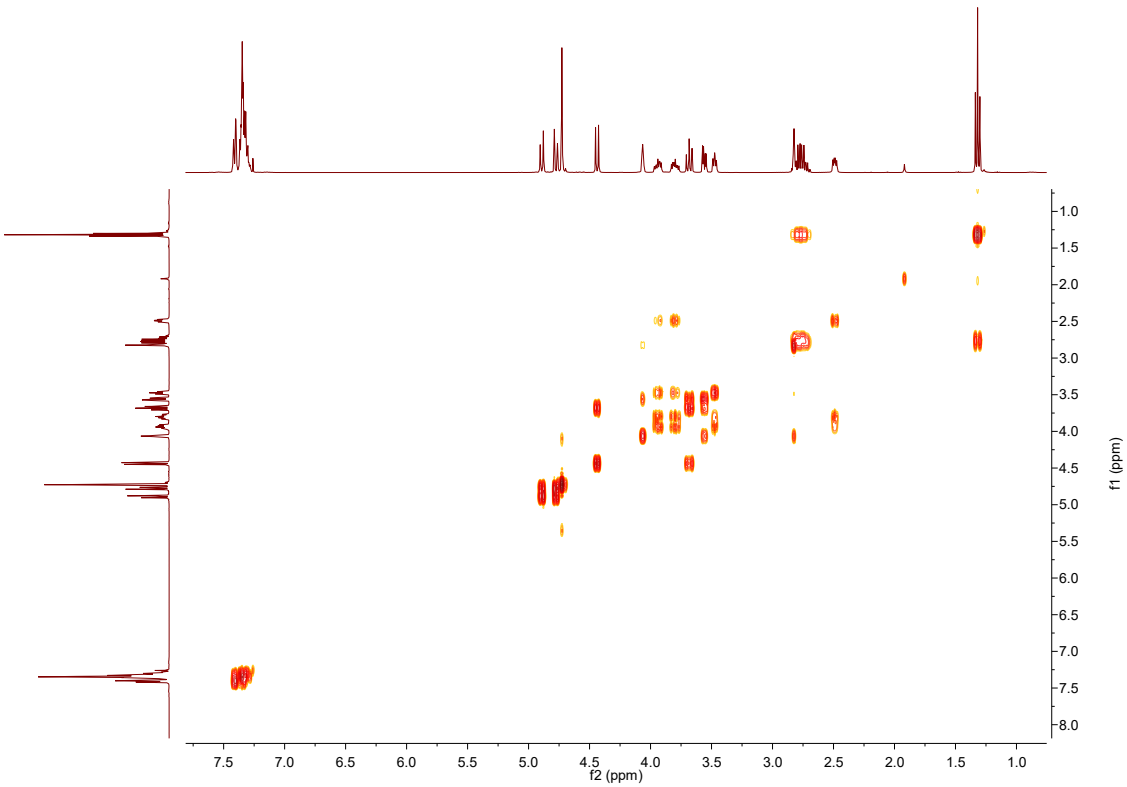

Figure A.92: COSY spectrum of **17**, in $CDCl_3$.

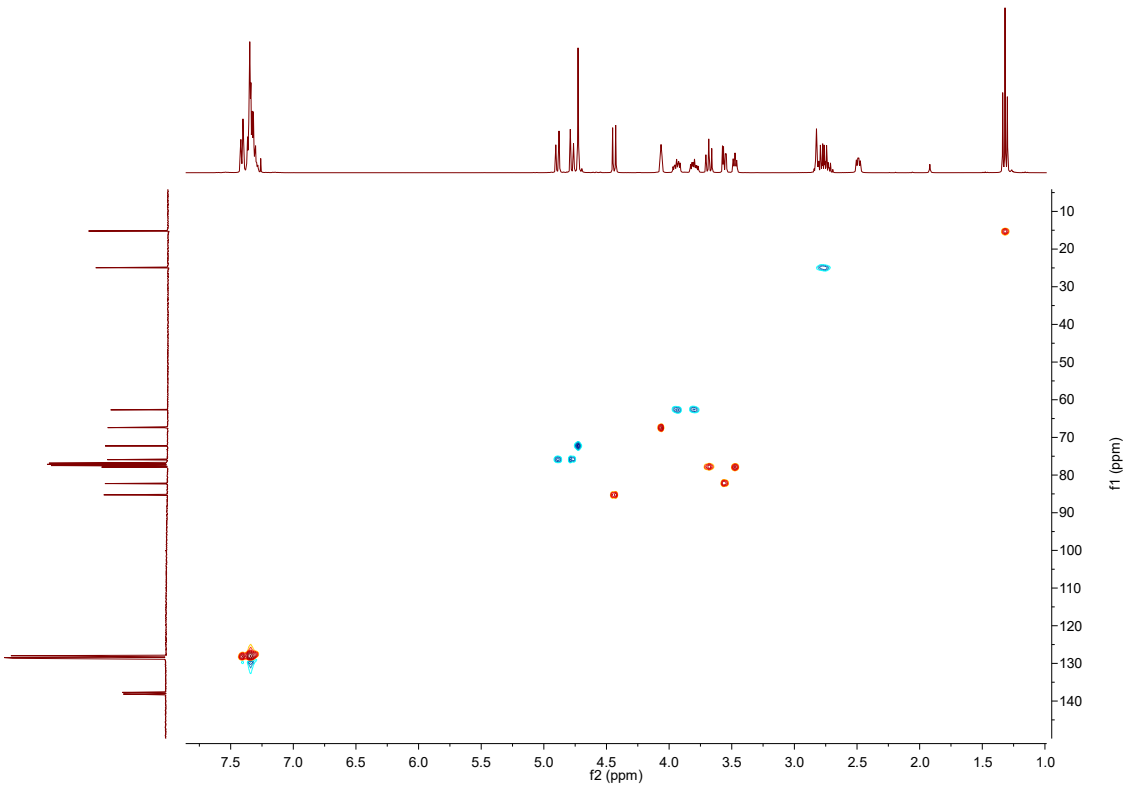

Figure A.93: HSQC spectrum of **17**, in $CDCl_3$.

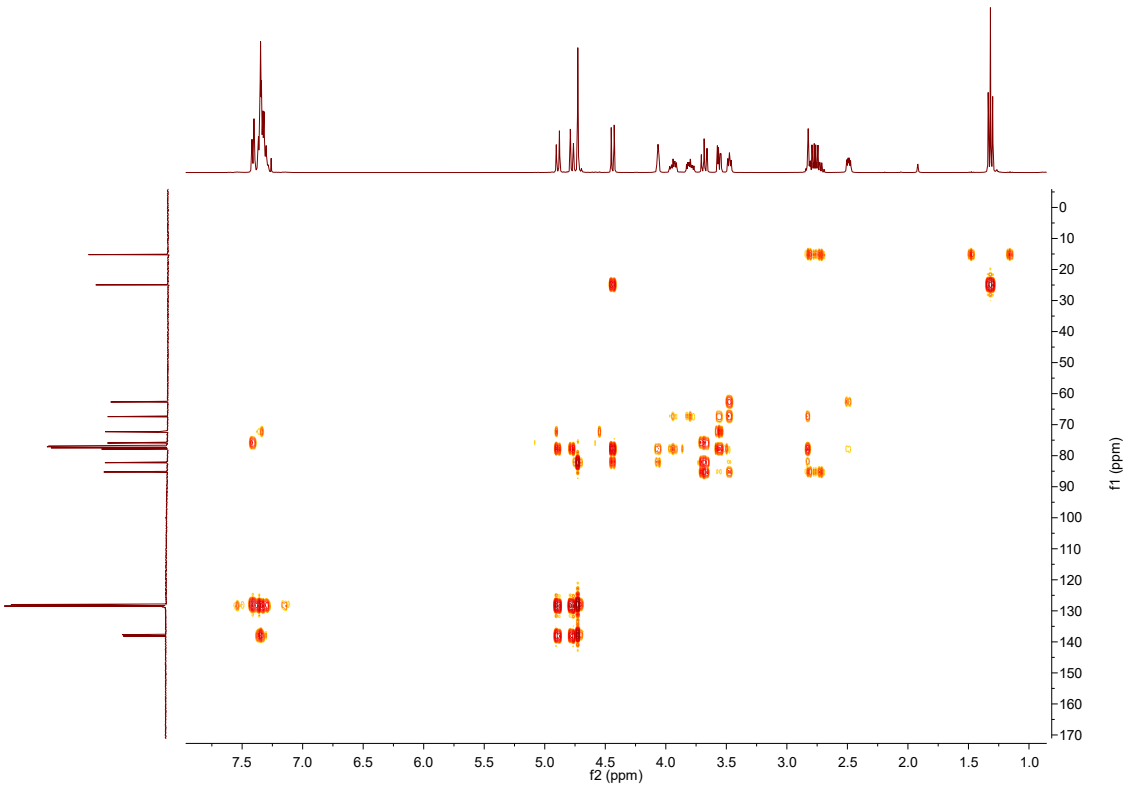

Figure A.94: HMBC spectrum of **17**, in $CDCl_3$.

A.23. Ethyl 2,3-di-*O*-benzyl-6-*O*-levulinoyl-1-thio-β-D-galactopyranoside (**18a**)

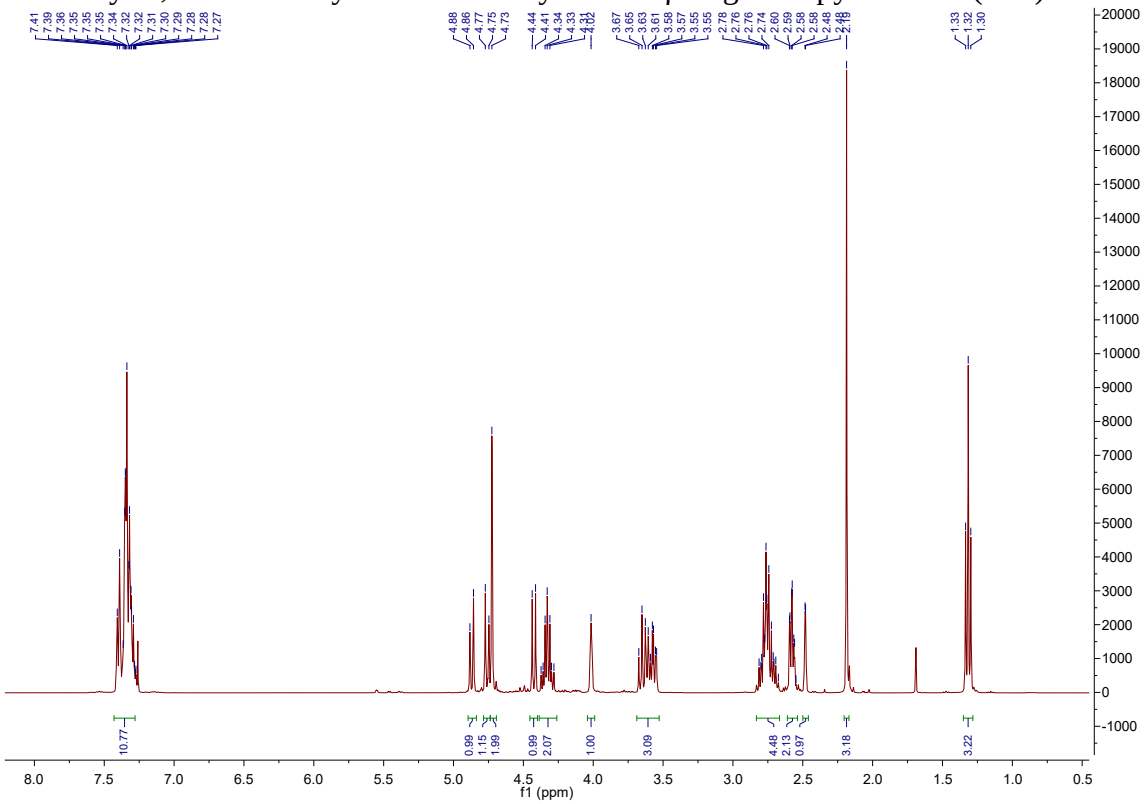

Figure A.95: ^{1}H NMR spectrum of **18a**, in $CDCl_3$.

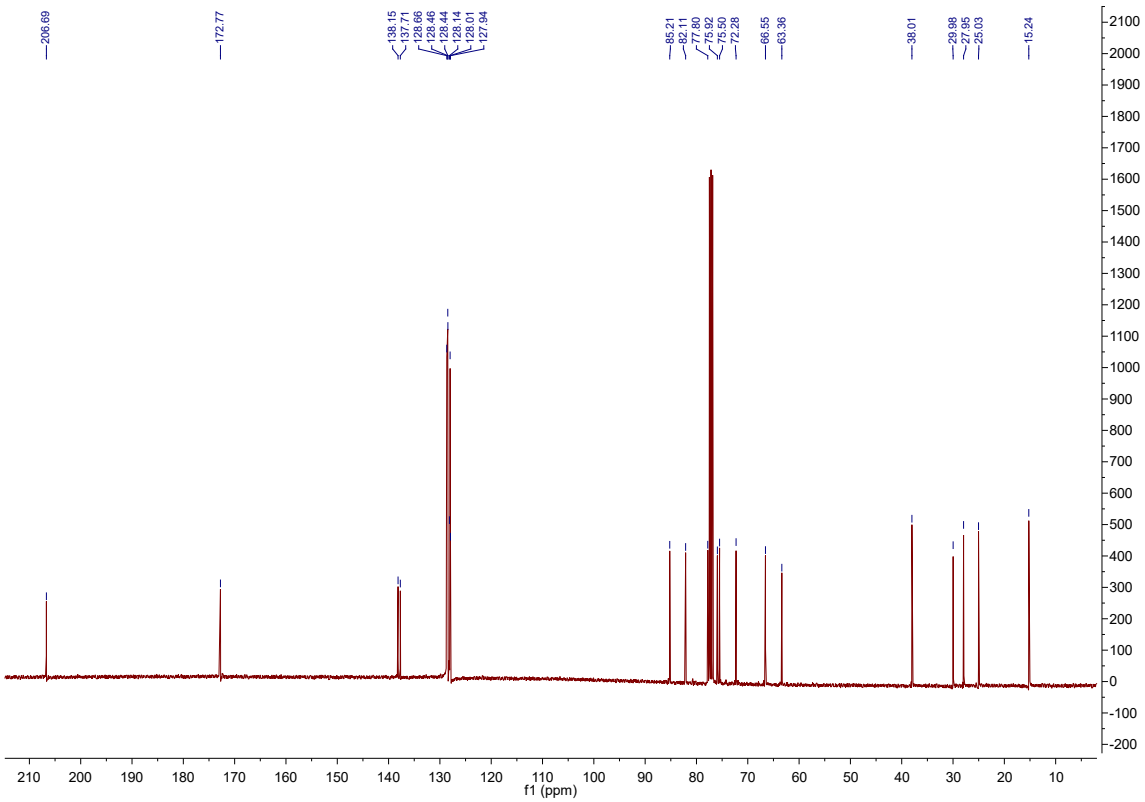

Figure A.96: ^{13}C NMR spectrum of **18a**, in $CDCl_3$.

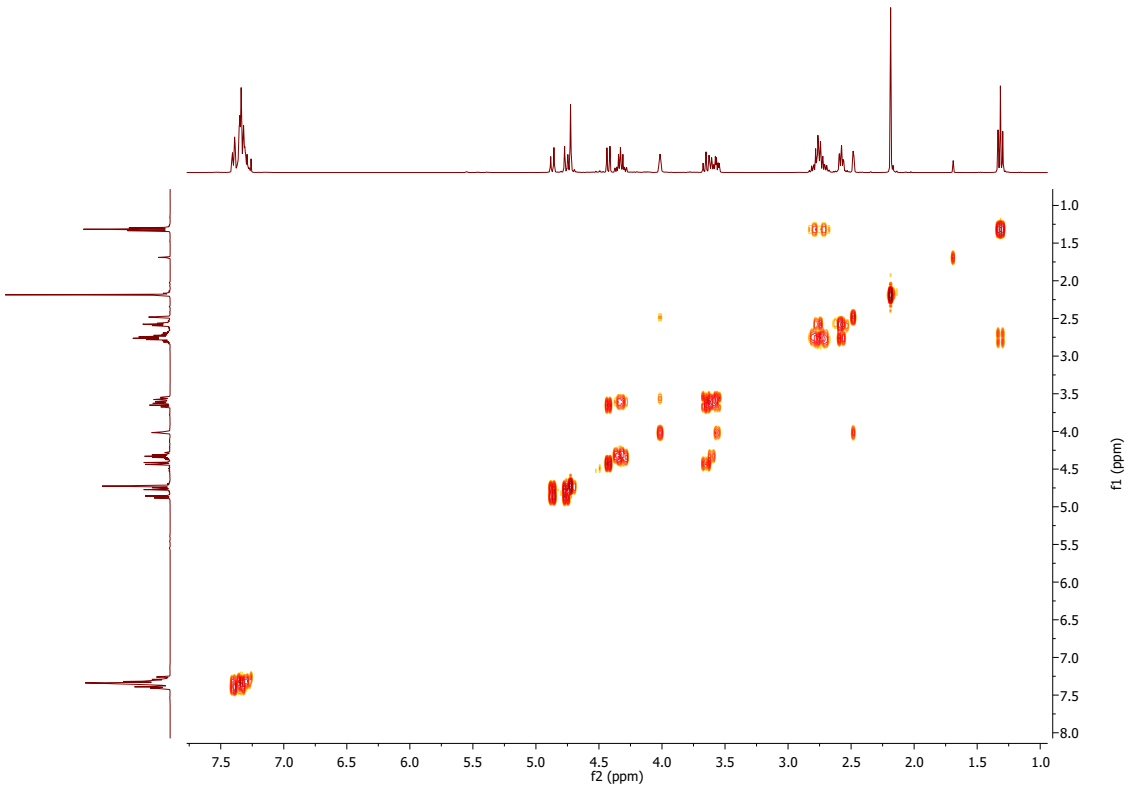

Figure A.97: COSY spectrum of **18a**, in $CDCl_3$.

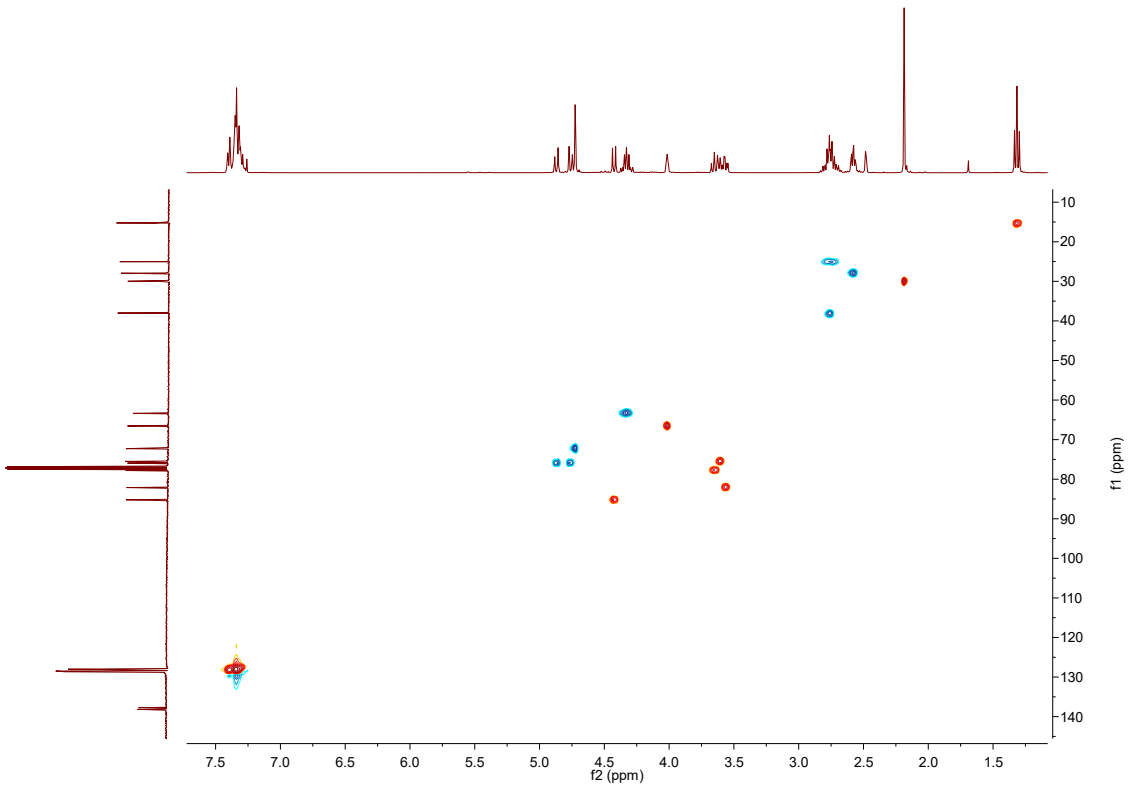

Figure A.98: HSQC spectrum of **18a**, in $CDCl_3$.

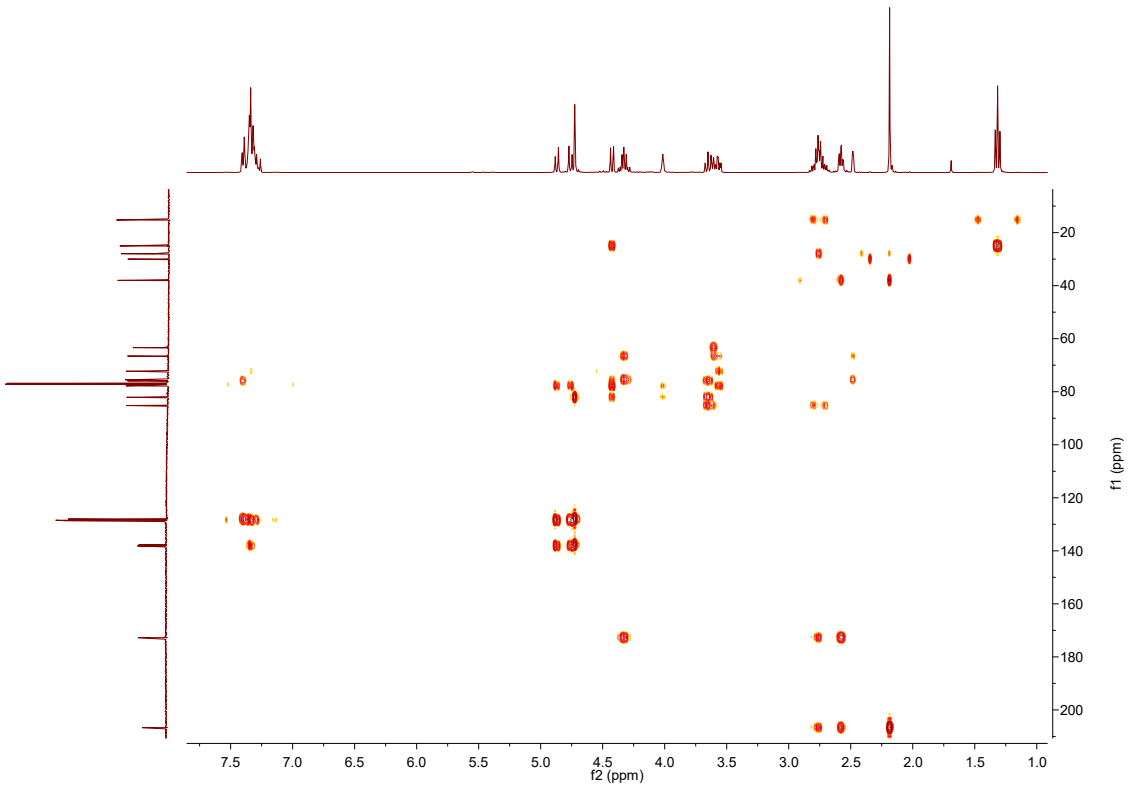

Figure A.99: HMBC spectrum of **18a**, in $CDCl_3$.

A.24. Ethyl 4-*O*-benzoyl-2,3-di-*O*-benzyl-6-*O*-levulinoyl-1-thio-β-D-galactopyranoside (**BB-2**)

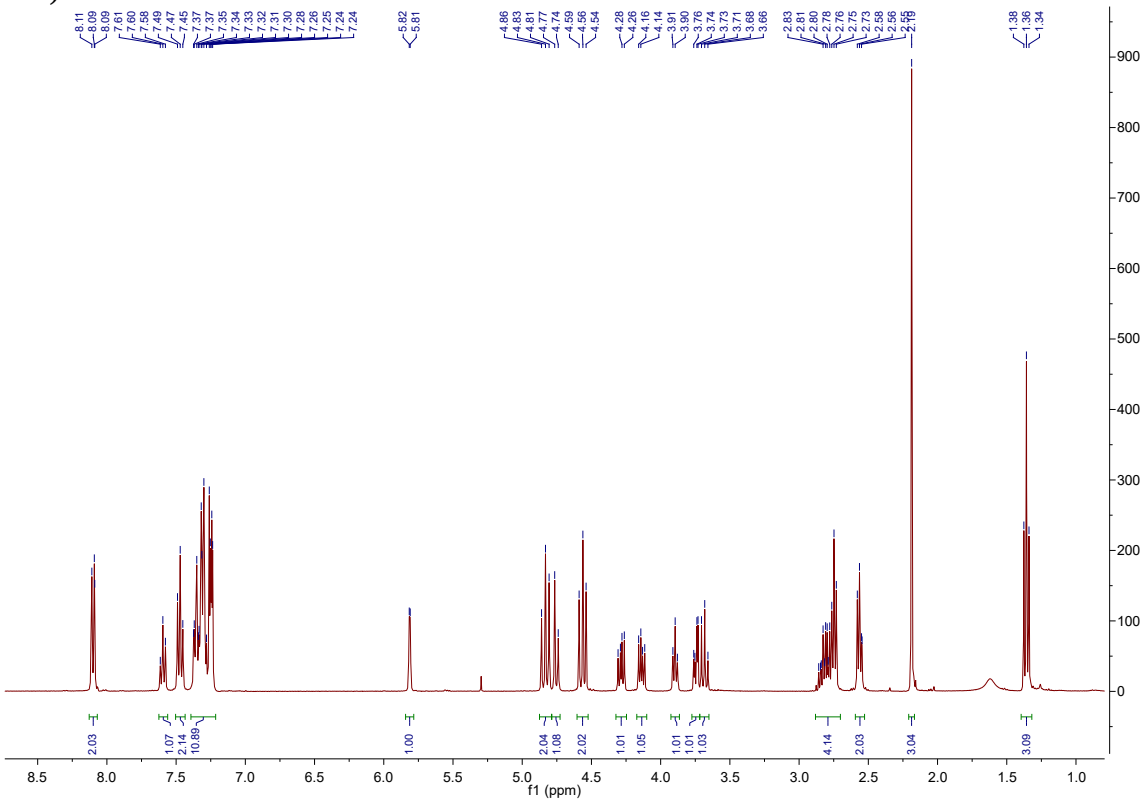

Figure A.100: ^{1}H NMR spectrum of **BB-2**, in $CDCl_3$.

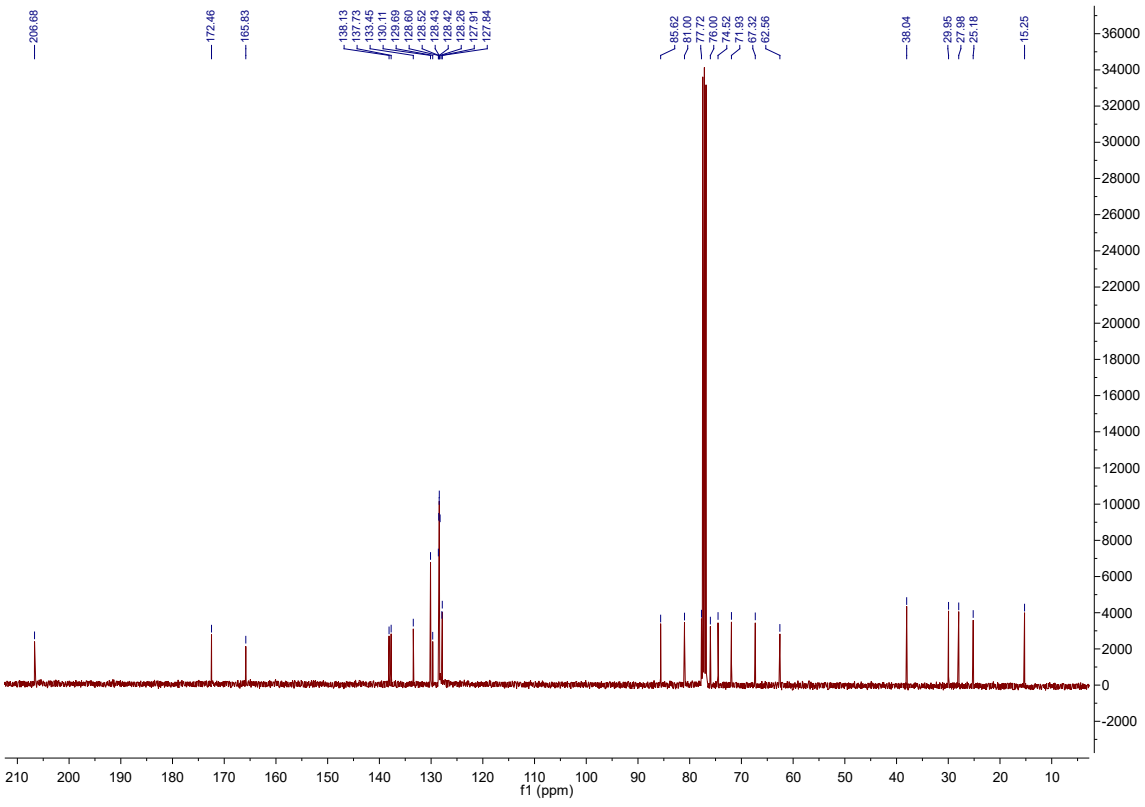

Figure A.101: ^{13}C NMR spectrum of **BB-2**, in $CDCl_3$.

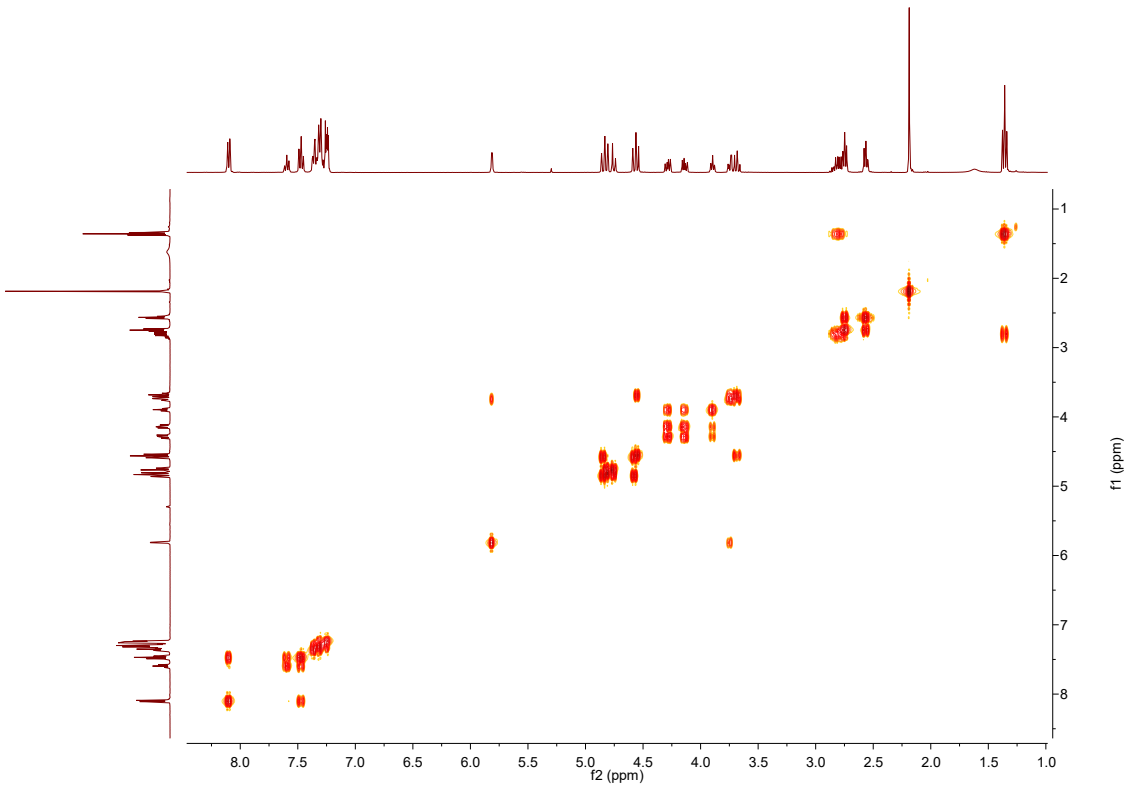

Figure A.102: COSY spectrum of **BB-2**, in $CDCl_3$.

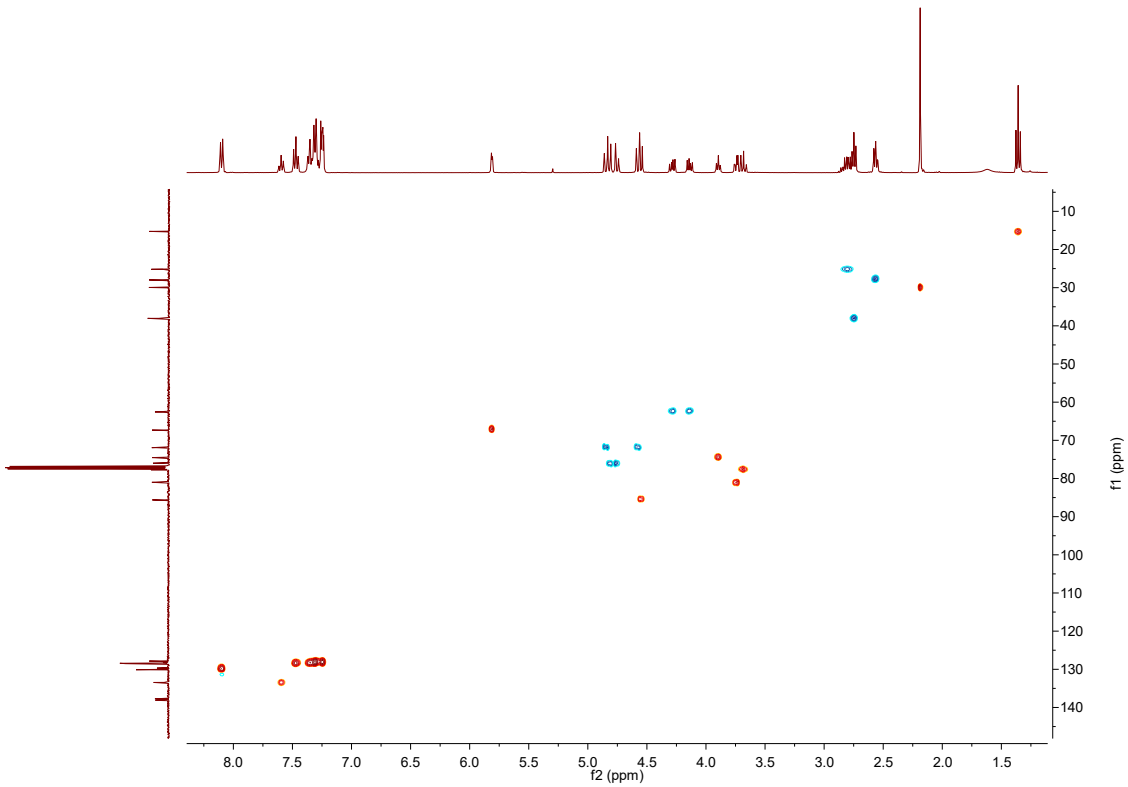

Figure A.103: HSQC spectrum of **BB-2**, in $CDCl_3$.

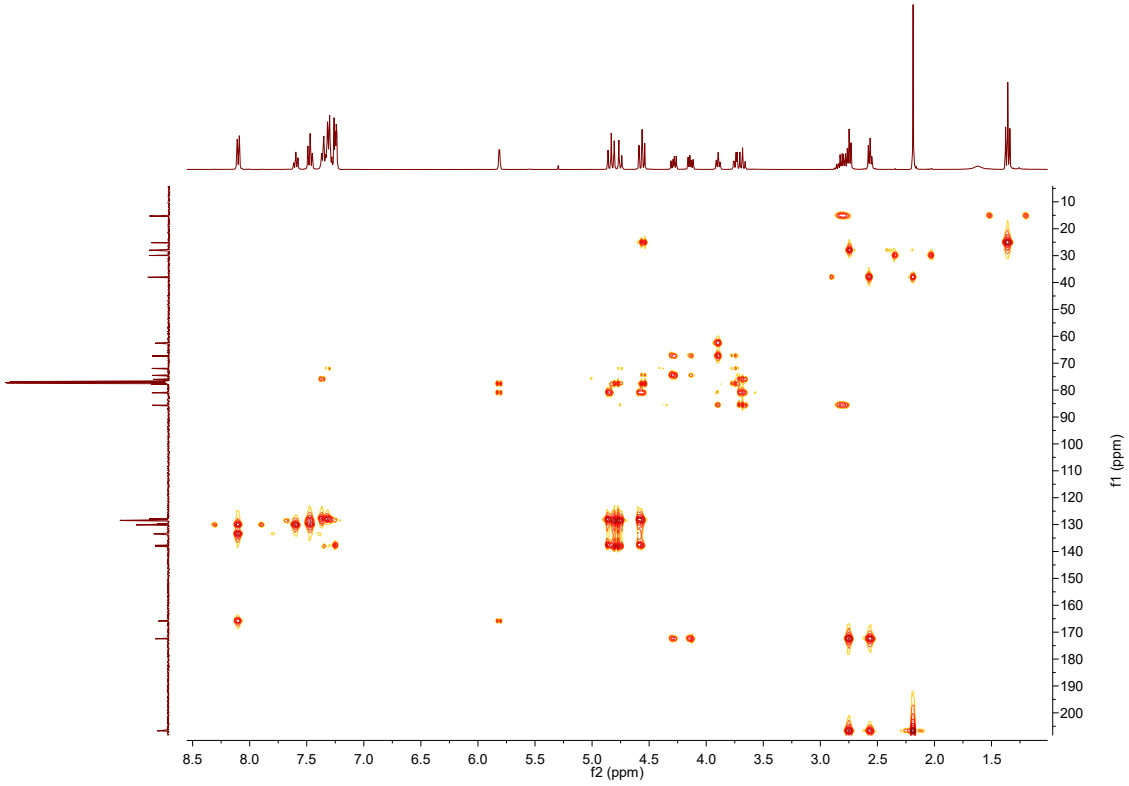

Figure A.104: HMBC spectrum of **BB-2**, in $CDCl_3$.

A.25. Contaminated Ethyl 4,6-*O*-benzylidene-3-*O*-(2-naphtylmethyl)-1-thio-α-D-mannopyranoside (**20**)

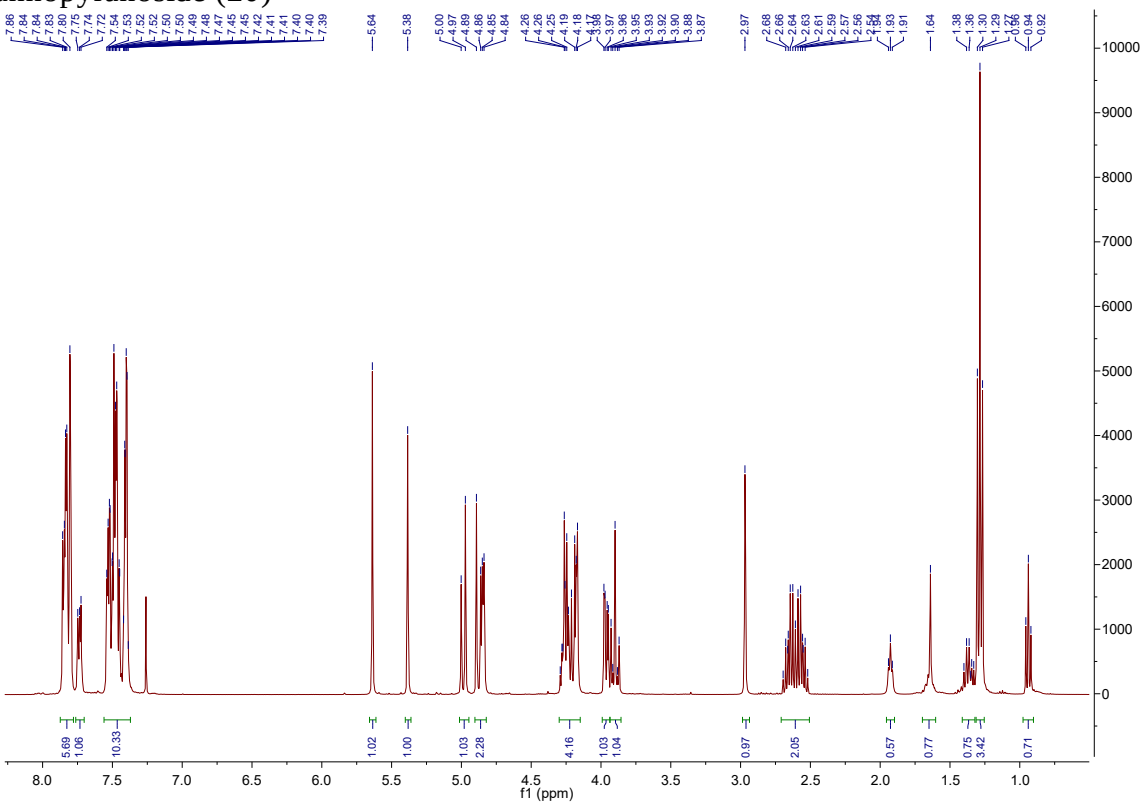

Figure A.105: ^{1}H NMR spectrum of contaminated **20**, in $CDCl_3$.

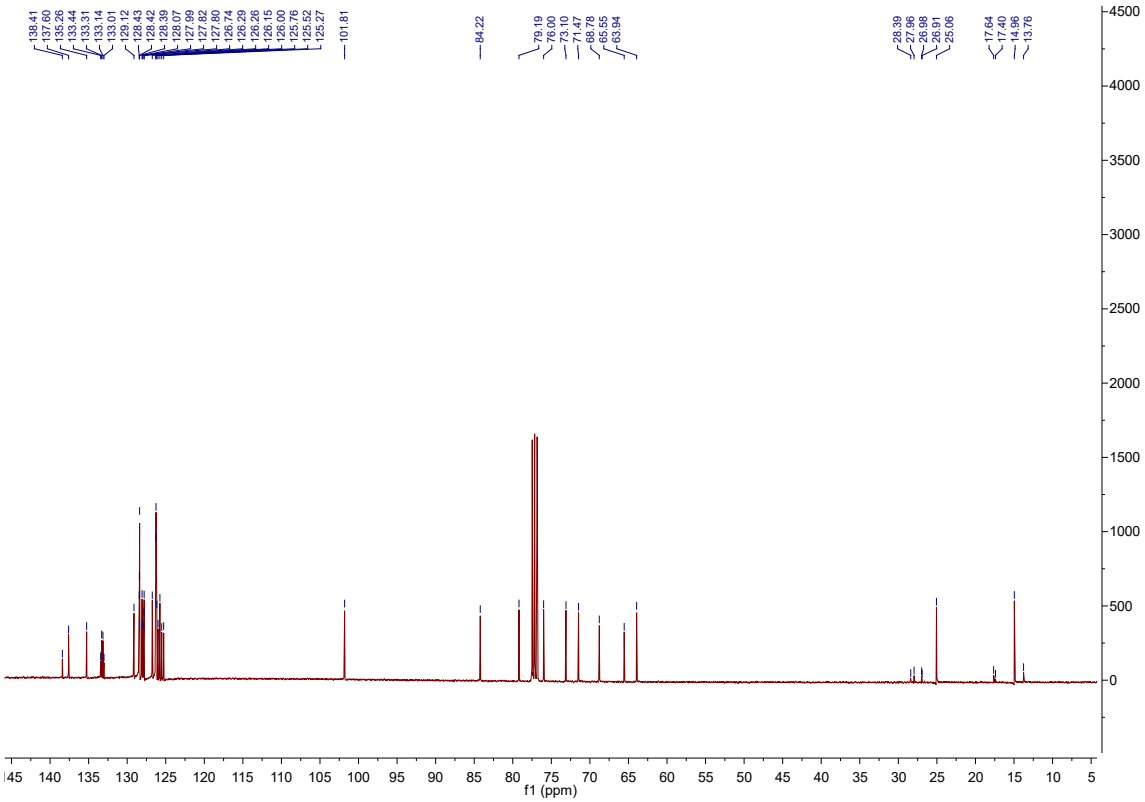

Figure A.106: ^{13}C spectrum of contaminated **20**, in $CDCl_3$.

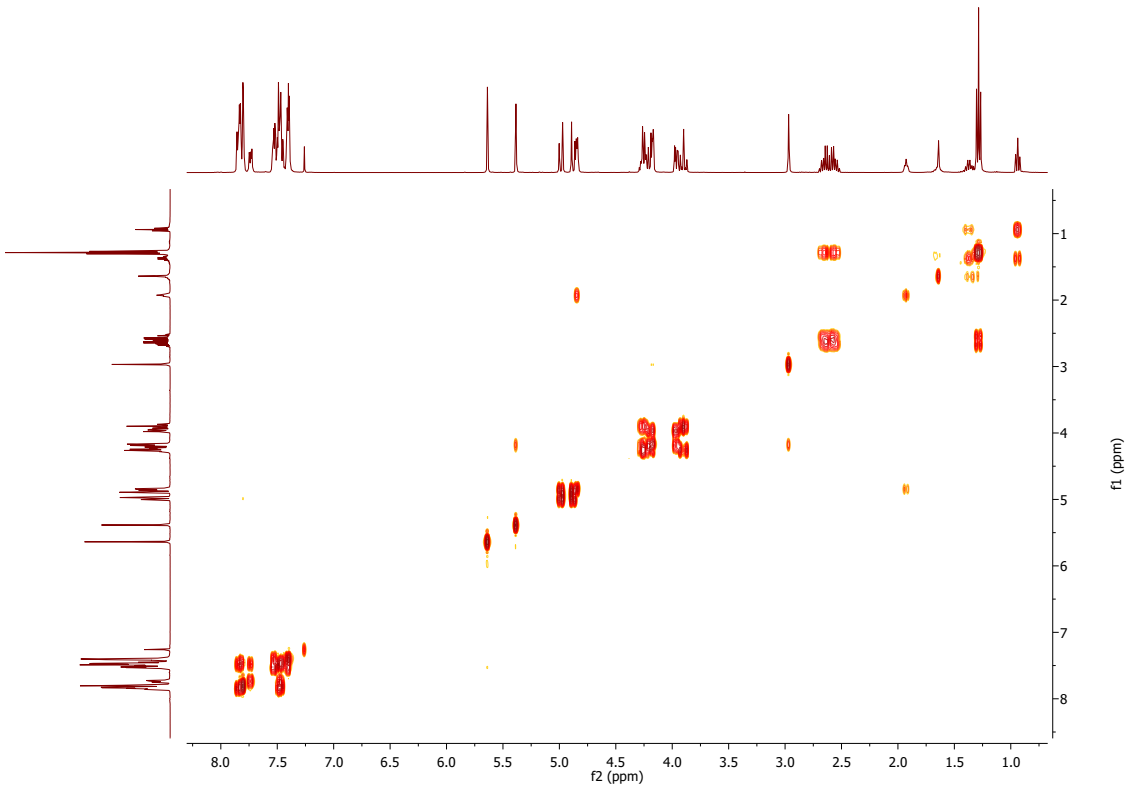

Figure A.107: COSY spectrum of contaminated **20**, in $CDCl_3$.

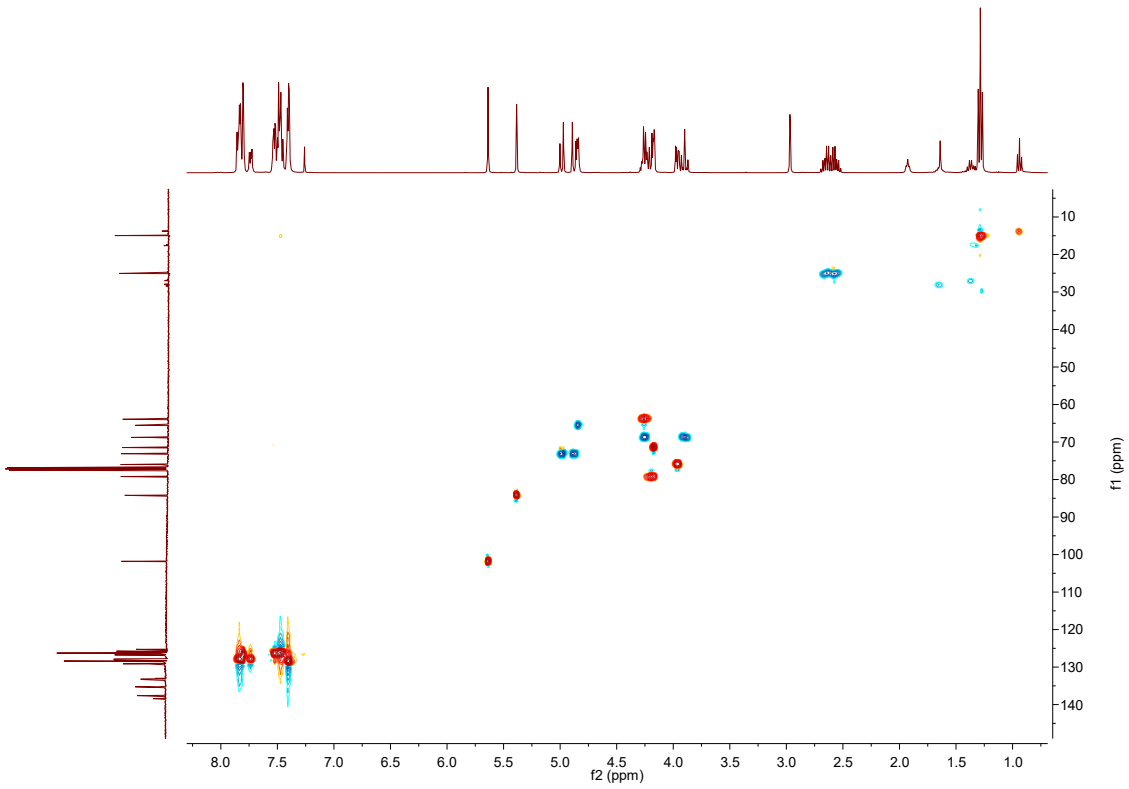

Figure A.108: HSQC spectrum of contaminated **20**, in $CDCl_3$.

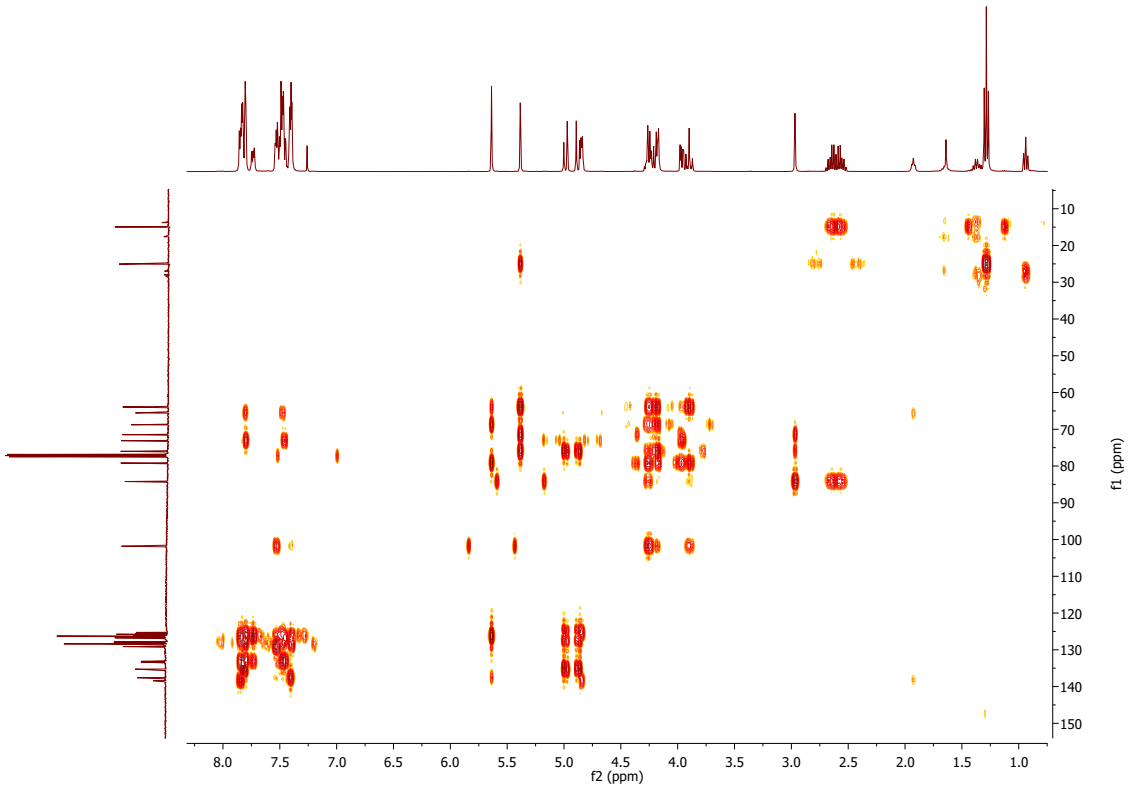

Figure A.109: HMBC spectrum of contaminated **20**, in $CDCl_3$.

A.26. Ethyl 2-O-benzoyl-4,6-O-benzylidene-3-O-(2-naphtylmethyl)-1-thio-α-D-mannopyranoside (21)

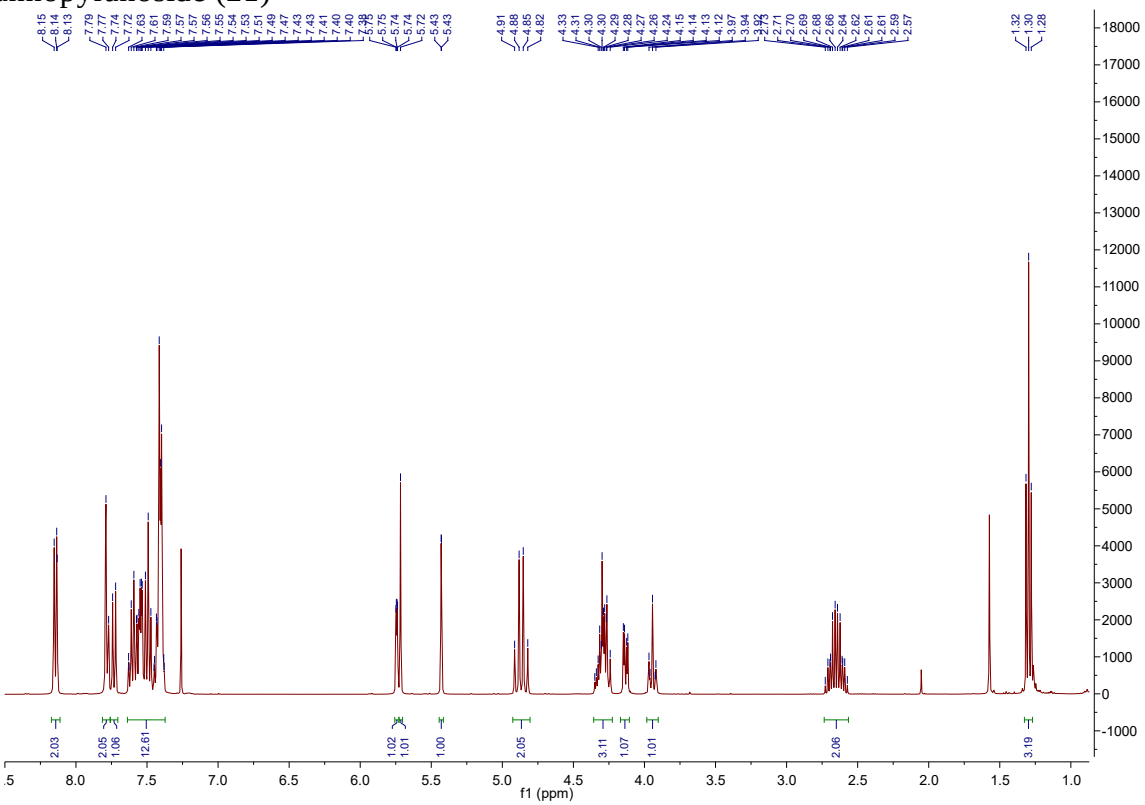

Figure A.110: ^{1}H NMR spectrum of **21**, in $CDCl_3$.

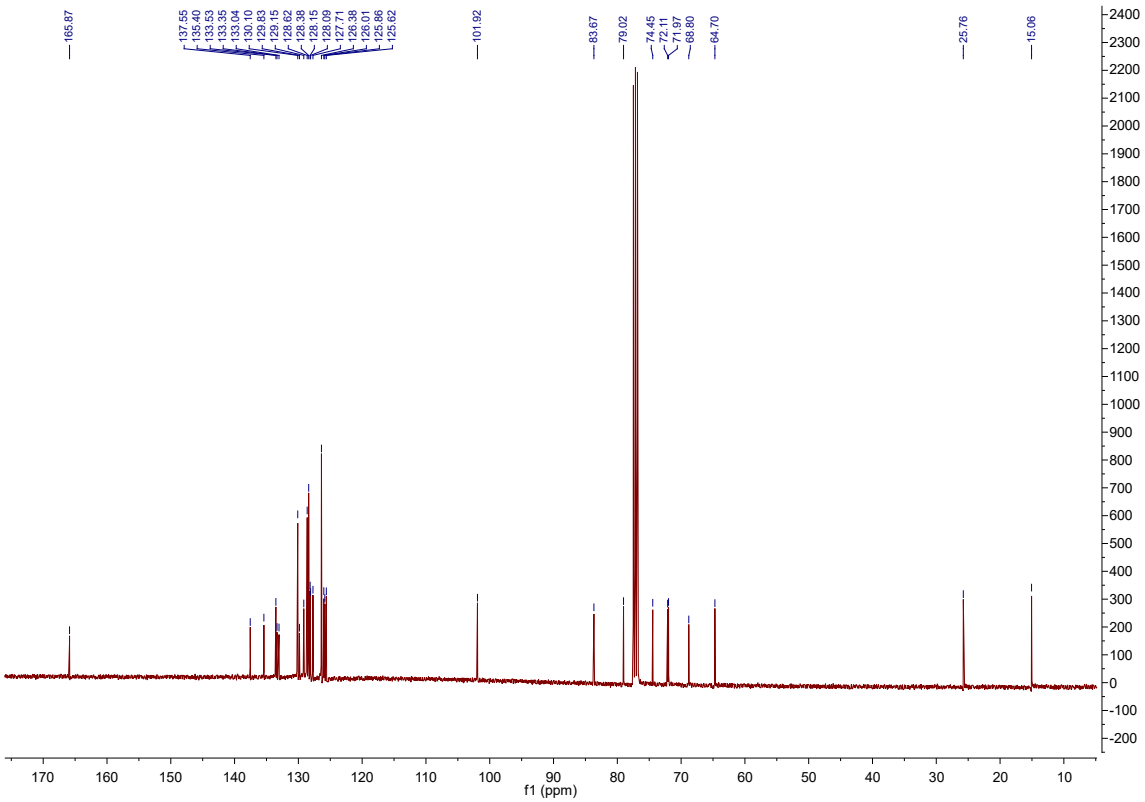

Figure A.111: ^{13}C NMR spectrum of **21**, in $CDCl_3$.

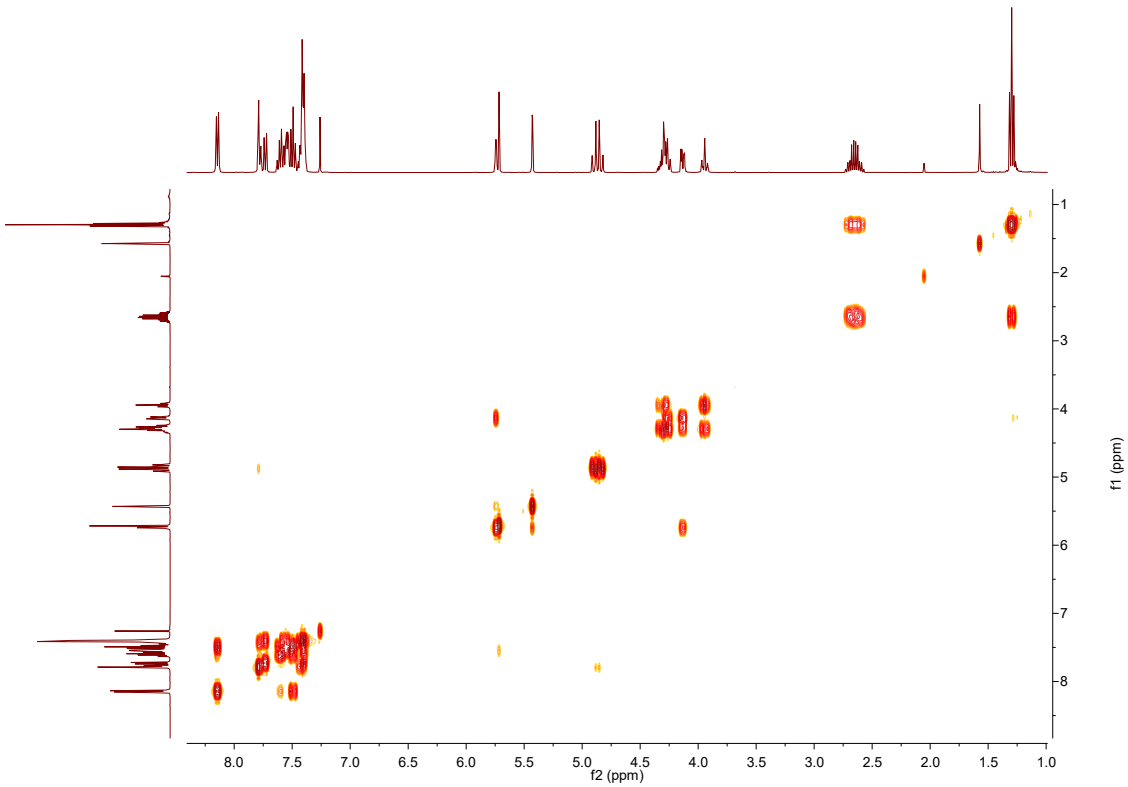

Figure A.112: COSY spectrum of **21**, in $CDCl_3$.

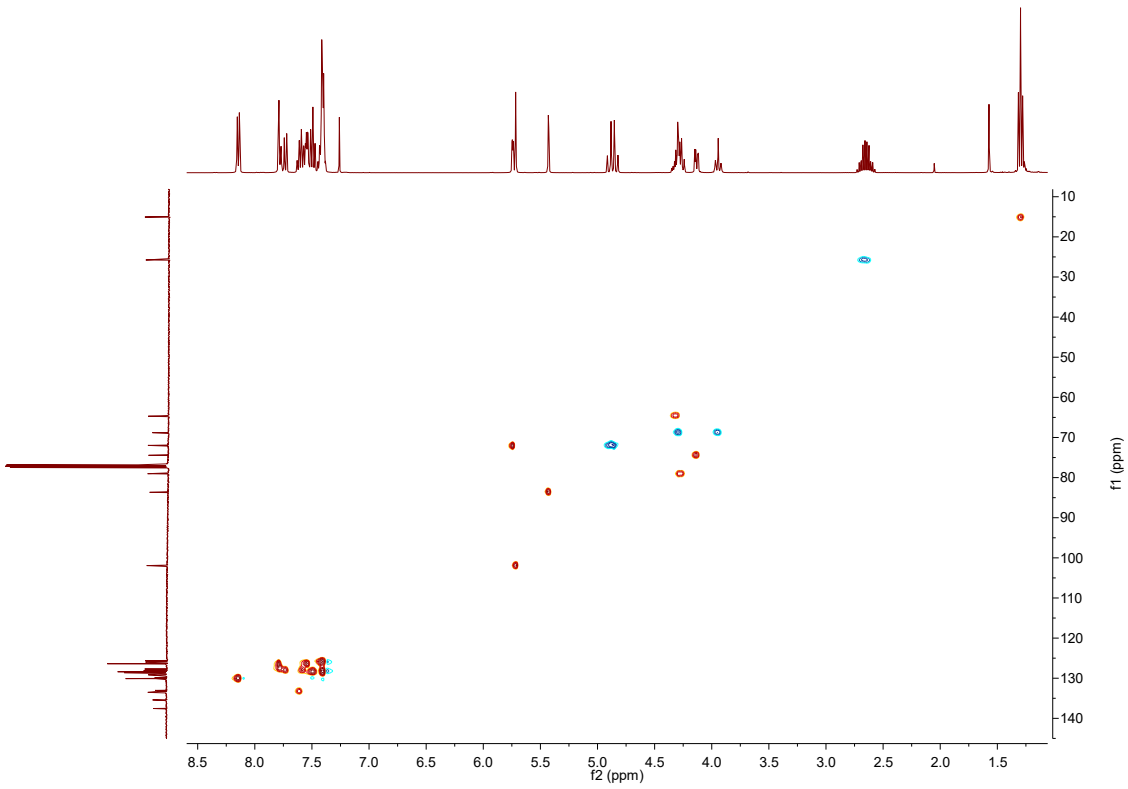

Figure A.113: HSQC spectrum of **21**, in $CDCl_3$.

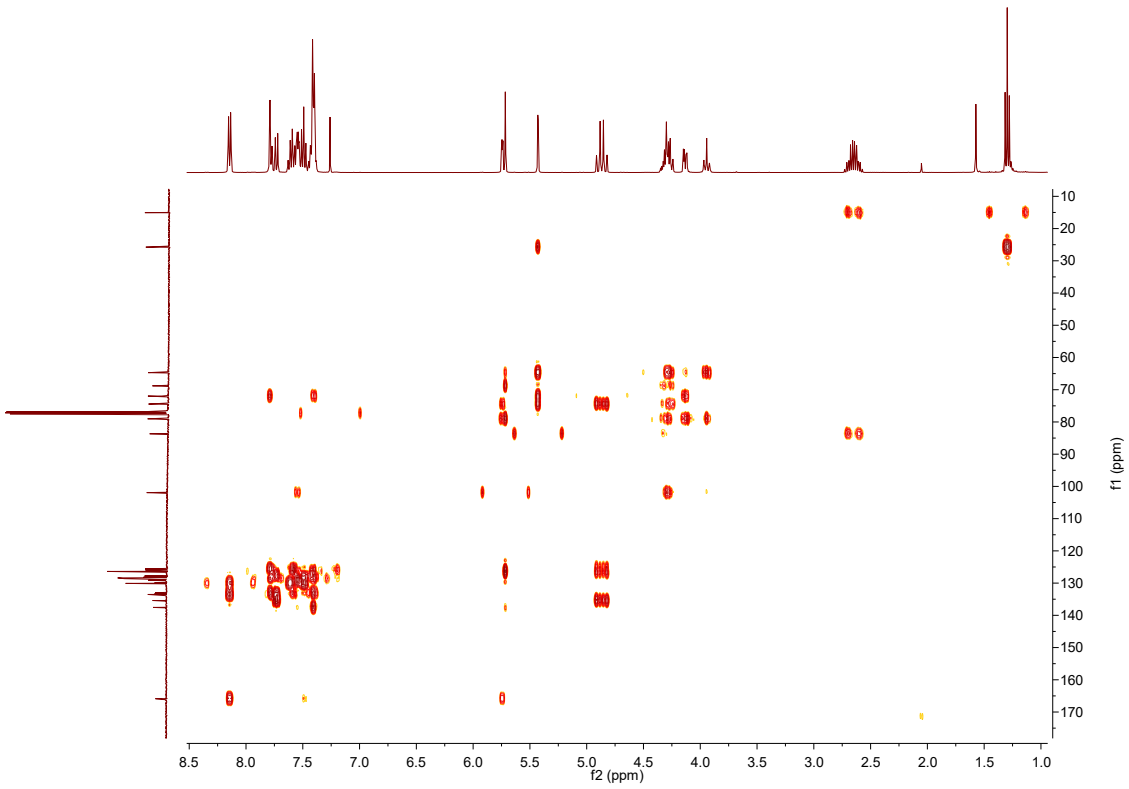

Figure A.114: HMBC spectrum of **21**, in $CDCl_3$.

A.27. Ethyl 2-*O*-benzoyl-3-*O*-(2-naphtylmethyl)-1-thio-α-D-mannopyranoside (**22**)

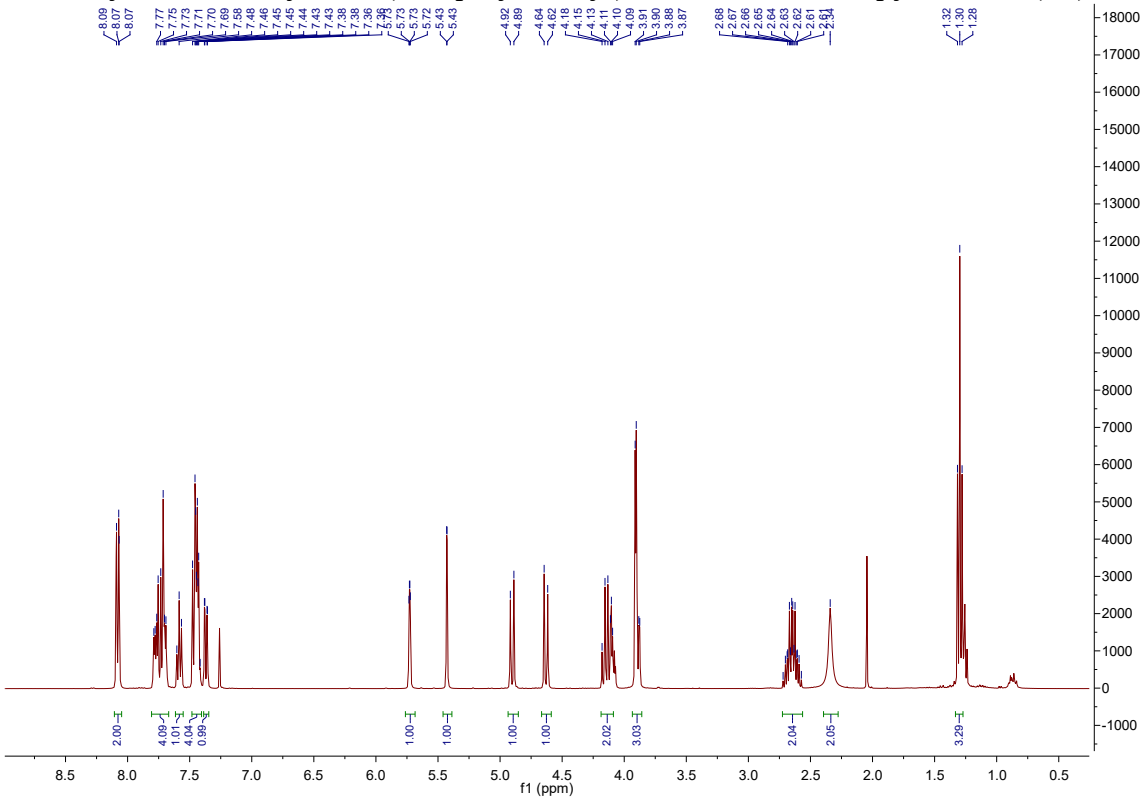

Figure A.115: ^{1}H NMR spectrum of **22**, in $CDCl_3$.

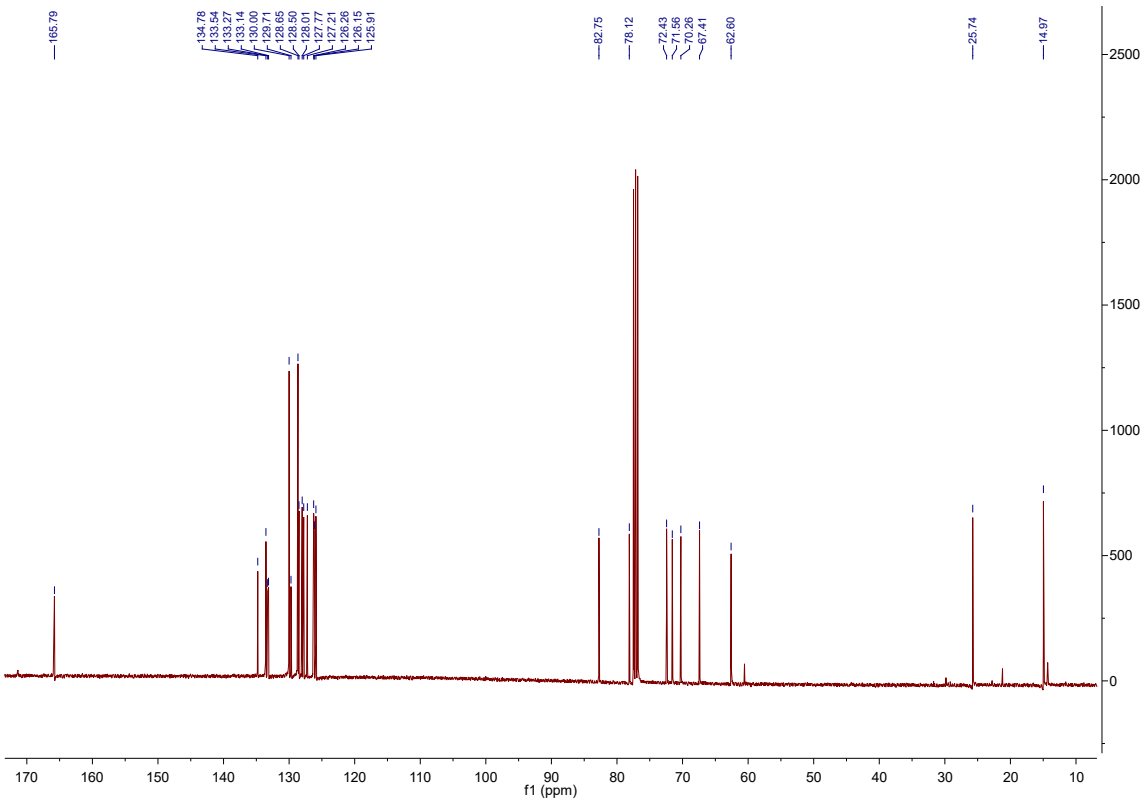

Figure A.116: ^{13}C NMR spectrum of **22**, in $CDCl_3$.

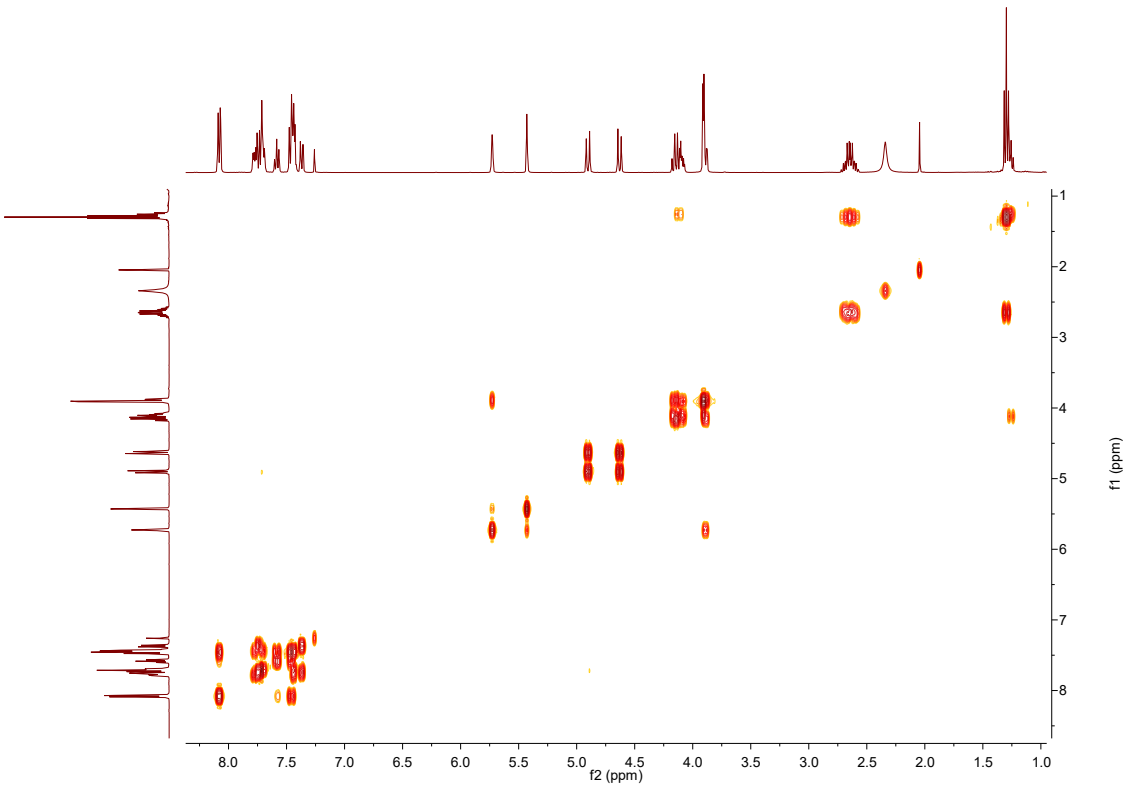

Figure A.117: COSY spectrum of **22**, in $CDCl_3$.

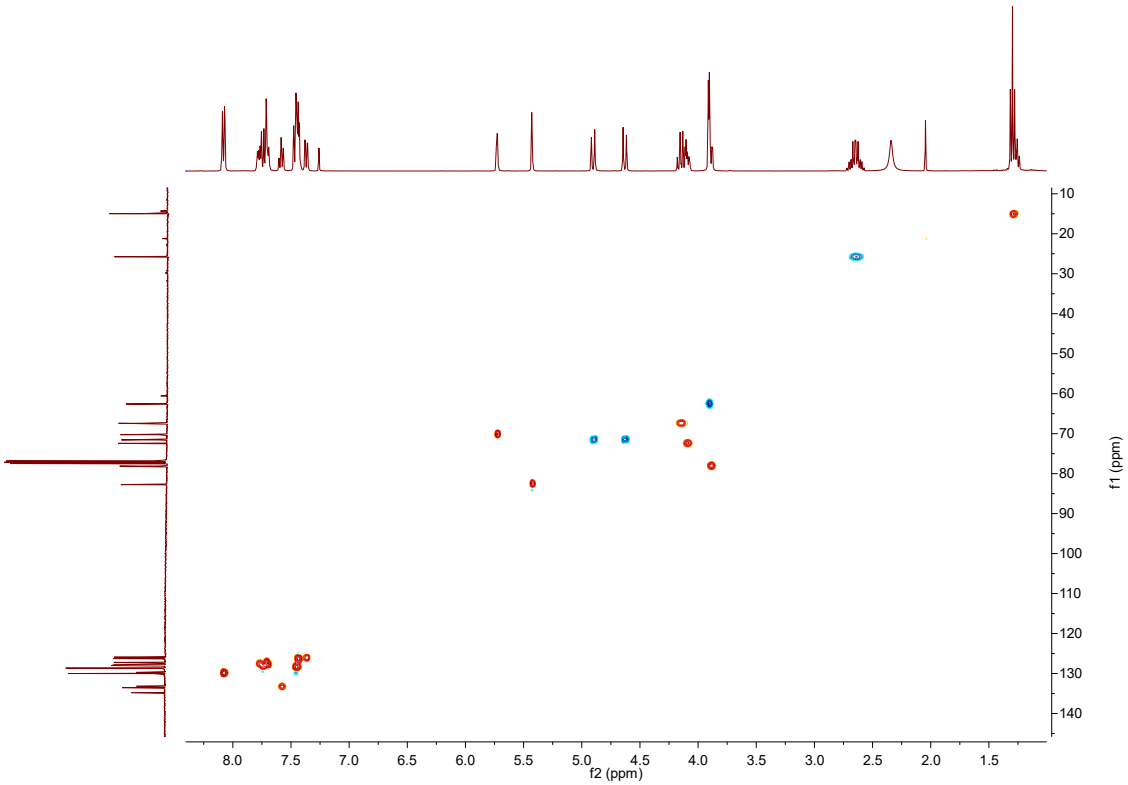

Figure A.118: HSQC spectrum of **22**, in $CDCl_3$.

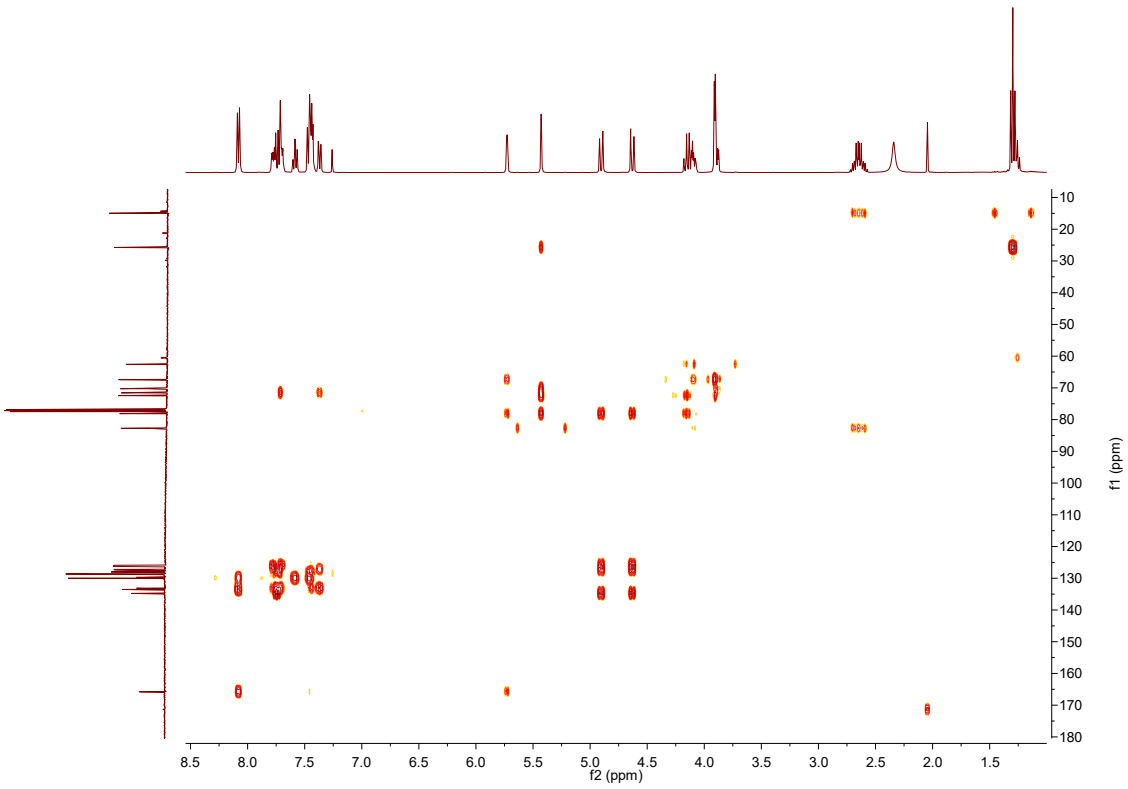

Figure A.119: HMBC spectrum of **22**, in $CDCl_3$.

A.28. Ethyl 2-*O*-benzoyl-4-*O*-benzyl-3-*O*-(2-naphtylmethyl)-1-thio-α-D-mannopyranoside (**23**)

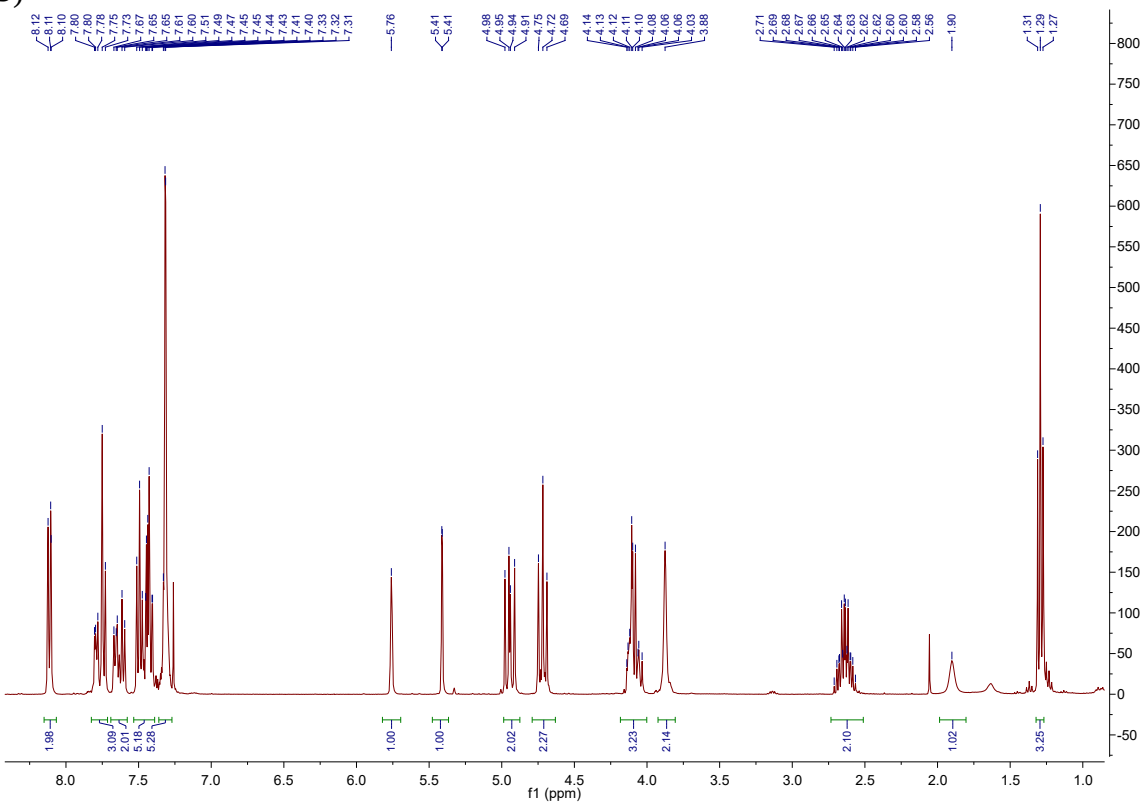

Figure A.120: ^{1}H NMR spectrum of **23**, in $CDCl_3$.

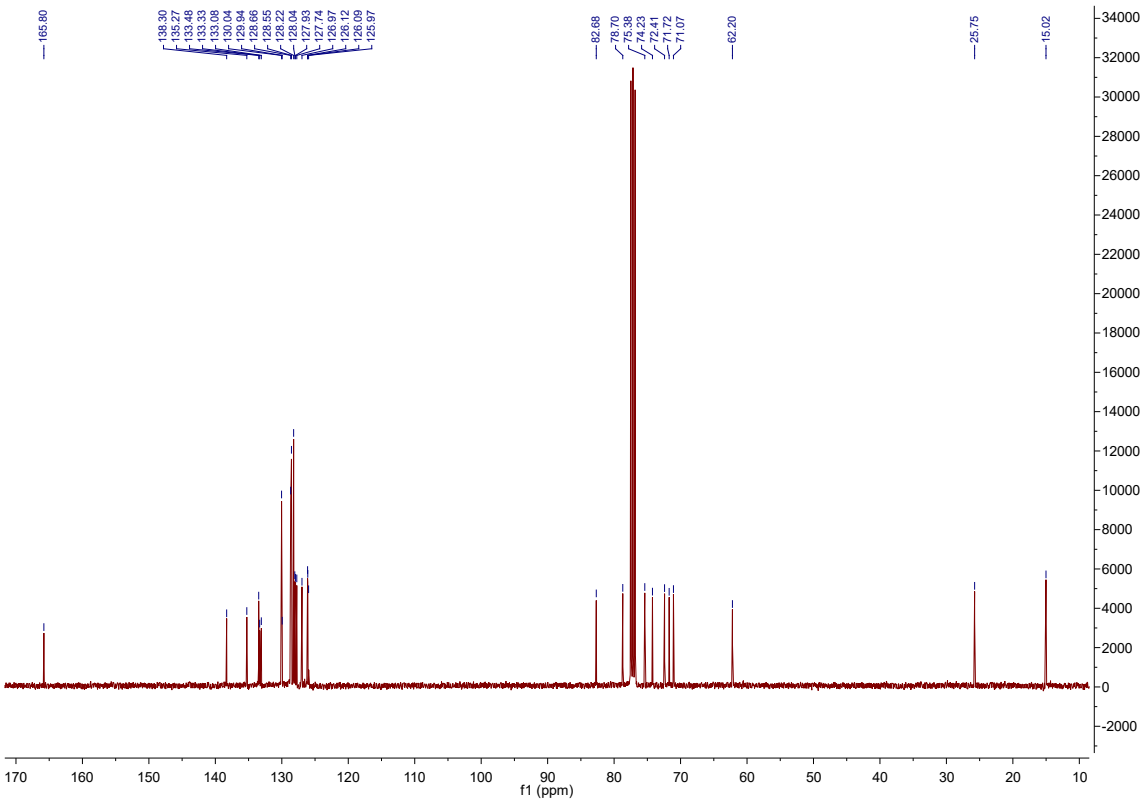

Figure A.121: ^{13}C NMR spectrum of **23**, in $CDCl_3$.

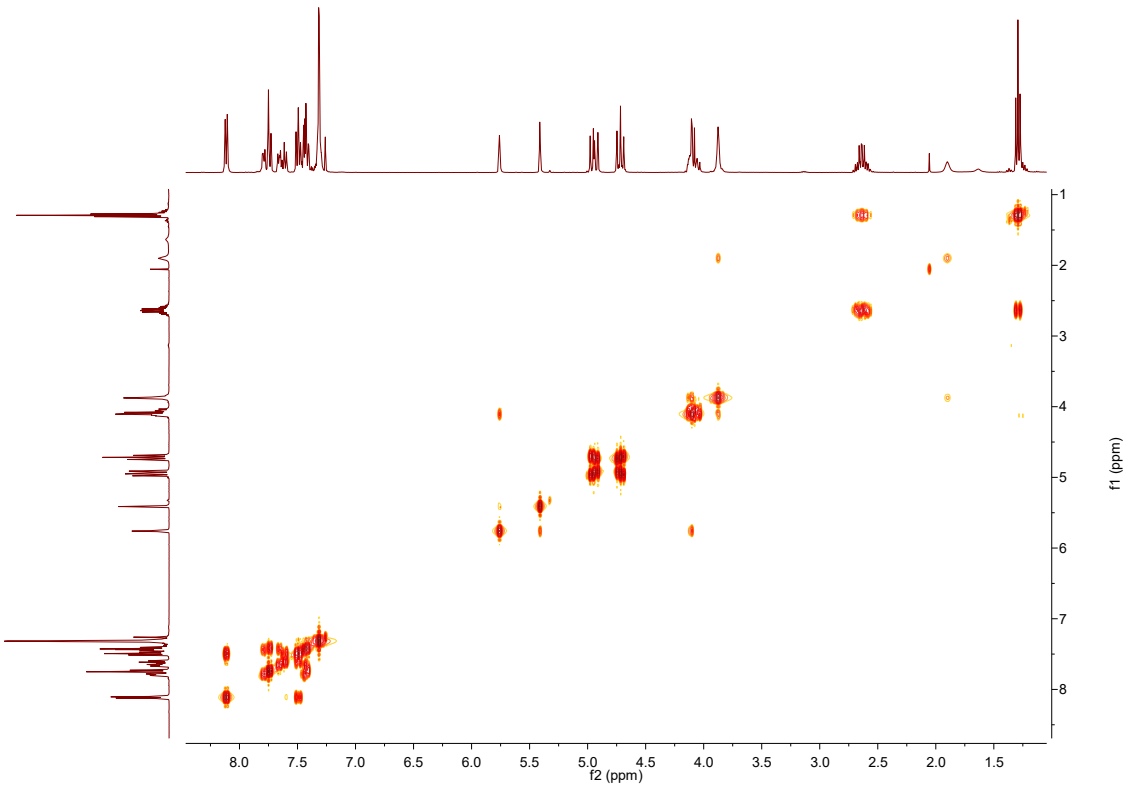

Figure A.122: COSY spectrum of **23**, in $CDCl_3$.

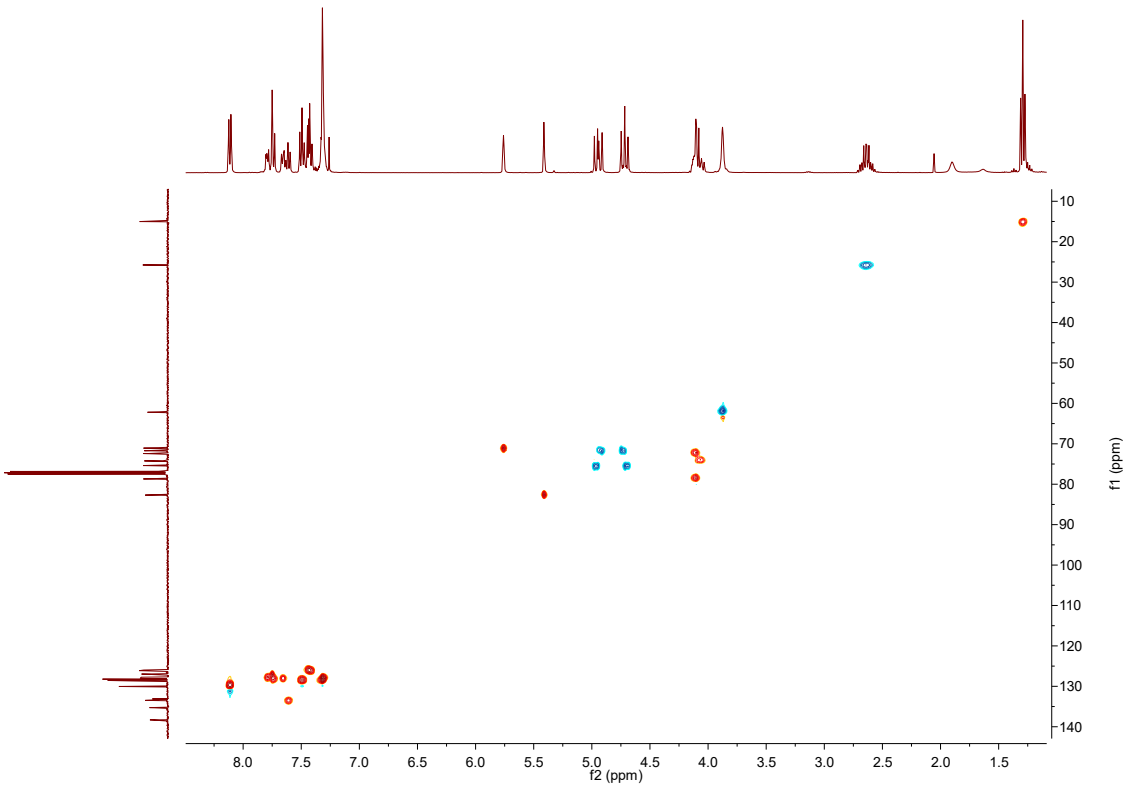

Figure A.123: HSQC spectrum of **23**, in $CDCl_3$.

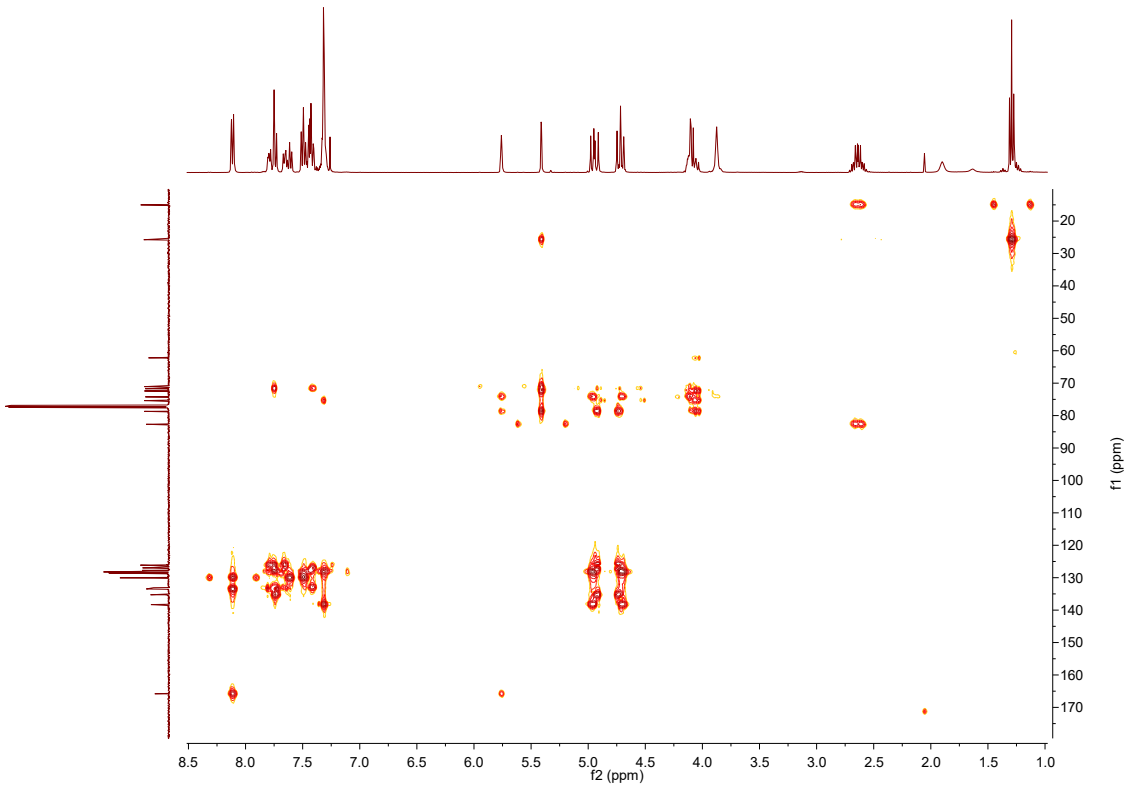

Figure A.124: HMBC spectrum of **22**, in $CDCl_3$.

A.29. Ethyl 2-*O*-benzoyl-4,6-di-*O*-benzyl-3-*O*-(2-naphtylmethyl)-1-thio-α-D-mannopyranoside (**BB-3**)

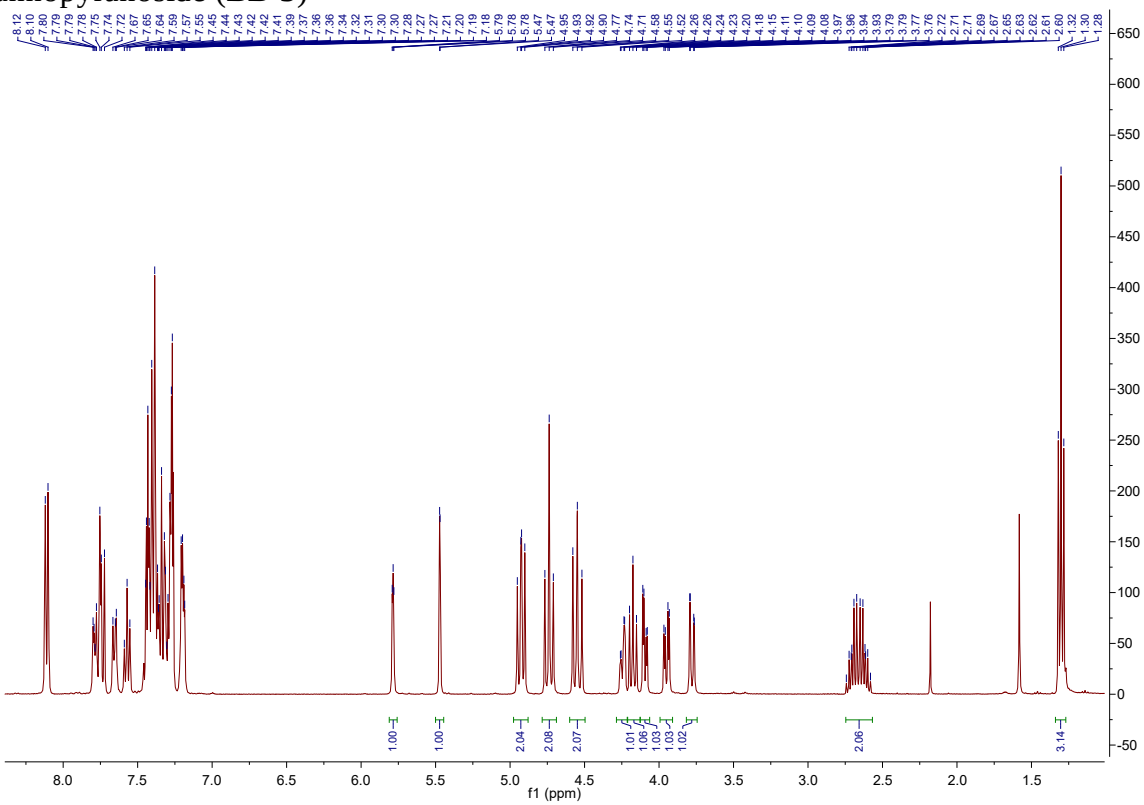

Figure A.125: ^{1}H NMR spectrum of **BB-3**, in $CDCl_3$.

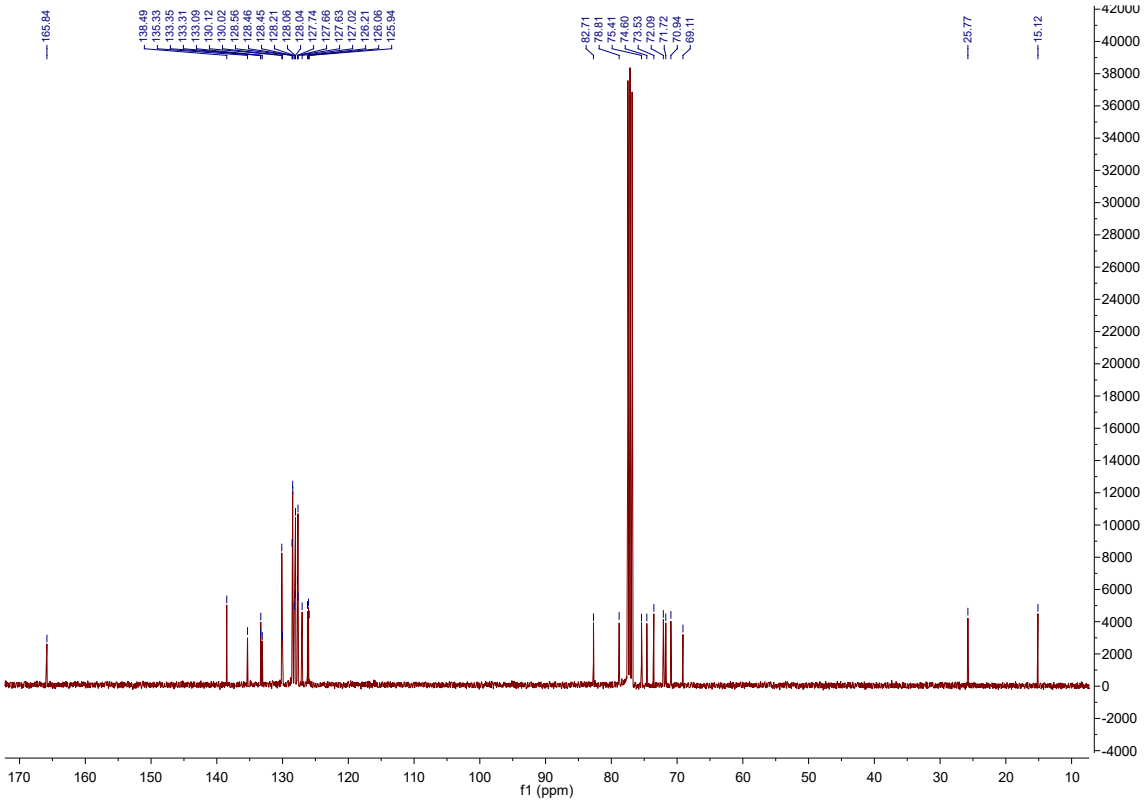

Figure A.126: ^{13}C NMR spectrum of **BB-3**, in $CDCl_3$.

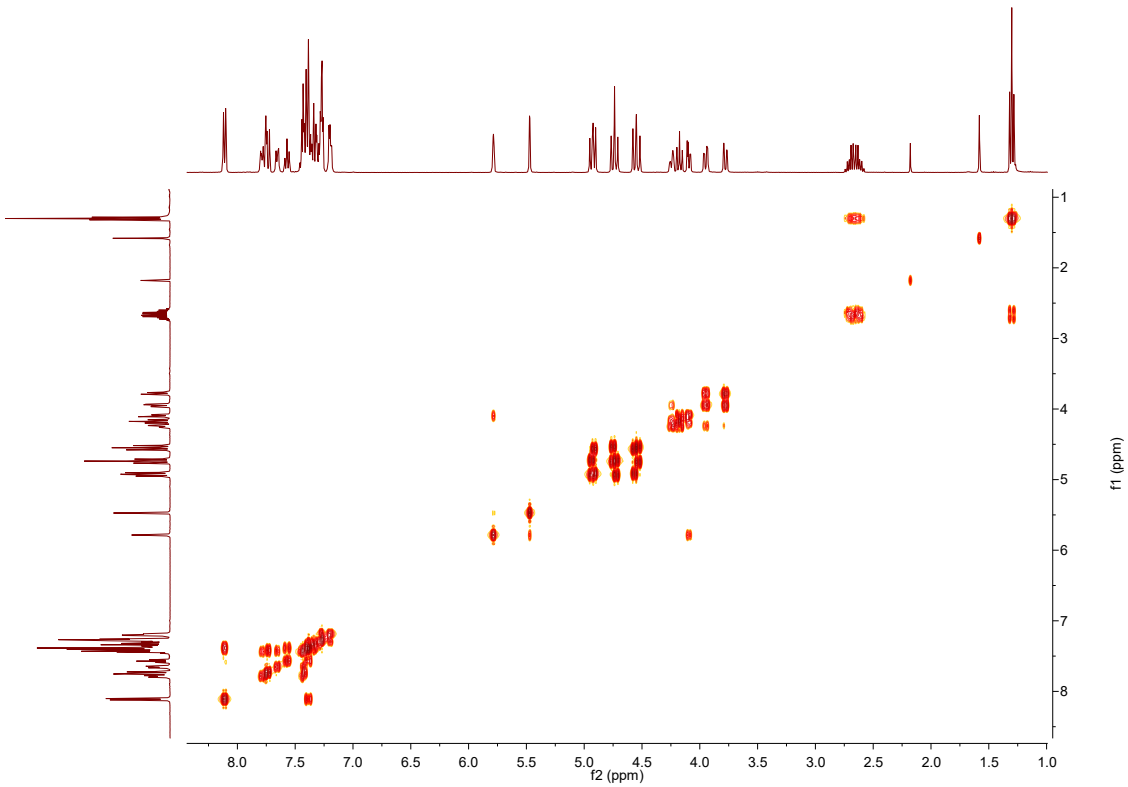

Figure A.127: COSY spectrum of **BB-3**, in $CDCl_3$.

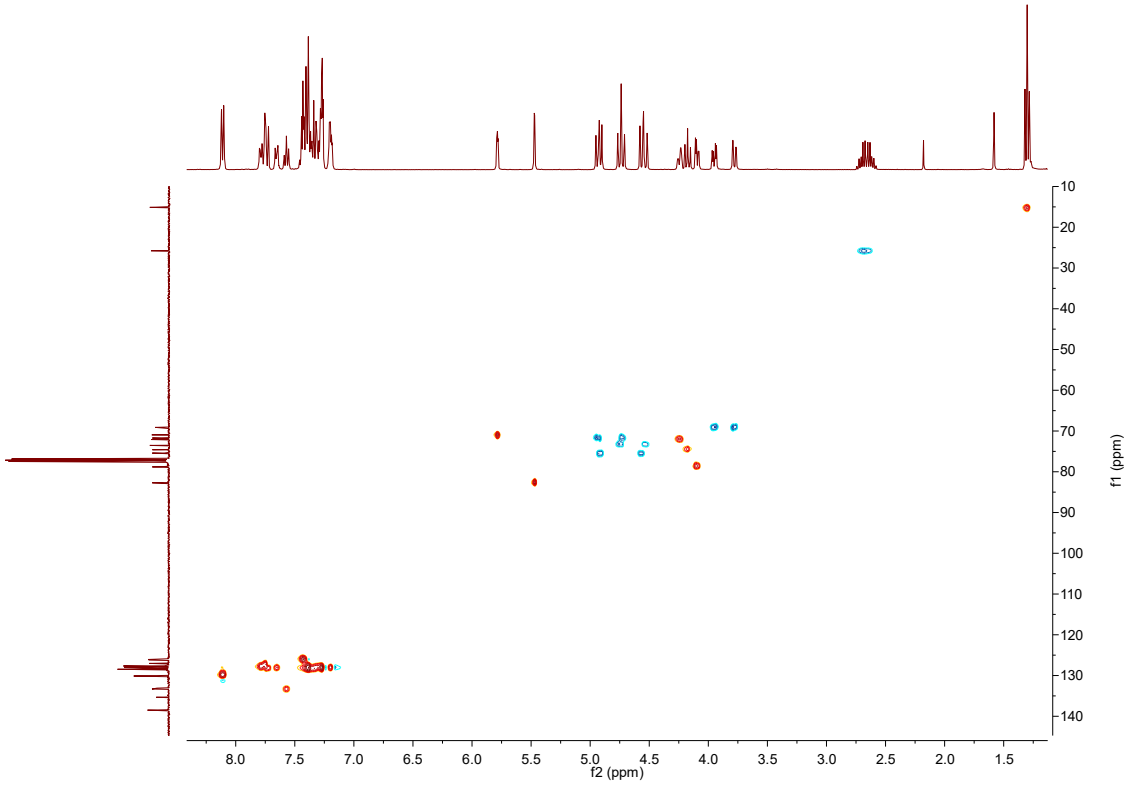

Figure A.128: HSQC spectrum of **BB-3**, in $CDCl_3$.

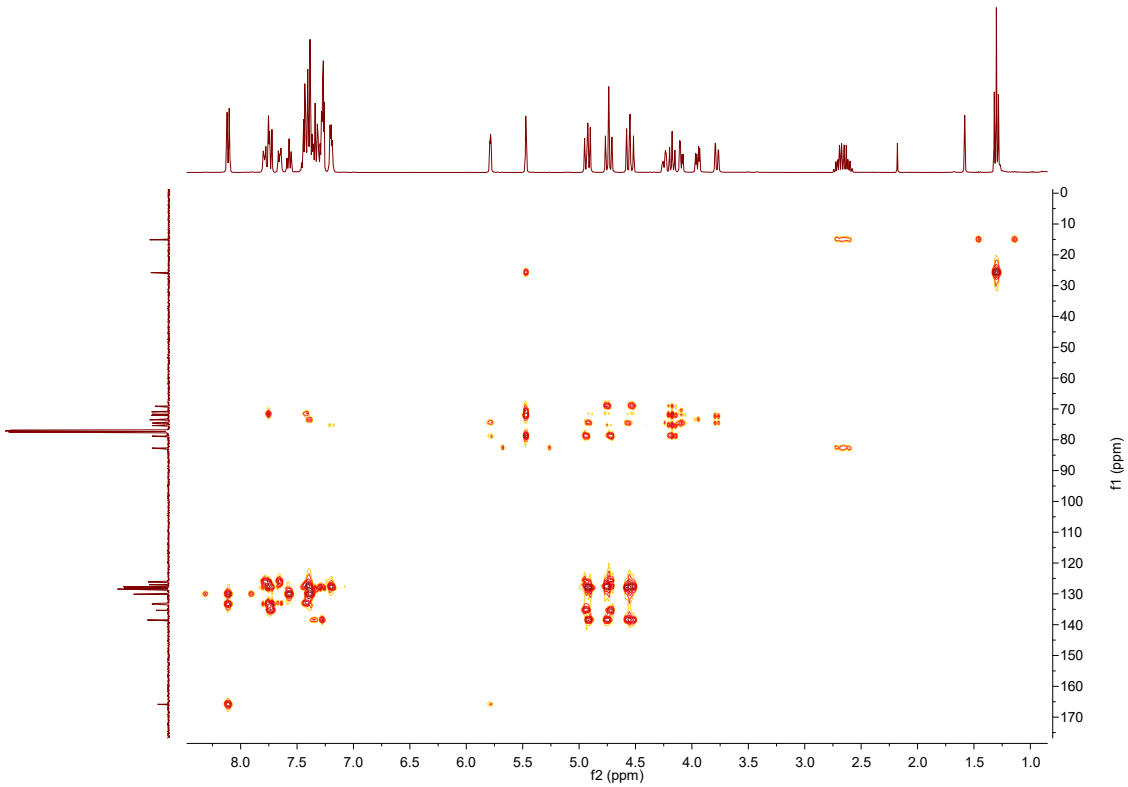

Figure A.129: HMBC spectrum of **BB-3**, in $CDCl_3$.

A.30. Ethyl 2-*O*-benzoyl-3-*O*-benzyl-4,6-*O*-benzylidene-1-thio-α-D-mannopyranoside (**25**)

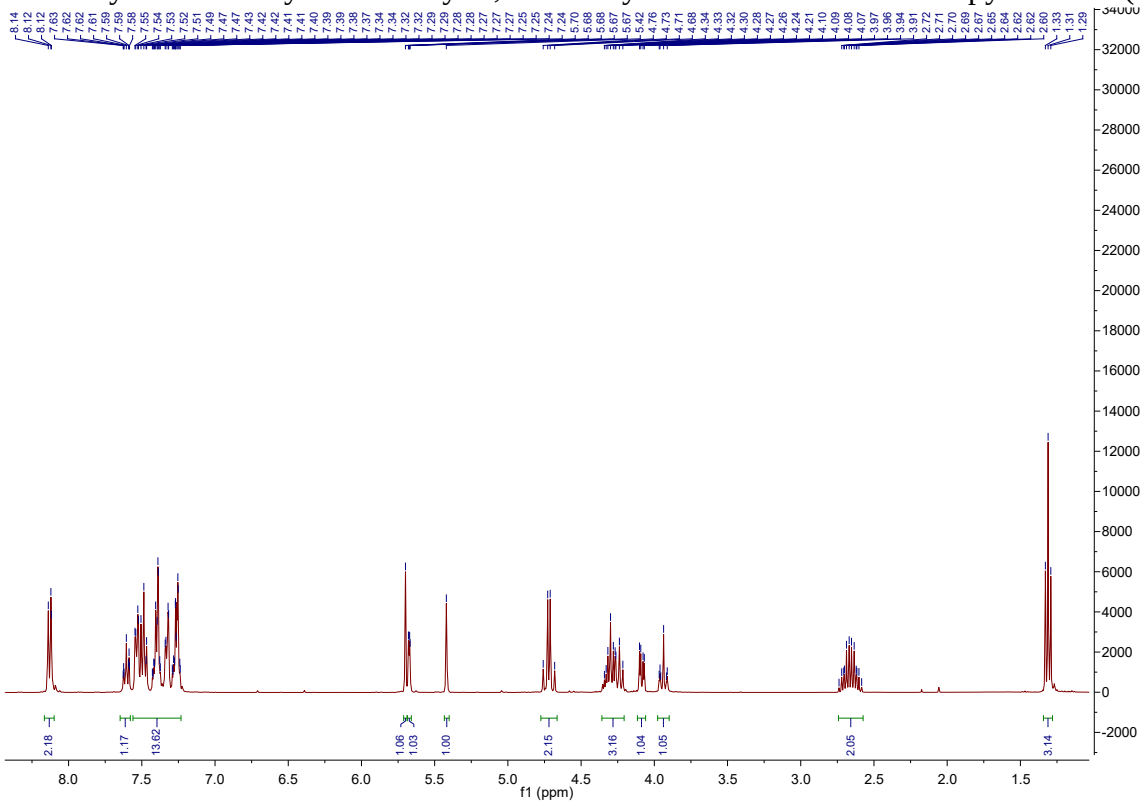

Figure A.130: ^{1}H NMR spectrum of **25**, in $CDCl_3$.

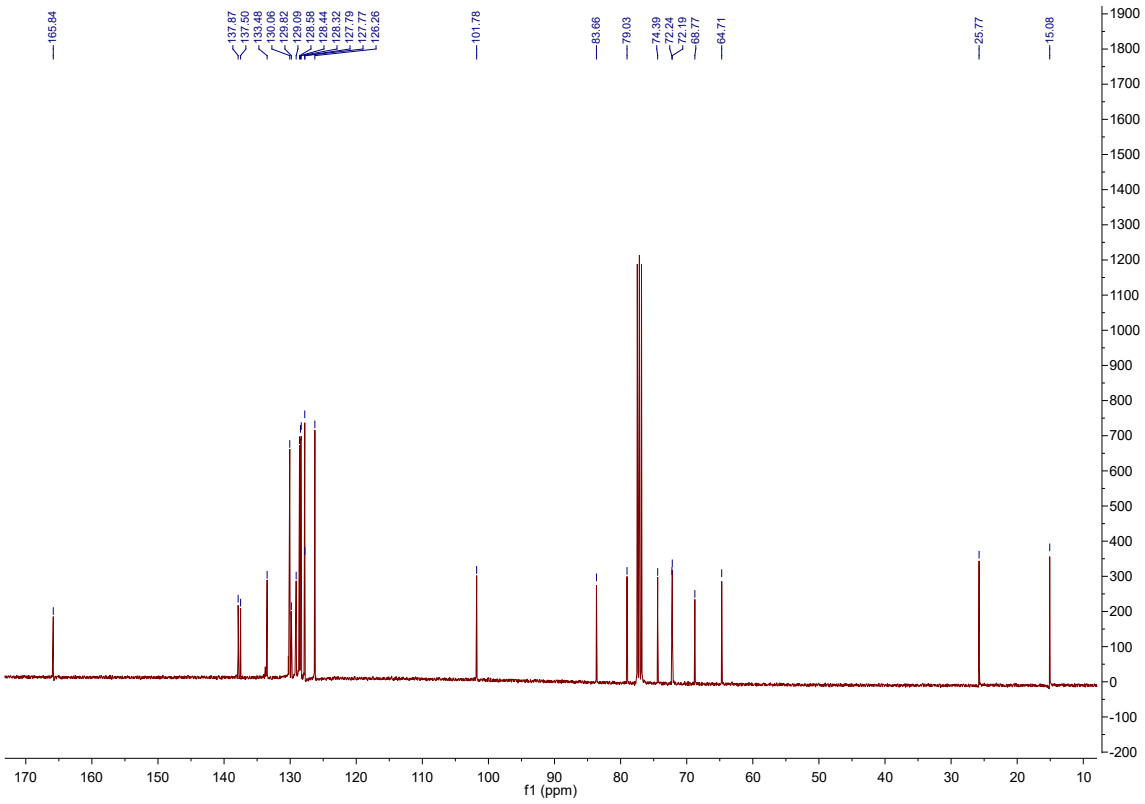

Figure A.131: ^{13}C NMR spectrum of **25**, in $CDCl_3$.

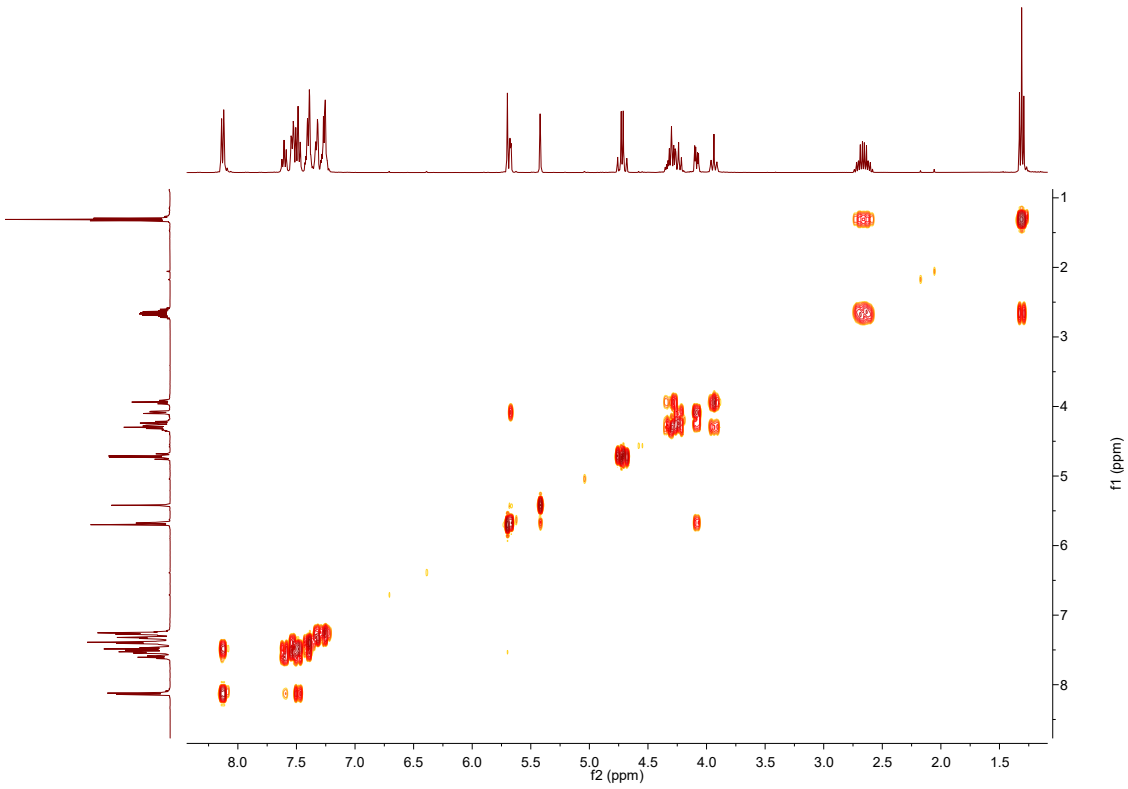

Figure A.132: COSY spectrum of **25**, in $CDCl_3$.

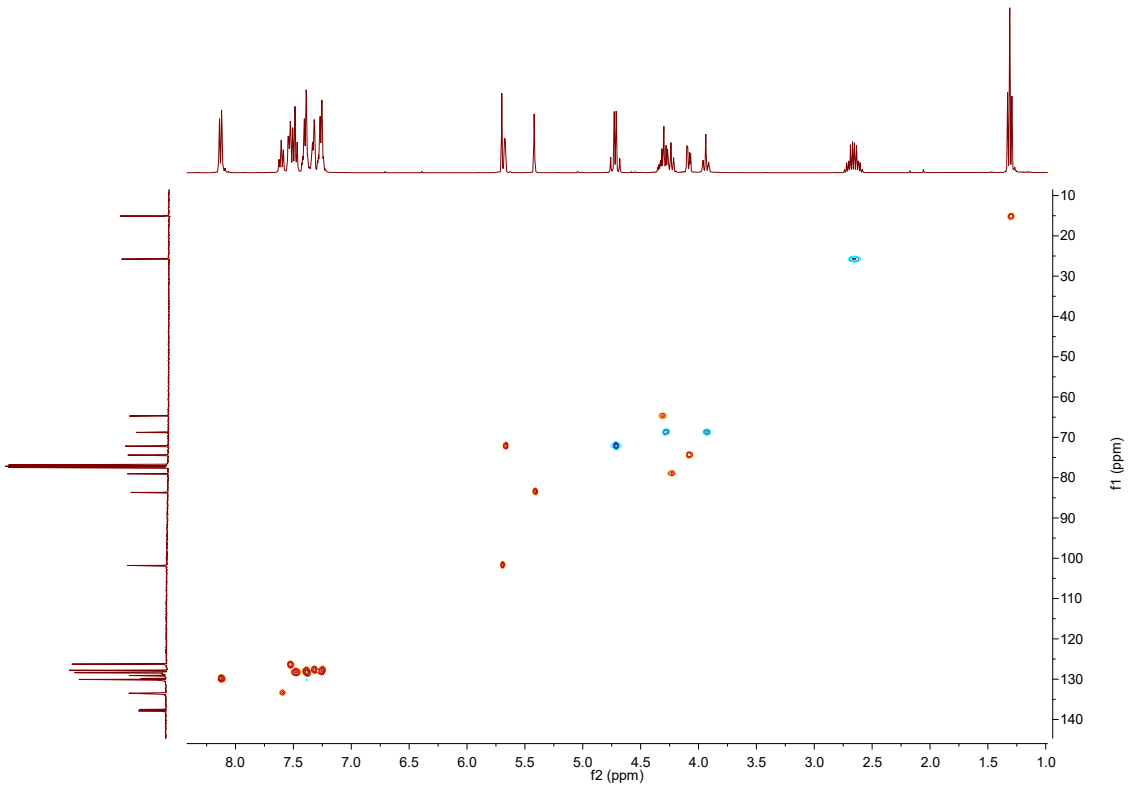

Figure A.133: HSQC spectrum of **25**, in $CDCl_3$.

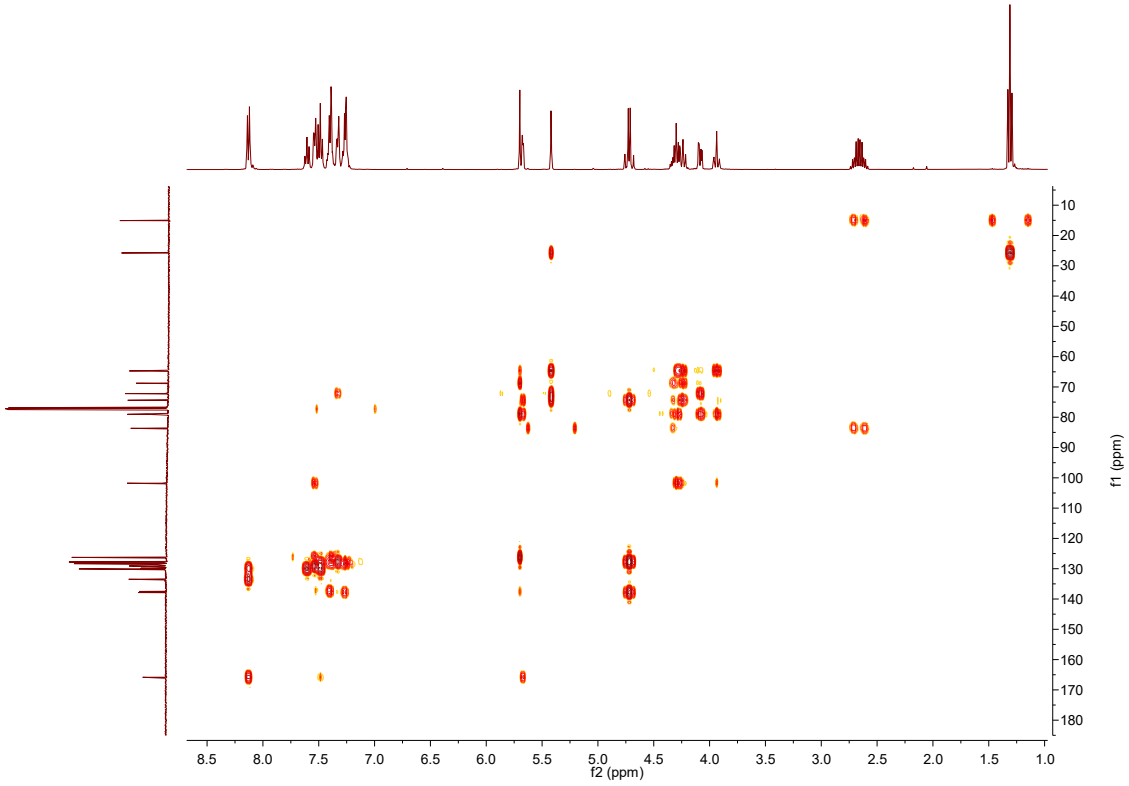

Figure A.134: HMBC spectrum of **25**, in $CDCl_3$.

A.31. Ethyl 2-*O*-benzoyl-3,4-di-*O*-benzyl-1-thio-α-D-mannopyranoside (**26**)

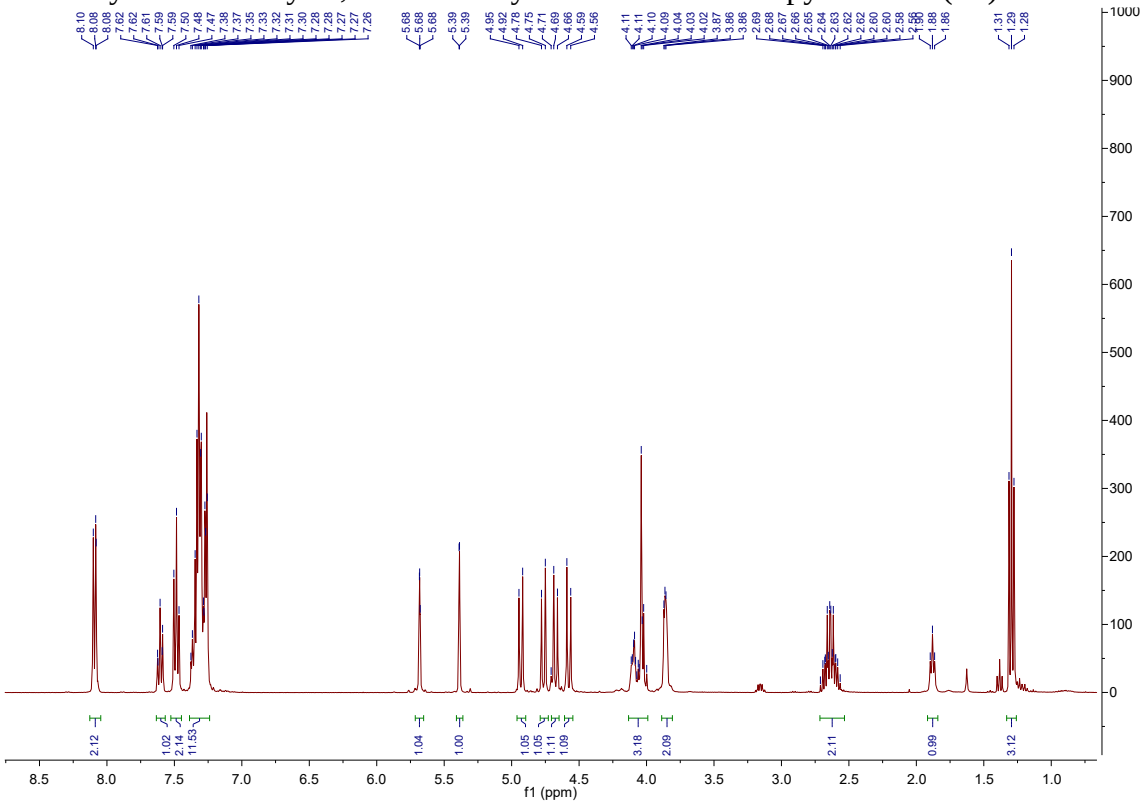

Figure A.135: ^{1}H NMR spectrum of **26**, in $CDCl_3$.

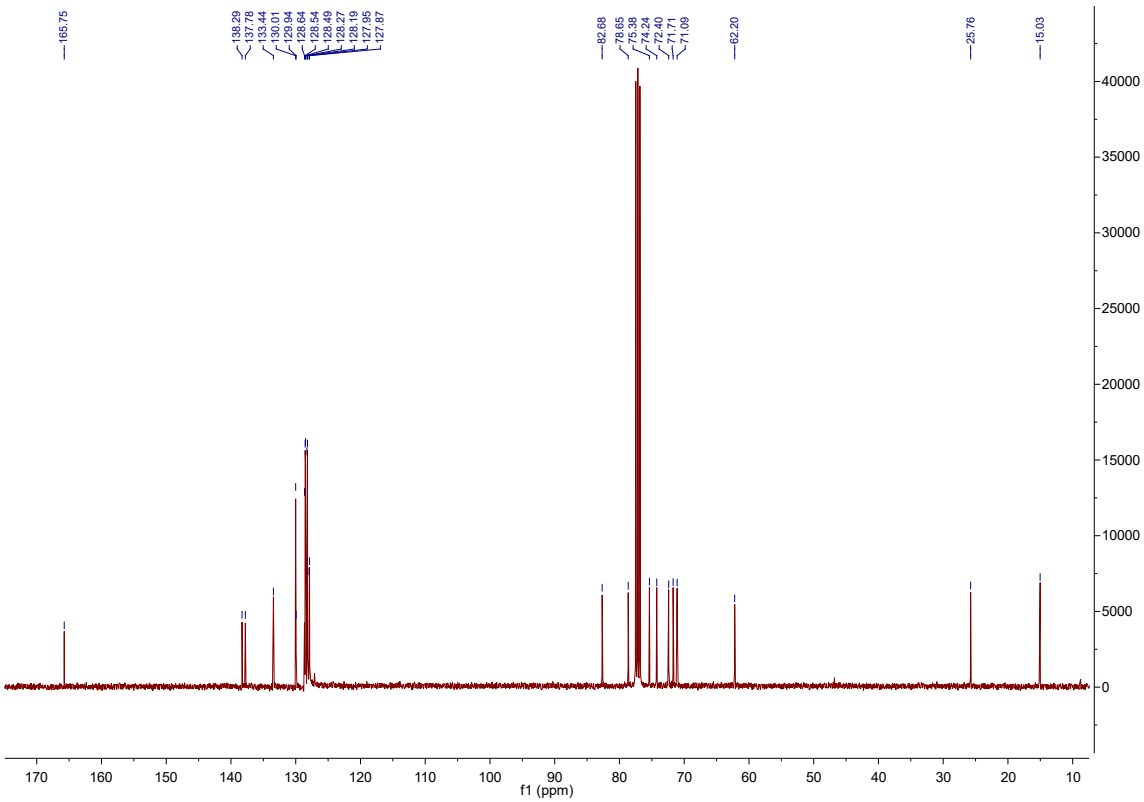

Figure A.136: ^{13}C NMR spectrum of **26**, in $CDCl_3$.

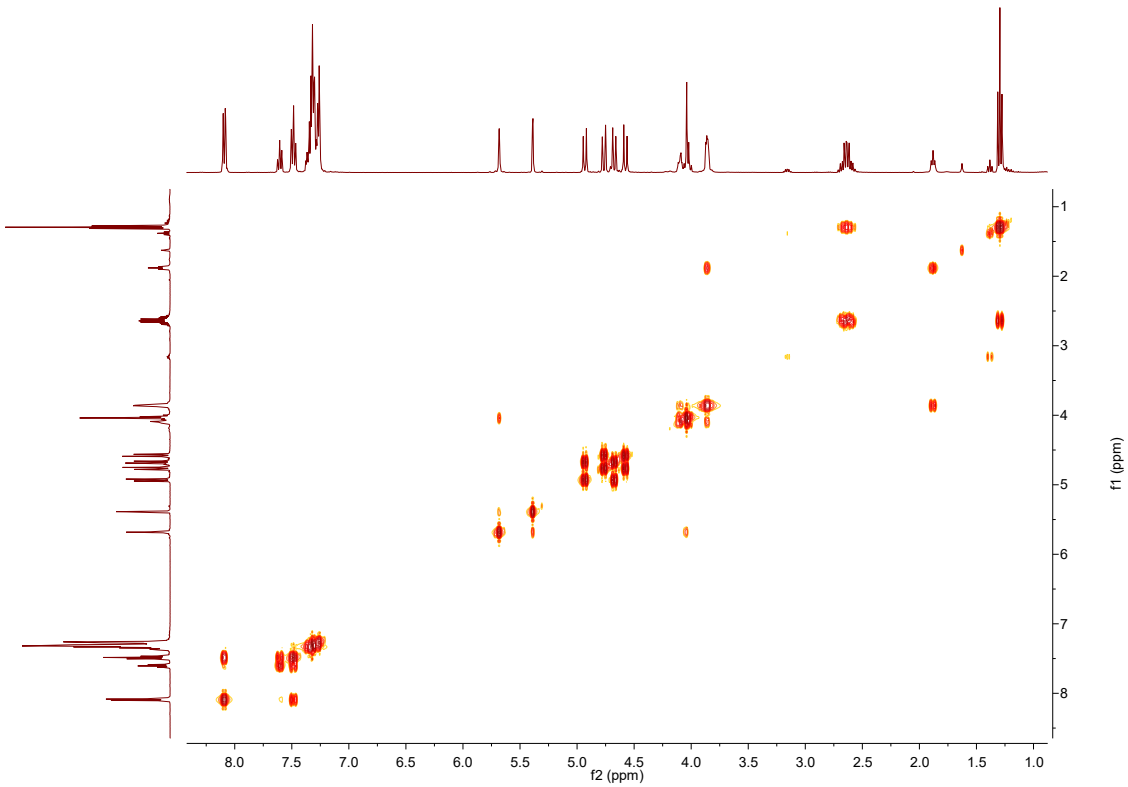

Figure A.137: COSY spectrum of **26**, in $CDCl_3$.

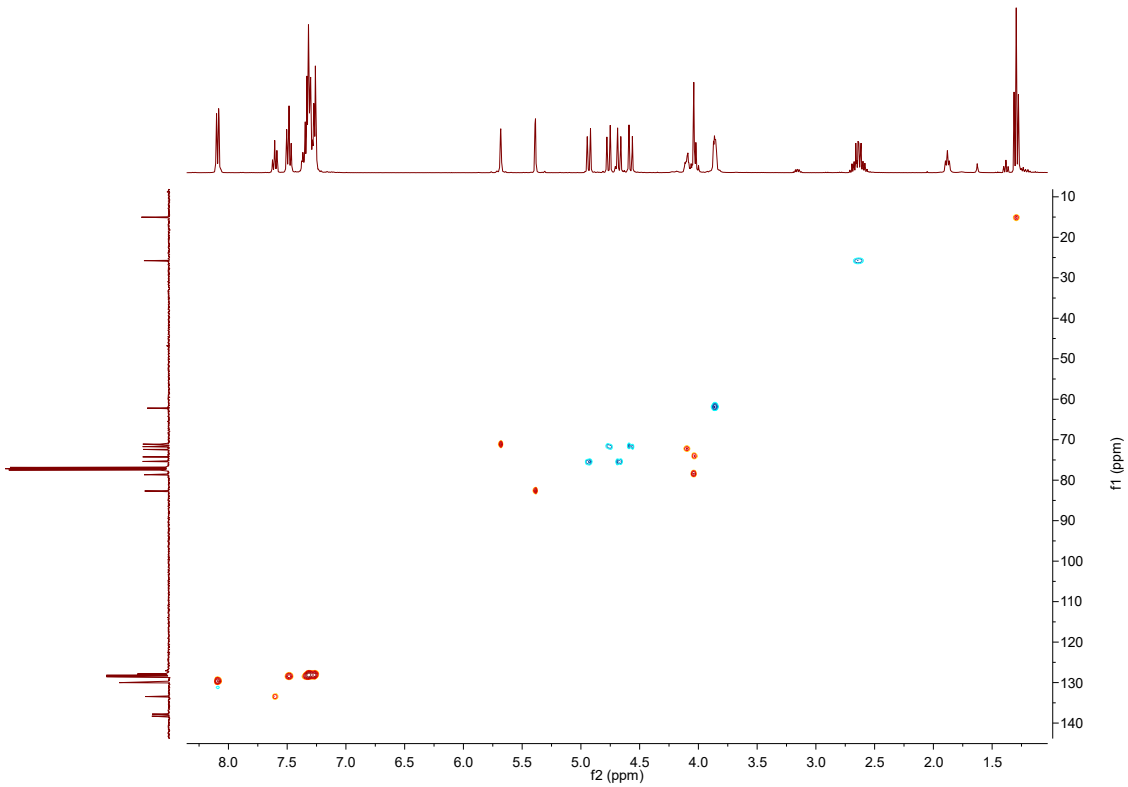

Figure A.138: HSQC spectrum of **26**, in $CDCl_3$.

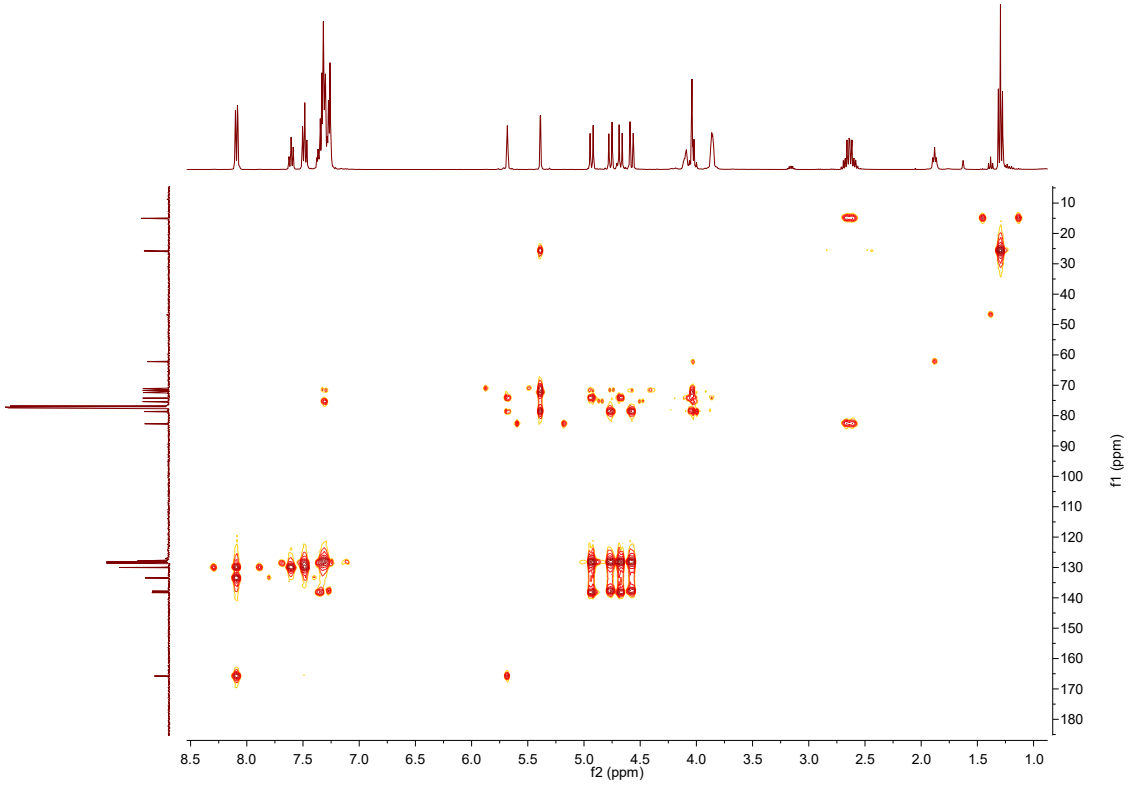

Figure A.139: HMBC spectrum of **26**, in $CDCl_3$.

A.32. Ethyl 2-*O*-benzoyl-3,4,6-tri-*O*-benzyl-1-thio-α-D-mannopyranoside (**BB-4**)

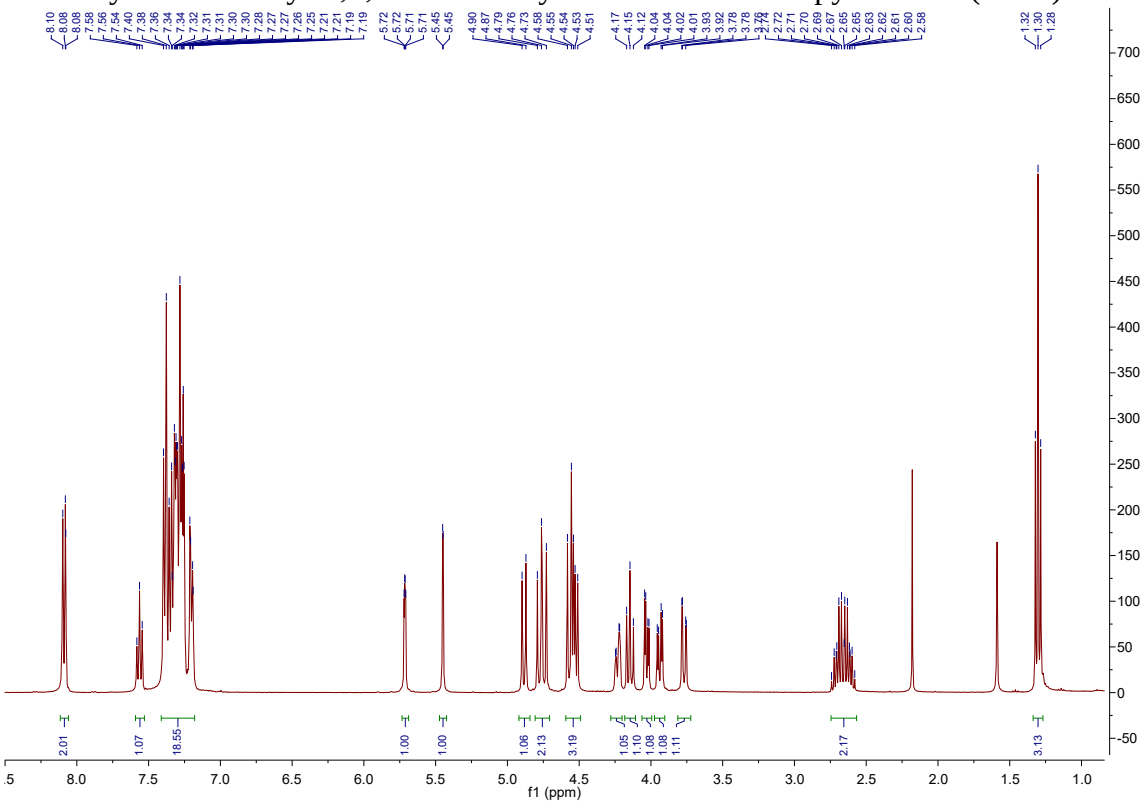

Figure A.140: ^{1}H NMR spectrum of **BB-4**, in $CDCl_3$.

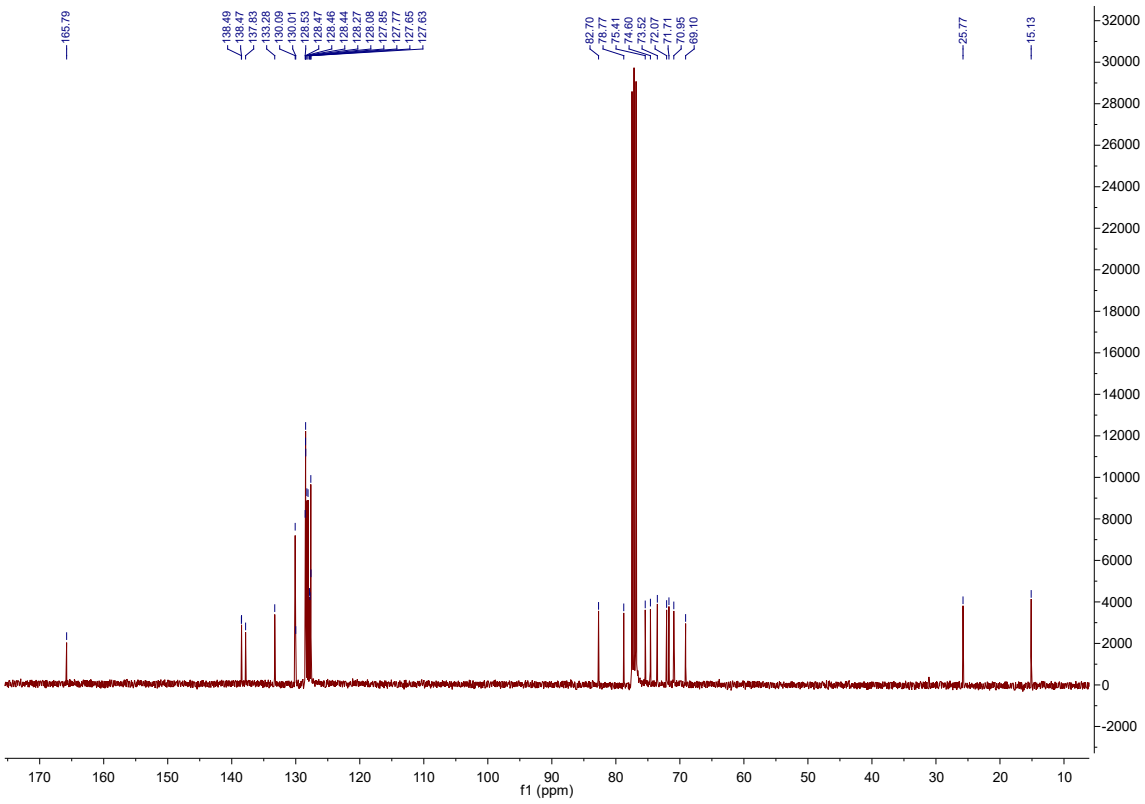

Figure A.141: ^{13}C NMR spectrum of **BB-4**, in $CDCl_3$.

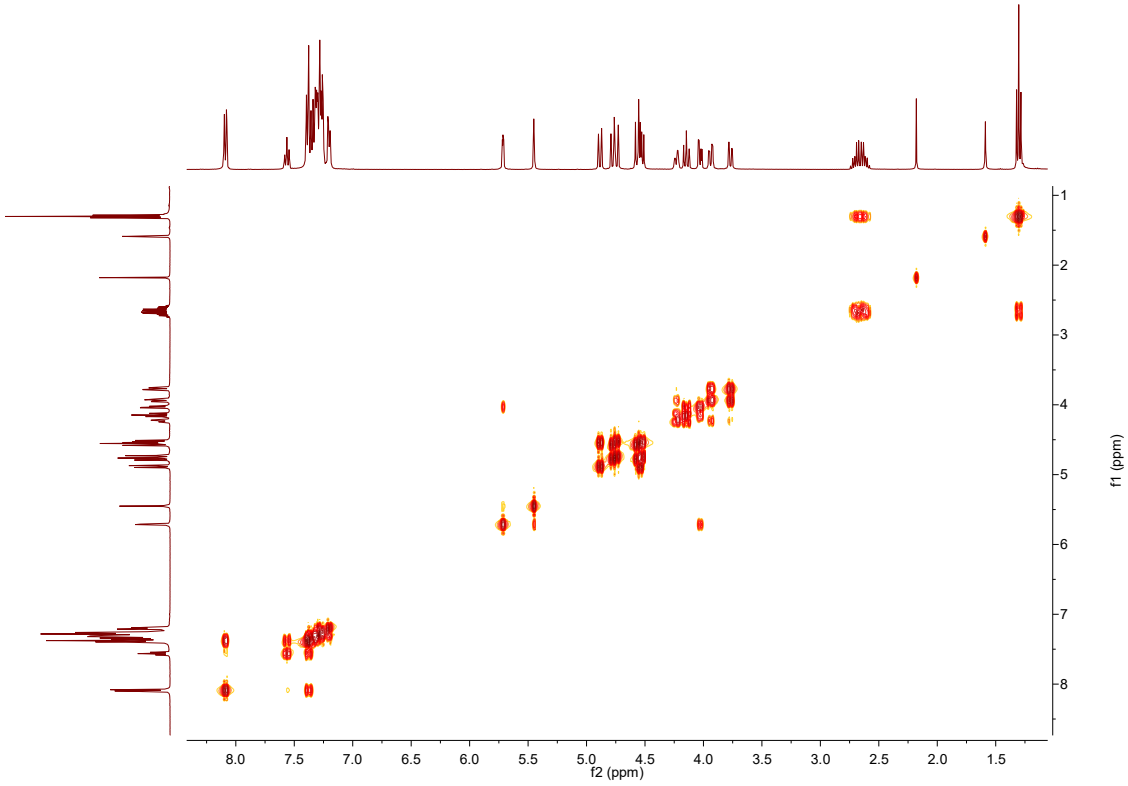

Figure A.142: COSY spectrum of **BB-4**, in $CDCl_3$.

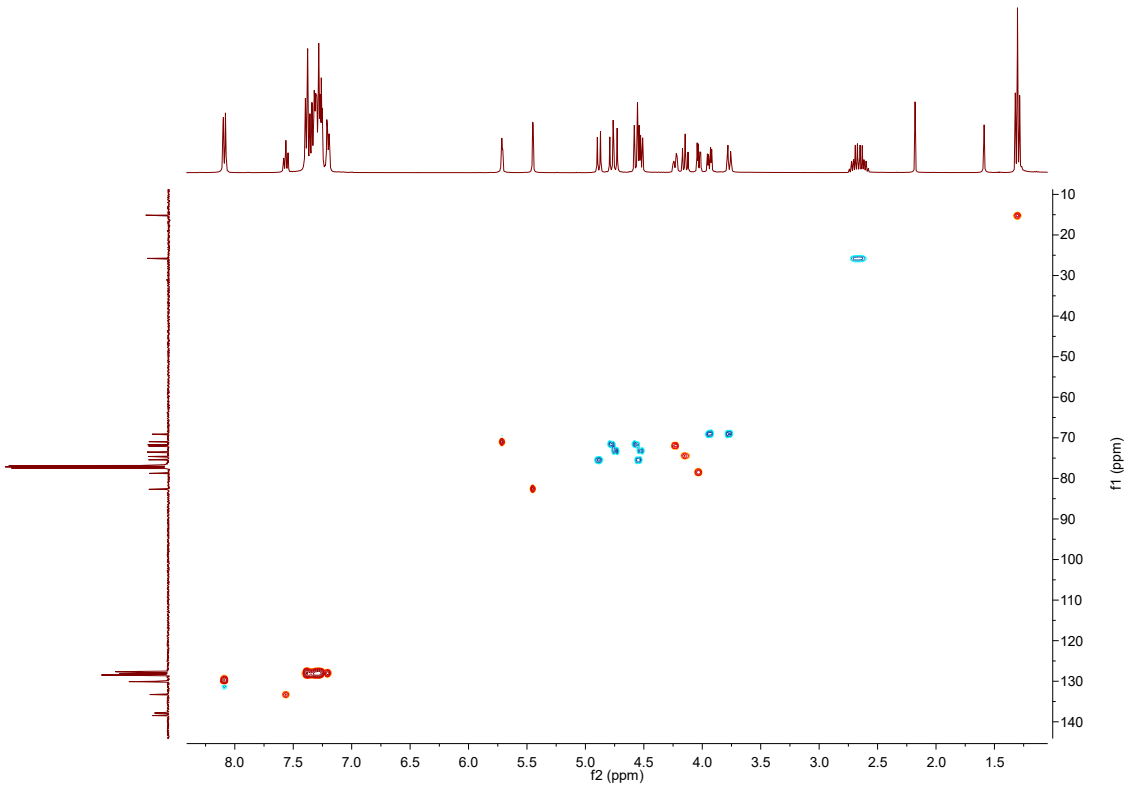

Figure A.143: HSQC spectrum of **BB-4**, in $CDCl_3$.

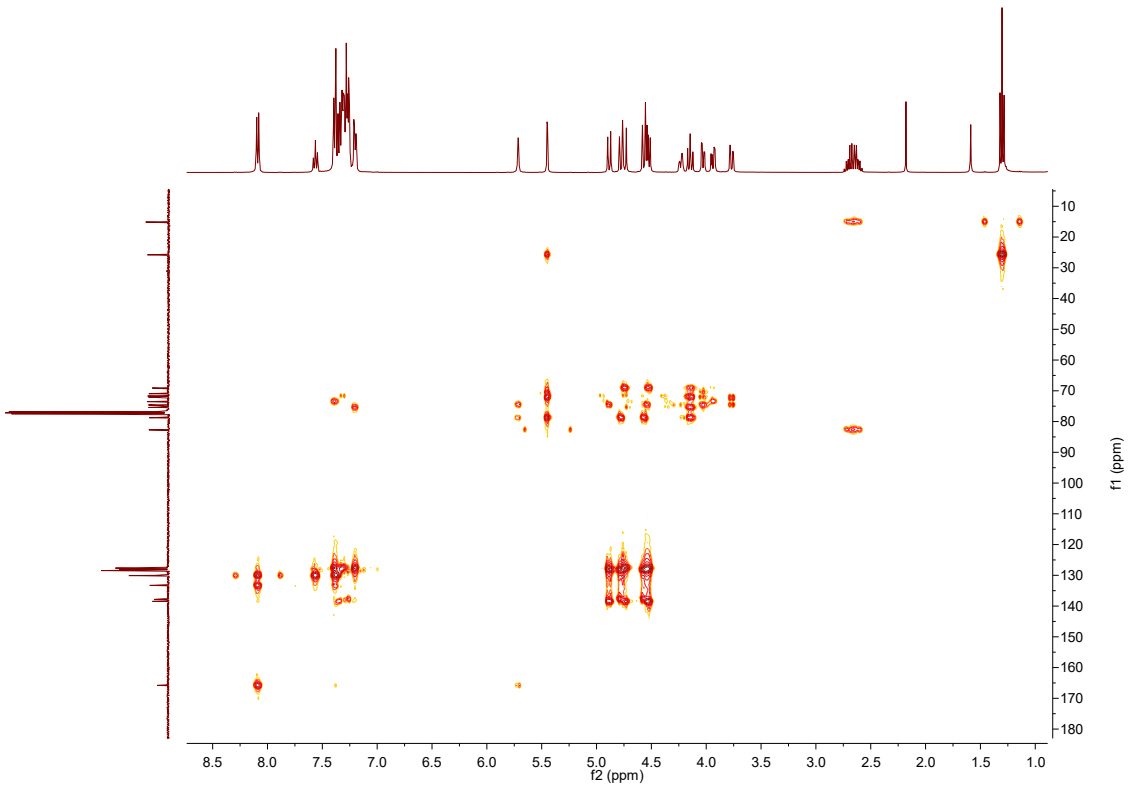

Figure A.144: HMBC spectrum of **BB-4**, in $CDCl_3$.